UNITED NATIONS EDUCATIONAL, SCIENTIFIC AND CULTURAL ORGANIZATION
INTERNATIONAL ATOMIC ENERGY AGENCY
INTERNATIONAL CENTRE FOR THEORETICAL PHYSICS
I.C.T.P., P.O. BOX 586, 34100 TRIESTE, ITALY, CABLE: CENTRATOM TRIESTE

H4.SMR/1013-28

SCHOOL ON THE USE OF SYNCHROTRON RADIATION
IN SCIENCE AND TECHNOLOGY:
"John Fuggle Memorial"

3 November - 5 December 1997

Miramare - Trieste, Italy

Dichroism and Spinpolarisation in Angular Resolved Photoemission

Gerhard H. Fecher
Johannes Gutenberg - Universität
Mainz - Germany

Gerhard H. Fecher

Johannes Gutenberg - Universität

Institut für Physik

D-55099 Mainz

Germany

universität mainz

Dichroism and Spinpolarisation in Angular Resolved Photoemission

Basic theory and Experiments

lecture presented at:

School on the Use of Synchrotron Radiation in Science and Technology

"John Fuggle Memorial"

International Centre for Theoretical Physics, Trieste, Italy November 1997

CONTENTS

I Introduction

In optics wavelength dependent differences in the absorption of light are observed illuminating a birefringend crystal by light linearly polarised in two orthogonal directions. This phenomenon is called dichroism for crystals with a single optical axis (uniaxial crystal) or trichroism in the case of two optical axes (biaxial). In strength, the polarisation of light has to be parallel or perpendicular to the optical axis, respectively. All other cases are called pleochroism if the polarisation has an arbitrary direction with respect to the optical axis [1.1]. This so called dispersion of polarisation is the color-decompositionof light in different directions in crystals.

In angular resolved photoemission spectroscopy, a difference in the photoelectron intensity or the differential cross section is obtained if the polarisation of the incoming photons is varied.

A strong difference in the angular resolved intensities can be obtained exciting the photoelectrons by circularly polarised light of opposite helicity. Initially, Ritchie [1.2] used the term „Circular Dichroism in the Angular Distribution of photoelectrons", or in short CDAD, for the difference of the differential photoemission cross-section for excitation by right or left-hand circularly polarised photons, respectively. The circular dichroism in the angular distribution of photoelectrons was later theoretically predicted by Cherepkov to occur for oriented molecules simply in dipole approximation. The effect was first experimentally verified by the group ofSchönhense.

If the photoelectrons are excited by linearly polarised light different intensities are observed. The case of switching the polarisation from parallel to perpendicular with respect to the quantisation axis is well known. In close analogy to the case of birefringence we call this effect Dichroism in the Angular Distribution (DAD) of photoelectrons. Another case, where the polarisation is switched between two orthogonal directions twisted by 45° with respect to the quantisation axis has not been treated explicitly but is included in the work of Cherepkov and Schönhense[1.3]. Below we will show that this leads to results very similar to that obtained from CDAD and therefore we call it Linear Dichroism in the Angular Distribution (LDAD) of photoelectrons.

Another type of so called dichroism is obtained from magnetic materials. In this case the electronic states are oriented by a magnetic field leading to differences in the angular resolved photoemission intensities if the sign or the direction of the magnetisation is switched. The effects are classified by CMDAD or LMDAD depending on the kind of photon polarisation. Recently Cherepkov has shown that there is no need to use polarised light to observe Magnetic Dichroism in the Angular Distribution of photoelectrons.

New types of insertion devices at the synchrotron facilities make it possible to work with elliptically polarised light and the polarisation can be chosen very arbitrary (for instance: elliptical Undulator at ALS, helical undulator at ESRF, and crossed undulator at BESSY). This opens a very wide field of new photoemission experiments by changing the linear or circular part of polarisation or both at once.

Below we give a single theoretical description for the angular resolved photoemission excited by arbitrarily polarised light. We will summarise all these phenomena by the term Pleochroism in Photoemission (PIPE). The splitting of m_l levels that is not seen in intensity spectroscopy can be observed by use of polarised light due to their different orientations as observed recently by Kisker in experiments and theoretically explained by Cherepkov. Similar results may be obtained if crystal field splitting of adsorbed atoms occurs. Therefor we suggest that the observed effects in angular resolved photoelectron spectroscopy from surfaces and adsorbates using polarised light are rather pleochroic than dichroic.

The term Dichroism originates from optics; it describes the different interaction of matter with light of two orthogonal states of polarisation. Meanwhile much work deals with the polarisation dependence of the photoemission cross-section and the effects arising from the orientation of the system under progress by magnetic fields are included. Following reference [1.4], a classification of the observed effects will be given here. The basic distinctions are that of magnetic and non-magnetic effects or the different polarisation of the photons.

Magnetic effects are distinguished for the different directions of the magnetisation or the applied magnetic field. The magnetisation can be applied in the plane of light incidence $M^{\pm p}$, perpendicular to it $M^{\pm s}$, or parallel to the surface normal $M^{\pm}$. The photon polarisation is classified according to the components vectors of the Stokes-vector. S_1 gives the linearly s, p polarisation in or perpendicular to the plane of incidence. S_2 corresponds to the linearly polarisation that is aligned with +45° (RLP) or –45° (LLP) to the plane of incidence and S_3 characterises the circular polarisation with right (RCP, σ^+) or left (LCP, σ^-) handed helicity.

Effect	switched	fixed
CDAD	S_3; RCP → LCP	Geometry
LDAD	S_2; RLP → LLP	
	S_1; s → p	
MCDAD	S_3	Magnetisation $M^{\pm s}$, $M^{\pm p}$, $M^{\pm}$
MLDAD	S_2	
	S_1	
CMDAD	Magnetisation $M^{\pm s}$, $M^{\pm p}$, $M^{\pm}$; $M^{+x} \rightarrow M^{-x}$	S_3 ; RCP or LCP
LMDAD		S_2 ; RLP or LLP
		S_1
UMDAD		unpolarised photons

The manifold of different effects and possibilities for variation of the quantities are used successfully in experiments by a lot of groups. Angular integrated or photoabsorbtion techniques like MCXD will not be described here.

For filled shells of free atoms CDAD cannot occur in pure atomic theory, because any filled shell has a spherical charge distribution, even the j-splitted subshells in the case of spin-orbit interaction. On the other hand differences in the spinresolved intensities can be observed. This effect will be discussed as a new class of CDAD the so called Spindependend Circular Dichroism in the Angular Distribution of photoelectrons(SCDAD).

We will start with the photoemission (PE) from free oriented or aligned atoms and finally we show for a very simple case that a surface is dichroic or pleochroic by itself. The latter means, one obtains CDAD in the case of initial states with spherical symmetry if an atom is adsorbed at a solid surface.

We calculate the photoemission cross section from Fermi's golden rule and use the dipole approximation in the relationship as used previously by other authors [1.6],[1.7]. The photoelectron intensity for a transition from a bound initial state $\phi_i = \phi_{n,l,x}$ to a free photoelectron final state $\phi_f = \phi_{E_{kin},\vec{k}}$ excited by a photon with energyhv is given in one electron approximation by:

$$I(\vartheta,\varphi) = \frac{d\sigma}{d\Omega}(E_{kin}) = c_\sigma \left| \left\langle \phi_{E_{kin},\vec{k}} \middle| \vec{A} \cdot \vec{p} - \vec{p} \cdot \vec{A} \middle| \phi_{n,l,x} \right\rangle \right|^2$$

$$I(\vartheta,\varphi) = c_\sigma \left| \left\langle \phi_{E_{kin},\vec{k}} \middle| \vec{\varepsilon} \cdot \vec{r} \middle| \phi_{n,l,x} \right\rangle \right|^2$$

$$c_\sigma = \frac{4\pi \cdot \alpha \cdot a_0^2}{3} \cdot h\nu$$

A and p are the vector potential and the total momentum of the electron, $\vec{\varepsilon} \bullet \vec{r} = \underline{p}$ is the dipole-operator. It is assumed that the vector potential keeps constant so that

$$\vec{p} \bullet \vec{A} = \nabla \bullet \vec{A} = 0$$

vanishes. The unit polarisation vector $\vec{\varepsilon}$ is extended to describe elliptically polarised light, what is discussed below in detail. a_0=0.529166Å is the first Bohr-radius and $\alpha \cong 1/137$ is the fine-structure constant. The polarisation vector does not depend on the integration variables and therefore can be separated from the transition matrix-element:

$$I(\vartheta,\varphi) = c_\sigma \left| \vec{\varepsilon} \bullet \left\langle \phi_f \middle| \vec{r} \middle| \phi_i \right\rangle \right|^2$$

From the equation it is seen that the photoelectron cross section can be described using products from the components of the polarisation vector.

$$I(\vec{\varepsilon}) = \frac{d\sigma}{d\Omega} \propto \left| \vec{\varepsilon} \bullet \vec{\xi} \right|^2 = \left| \varepsilon_x \xi_x + \varepsilon_y \xi_y + \varepsilon_z \xi_z \right|^2$$

where ε_i are the real (x,z) and complex (y) components of the polarisation vector describing elliptically polarised light. $\xi_i(\vartheta,\varphi)$ are complex functions describing the photoelectron wavefunction and therefore the angular distribution of the emitted photoelectrons. The transition matrix-element is separated in a vector whose components are excited by the corresponding parts of the position vector. Each function is „produced" by the corresponding part of the dipole operator or the position vector, respectively: ξ_x by $\varepsilon_x r_x$, ξ_y by $\varepsilon_y r_y$ and ξ_z by $\varepsilon_z r_z$. They depend on the initial and final states and are discussed in more detail in chapter V. Solving and interpreting this equation will be the main part of the present work.

We simplify the expression by taking only the y-component of the polarisation vector as complex and assuming the x- and z- components to be real. The explanation for these assumptions to be correct is given below. In a length representation the matrixelement describing the angular dependent amplitude of the outgoing photoelectron is given by:

$$M_{i,f} = \vec{\varepsilon} \bullet \vec{\xi} = \begin{pmatrix} \varepsilon_x \\ \varepsilon_{yr} + i \cdot \varepsilon_{yi} \\ \varepsilon_z \end{pmatrix} \bullet \begin{pmatrix} \xi_{xr} + i \cdot \xi_{xi} \\ \xi_{yr} + i \cdot \xi_{yi} \\ \xi_{zr} + i \cdot \xi_{zi} \end{pmatrix}$$

(the prefactor c_σ is neglected here) The photoelectron current is proportional to the square absolute of the matrix element that can be build by separation into its real and imaginary part, leading to:

$$\Re(M_{i,f}) = \varepsilon_x \xi_{xr} + \varepsilon_{yr} \xi_{yr} - \varepsilon_{yi} \xi_{yi} + \varepsilon_z \xi_{zr}$$

$$\Im(M_{i,f}) = \varepsilon_x \xi_{xi} + \varepsilon_{yr} \xi_{yi} + \varepsilon_{yi} \xi_{yr} + \varepsilon_z \xi_{zi}$$

$$I \propto \left| \vec{\varepsilon} \bullet \vec{\xi} \right|^2 = \left| M_{i,f} \right|^2 = \Re^2(M_{i,f}) + \Im^2(M_{i,f})$$

It is seen that the sum of two intensities leads to a simplified equation if they are calculated or measured with differing sign of one of the ε_y-components. As shown below, these sums (or better differences) are the dichroic signals called CDAD in the case of switching the imaginary part of ε_y and LDAD in the case of switching the real part. The simplified expressions are given by

a) switching the real part of the ε_y-component from $\varepsilon_{yr}>0$ to $\varepsilon_{yr}<0$:

$$I_{LDAD} = I^{\varepsilon_y} - I^{-\varepsilon_y} \propto 2 \cdot \varepsilon_{yr} \cdot \left\{ 2 \cdot \varepsilon_x \cdot \Re(\xi_x \xi_y^*) + 2 \cdot \varepsilon_z \cdot \Re(\xi_y^* \xi_z) \right\}$$

b) switching the imaginary part of the ε_y-component from $\varepsilon_{yi}>0$ to $\varepsilon_{yi}<0$:

$$I_{CDAD} = I^{i\varepsilon_y} - I^{-i\varepsilon_y} \propto 2 \cdot \varepsilon_{yi} \cdot \left\{ 2 \cdot \varepsilon_x \cdot \Im(\xi_x \xi_y^*) + 2 \cdot \varepsilon_z \cdot \Im(\xi_y^* \xi_z) \right\}$$

If we are able to show that these expressions do not vanish then we have an instrumentation that makes it easier to determine the dynamical parameters in photoemission compared to measurements of the complete differential cross sections for different type of polarised or unpolarised light.

One may think about a further simplification by setting one of the components either ε_x or ε_z to Zero, at this point. Indeed, this is applicable in gas phase physics but unfortunately not generally in surface physics, because it presumes that either light incidence or electron emission is observed in a direction parallel to the surface, as shown and discussed below. The first case (light incidence parallel to the surface for ε_x=0) is not applicable and the second (normal light incidence for ε_z=0) is in gas phase physics only useful for truly oriented states and in spin resolved observations. Below it will be shown that normal light incidence in emission from adsorbates or the bare substrate leads to a new type of CDAD asymmetries.

For completeness we give the intensities for fully linear s(ε_x=0, ε_z=0) or p- (ε_y=0) polarisation, too:

$$I_{s-pol} \propto \left| \varepsilon_y \right|^2 \cdot \left| \xi_y \right|^2$$

$$I_{p-pol} \propto \varepsilon_x^2 |\xi_x|^2 + \varepsilon_z^2 |\xi_z|^2 + 2\varepsilon_x \varepsilon_z \Re(\xi_x \xi_z^*)$$

At first sight these expressions look also simple, but note that we made no assumptions on the degree of polarisation to derive I_{CDAD} or I_{LDAD} whereas we used completely polarised light here. The intensity for unpolarised light can be found for example by adding the intensities for two orthogonal polarisation states (e.g. s- and p- polarised, or RCP and LCP) of the light incoherently:

$$I_0 = \frac{I_s + I_p}{2} \propto \frac{1}{2} \cdot \left(\varepsilon_x^2 |\xi_x|^2 + \left| \varepsilon_y \right|^2 \cdot \left| \xi_y \right|^2 + \varepsilon_z^2 |\xi_z|^2 + 2\varepsilon_x \varepsilon_z \Re(\xi_x \xi_z^*) \right) ,$$

whereas the intensity for any arbitrary elliptical polarisation has to include all four terms.

Multiplying out the components of the polarisation vector $\varepsilon_i \varepsilon_j$ we will find that the cross section for arbitrary elliptically polarised light can be calculated using the components S_i of the Stokes-vector from:

$$I(\vartheta,\varphi) = c_\sigma \left[S_0 G_0 + S_1 G_1 + S_2 G_2 + S_3 G_3 \right]$$

The functions $G_i(\vartheta,\varphi,\vartheta_q)$ depend on the transition matrix element via the ξ-functions and on the angle of photon incidence, as will be discussed in the main part of this work.

In the following we will discuss these equations together with other pleochroic effects. We will do this from the experimentalist's point of view and therefore have to give some remarks on the experimental geometry, firstly.

I.1 References

[1] Born and Wolf; „*Principles of Optics*"

[2] B.Ritchie, Phys.Rev A12 (1975) 567

[3] N.A.Cherepkov, and G.Schönhense; Europhys.Lett 24 (2) (1993) pp.79-85

[4] D.Venus, Phys.Rev. B49 (1994) 8821

[6] J.E.Inglesfield, and B.W.Holland; in „*The Chemical Physics of Solid Surfaces and Heterogeneous Catalysis*"; Ed.: D.A.King and D.P.Woodruf; Elsevier; Amsterdam (1981) pp.183-363

[7] S.M.Goldberg, C.S.Fadley, S.Kono; J.Elec.Spec.Rel.Phen. 21 (1981) pp.285-363

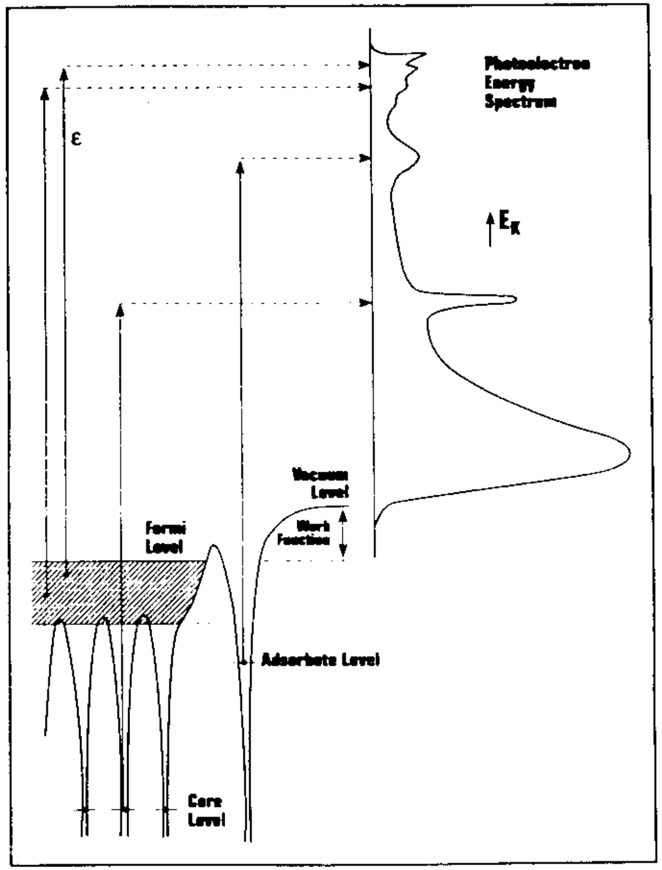

This schematic diagram shows that peaks in the photoelectron spectrum of a metallic solid correspond to the quantum states from which the electrons are emitted. The diagram shows core states in atomic potential energy wells, the portion of the valence band occupied by electrons (i.e. below the Fermi level), and a state in a potential energy well associated with the surface. There is also a large secondary peak due to inelastically scattered electrons. Adapted from [illegible]

Circular Dichroism (CD)
"optical activity"

Pasteur ~1850

CD in the Angular Distribution (CDAD)

Ritchie 1975
Cherepkov 1982
Exp. 1988

Optical Spin Orientation

Fano 1969
Exp. 1970

Spinpol. Photoelectrons from Ferromagnets

Bänninger, Busch, Campagna, Siegmann 1970

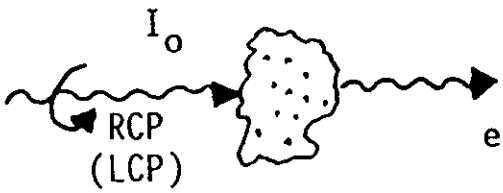

PHOTONS:

$I_{RCP} \neq I_{LCP}$

e dipole – m dipole

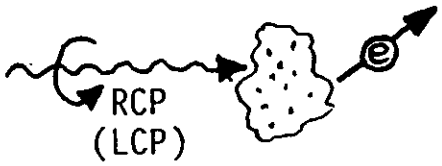

PHOTOELECTRONS:

$I_{RCP} \neq I_{LCP}$

pure e dipole

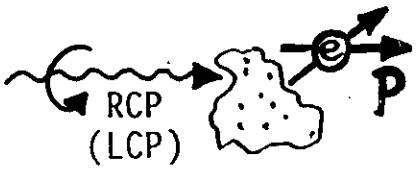

SPIN POLARIZATION optically induced

spin–orbit interaction

SPIN POLARIZATION of initial state

exchange interaction

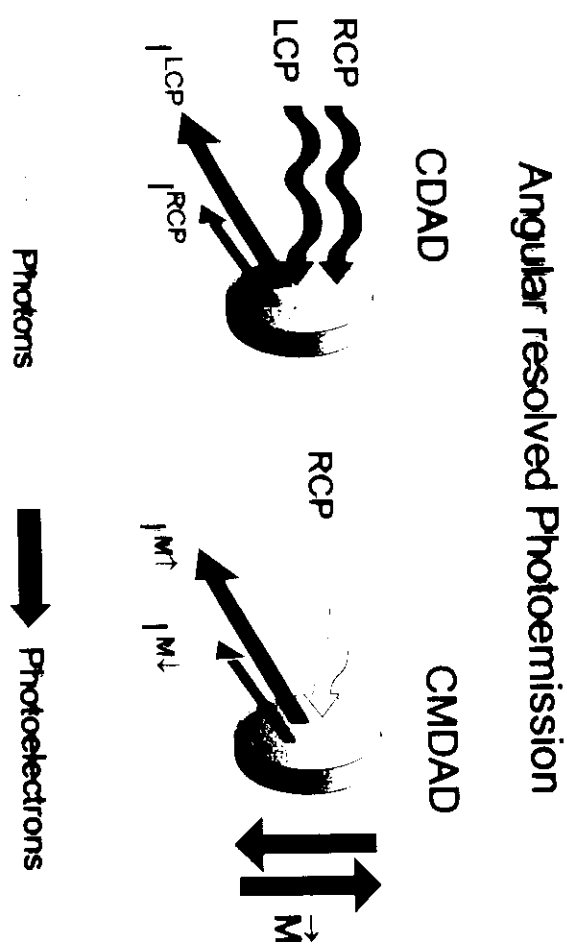

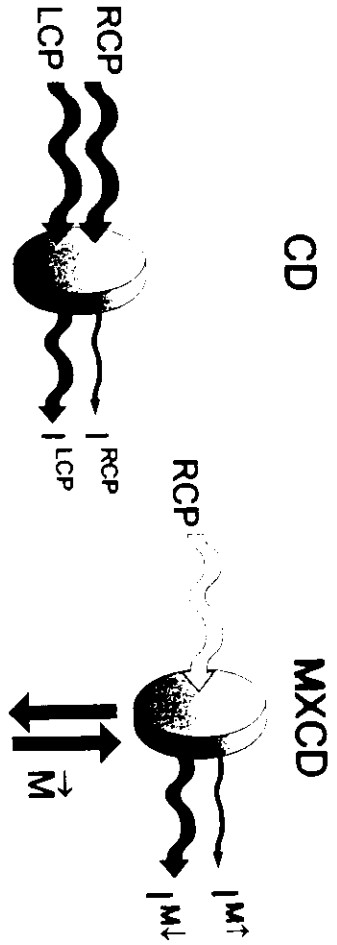

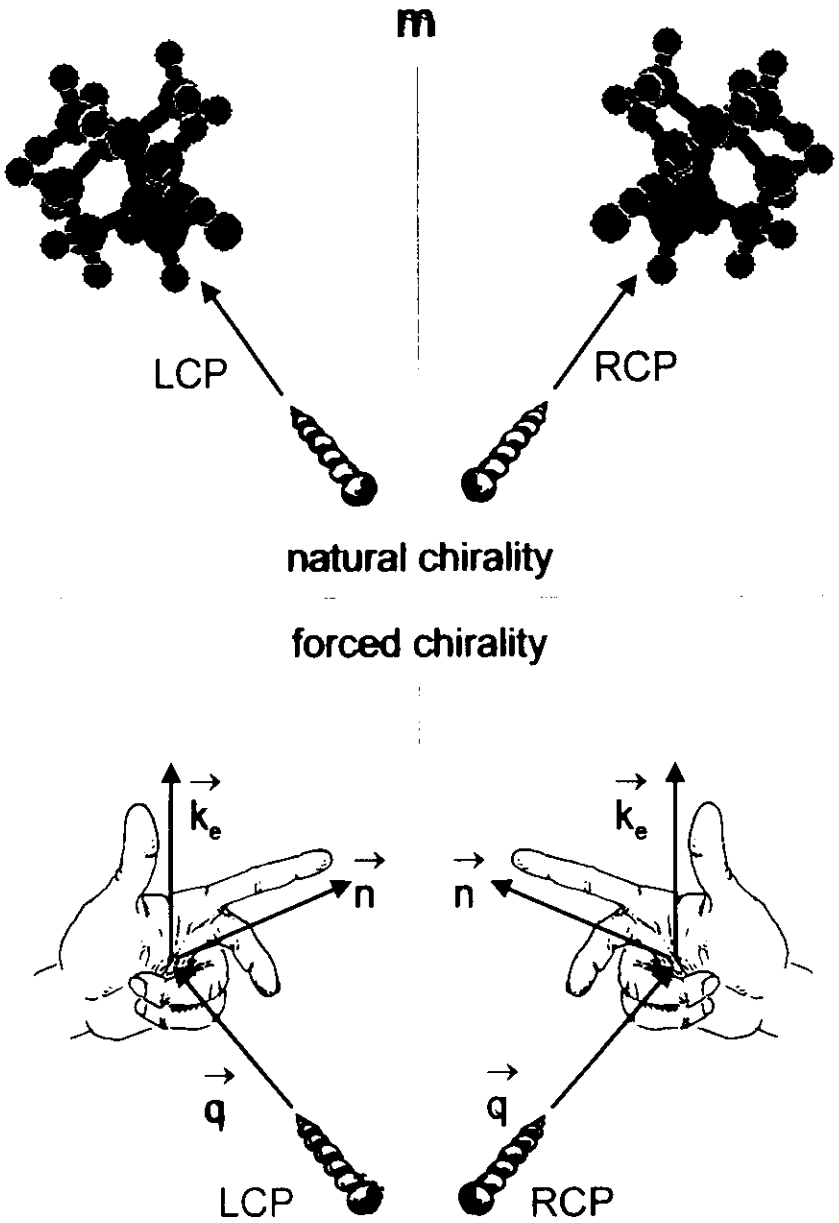

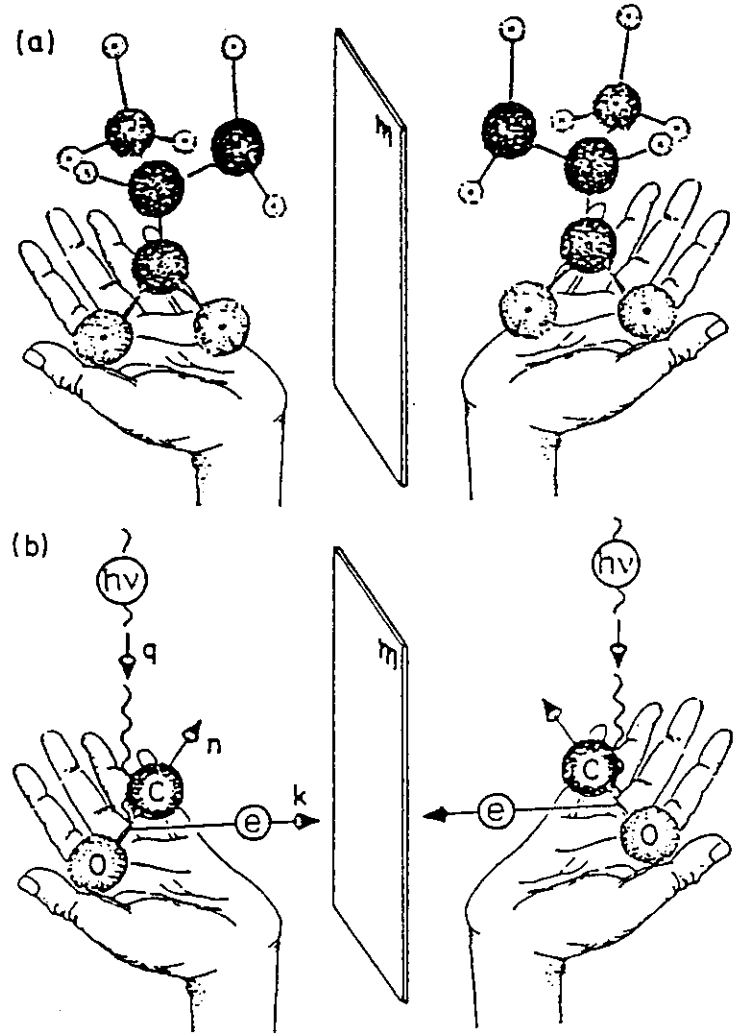

Fig. 1. "Natural" handedness of a chiral molecule (a) and handedne "induced" by a dissymmetric experimental arrangement (b). Photon prop gation direction q, electron momentum k and molecular axis n define handed coordinate system. Both (a) and (b) exhibit a lack of inversic symmetry thus allowing for circular dichroic effects.

Winkelaufgelöste Photoemission:

Symmetrie-Auswahlregeln für lin. pol. Licht

Vol. A57 (1980) ACTA PHYSICA POLONICA No 1

CIRCULAR DICHROISM OF ANGULAR DISTRIBUTIONS OF PHOTOELECTRONS EMITTED FROM HEAVY POLARIZED ALKALI ATOMS*

By R. Parzyński

Institute of Physics, A. Mickiewicz University, Poznań**

(Received October 27, 1978; revised version received February 12, 1979)

The angular distributions of photoelectrons, emitted from the ground state of polarized heavy alkali atoms, are predicted to depend on the helicity of the photon. The effects should occur, in the purely electric dipole approximation, for photon energies from the region of so-called nonzero minimum of the photoionization cross-section. Formulae are proposed for experimental determination of the frequency-dependence of Fano's parameter x.

CDAD appears in purely dipole approximation

ıe 87, number 4 CHEMICAL PHYSICS LETTERS 2 April 198

CIRCULAR DICHROISM OF MOLECULES IN THE CONTINUOUS ABSORPTION REGION

N.A. CHEREPKOV

A.F. Ioffe Physico-Technical Institute, 194021 Leningrad, USSR

Received 7 August 1981; in final form 18 January 1982

The angular distribution of photoelectrons with defined spin polarization ejected from oriented optically active molecules is derived. Circular dichroism in the angular distribution of photoelectrons from unoriented chiral molecules appears already in the electric dipole approximation.

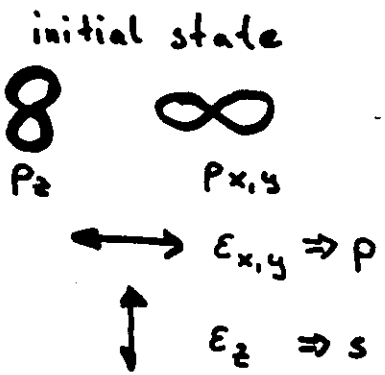

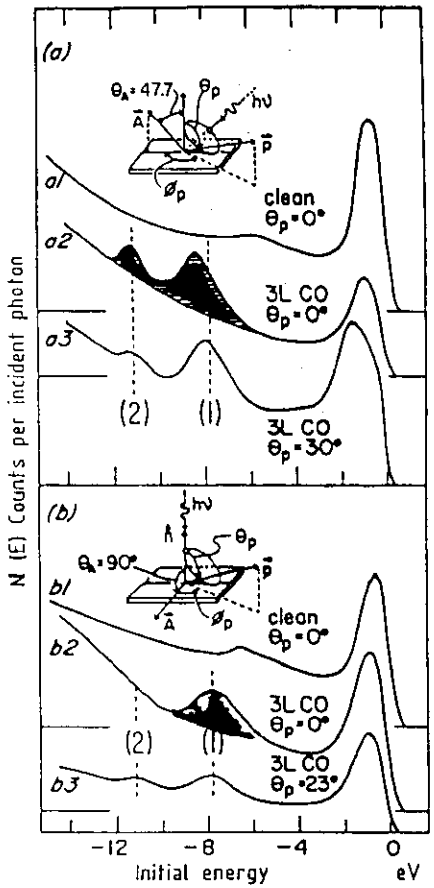

Fig. 4.38. Angle resolved photoelectron spectra of clean Ni(100), curves a1) and b1) and of a Ni(100) surface exposed to 3 L of CO, curves a2) and b2). Photon energy = 28 eV.
a) Nearly p-polarization, normal emission with two upper curves;
b) s-polarization, normal emission with two upper curves.
The insets in each diagram illustrate the experimental configuration. θ_p and ϕ_p denote the polar and azimuthal emission angles; θ_A specifies the angle between A and the surface normal. Note that the 5σ and 1π levels have changed order with respect to the gas phase. From Smith et al. [99]. (EK)

CO/Ni(100)

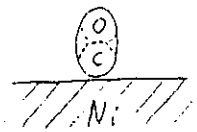

Circular Dichroism in the Angular Distribution of Photoelectrons from Oriented CO Molecules

C. Westphal, J. Bansmann, M. Getzlaff, and G. Schönhense
Fakultät für Physik, Universität Bielefeld, D-4800 Bielefeld, Federal Republic of Germany
(Received 17 March 1989)

Theoretical predictions of a new phenomenon arising in photoelectron emission from oriented molecules by circularly polarized light have been experimentally verified for CO. For a special geometry photoelectron-intensity differences occur upon reversal of photon helicity. The measured asymmetries (up to 80%) show good agreement with an *ab initio* calculation at photon energies between 20 and 40 eV. Theoretically, the new manifestation of circular dichroism is already obtained in the pure electric dipole approximation without inclusion of spin-orbit interaction.

PACS numbers: 33.60.Cv, 33.55.Ad, 33.80.Eh

First experimental verification of CDAD in photoemission from adsorbed molecules

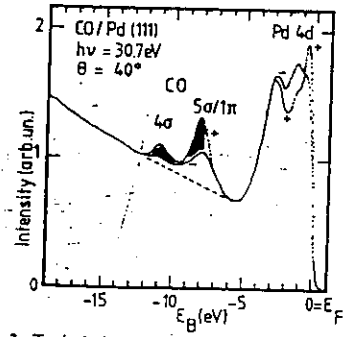

FIG. 2. Typical photoelectron spectra of CO on Pd(111) illustrating CDAD. + and − denote right- and left-handed circularly polarized light, respectively. The binding-energy scale refers to the Fermi energy E_F of the substrate crystal. Dashed lines, see text.

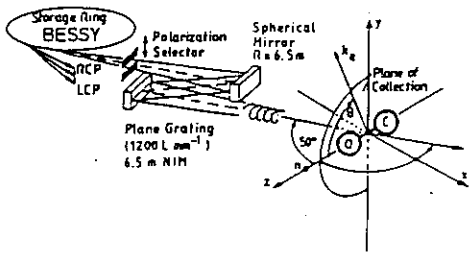

FIG. 1. Schematic drawing of the experimental geometry at the 6.5-m normal-incidence monochromator (NIM) at BESSY. Molecular axis a and incoming light beam span x plane perpendicular to the plane of photoelectron collection, by a and the photoelectron momentum k_e.

Theoretical studies in photoelectron spectroscopy. Molecular optical activity in the region of continuous absorption and its characterization by the angular distribution of photoelectrons

Burke Ritchie
Chemistry Department, University of Alabama, Tuscaloosa, Alabama 35486
(Received 30 December 1974; revised manuscript received 6 March 1975)

The phenomenon of molecular optical activity is examined in the region of continuous absorption. When the "excited" state of the molecule describes an infinite (ionized) system, then the angular distribution of photoelectrons is the sum of coherent contributions corresponding to different magnitudes and interferences of $\hbar\vec{l}$, the angular momentum of the photoelectron. The amplitude for such a process is the sum of terms for each l; thus, since both even and odd values of l can coexist at a single energy in the continuous spectrum, the electric and magnetic dipole matrix elements can *coexist* in this amplitude, making possible the existence of electric-dipole–magnetic-dipole interference in the angular distribution even for a molecule with a center or plane of symmetry. For discrete absorption, in which the intensity is the sum of incoherent contributions corresponding to the intensities for populating the fine-structure levels of a given excited state, the coexistence of the electric and magnetic dipole matrix elements in the amplitude is possible only for a molecule with a site which is asymmetric with respect to inversion or reflection; otherwise both even and odd values of l could not coexist at a single energy in the discrete spectrum. The signs of the electric-dipole–magnetic-dipole interference terms are opposite for left and right circularly polarized light; thus there exists a signal for the angular distribution difference for absorption of left and right circularly polarized light of order α relative to the angular distribution for absorption of light of either polarization. This is just the phenomenon of "circular dichroism" which characterizes molecular "optical activity" in the region of absorption. It exists for the angular distribution of photoelectrons ejected from an *oriented* molecule with a center or plane of symmetry, but vanishes for isotropic systems (atoms) owing to the independence of the radial wave functions from the magnetic quantum number. This ensures the orthogonality of atomic radial wave functions belonging to states of different m and is responsible for the selection rule in atomic spectroscopy that magnetic-dipole transitions are possible only between the fine-structure levels of a given multiplet. Measurement of the angular distribution characteristic for this process would provide a sensitive probe of the parameters of the initial molecular orbital. The existence of even-odd–type interferences of the partial waves of the photoelectron would provide a test of the time-reversal invariance of the wave function for the ionized system, since these interferences depend on the sine rather than the cosine of the phase-shift difference and hence on the normalization of the wave function to satisfy incoming boundary conditions. Calculations are carried out to illustrate these and other points.

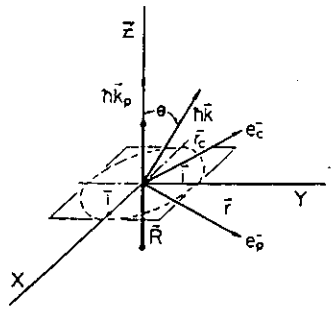

FIG. 1. Coordinate system. $\hbar\vec{k}$ and $\hbar\vec{k}_p$ are the momenta of the ejected electron and incident photon, respectively. $\vec{i}$ and $\vec{j}$ are unit vectors in the direction of the polarization of the light. $\vec{R}$ is the relative position of the nuclei, $\vec{r}$ the position of the photoelectron, and $\vec{r}_c$ the position of the core electron

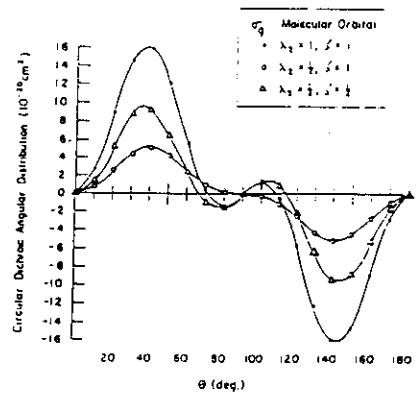

FIG. 2. Circular dichroic angular distribution for a molecular orbital of σ_g symmetry.

CDAD is the difference in the photoemission cross section excited by photons of opposite helicity

$I_{+-} - I_{--} = I_{++} - I_{-+}$

II The co-ordinate systems

To avoid confusion we will give at first a description of the co-ordinates used.

II.1 The quantisationaxis

This work deals with photoemission from surfaces and adsorbates, so the first to do is defining a proper axis of quantisation. In the theory of photoemission from aligned or oriented free atoms and molecules usually the direction of light incidence (for circularly polarised light) or the direction of the electric field vector (for linearly polarised light) is used. This is not always useful in photoemission from atoms or molecules oriented or aligned by adsorption on a surface. Here the surface normal plays the role of a natural quantisation axis and therefore has to be used rigorously. From this definition we have the z-axis of the co-ordinate system always parallel to the surface normal, whereas the x- and y-axes always are within the surface plane. In the most cases, these axes can be defined with respect to low index crystallographic directions.

II.2 The Laboratory Frame

Mainly influenced by the experimental set-up we use the following convention to define the various angles and vectors. However, in some cases a problem arises from the definition of the polarisation by the photon momentum $\vec{q}$ or the electric field vector $\vec{E}$ or $\vec{\varepsilon}$ to describe the CDAD and the LDAD in theoretical works, hopefully this is removed in the description below. For the experiments we need an unambiguous definition of all vectors included in the laboratory system.

The X-Z plane is always the plain build from the photon momentum and the surface normal. In our experiment this X-Z plane is defined by the plane of the BESSY storage ring (or the ESRF) this is also the plane of incidence of the incoming photons. At BESSY the linearly polarised light has the electric field vector $\vec{E}$ fixed in this plane. This is called the $E_\parallel$ component. The Z-axis is parallel to the surface normal $\vec{n}$. The X-Y plane lies in the surface and the X-axis is defined by a low index crystallographic direction. This crystallographic direction is determined, if the sample is once build in the vacuum chamber. Furthermore we are able to rotate the sample around the surface normal to change the crystallographic direction. The usable angular range is approximately $\Gamma_{sample}=\pm45°...\pm90°$, depending on the sample size. The vectors and the corresponding angles we use are defined in the figure (uppercase letters are used to assign the laboratory frame).

II.2.1 Special laboratory co-ordinates

The origin to use this XYZ co-ordinate system is the rotation of the spectrometer we use. We measure Θ with respect to the Z-axis in the XZ-plane and Φ with respect to the XZ-plane.

$\hat{q}$ is used for the unit momentum vector of the photons and it is always parallel to the direction of incidence:

$$\hat{q}=\frac{\vec{q}}{|\vec{q}|}=\begin{Bmatrix}\sin(\Theta_q)\cos(\Phi_q)\\ \sin(\Phi_q)\\ \cos(\Theta_q)\cos(\Phi_q)\end{Bmatrix}\overset{\Phi_q=0}{\equiv}\begin{Bmatrix}\sin(\Theta_q)\\ 0\\ \cos(\Theta_q)\end{Bmatrix}$$

The identity arises from the fact, that we have always $\Phi_q=0$ in our experiments. It is worthwhile to note that it may be more convenient in some cases to use the angles that describe $-\vec{q}$ in the laboratory

frame, namely $\Phi_{q,L}=-\Phi_q$ and $\Theta_{q,L}=\Theta_q-\pi$, what is a definition like in optics where one uses α as angle of incidence with $\Theta_{q,L}=\alpha=\Theta_q-\pi$.

The polarisation vector $\vec{\varepsilon}$ is defined by the electric field vector $\vec{E}$ and describes the polarisation of the light:

$$\vec{\varepsilon}=\frac{\vec{E}}{|\vec{E}|}=\begin{Bmatrix}\varepsilon_\parallel\\ \varepsilon_\perp\end{Bmatrix}=\begin{Bmatrix}\varepsilon_X\\ \varepsilon_{Yr}+i\varepsilon_{Yi}\\ \varepsilon_Z\end{Bmatrix}=\begin{Bmatrix}\cos(\Theta_q) & \cos(\Gamma_q)\\ & \sin(\Gamma_q)\ \exp(i\Delta)\\ -\sin(\Theta_q) & \cos(\Gamma_q)\end{Bmatrix}$$

$\varepsilon_\parallel$ || x,z is the component lying in the plane of the storage ring and $\varepsilon_\perp$ || y is the component perpendicular to it. For a more detailed description see next chapter.

$\vec{k}_e$ is used for the momentum of the emitted electrons:

$$\vec{k}_e=k_0\cdot\begin{Bmatrix}\sin(\Theta_e)\cos(\Phi_e)\\ \sin(\Phi_e)\\ \cos(\Theta_e)\cos(\Phi_e)\end{Bmatrix};\ k_0=\sqrt{2m_eE_{kin}}$$

II.2.2 The standard spherical co-ordinates

In some cases it is more convenient to use the alternative co-ordinates xyz to describe the problem, this is the case if we use spherical harmonics $Y_{\ell m}(\vartheta,\varphi)$ or the molecular frame. We use these co-ordinates in all theoretical calculations. The position vector is then given by:

$$\vec{r}=r\cdot\hat{r}=r\cdot\begin{Bmatrix}\sin(\vartheta)\cos(\varphi)\\ \sin(\vartheta)\sin(\varphi)\\ \cos(\vartheta)\end{Bmatrix}$$

For the unit vectors of the momentum of the electrons and the photons we have:

$$\hat{k}_e=\begin{Bmatrix}\sin(\vartheta_e)\cos(\varphi_e)\\ \sin(\vartheta_e)\sin(\varphi_e)\\ \cos(\vartheta_e)\end{Bmatrix};\ \hat{q}=\begin{Bmatrix}\sin(\vartheta_q)\\ 0\\ \cos(\vartheta_q)\end{Bmatrix},$$

light incidence in thex-z plane is assumed here.

The angles are easily transformed by the following relations, if the co-ordinates xyz coincidence with XYZ:

$$\tan(\vartheta)=\frac{\sqrt{\sin^2(\Phi)+\cos^2(\Phi)\sin^2(\Theta)}}{\cos(\Phi)\cos(\Theta)};\ \tan(\Phi)=\frac{\sin(\vartheta)\sin(\varphi)}{\sqrt{\sin^2(\vartheta)\cos^2(\varphi)+\cos^2(\vartheta)}}$$

$$\tan(\varphi)=\frac{\tan(\Phi)}{\sin(\Theta)};\qquad \tan(\Theta)=\tan(\vartheta)\cos(\varphi)$$

However, there may be more complicated cases. We use the Euler angles $\underline{\omega}=(\alpha,\beta,\gamma)$ and the Wigner rotational matrix if the two systems are rotated with respect to each other. This is the case where the molecules are adsorbed at the surface with a tilt angle between the molecular axis and the surface normal, for instance.

Please note that for arbitrary photon incidence the polarisation vector becomes very puzzling in spherical co-ordinates. In comparison to the laboratory frame we have:

$$\vec{\varepsilon} = \begin{Bmatrix} [\varepsilon_{\parallel} - \varepsilon_{\perp}\sin(\Phi_q)]\cos(\Theta_q) \\ \varepsilon_{\perp}\cos(\Phi_q) \\ -[\varepsilon_{\parallel} + \varepsilon_{\perp}\sin(\Phi_q)]\sin(\Theta_q) \end{Bmatrix}$$

$$= \begin{Bmatrix} \dfrac{\varepsilon_{\parallel} - \varepsilon_{\perp}\sin(\vartheta_q)\sin(\varphi_q)}{\sqrt{\cos^2(\vartheta_q) + \sin^2(\vartheta_q)\cos^2(\varphi_q)}}\cos(\vartheta_q) \\ \varepsilon_{\perp}\sqrt{\cos^2(\vartheta_q) + \sin^2(\vartheta_q)\cos^2(\varphi_q)} \\ -\dfrac{\varepsilon_{\parallel} + \varepsilon_{\perp}\sin(\vartheta_q)\sin(\varphi_q)}{\sqrt{\cos^2(\vartheta_q) + \sin^2(\vartheta_q)\cos^2(\varphi_q)}}\sin(\vartheta_q)\cos(\varphi_q) \end{Bmatrix}$$

Special cases of some other laboratory co-ordinate systems used to simplify the calculations will be given in context with the discussion of magnetic effects.

Orbital Frame
(Standard Spherical Co-Ordinates)

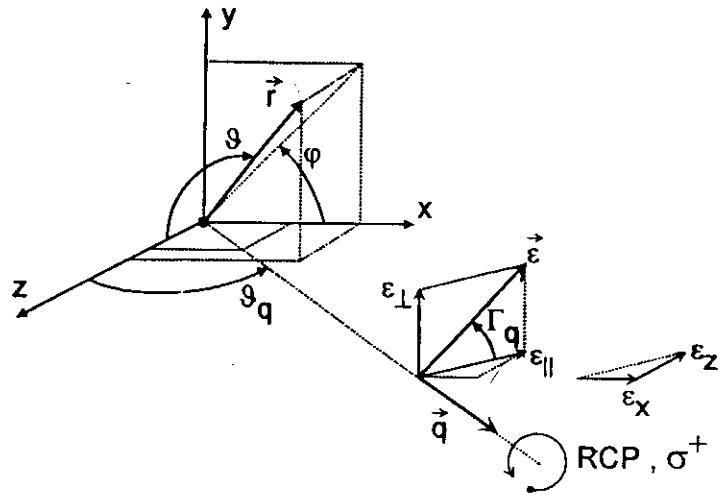

Laboratory Frame

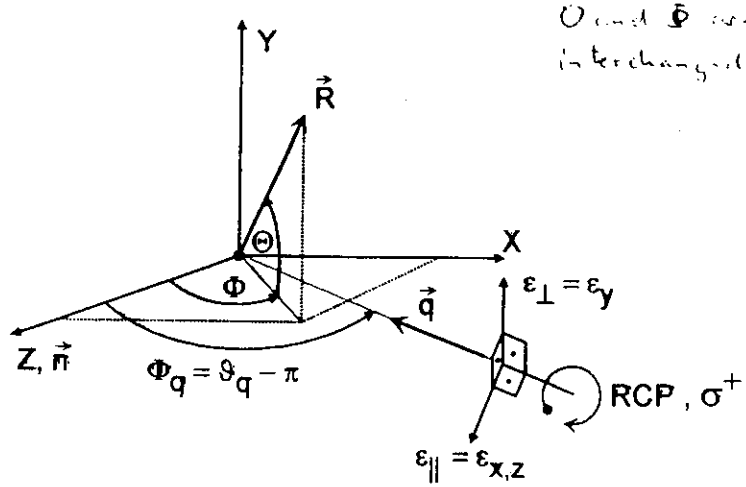

6.5m-NIM

BESSY
Berlin

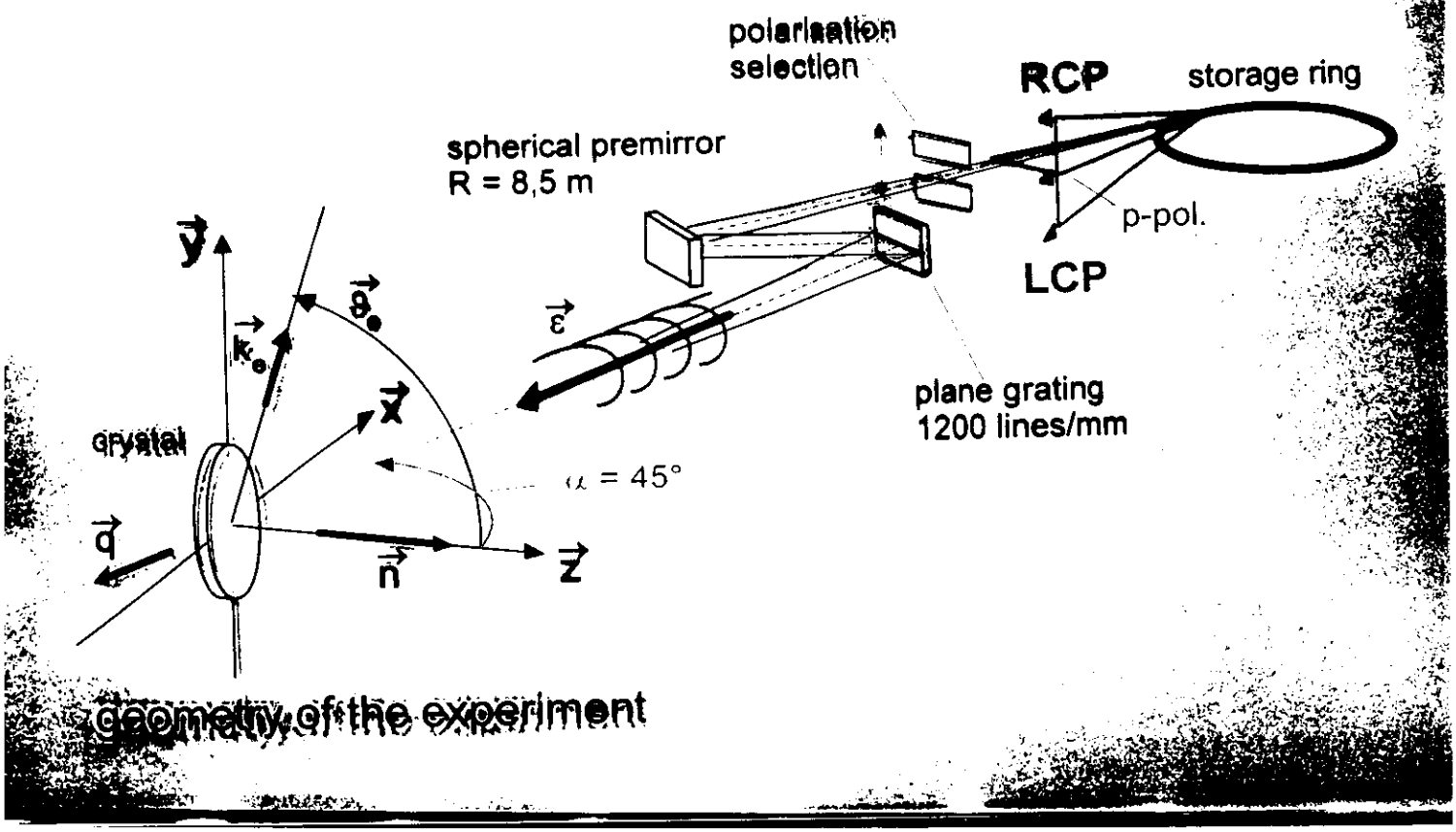

geometry of the experiment

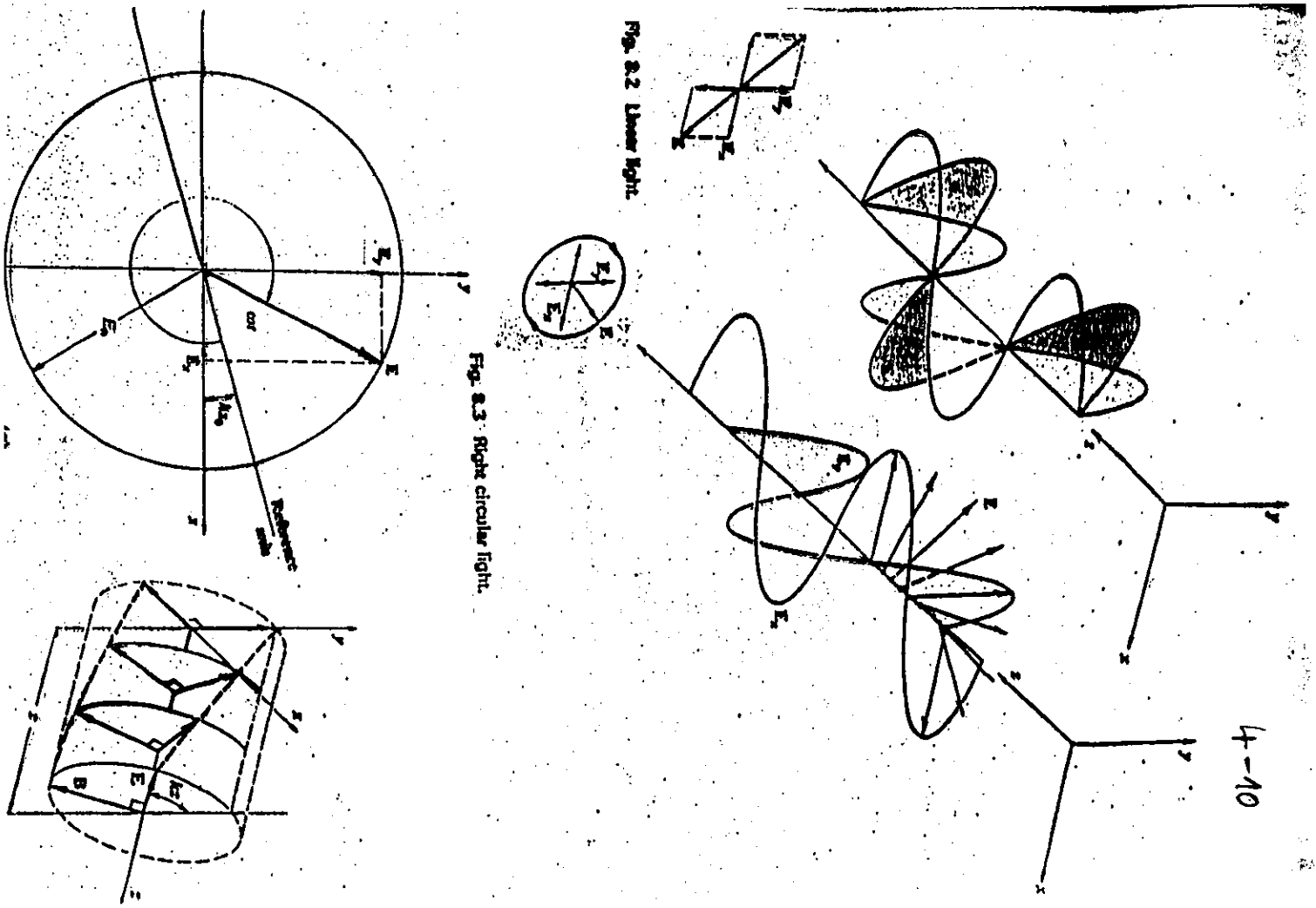

Fig. 8.2 Linear light.

Fig. 8.3 Right circular light.

4-10

III The polarisation of the photons

In this chapter we will give a description of the polarisation of the photons playing the most important role throughout this work. Most of the properties of the photons can be found in standard textbooks on optics [3.1],[3.2], therefore we concentrate more on the things necessary to describe the photoemission process. We start with a more general description of the polarisation, namely elliptical polarisation. The next step will be to examine the influence of the photon polarisation on the properties of the pleochroism. In the remaining part we will discuss the influence of a mixed or incomplete polarisation. Such effects can arise if the polarisation is changed by some optical components of the experimental set-up. But, more important is, that the sample itself is able to change the properties of the photon field, at least in the VUV range of impact energies.

III.1 Description of elliptically polarised light

We will start this chapter giving the apparatus to describe the polarisation of the photons. As we have seen before, we need the x-, y-, and z-component of the electric field or polarisation vector to describe the photoemission process. On the other hand in most textbooks only two components of the electric field are given and we have to find a way to get what we need. Usually the electric field vector $\vec{E}$ is separated into two orthogonal components, that are always in a plane perpendicular to the photon momentum $\vec{q}$. They are called the parallel p-component and the perpendicular s-component (s from German senkrecht). The p-component is defined as the one lying in the plane of incidence, but this makes the definition of a co-ordinate system necessary. We will use a slightly different definition that follows from the experimental set-up in use. The radiation emitted from (the bending magnets at) an electron storage ring is in the plane of the ring is polarised linearly with the electric field vector lying in this plane. Therefor, it is most useful to define in close connection to our experiments the parallel component to be lying in the plane of the electron storage ring 1. (Note: finally the pleochroism will not depend on this definition. It is just given because its most illustrative.)

Using this definition the field vector separated into its components is given by:

$$\vec{E} = \begin{Bmatrix} E_\parallel \\ E_\perp \end{Bmatrix} = E \cdot \vec{\varepsilon} = E \cdot \begin{Bmatrix} \cos(\Gamma_q) \\ \sin(\Gamma_q)\exp(i\Delta_q) \end{Bmatrix}$$

$\vec{\varepsilon}$ is the polarisation vector and Δ_q is the phaseshift between the components that is needed to describe elliptically polarised light, what is particularly the case if $\Delta_q \neq 0$. The angle Γ_q gives the relation between the electric field vector components $E_\perp$ and $E_\parallel$ via $\tan(\Gamma_q)=|E_\perp|/|E_\parallel|$, but says nothing about their orientation in space. For later use, we define the direction of $E_\parallel$ being parallel to the positive x'-axis and of $E_\perp$ being parallel to the y'-axis, if the direction of photon propagation is along the z'-axis (see chapter II). This ensures that we work only with right-handed co-ordinate systems. We find two special cases of polarisation depending on the parameters Γ_q and Δ_q. These special cases are $\Delta_q=0$ for linearly polarised light and $\Delta_q=\pm\pi/2$ with equal values of the E-components for circularly polarised light.

We define the case with $\Gamma_q=\pi/4$, $\Delta_q=+\pi/2$ ($\Delta m=+1$, σ^+) as **right circularly** (*RCP*) and that with $\Gamma_q=\pi/4$; $\Delta_q=-\pi/2$ ($\Delta m=-1$, σ^-) as **left circularly** (*LCP*) polarised light [3.3].

(Please note: a) LCP can be represented by $\Gamma_q=3\pi/4$ or $\Gamma_q=-\pi/4$; $\Delta_q=+\pi/2$; b) the terms RCP and LCP depend on the direction of observation [3.4].)

1 A detail of the co-ordinates was shown in chapter 2. We will keep that definition for the cases where we work at insertion devices or with a laboratory source (gas discharge lamp, etc.) . In the later case we use the same port to apply the source.

A easy we to describe the polarisation is the density formalism [3.5]. The intensity of the photon beam is given by: $I \sim E_\perp E_\perp^* + E_\parallel E_\parallel^*$ and the density matrix describing the photon polarisation can be calculated from:

$$\rho_1 = \frac{1}{\langle E_\perp E_\perp^* \rangle + \langle E_\parallel E_\parallel^* \rangle} \begin{bmatrix} \langle E_\perp E_\perp^* \rangle & \langle E_\perp E_\parallel^* \rangle \\ \langle E_\parallel E_\perp^* \rangle & \langle E_\parallel E_\parallel^* \rangle \end{bmatrix}$$

The expectation values "<>" (that are time averaged) describe the degrees of polarisation. By use of the complex E-vector components we can calculate the different degrees of polarisation for circularly and linearly polarised light. In the case of circularly polarised light we have:

$$P_{circ} = \frac{\langle |E_\parallel - iE_\perp|^2 \rangle - \langle |E_\parallel + iE_\perp|^2 \rangle}{\langle |E_\parallel - iE_\perp|^2 \rangle + \langle |E_\parallel + iE_\perp|^2 \rangle} = \frac{-2 \cdot \Im m(E_\parallel E_\perp^*)}{E_\parallel E_\parallel^* + E_\perp E_\perp^*}$$

From the definition given above we see that RCP is described by $P_{circ}=+1$ and LCP by $P_{circ}=-1$.

The case of linearly polarised light is some more complicated because we can define two different degrees of polarisation by:

$$P_\parallel = \frac{\langle |E_\parallel|^2 \rangle - \langle |E_\perp|^2 \rangle}{\langle |E_\parallel|^2 \rangle + \langle |E_\perp|^2 \rangle} = \frac{E_\parallel E_\parallel^* - E_\perp E_\perp^*}{E_\parallel E_\parallel^* + E_\perp E_\perp^*} = \frac{2 \cdot E_\parallel E_\parallel^*}{E_\parallel E_\parallel^* + E_\perp E_\perp^*} - 1$$

and

$$P_{45} = \frac{\langle |E_\parallel + E_\perp|^2 \rangle - \langle |E_\parallel - E_\perp|^2 \rangle}{\langle |E_\parallel + E_\perp|^2 \rangle + \langle |E_\parallel - E_\perp|^2 \rangle} = \frac{2 \cdot \Re e(E_\parallel E_\perp^*)}{E_\parallel E_\parallel^* + E_\perp E_\perp^*}$$

The first polarisation term describes p-polarisation ($P_P=+1$) and s-polarisation ($P_P=-1$). In the case of a complete linear polarisation parallel to the plane of incidence we have $P_P=+1$ this will be named **PP** light. For light polarised perpendicular to the plane of incidence we have $P_P=-1$ or $P_\perp=-P_P=+1$ what will be called **SP** light.

The case of circularly polarised light can be understood as a coherent superposition of the s- and p-component being equal in magnitude and having a phase shift of $\pm\pi/2$ between them.

The second term P_{45} looks very similar to P_{circ}, therefore we define in close analogy right linearly polarised light (**RLP**) by $P_{45}=+1$ and left linearly polarised light (**LLP**) by $P_{45}=-1$. This case of polarisation can be understood as a coherent superposition of the s- and p-component being equal in magnitude without any phase shift. Below we will show that such kind of terms describe the LDAD in close analogy to the CDAD.

The total linear polarisation is given by:

$$P_{lin}^2 = P_\parallel^2 + P_{45}^2$$

By use of the degrees of polarisation we can rewrite the density matrix to be given by:

$$\rho_1 = \begin{bmatrix} 1 - \frac{1}{2}P_\parallel & \frac{1}{2}(P_{45} - iP_{circ}) \\ \frac{1}{2}(P_{45} + iP_{circ}) & 1 + \frac{1}{2}P_\parallel \end{bmatrix}$$

The index 1 indicates that we have totally polarised light and no part of unpolarised light.

We have seen, however, that we need in its general form only two components to describe the polarisation, because $\vec{E}$ has no component parallel to $\vec{q}$. To calculate the differential cross sections we need the polarisation vector in the XYZ or xyz co-ordinates and we have to use 3-component vectors. First, we assume an arbitrary direction of incidence and describe the photon momentum by:

$$\frac{\vec{q}}{|\vec{q}|} = \begin{Bmatrix} \sin(\vartheta_q)\cos(\varphi_q) \\ \sin(\vartheta_q)\sin(\varphi_q) \\ \cos(\vartheta_q) \end{Bmatrix}$$

and the complex polarisation vector by:

$$\vec{\varepsilon} = \begin{Bmatrix} \varepsilon_X + i\varepsilon'_X \\ \varepsilon_Y + i\varepsilon'_Y \\ \varepsilon_Z + i\varepsilon'_Z \end{Bmatrix} = \begin{Bmatrix} \left[\varepsilon_\parallel - \varepsilon_\perp \sin(\Phi_q)\right]\cos(\Theta_q) \\ \varepsilon_\perp \cos(\Phi_q) \\ -\left[\varepsilon_\parallel + \varepsilon_\perp \sin(\Phi_q)\right]\sin(\Theta_q) \end{Bmatrix}$$

where we made the choice that ε_y has always only a $\varepsilon_\perp$-component. For easier use we used here the laboratory co-ordinates for the polarisation vector, the transformation to spherical co-ordinates was given in the previous chapter II. Experiments are done easiest if the plane of light incidence coincides with the parallel component of the photon polarisation. This is fulfilled in our experiments where the plane of light incidence is defined by the plane of the electron storage ring with the sample surface fixed in a perpendicular plane and therefore we have in spherical co-ordinates with φ_q=0:

$$\vec{\varepsilon} = \begin{Bmatrix} \varepsilon_X \\ \varepsilon_{Yr} + i\varepsilon_{Yi} \\ \varepsilon_Z \end{Bmatrix} = \begin{Bmatrix} \cos(\vartheta_q) & \cos(\Gamma_q) \\ & \sin(\Gamma_q)\ \exp(i\Delta_q) \\ -\sin(\vartheta_q) & \cos(\Gamma_q) \end{Bmatrix}$$

and the degrees of polarisation are given by:

$$\begin{aligned} P_{circ} &= 2\sin(\Gamma_q)\cos(\Gamma_q)\sin(\Delta_q) &&= \sin(2\Gamma_q)\sin(\Delta_q) \\ P_\parallel &= 1 - 2\sin^2(\Gamma_q) = 2\cos^2(\Gamma_q) - 1 &&= \cos(2\Gamma_q) \\ P_{45} &= 2\sin(\Gamma_q)\cos(\Gamma_q)\cos(\Delta_q) &&= \sin(2\Gamma_q)\cos(\Delta_q) \\ P_{lin} &= &&= \sqrt{\cos^2(2\Gamma_q) + \sin^2(2\Gamma_q)\cos^2(\Delta_q)} \end{aligned}$$

As shown above, the three polarisation components are described by only two angles, namely Γ_q and Δ_q, meaning that only two of the polarisation components can be changed independently at once:

$$\tan(\Delta_q) = \frac{P_{circ}}{P_{45}}$$

and

$$\tan(2\Gamma_q) = \sqrt{\frac{P_{circ}^2 + P_{45}^2}{P_\parallel^2}} = \sqrt{\frac{P_{circ}^2 + P_{45}^2}{1 - [P_{circ}^2 + P_{45}^2]}}$$

Finally we like to express the polarisation vector in terms of the polarisation. Applying the relations given above we calculate the polarisation vector using the degree of polarisation to be given by:

$$\vec{\varepsilon}(P) = \sqrt{\frac{1}{2}} \begin{Bmatrix} \cos(\vartheta_q)\sqrt{1+P_\parallel} \\ \frac{P_{45}}{\sqrt{1+P_\parallel}} + i\frac{P_{circ}}{\sqrt{1+P_\parallel}} \\ -\sin(\vartheta_q)\sqrt{1+P_\parallel} \end{Bmatrix} \begin{matrix} P_\parallel = -1 \\ P_\perp = +1 \\ \Rightarrow \end{matrix} \begin{Bmatrix} 0 \\ 1 \\ 0 \end{Bmatrix}$$

For completeness, the latter relation is only needed to avoid a division by Zero and to give $\varepsilon(P_\perp)$ correctly but not to describe the differential cross section.

As shown in the introduction (see Chapter I and also below), we need products calculated from the different components of the polarisation vector to calculate the cross sections. These are calculated to be:

$$\begin{aligned} \varepsilon_X^2 &\quad \tfrac{1}{2}(1+P_\parallel)\cos^2(\vartheta_q) \\ \varepsilon_{Yr}^2 + \varepsilon_{Yi}^2 &\quad \tfrac{1}{2}(1-P_\parallel) = \frac{P_{45}^2 + P_{circ}^2}{2(1+P_\parallel)} \\ \varepsilon_Z^2 &\quad \tfrac{1}{2}(1+P_\parallel)\sin^2(\vartheta_q) \\ 2\varepsilon_X\varepsilon_{Yr} &\quad P_{45}\cos(\vartheta_q) \\ 2\varepsilon_X\varepsilon_{Yi} &\quad P_{circ}\cos(\vartheta_q) \\ 2\varepsilon_X\varepsilon_Z &\quad -\tfrac{1}{2}(1+P_\parallel)\sin(2\vartheta_q) \\ 2\varepsilon_{Yr}\varepsilon_Z &\quad -P_{45}\sin(\vartheta_q) \\ 2\varepsilon_{Yi}\varepsilon_Z &\quad -P_{circ}\sin(\vartheta_q) \end{aligned}$$

Notes: a) For $P_{lin}=1$ we have no ε_{Yi} terms, meaning that the polarisation vector is reel. Do not confuse P_{lin} and $P_{\perp L}$. b) At 100% polarisation the CDAD is calculated from terms with $P_{circ}=\pm1$, the LDAD from $P_{45°}=\pm1$, and the spDAD from $P_\parallel=\pm1$. c) Do not use these equations for totally unpolarised light with P_i=0, because one has no well defined direction of the electric field but an average on statistically distributed directions.

In PE-experiments at surface it may not be convenient to use an angle of light incidence parallel to the surface ($\vartheta_q=\pm\pi/2$) due to the vanishing intensity and spread of the light spot. At normal incidence the photon beam may be shut by the electron analyser in a certain range of angles making impossible to determine a complete angular distribution of the ejected photoelectrons. A good compromise may be therefore to set $\vartheta_q=\pm\pi/4$ making use of the symmetry properties of Sine and Cosine.

Until now we made no assumption on the total degree of polarisation that may be effected by unpolarised light. The total polarisation is given by the sum of the squares of the three different degrees of polarisation:

$$P = \sqrt{P_\parallel^2 + P_{45}^2 + P_{circ}^2} = \sqrt{P_{lin}^2 + P_{circ}^2}$$

By use of the polarisation vector given above we have $P=1$.

A partially polarised state (with $|P|<1$) can be obtained by a superposition of a totally polarised and a totally unpolarised part using the density matrix formalism:

$$\rho_P = (1-P)\cdot\rho_0 + P\cdot\rho_1 = \frac{1-P}{2}\begin{pmatrix}1&0\\0&1\end{pmatrix} + \frac{P}{2}\begin{pmatrix}\rho_{11}&\rho_{12}\\\rho_{21}&\rho_{22}\end{pmatrix}$$

To include effects arising from partially unpolarised light another kind of the description of the photon properties is very useful. The polarisation can be described by a 4-component Stokes-vector [3.6] that is given by:

$$\underline{S} = \begin{Bmatrix} S_0 = I \\ S_1 = \Delta I_{\parallel} \\ S_2 = \Delta I_{45} \\ S_3 = \Delta I_{circ} \end{Bmatrix} \overset{P=1}{\rightarrow} \begin{Bmatrix} \rho_{11}+\rho_{22} \\ -(\rho_{11}-\rho_{22}) \\ \rho_{12}+\rho_{21} \\ i(\rho_{12}-\rho_{21}) \end{Bmatrix} \rightarrow \begin{Bmatrix} 1 \\ \cos^2(\Gamma_q)-\sin^2(\Gamma_q) \\ 2\sin(\Gamma_q)\cos(\Gamma_q)\cos(\Delta_q) \\ 2\sin(\Gamma_q)\cos(\Gamma_q)\sin(\Delta_q) \end{Bmatrix}$$

The two relations at the right using I=1 are only true for totally polarised light. To describe partially polarised and unpolarised light, we have to drop the assumption I=1, that means the Stokes-vector has to be used in its general form, this case is automatically included in the first form of the definition for the Stokes-vector in the equation above. In this case we define the different degrees of polarisation by:

$$p_{\parallel}=S_1/S_0, \qquad p_{45}=S_2/S_0, \qquad \text{and } p_{circ}=S_3/S_0$$

We use the lower case p to assign that the total degree of polarisation is not longer unity.

In the following we will apply the equations derived here to describe the pleochroism depending on the photon properties.

III.2 Photon polarisation and the pleochroic effects

We describe now the pleochroism without any knowledge on the particular kind of the photoemission matrix element. That is we like to determine the properties of the photoemission process that depend on the photon polarisation. Properties that depend on the electron momentum will be discussed later. We assume that the Ξ, or ξ-functions exist and depend only on the electron momentum but not on the properties of the photons. The later was already shown in the introduction. It is easily seen that the equation we presented at the beginning can be rewritten to be:

$$\frac{I(\vec{\varepsilon})}{c_\sigma} = \left|\vec{\varepsilon}(\vartheta_q,\varphi_q)\bullet\vec{\xi}(\vartheta,\varphi)\right|^2$$
$$= (1+P_{\parallel})G_{\parallel} + (1-P_{\parallel})G_{\perp} + P_{45}G_{45} + P_{circ}G_{circ} = \frac{I(P)}{c_\sigma}$$

$$c_\sigma = \frac{4\pi a_0 a_0^2}{3}h\nu\,.$$

where the functions $G_p=G_p(\vartheta,\varphi,\vartheta_q,\varphi_q)$ depend now on the electron and the photon momentum. The first two can be interpreted as differential cross sections for 100% s- or p-polarised light. The functions G_i can be calculated from the ξ-functions by determining the first line of the equation. The different products of the polarisation vector have already been given in the previous chapter. Assuming a

complete polarisation (P=1) and inserting the products from the previous chapter we find the G-functions to be given by:

$$G_{\parallel} = \tfrac{1}{2}\cos^2(\vartheta_q)\cdot|\xi_x|^2 + \tfrac{1}{2}\sin^2(\vartheta_q)\cdot|\xi_z|^2 - \sin(2\vartheta_q)\cdot\Re(\xi_x\xi_z^*)$$
$$G_{\perp} = \tfrac{1}{2}|\xi_y|^2$$

$$G_2 = G_{45} = 2\cdot\left\{\cos(\vartheta_q)\cdot\Re(\xi_x\xi_y^*) - \sin(\vartheta_q)\cdot\Re(\xi_y^*\xi_z)\right\}$$
$$G_3 = G_{circ} = 2\cdot\left\{\cos(\vartheta_q)\cdot\Im(\xi_x\xi_y^*) - \sin(\vartheta_q)\cdot\Im(\xi_y^*\xi_z)\right\}$$

The first two functions are rather non symmetric therefore we combine them in a different way:

$$G_0 = G_{\parallel} + G_{\perp} = \tfrac{1}{2}\left\{\cos^2(\vartheta_q)\cdot|\xi_x|^2 + |\xi_y|^2 + \sin^2(\vartheta_q)\cdot|\xi_z|^2\right\} - \sin(2\vartheta_q)\cdot\Re(\xi_x\xi_z^*)$$

$$G_1 = G_{\parallel} - G_{\perp} = \tfrac{1}{2}\left\{\cos^2(\vartheta_q)\cdot|\xi_x|^2 - |\xi_y|^2 + \sin^2(\vartheta_q)\cdot|\xi_z|^2\right\} - \sin(2\vartheta_q)\cdot\Re(\xi_x\xi_z^*)$$

These two functions can be interpreted easily. The photoemission cross section for unpolarised light is equivalent to an incoherent superposition of the cross sections for polarised light with $P_{circ}=\pm1$, $P_{\parallel}=\pm1$, or $P_{45}=\pm1$, as seen from the equations above. In the case of 100% polarisation (and only in this case) the photoelectron intensity for unpolarised light can be determined from the measurements with polarised light:

$$2\cdot I_0 = \begin{cases} (I^{RCP}+I^{LCP}) \\ \text{or } (I^{RLP}+I^{LLP}) \\ \text{or } (I^{PP}+I^{SP}) \end{cases} \propto 2\cdot(G_{\parallel}+G_{\perp})$$

Using $G_0=G_{\parallel}+G_{\perp}$, $G_1=G_{\parallel}-G_{\perp}$, $G_2=G_{45}$, and $G_3=G_c$ we find the final form of the equation describing the photoelectron intensity depending on the degree of polarisation. In direct relation to the Stokes-vector we have:

$$I(P) = c_\sigma\cdot S_0\cdot[G_0 + P_{\parallel}G_1 + P_{45}G_2 + P_cG_3]$$
$$= c_\sigma\cdot[S_0G_0 + S_1G_1 + S_2G_2 + S_3G_3]$$

To describe partially polarised and unpolarised light, we have to drop the assumption I=1, that means the Stokes-vector has to be used in its general form, this case is automatically included in the complete form of the equation above. According to the density matrix formalism, the cross sections in the photoemission can be calculated by an incoherent superposition of a totally polarised and a totally unpolarised part:

$$\frac{d\sigma}{d\Omega}_P = (1-P)\cdot\frac{d\sigma}{d\Omega}_{0\%} + P\cdot\frac{d\sigma}{d\Omega}_{100\%}$$

Products of the overall polarisation P with the components of elliptical polarisation P_{ell} are obtained by the incoherent superposition of the cross sections, if P does not equal 1. Therefore, we define the degrees of polarisation by $p_{abc}=P*P_{abc}$ and calculate the products needed by replacing the capital P's by lower case letters in the equations given above.

$$I(p) = (1-P)\cdot I_0 + P\cdot I(P) \propto G_0 + p_{\parallel}G_1 + p_{45}G_2 + p_cG_3$$

The intensity is proportional to $c_\sigma S_0$. In this equation we have divided the photocurrent in an part arising from unpolarised light (G_0) and a part arising from polarised light, if one of the Stokes-components S_i, $i\neq 0$ is present.

Now, having a general equation of the photoemission cross-section depending on the polarisation of the photons, we are able to determine easily the pleochroism.

We are now able to give a very simple definition of thpleochroism in photoemission (PIPE):

The Pleochroism in photoemission is the difference in the photoelectron intensities that is obtained by switching the sign of one polarisation component:

$$I_{PIPE} = I^{+} - I^{-}$$

The three cases singled out are given by:

$$\begin{aligned} I_{s-pDAD} &= I^{PP} - I^{SP} &&= 2\cdot|p_{\parallel}|\cdot(G_{\parallel} - G_{\perp}) \\ I_{LDAD} &= I^{RLP} - I^{LLP} &&= 2\cdot|p_{45}|\cdot G_{45} \\ I_{CDAD} &= I^{RCP} - I^{LCP} &&= 2\cdot|p_{circ}|\cdot G_{circ} \end{aligned}$$

In some cases it is more useful to give not the differences themselves, but some normalised quantities. The asymmetries, that are the normalised pleochroic differences in the case of 100% polarisation, are given by:

$$\begin{aligned} A_{s-pDAD} &= \frac{I^{PP} - I^{SP}}{2I_0} = \frac{G_{\parallel} - G_{\perp}}{G_{\parallel} + G_{\perp}} = \frac{G_1}{G_0} \\ A_{LDAD} &= \frac{I^{RLP} - I^{LLP}}{2I_0} = \frac{G_{45}}{G_{\parallel} + G_{\perp}} = \frac{G_2}{G_0} \\ A_{CDAD} &= \frac{I^{RCP} - I^{LCP}}{2I_0} = \frac{G_{circ}}{G_{\parallel} + G_{\perp}} = \frac{G_3}{G_0} \end{aligned}$$

. In more general, we define the PIPE-asymmetry by:

$$A_{PIPE} = \frac{I^{+} - I^{-}}{I^{+} + I^{-}}$$

At the first sight it seems that the normalisation by $I^{+}+I^{-}$ may not be useful if $|P_j|\neq 100\%$ leading to $I^{+}+I^{-}\neq 2I_0$. Nevertheless, we will show below that this normalisation has some advantages. In some cases it may be more convenient to normalised$_{PIPE}$ by the normal emission intensityI(ϑ=0).

An important case is the simultaneous occurrence of CDAD and LDAD, as will be shown later. By switching the sign (notchanging the absolute value !) of both components p_{45} and p_c at once we have:

$$A_{PIPE} = \frac{|p_c|G_3 \pm |p_{45}|G_2}{G_0 + p_{\parallel}G_1}$$

that becomes more simple if $p_{\parallel}$ vanishes. The double sign arises not from the switching of polarisation but from the initial orientation of p_{45} that can either be positive or negative. A similar expression can be found for the linear case.

We have now a complete formalism to describe the pleochroism in terms of the photon properties. Nevertheless, we have to show that the G-functions do not vanish. As the experience tells us that the

photoelectron intensities are in general different if we use different kinds of polarisation or unpolarised light we can be sure that our work was not done for nothing.

From the properties of the G-functions we can derive some properties of the pleochroism. An interesting question is what conditions are necessary that the pleochroism vanishes depending on the photon incidence. We will use the CDAD as an example, the case of LDAD can be derived straight forward, simply by inserting the real parts instead of the imaginary parts occurring in the following equations.

The CDAD is described by:

$$G_3 = G_{circ} \propto \cos(\vartheta_q)\cdot\Im(\xi_x\xi_y^*) - \sin(\vartheta_q)\cdot\Im(\xi_y^*\xi_z)$$

It is easily seen that it vanishes for the condition:

$$I_{CDAD} = 0 \Leftrightarrow \cos(\vartheta_q)\Im(\xi_x\xi_y^*) = \sin(\vartheta_q)\Im(\xi_y^*\xi_z) \Leftrightarrow \tan(\vartheta_q^0) = \frac{\Im(\xi_x\xi_y^*)}{\Im(\xi_y^*\xi_z)}$$

assuming that at least one of the functions $\Im(\xi_x\xi_y^*)\neq 0$ or $\Im(\xi_y^*\xi_z)\neq 0$ does not vanish. Additionally we find Zeros in the CDAD if ϑ_q=0,π or $|\vartheta_q|=\pi/2$ just if the first or second imaginary part vanishes. That leads to the conclusion that $\Im(\xi_x\xi_y^*)$ describes the normal incidence ($\vartheta_q=\pi$) and $\Im(\xi_y^*\xi_z)$ the gracing incidence($|\vartheta_q|=\pi/2$) properties of the CDAD.

IV The Influence of mixed or incomplete polarisation on the pleochroism

Up to now we implicitly made use that we describe the photons in vacuum and that we know the polarisation. In this chapter we will examine what happens if the initial polarisation is changed by effects that cannot be corrected simply by the performer of the experiment. Firstly, this is the change of the polarisation of the synchrotron radiation by optical components, and secondly it is the change of the photons by the sample under investigation itself.

IV.1 Perturbations of the photon polarisation by optical components

The polarisation of the photons used to excite the photoelectrons can be altered by different processes. In the case of reflection at absorbing metal surfaces different reflection factors $r_\parallel$ and $r_\perp$ occur for the parallel and the perpendicular components of the electric field vector as well as an additional phase shift δ between these components. Such reflections are observed at the optical components of a monochromator changing the polarisation of the incoming photons as discussed in the following part. Unwanted changes in the photon polarisation may be avoided by a careful arrangement of the optical components. Nevertheless, one has always a reflection at the substrate surface itself that cannot be neglected.

We assume that all reflections occur in the same plane with $\varphi_q=0$, for simplification. We make use that $\vartheta_r=\pi-\vartheta_q$ for the reflected beam and find that the electric field vector of the reflected photon beam is given by:

$$\frac{\vec{E_r}}{E_0} = \begin{Bmatrix} r_\parallel & \cos(\vartheta_r)\cos(\Gamma_0) \\ r_\perp & \sin(\Gamma_0)\; e^{\{i(\Delta_0+\delta)\}} \\ -r_\parallel & \sin(\vartheta_r)\cos(\Gamma_0) \end{Bmatrix} = \begin{Bmatrix} -r_\parallel & \cos(\vartheta_q)\cos(\Gamma_0) \\ r_\perp & \sin(\Gamma_0)\; e^{\{i(\Delta_0+\delta_r)\}} \\ -r_\parallel & \sin(\vartheta_q)\cos(\Gamma_0) \end{Bmatrix}$$

(Index 0 is used for the polarisation of the primary photons.) In general, and especially for the UV-range the reflectivities r are complex numbers.

As in the case of the incoming beam, the degrees of polarisation do not depend directly on the angle of light incidence ϑ_q:

$$P_{\parallel,r} = \frac{|r_\parallel|^2\cos^2(\Gamma_0)-|r_\perp|^2\sin^2(\Gamma_0)}{|r_\parallel|^2\cos^2(\Gamma_0)+|r_\perp|^2\sin^2(\Gamma_0)}$$

$$P_{c,r} = \frac{|r_\parallel||r_\perp|\cdot\sin(2\Gamma_0)\sin(\Delta_0+\delta_r)}{|r_\parallel|^2\cos^2(\Gamma_0)+|r_\perp|^2\sin^2(\Gamma_0)}$$

$$P_{45,r} = \frac{|r_\parallel||r_\perp|\cdot\sin(2\Gamma_0)\cos(\Delta_0+\delta_r)}{|r_\parallel|^2\cos^2(\Gamma_0)+|r_\perp|^2\sin^2(\Gamma_0)}$$

On the other hand the reflection (or transmission) coefficient's $r_\parallel$ for the p-component and $r_\perp$ for the s-component as well as the relative phase δ_r between them depend on the angle of photon propagation. They can be calculated in the Fresnel prescription. The coefficients become dependent on the angle of incidence and therefore the polarisation depends on the light incidence, too. The complex law of refraction (Snell's law) becomes $\sin(\vartheta_{refr}) = (n-ik)\sin(\vartheta_q)$ if the photons cross the barrier from vacuum to the substrate (note that in the co-ordinates used the angle of incidence is $\alpha=\vartheta_q-\pi$). Using the Fresnel

equations, the complex reflection coefficients and the relative phase can be calculated from Fresnel's equations to be [3.1]:

$$r_\parallel = \frac{(n-ik)-f_a}{(n-ik)+f_a}$$

$$r_\perp = \frac{(n-ik)f_a-1}{(n-ik)f_a+1}$$

$$f_a = \frac{\sqrt{(n-ik)^2-\sin^2(\vartheta_q)}}{(n-ik)\cos(\vartheta_q)}$$

The phase $\delta=\delta_\parallel-\delta_\perp$ can be calculated from the real and imaginary part of the reflection coefficients.

Far away from the surface the photon beam is described by the reflected wave directly, because incoming and outgoing waves do not interact coherently. In the case of completely s or p polarised light the reflection does not change the polarisation, but remarkably in the case of completely S_3- or S_2- polarised light the reflection results in elliptically polarised light. In the case of a complete linear (S_2) polarisation we have:

$$\underline{S}' = \begin{pmatrix} 1 \\ 0 \\ \pm1 \\ 0 \end{pmatrix} \rightarrow \underline{S}^r = \begin{pmatrix} |r_\parallel|^2+|r_\perp|^2 \\ 2\cdot|r_\parallel|^2-\left[|r_\parallel|^2+|r_\perp|^2\right] \\ \pm2\cdot|r_\parallel||r_\perp|\cos(\delta) \\ \pm2\cdot|r_\parallel||r_\perp|\sin(\delta) \end{pmatrix}$$

and for a complete circular (S_3) polarisation of the incident photons we find:

$$\underline{S}' = \begin{pmatrix} 1 \\ 0 \\ 0 \\ \pm1 \end{pmatrix} \rightarrow \underline{S}^r = \begin{pmatrix} |r_\parallel|^2+|r_\perp|^2 \\ 2\cdot|r_\parallel|^2-\left[|r_\parallel|^2+|r_\perp|^2\right] \\ \pm2\cdot|r_\parallel||r_\perp|\sin(\delta) \\ \pm2\cdot|r_\parallel||r_\perp|\cos(\delta) \end{pmatrix}$$

The crucial point is that the change of the helicity for 100% circularly polarised photons causes a change of the sign of the reflected S_2 component, too, and vice versa. Therefore, the reflected photon beam leads to the occurrence of an additional LDAD effect.

The S_2 or S_3 polarisation is not influenced at normal incidence, reversing only the z-direction of the photon beam. Therefore this geometry may be the best to build monochromators to work with circularly polarised synchrotron radiation. Unfortunately this design cannot be used for photon energies above about 40eV. On the other hand, for most materials the index of refraction is not very different from unity for photon energies above hν=100eV. The behaviour of the polarisation at two typical monochromators at BESSY (Berlin) is discussed in the next chapter.

In principle not only a single reflection occurs in typical monochromator set-ups what can be treated by using matrix methods as can be found in the literature [3.6].

Before discussing the influence of the sample itself, we will give a short description of the polarisation at some monochromators that we use using in the experiments.

IV.1.1 Polarisation of the Synchrotron Radiation

At the BESSY storage ring (6.5m NIM, SX700-III monochromator) we obtain σ^+ (RCP) polarised light above and σ^- (LCP) polarised light below the ring plane as well as linear polarised light (PP) in the plane of the storage ring. Note, in some work the notation RCP, LCP is used with respect to the view in the direction opposite to the photon beam (view to the BESSY storage ring) rather than in the direction of the photon beam, leading to confusion if different kinds of pleochroism are compared. The degree of polarisation depends on the monochromator that is used. Circularly polarised light can be obtained at the 6.5m NIM and the SX700-III monochromator for different photon energy ranges.

At the 6.5m NIM one has photon energies in the range of approximately hν=0...40eV with the circular polarisation varying between 87% and 98% (150nm...30nm) [3.7]. Furthermore the degree of polarisation depends on the opening of the slits that act as polarisation selector (see figure in ref.[3.7]). However, the light is always polarised with P=100%, meaning that $P^2 = P_{circ}^2 + P_l^2 = 1$. We have $P_{lin}=P_\parallel>0$ and the normal incidence design of the monochromator ensures that there is no phaseshift observed between the s- andp-components, such that $P_{45}=0$. The CDAD-asymmetry is given by:

$$A_{CDAD} = \frac{|p_{circ}| \cdot G_{circ}}{(G_\parallel + G_\perp) + p_\parallel (G_\parallel - G_\perp)} = \frac{|P_{circ}| \cdot G_3}{G_0 + G_1 \sqrt{1 - P_{circ}^2}}$$

The root in the denominator is about 0.3 even if the circular polarisation is in the order of 95%, and therefore it cannot be neglected. The asymmetry does not scale linearly with the degree of circular polarisation P_c, what has to be taken into account if one likes to compare it to measurements taken at other devices.

The situation of the polarisation is more complicated at the SX700-III monochromator [3.8],[3.9] having a gracing incidence design. Here, P_c can be as low as 30% (depending on the wavelength) and one finds in addition a P_{45}-component that is nearly as high as P_c depending on the photon energy. Moreover its sign is switched simultaneously with the circular component. The Stokes parameters for the VUV and XUV energy range given in thetable below were measured by theBESSY crew.

hν	P_{ges}	$S_1=P_\parallel$	$S_2=P_{45°}$	$S_3=P_{circ}$
30eV	85%	75%	±21%	±32%
50eV	94%	73%	±30%	±52%
70eV	95%	75%	±21%	±55%
90eV	63%	67%	±15%	±40%

Due to switching of the sign (not the absolute value!) of both components P_{45} and P_c at once we have:

$$A_{CDAD} = \frac{|p_c| G_3 \pm |p_{45}| G_2}{G_0 + p_\parallel G_1}$$

The double sign arises *not* from the switching of polarisation but from the initial orientation of P_{45} that can either be positive or negative, in general. For the SX700-III both components have initially the

same sign and therefore the sign in the equation above has to be „+" .The origin of the changes in the photon polarisation was discussed in the previous chapter.

However, there is an unpolarised contribution. The origin is unclear at the moment, but possibly radiation from above and below the plane of the storage ring adds incoherently.

IV.2 Misalignment of the Experiment

In the experiments one has oftenly a slight misalignment of the sample with respect to the light incidence. In this case we have to take into account that the photon propagation vector has a φ_q component. The polarisation vector is then complex in all three components and given by:

$$\vec{\varepsilon} = \begin{Bmatrix} \varepsilon_X + i\varepsilon'_X \\ \varepsilon_Y + i\varepsilon'_Y \\ \varepsilon_Z + i\varepsilon'_Z \end{Bmatrix} = \begin{Bmatrix} \left[\varepsilon_\parallel - \varepsilon_\perp \sin(\Phi_q)\right]\cos(\Theta_q) \\ \varepsilon_\perp \cos(\Phi_q) \\ -\left[\varepsilon_\parallel + \varepsilon_\perp \sin(\Phi_q)\right]\sin(\Theta_q) \end{Bmatrix} \simeq \begin{Bmatrix} \left[\varepsilon_\parallel - \varepsilon_\perp \sin(\varphi_q)\right]\cos(\vartheta_q) \\ \varepsilon_\perp \cos(\varphi_q) \\ -\left[\varepsilon_\parallel + \varepsilon_\perp \sin(\varphi_q)\right]\sin(\vartheta_q) \end{Bmatrix}$$

As far as φ_q is small, we may set the Cosine term in the y-component to unity but leave the additional imaginary part in the x- and z-components, that become now complex, too. Furthermore we assume a situation were no S_2 Stokes component is present, that is: $P_{45}=0$. The LDAD case can then be treated by replacing simply iP_{circ} by P_{45} and the imaginary parts of the products between the components of ξ-functions by their real parts. The simplified polarisation vector for slightly out of plane incidence is then given by:

$$\vec{\varepsilon} = \begin{Bmatrix} \varepsilon_{xr} + i\varepsilon_{xi} \\ i\varepsilon_{yi} \\ \varepsilon_{zr} + i\varepsilon_{zi} \end{Bmatrix} = \sqrt{\frac{1}{2(1+P_\parallel)}} \begin{Bmatrix} \cos(\vartheta_q) & \left[(1+P_\parallel) - iP_{circ}\sin(\varphi_q)\right] \\ & +iP_{circ} \\ -\sin(\vartheta_q) & \left[(1+P_\parallel) + iP_{circ}\sin(\varphi_q)\right] \end{Bmatrix}$$

To determine the CDAD, we have to calculate the difference of the square absolute of the product of the polarisation vector (with opposite sign of the imaginary parts) and the Ξ-function:

$$I_{CDAD} \propto \left| \begin{Bmatrix} \varepsilon_{xr} + i\varepsilon_{xi} \\ i\varepsilon_{yi} \\ \varepsilon_{zr} + i\varepsilon_{zi} \end{Bmatrix} \bullet \begin{Bmatrix} \xi_{xr} + i\xi_{xi} \\ \xi_r + i\xi_{yi} \\ \xi_{zr} + i\xi_{zi} \end{Bmatrix} \right|^2 - \left| \begin{Bmatrix} \varepsilon_{xr} - i\varepsilon_{xi} \\ -i\varepsilon_{yi} \\ \varepsilon_{zr} - i\varepsilon_{zi} \end{Bmatrix} \bullet \begin{Bmatrix} \xi_{xr} + i\xi_{xi} \\ \xi_r + i\xi_{yi} \\ \xi_{zr} + i\xi_{zi} \end{Bmatrix} \right|^2$$
$$= 4\left\{(\varepsilon_{xr}\varepsilon_{zi} - \varepsilon_{xi}\varepsilon_{zr}) \cdot \Im(\xi_x^*\xi_z) + \varepsilon_{xr}\varepsilon_{yi} \cdot \Im(\xi_x\xi_y^*) + \varepsilon_{yi}\varepsilon_{zr} \cdot \Im(\xi_y^*\xi_z)\right\}$$

The last two terms are just the same as for in-plane photon incidence. The products of the polarisation vector components of the first term is given by:

$$(\varepsilon_{xr}\varepsilon_{zi} - \varepsilon_{xi}\varepsilon_{zr}) = \frac{-P_{circ}}{2}\sin(2\vartheta_q)\sin(\varphi_q)$$

Using this equation the CDAD for slightly out of plane photon incidence is given approximately by:

$$I_{CDAD} \simeq \cos(\varphi_q) \cdot I^0_{CDAD} - 2P_{circ}\sin(2\vartheta_q)\sin(\varphi_q) \cdot \Im(\xi_x^*\xi_z)$$

The superscript 0 hints on the CDAD for in-plane photon incidence as described before. The additional term has at α=45° photon incidence a maximum, but it is always small because we assumed $\sin(\varphi_q)$ to be small. Nevertheless, in special cases of the direction of electron emission the first term may vanish and one has to prove that the xz-term does not become large. In such a case we may observe some unexpected CDAD.

Note 1: Even in the more general case where a non-switching S_2-component is present, we have the same result:

$$I_{CDAD} \propto 2\left\{\varepsilon_{xz}\cdot\Im(\xi_x^*\xi_z)+\varepsilon_{xy}\cdot\Im(\xi_x\xi_y^*)+\varepsilon_{yz}\cdot\Im(\xi_y^*\xi_z)\right\}$$
$$\varepsilon_{xz}=2(\varepsilon_{xr}\varepsilon_{zi}-\varepsilon_{xi}\varepsilon_{zr})=-\tfrac{1}{2}\sin(2\vartheta_q)\sin(\varphi_q)\cdot P_{circ}$$
$$\varepsilon_{xy}=2(\varepsilon_{xr}\varepsilon_{yi}-\varepsilon_{xr}\varepsilon_{yi})=\cos(\vartheta_q)\cos(\varphi_q)\cdot P_{circ}$$
$$\varepsilon_{yz}=2(\varepsilon_{yi}\varepsilon_{zr}-\varepsilon_{yr}\varepsilon_{zi})=-\sin(\vartheta_q)\cos(\varphi_q)\cdot P_{circ}$$

That is what we expected, because the difference is always effected only by the circularly polarised component of the polarisation vector. So far the result can be generalised for any arbitrary photon incidence, if we take into account the dependence on both angles of photon propagation to be more complicated (simply replace ϑ,φ by Θ,Φ and use the transformation given in the previous chapter). But, remember: the intensity for unpolarised photons gets some additional terms, too, what will effect the asymmetry!

Note 2: If additionally a switching S_2-component is present, we have to add both terms to find the dichroic signal: $I_{PIPE}=I_{CDAD}+I_{LDAD}$!

IV.3 The polarisation near the sample surface and inside of thin films

So far we have omitted the adsorbate layer. The changes in the polarisation caused by an adsorbate are successfully used for ellipsometric measurements or the magneto-optic Kerr-effect (MOKE).

To calculate the behaviour of the electric field vector we can in principle proceed as follows. A part of the incoming wave is reflected by the vacuum-adsorbate interface The transmitted wave is damped and partially reflected at the adsorbate-substrate interface. The reflected part of the wave going through the adsorbate backwards leads finally to multiple reflections inside of the adsorbate layer. Now we can calculate the reflection and transmission coefficients at each boundary using the Fresnel equations and sum up the infinite series.

We will describe first the behaviour of the photon polarisation in dichroic films on isotropic substrates and for dichroic substrates without adsorbates. Then we simplify these equations for isotropic films.

IV.3.1 Thin bifringent, dichroic films

We start with the general case of an anisotropic adsorbate on an isotropic substrate. The photons cross in this case the adsorbate with thickness d and a complex index of refraction $n_{c,a}=n_a-i\,k_a$ before entering the substrate with $n_{c,s}=n_s-i\,k_s$. In general, the optical constants can differ in directions in and perpendicular to the thin film. We write the complex index of refraction of the thin film as $n_{c,j}=n_j-i\,k_j$ (j=x,y,z) and assume that the substrate is not dichroic. To calculate the reflection and transmission coefficients we make use that the tangential components of the electric field E and the magnetic field H are continuous at the boundary.

A complete description of the derivation for the Fresnel coefficients for thin anisotropic films can be found in textbooks on optics.

We find that our problem can be described by the four coefficients for the amplitude of electric field of the reflected (R), the transmitted (T) and the beam inside the adsorbate travelling into the adsorbate (A) and back (B).

$$R=\frac{r^{(a)}+r^{(s)}\exp\{-i2\kappa_z^{(a)}d\}}{1+r^{(a)}r^{(s)}\exp\{-i2\kappa_z^{(a)}d\}}$$
$$A=\frac{t^{(a)}}{1+r^{(a)}r^{(s)}\exp\{-i2\kappa_z^{(a)}d\}}$$
$$B=\frac{t^{(a)}r^{(s)}}{1+r^{(a)}r^{(s)}\exp\{-i2\kappa_z^{(a)}d\}}$$
$$T=\frac{t^{(a)}t^{(s)}\exp\{-i(\kappa_z^{(a)}-\kappa_z^{(s)})d\}}{1+r^{(a)}r^{(s)}\exp\{-i2\kappa_z^{(a)}d\}}$$

These equations depend not directly on the polarisation of the photons. On the other hand, the coefficients r and t depend not only on the material but also on the kind of photon polarisation as well as the direction of photon propagation.

The single-boundary coefficients for reflection and transmission of *s-polarised* photons at the adsorbate or the substrate are given by:

$$r_s^{(a)}=\frac{\kappa_z^{(0)}-\kappa_z^{(a)}}{\kappa_z^{(0)}+\kappa_z^{(a)}}\qquad t_s^{(a)}=[1+r_s^{(a)}]=\frac{2\kappa_z^{(0)}}{\kappa_z^{(0)}+\kappa_z^{(a)}}$$

$$r_s^{(s)}=\frac{\kappa_z^{(a)}-\kappa_z^{(s)}}{\kappa_z^{(a)}+\mu_a\kappa_z^{(s)}}\qquad t_s^{(s)}=[1+r_s^{(s)}]=\frac{2\kappa_z^{(a)}}{\kappa_z^{(a)}+\kappa_z^{(s)}}$$

The wave-vector for s-polarised photons inside of the anisotropic adsorbate is given by:

$$\kappa_{z,s}^{(a)}=\sqrt{\varepsilon_y\kappa_0^2-(\kappa_x^{(0)})^2}$$

In the case of *p-polarised* photons the single reflection and transmission coefficients given by:

$$r_p^{(a)}=\frac{\varepsilon_x\kappa_z^{(0)}-\kappa_z^{(a)}}{\varepsilon_x\kappa_z^{(0)}+\kappa_z^{(a)}}\qquad t_p^{(a)}=[1+r_p^{(a)}]\sqrt{\frac{1}{\varepsilon_x}}=\frac{2\varepsilon_x\kappa_z^{(0)}}{\varepsilon_x\kappa_z^{(0)}+\kappa_z^{(a)}}\sqrt{\frac{1}{\varepsilon_x}}$$

$$r_p^{(s)}=\frac{\varepsilon_x\kappa_z^{(a)}-\varepsilon_x\kappa_z^{(s)}}{\varepsilon_x\kappa_z^{(a)}+\varepsilon_x\kappa_z^{(s)}}\qquad t_p^{(s)}=[1+r_p^{(s)}]\sqrt{\frac{\varepsilon_x}{\varepsilon_s}}=\frac{2\varepsilon_x\kappa_z^{(a)}}{\varepsilon_x\kappa_z^{(a)}+\varepsilon_x\kappa_z^{(s)}}\sqrt{\frac{\varepsilon_x}{\varepsilon_s}}$$

The wave-vector for p-polarised photons inside of the anisotropic adsorbate is given by:

$$\kappa_{z,p}^{(a)}=\sqrt{\varepsilon_x\kappa_0^2-\frac{\varepsilon_x}{\varepsilon_z}(\kappa_x^{(0)})^2}$$

Furthermore we find the Cosines and Sins of the angles to evaluate the photoemission intensity depending on the angle of refraction inside of the anisotropic adsorbate and the substrate.

We insert the expression for the wave-vector depending on the index of refraction and find for the Cosine-terms:

$$\cos(\vartheta_s^{(a)}) = \frac{\sqrt{(n_y - ik_y)^2 - \sin^2(\vartheta_0)}}{(n_z - ik_z)}$$

$$\cos(\vartheta_p^{(a)}) = \frac{(n_x - ik_x)\sqrt{(n_z - ik_z)^2 - \sin^2(\vartheta_0)}}{(n_z - ik_z)^2}$$

$$\cos(\vartheta^{(s)}) = \frac{\sqrt{(n_s - ik_s)^2 - \sin^2(\vartheta_0)}}{(n_s - ik_s)}$$

and the Sine-terms:

$$\sin^2(\vartheta_s^{(a)}) = \frac{\sin^2(\vartheta_0) - (n_y - ik_y)^2 + (n_z - ik_z)^2}{(n_z - ik_z)^2}$$

$$\sin^2(\vartheta_p^{(a)}) = \frac{(n_x - ik_x)^2 \sin^2(\vartheta_0) - (n_x - ik_x)^2(n_z - ik_z)^2 + (n_z - ik_z)^4}{(n_z - ik_z)^4}$$

$$\sin^2(\vartheta^{(s)}) = \frac{\sin^2(\vartheta_0)}{(n_s - i \cdot k_s)^2}$$

In all cases we have set the relative permeability to be $\mu=1$ in the adsorbate and substrate. The angle of refraction is now depending on the state of polarisation of the photons, as is typical for dichroic materials.

On the first sight this seems to be puzzling, but to calculate the photoemission we do not need the angle of refraction directly but only the components of the electric field.

Before looking at the particular case of an isotropic adsorbate in more detail, we like to express the single reflection and transmission coefficients in terms of the complex index of refraction (for short we use $\underline{n}$ instead of $(n\text{-}ik)$:

a) s-polarised photons

$$r_s^{(a)} = \frac{\cos(\vartheta_0) - \sqrt{\underline{n}_y^2 - \sin^2(\vartheta_0)}}{\cos(\vartheta_0) + \sqrt{\underline{n}_y^2 - \sin^2(\vartheta_0)}}$$

$$r_s^{(s)} = \frac{\sqrt{\underline{n}_y^2 - \sin^2(\vartheta_0)} - \sqrt{\underline{n}_s^2 - \sin^2(\vartheta_0)}}{\sqrt{\underline{n}_y^2 - \sin^2(\vartheta_0)} + \sqrt{\underline{n}_s^2 - \sin^2(\vartheta_0)}}$$

$$t_s^{(a)} = \frac{2\cos(\vartheta_0)}{\cos(\vartheta_0) + \sqrt{\underline{n}_y^2 - \sin^2(\vartheta_0)}}$$

$$t_s^{(s)} = \frac{2\sqrt{\underline{n}_y^2 - \sin^2(\vartheta_0)}}{\sqrt{\underline{n}_y^2 - \sin^2(\vartheta_0)} + \sqrt{\underline{n}_s^2 - \sin^2(\vartheta_0)}}$$

b) p-polarised photons

$$r_p^{(a)} = \frac{\underline{n}_x \underline{n}_z \cos(\vartheta_0) - \sqrt{\underline{n}_z^2 - \sin^2(\vartheta_0)}}{\underline{n}_x \underline{n}_z \cos(\vartheta_0) + \sqrt{\underline{n}_z^2 - \sin^2(\vartheta_0)}}$$

$$r_p^{(s)} = \frac{\underline{n}_s^2 \sqrt{\underline{n}_z^2 - \sin^2(\vartheta_0)} - \underline{n}_x \sqrt{\underline{n}_s^2 - \sin^2(\vartheta_0)}}{\underline{n}_s^2 \sqrt{\underline{n}_z^2 - \sin^2(\vartheta_0)} + \underline{n}_x \sqrt{\underline{n}_s^2 - \sin^2(\vartheta_0)}}$$

$$t_p^{(a)} = \frac{2\underline{n}_x \underline{n}_s \cos(\vartheta_0)}{\underline{n}_x \underline{n}_z \cos(\vartheta_0) + \sqrt{\underline{n}_z^2 - \sin^2(\vartheta_0)}}$$

$$t_p^{(s)} = \frac{2\underline{n}_x \underline{n}_s \sqrt{\underline{n}_z^2 - \sin^2(\vartheta_0)}}{\underline{n}_s^2 \sqrt{\underline{n}_z^2 - \sin^2(\vartheta_0)} + \underline{n}_x \sqrt{\underline{n}_s^2 - \sin^2(\vartheta_0)}}$$

IV.3.2 Isotropic samples

In this case all n_j, k_j are equal and Snell's law of refraction becomes:

$$\sin(\vartheta_0) = (n_a - i \cdot k_a) \cdot \sin(\vartheta^{(a)}) = (n_s - i \cdot k_s) \cdot \sin(\vartheta^{(s)})$$

The reflected photon beam is not influenced alone, but the transmitted wave too. This will influence the measurements of dichroism in photoemission from substrate states. Firstly refraction occurs with a complex index of refraction n-ik, that changes the direction of the photon propagation. We will rewrite Snell's law and the Fresnel equations to include the transmission coefficients:

$$\sin(a) = n\sin(\beta) \qquad n\cos(\beta) = \sqrt{n^2 + \sin^2(a)} = g_\vartheta$$

$$r_\perp = \frac{\cos(a) - g_\vartheta}{\cos(a) + g_\vartheta} \qquad t_\perp = \frac{2\cos(a)}{\cos(a) + g_\vartheta}$$

$$r_\parallel = \frac{n^2\cos(a) - g_\vartheta}{n^2\cos(a) + g_\vartheta} \qquad t_\parallel = \frac{2n\cos(a)}{n^2\cos(a) + g_\vartheta}$$

First, we assume that the adsorbate is located in the coherence zone of the direct and the reflected wave. Directly outside the surface we find for the polarisation vector:

$$\vec{\varepsilon}_{out} = \frac{1}{\sqrt{2}} \begin{Bmatrix} -\cos(a)\ (1 - r_\parallel)\ \sqrt{1 + P_\parallel} \\ (1 + r_\perp)\ \frac{P_{45} + iP_c}{\sqrt{1 + P_\parallel}} \\ \sin(a)\ (1 + r_\parallel)\ \sqrt{1 + P_\parallel} \end{Bmatrix}$$

and for the wave just inside of the sample we find for the polarisation vector:

$$\vec{\varepsilon}_{in} = \frac{1}{\sqrt{2}} \begin{Bmatrix} -\cos(\beta)\ t_{\parallel}\ \sqrt{1+P_{\parallel}} \\ t_{\perp}\ \frac{P_{45}+iP_c}{\sqrt{1+P_{\parallel}}} \\ \sin(\beta)\ t_{\parallel}\ \sqrt{1+P_{\parallel}} \end{Bmatrix}$$

If the initial photon beam was completely circularly polarised, we find:

$$\vec{\varepsilon}_{in}^{circ} = \sqrt{2}\cos(\vartheta) \begin{Bmatrix} \frac{-\cos(\beta)}{(n+ik)((n+ik)^2\cos(\vartheta)+g_\vartheta)} \\ \frac{iP_c}{\cos(\vartheta)+g_\vartheta} \\ \frac{2\sin(\beta)}{(n+ik)((n+ik)^2\cos(\vartheta)+g_\vartheta)} \end{Bmatrix}$$

IV.4 Description of the Dichroism in isotropic samples

We have found that all three components of the polarisation vector become complex inside of the adsorbate. On the other hand, only the sign of the y-component is changed, if we switch the sign of the initial polarisation. The difference is that now both components, the real and the imaginary part of the y-component, are switched at once. This leads to a simultaneous occurrence of CDAD and LDAD. We write the polarisation vector inside of the adsorbate for the two opposite signs of the polarisation as:

$$\vec{\varepsilon}_a^{\pm} = \begin{pmatrix} \varepsilon_{xr} + i\cdot\varepsilon_{xi} \\ \pm(\varepsilon_{yr} + i\cdot\varepsilon_{yi}) \\ \varepsilon_{zr} + i\cdot\varepsilon_{zi} \end{pmatrix}$$

The components ε_x, ε_y and ε_z are those being changed by the adsorbate and substrate as described above. The dichroism is as before given by the difference of the cross-sections for the polarisation of opposite sign:

$$I_{DAD} \propto \left|\vec{\varepsilon}_a^{+}\bullet\Xi\right|^2 - \left|\vec{\varepsilon}_a^{-}\bullet\Xi\right|^2$$

If we insert the complexΞ-functions and calculate the dichroism, we find the result:

$$I_{DAD} = I_{CDAD} + I_{LDAD}$$

$$I_{LDAD} \propto 4\left\{\mathrm{Re}(\varepsilon_x\varepsilon_y^*)\,\mathrm{Re}(\xi_x\xi_y^*) + \mathrm{Re}(\varepsilon_y\varepsilon_z^*)\,\mathrm{Re}(\xi_y\xi_z^*)\right\}$$
$$I_{CDAD} \propto -4\left\{\mathrm{Im}(\varepsilon_x\varepsilon_y^*)\,\mathrm{Im}(\xi_x\xi_y^*) + \mathrm{Im}(\varepsilon_y\varepsilon_z^*)\,\mathrm{Im}(\xi_y\xi_z^*)\right\}$$

These equations are essentially the same as those we derived before. In particular all properties connected to the Ξ-functions keep the same. The only difference is that both kind of dichroism occur simultaneously making a distinction of CDAD and LDAD impossible. To distinguish the effects we must make use of the symmetry properties of the Ξ-functions, that will possibly allow to suppress one kind of dichroism, if the measurement makes use of a special geometry or initial states.

IV.4.1 The field at the boundaries and in an adsorbate:

Directly at the vacuum-adsorbate interface we find for the electric field:

$$\frac{\hat{E}}{\hat{E}^{(0)}} = 1 + R = \frac{(1+r_{v-a})(1+r_{a-s}\exp\{-i2\kappa_z^{(a)}d\})}{1+r_{v-a}r_{a-s}\exp\{-i2\kappa_z^{(a)}d\}}$$

In the middle of the adsorbate we find for the electric field:

$$\frac{E^{(a)}}{E^{(0)}} = A\exp\{-i\cdot\kappa_z^{(a)}\tfrac{d}{2}\} + B\exp\{i\cdot\kappa_z^{(a)}\tfrac{d}{2}\}$$
$$= \frac{t_{v-a}[1+r_{a-s}\exp\{-i\kappa_z^{(a)}d\}]}{1+r_{v-a}r_{a-s}\exp\{-i2\kappa_z^{(a)}d\}}\exp\left\{-i\frac{\kappa_z^{(a)}d}{2}\right\}$$

As an example, we will now examine these equations for a alkali monolayer on a non-chiral d-band substrate. We assume that the excitation energy is well above the plasma frequency and well beside of semi-corelevel or corelevel excitations. In this case no damping of the wave occurs and we have k_a=0. The index of refraction is than between $1<n_a<0.9$. Furthermore we assume that the index of refraction differs for the directions in the layer and perpendicular to it, that is $n_z=n_\perp, n_x, n_y$. For fourfold order of the adsorbate both in plane components should be equal and we will write them like: $n_\parallel=n_\perp+\Delta n$. In case of adsorbates in two-fold or hexagonal symmetry the in-plane components can differ from each other, in this case we at the direction as an index toΔn.

a) We assume that the index of refraction in the z-direction is that of the vacuum (n_z=1) and only the in-plane components differ from 1. The Fresnel coefficients read than:

for s-polarisation they stay the same as before:

$$r_s^{(a)} = \frac{\cos(a)-f_s^{(a)}}{\cos(a)+f_s^{(a)}} \qquad t_s^{(a)} = \frac{2\cos(a)}{1+f_s^{(a)}}$$
$$f_s^{(a)} = \sqrt{n_y^2-\sin^2(a)}$$
$$r_s^{(s)} = \frac{f_s^{(a)}-f_s^{(s)}}{f_s^{(a)}+f_s^{(s)}} \qquad t_s^{(s)} = \frac{2\cdot f_s^{(a)}}{f_s^{(a)}+f_s^{(s)}}$$
$$f_s^{(s)} = \sqrt{(n_s-ik_s)^2-\sin^2(a)}$$
$$\delta_s = 4\pi\cdot f_s^{(a)}\cdot\frac{d}{\lambda_0}$$

for p-polarisation:

$$r_p^{(a)} = \frac{n_x - 1}{n_x + 1} \qquad t_p^{(a)} = \frac{2}{n_x}$$

$$r_p^{(s)} = \frac{\cos(a) - f_p^{(s)}}{\cos(a) + f_p^{(s)}} \qquad t_p^{(s)} = \frac{n_x}{n_s - ik_s} \cdot \frac{2\cos(a)}{\cos(a) + f_p^{(s)}}$$

$$f_p^{(s)} = \frac{n_x \sqrt{(n_s - ik_s)^2 - \sin^2(a)}}{(n_s - ik_s)^2}$$

$$\delta_p = 4\pi n_x \cos(a) \frac{d}{\lambda_0}$$

In a monolayer we can assume thatd<<λ_0 and the phasefactor exp(-iδ) becomes unity. This results in:

$$R_p = \frac{\cos(a) - f_p^{(s)}}{\cos(a) + f_p^{(s)}}$$

$$T_p = \frac{2(n_s + 1)}{n_x(n_s - ik_s)} \cdot \frac{\cos(a)}{\cos(a) + f_p^{(s)}}$$

$$f_p^{(s)} = \frac{\sqrt{(n_s - ik_s)^2 - \sin^2(a)}}{(n_s - ik_s)^2}$$

We find for the reflection and transmission coefficients:

$$R = \frac{r^{(a)} + r^{(s)} \exp\{-i\delta\}}{1 + r^{(a)} r^{(s)} \exp\{-i\delta\}}$$

$$A = \frac{t^{(a)}}{1 + r^{(a)} r^{(s)} \exp\{-i\delta\}}$$

$$B = \frac{t^{(a)} r^{(s)} \exp\{-i\delta\}}{1 + r^{(a)} r^{(s)} \exp\{-i\delta\}}$$

$$T = \frac{t^{(a)} t^{(s)} \exp\{-i\delta\}}{1 + r^{(a)} r^{(s)} \exp\{-i\delta\}} \exp\{i(\kappa_z^{(a)} + \kappa_z^{(s)})d\}$$

$$\delta = 2\kappa_z^{(a)} d$$

in this case we have for the field inside of the adsorbate:

$$A_p = \frac{\hat{E}_A^{(a)}}{\hat{E}^{(0)}} = \frac{2n_s}{n_x + 1 + (n_x - 1) r_{a-s} \exp\{-i2\kappa_z^{(a)} d\}}$$

$$B_p = \frac{\hat{E}_B^{(a)}}{\hat{E}^{(0)}} = \frac{2n_s r_{a-s} \exp\{-i2\kappa_z^{(a)} d\}}{n_x + 1 + (n_x - 1) r_{a-s} \exp\{-i2\kappa_z^{(a)} d\}}$$

$$C_p = \frac{\hat{E}_A^{(a)} + \hat{E}_B^{(a)}}{\hat{E}^{(0)}} = \frac{\hat{E}^{(a)}}{\hat{E}^{(0)}} = \frac{2n_s[1 + r_{a-s} \exp\{-i\kappa_z^{(a)} d\}]}{n_x + 1 + (n_x - 1) r_{a-s} \exp\{-i2\kappa_z^{(a)} d\}}$$

IV.5 A Concluding Remark

We have seen that the use of Fresnel equations leads to substantial effects on the photon polarisation. Nevertheless, the Fresnel equations are a strong oversimplification of the problem. The complete influence of the surface has to be treated in a microscopic theory. The dichroic measurements can provide to be a tool to measure the local optical properties on a microscopic scale in photon energy ranges were ellipsometric measurements can not be performed.

IV.6 References

[3.1] Bergmann/ Schäfer „Lehrbuch der Experimentalphysik", Bd.III Optik

[3.2] Born and Wolf, *Principles of Optics*

[3.3] Zare R.N. „Angular momentum"

[3.4] Bergmann / Schäfer „Lehrbuch der Experimentalphysik", Bd.III Optik: p505 and Bd.IV Aufbau der Materie: p79; W.deGruyther

view in direction of propagationσ^+; $\Delta m=+1 \Rightarrow$ RCP and σ^-; $\Delta m=-1 \Rightarrow$ LCP

or opposite to propagation-directionσ^+; $\Delta m=+1 \Rightarrow$ LCP and σ^-; $\Delta m=-1 \Rightarrow$ RCP

[3.5] Blume M., Gibbs R.; Phys.Rev. B37 (1988) p1779

[3.6] Klinger D.S., Lewis J.W., Randall C.E.; *„Polarized Light in Optics and Spectroscopy"*; Academic Press, Boston...Toronto (1990)

[3.7] F.Schäfers, W.Peatman, A.Eyers, Ch.Heckenkamp, G.Schönhense, and U.Heinzmann, Rev.Sci.Instr. 57 (1986) 1032

[3.8] H.Petersen, M.Willmann, F.Schäfers, and W.Gudat, Nucl.Instr.Meth. Phys.Res. A333 (1993) 594

[3.9] M.Willmann, H.Petersen, F.Schäfers, M.Mast, B.R.Müller, and W.Gudat, BESSY Annual Report, (1991) 466

see also:

O.S.Heavens; "Optical Properties of Thin Solid Films"; Dover Publications, New York (1991)

H.Schopper; Z. f. Physik 132 (1952) 146

P.J.Feibelman; Surf.Sci. 46 (1974) 558

P.J.Feibelman; Phys.Rev. B12 (1975) 1319

S.P.Weeks, E.W.Plummer; Solid State Comm. 21 (1977) 695

R.McLean, R.Haydock; J.Phys. C: Solid State Phys. 10 (1977) 1929

M.A.B. Whitaker; J.Phys. C: Solid State Phys. 11 (1978) L151

N.V.Smith, R.L.Benbow, Z.Hurych; Phys.Rev. B21 (1980) 4331

A.Goldmann, A.Rodriquez, R.Feder; Solid State Comm. 45 (1983) 449

R.Courths, S.Hüfner; Phys.Rep. 112 (1984) 53

H.Wern, R.Courths; Surf.Sci. 162 (1985) 29

F.Forstmanns, R.R.Gerhardts; *"Metal Optics Near the Plasma Frequency"*; Springer Verlag, Berlin (1986)

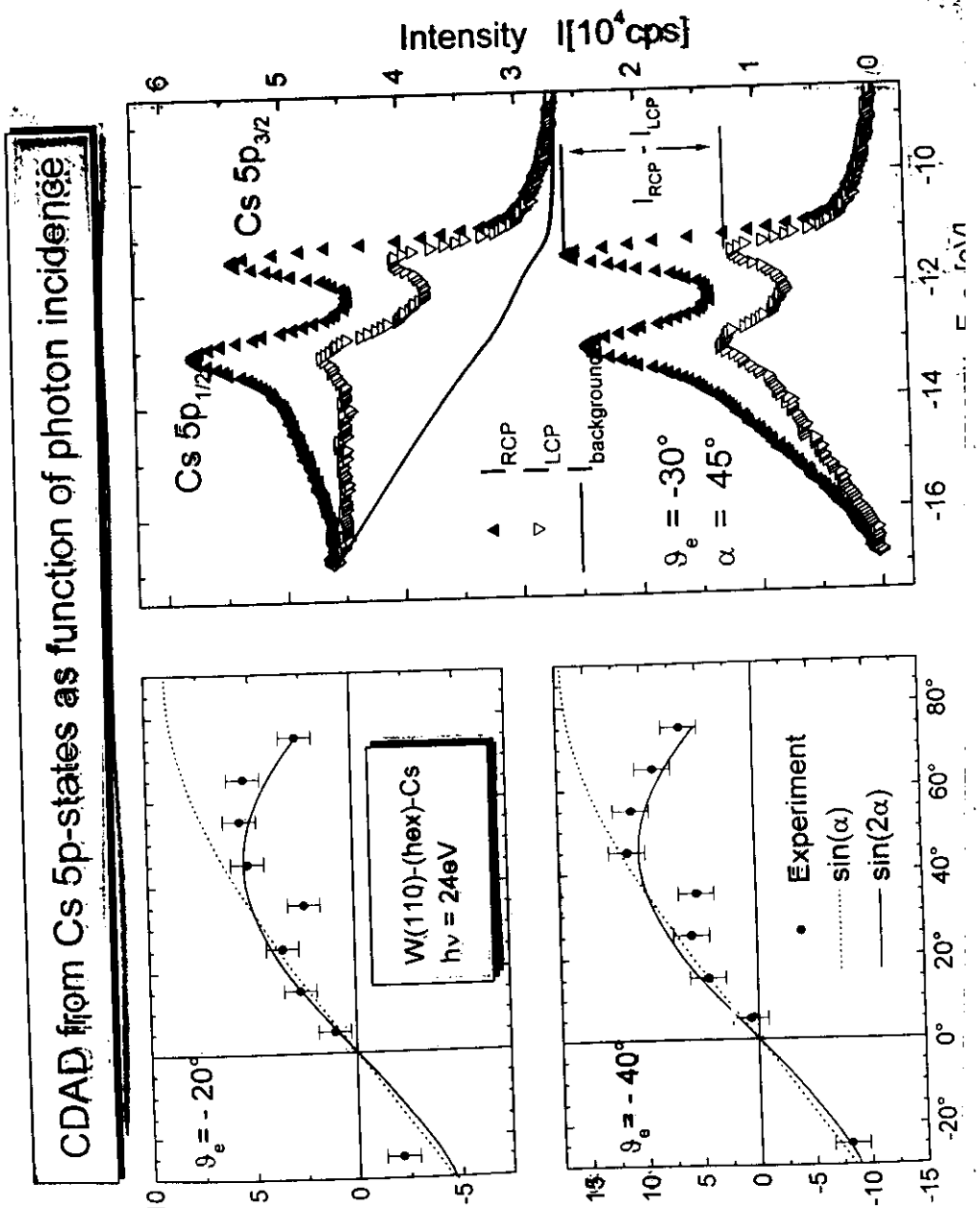

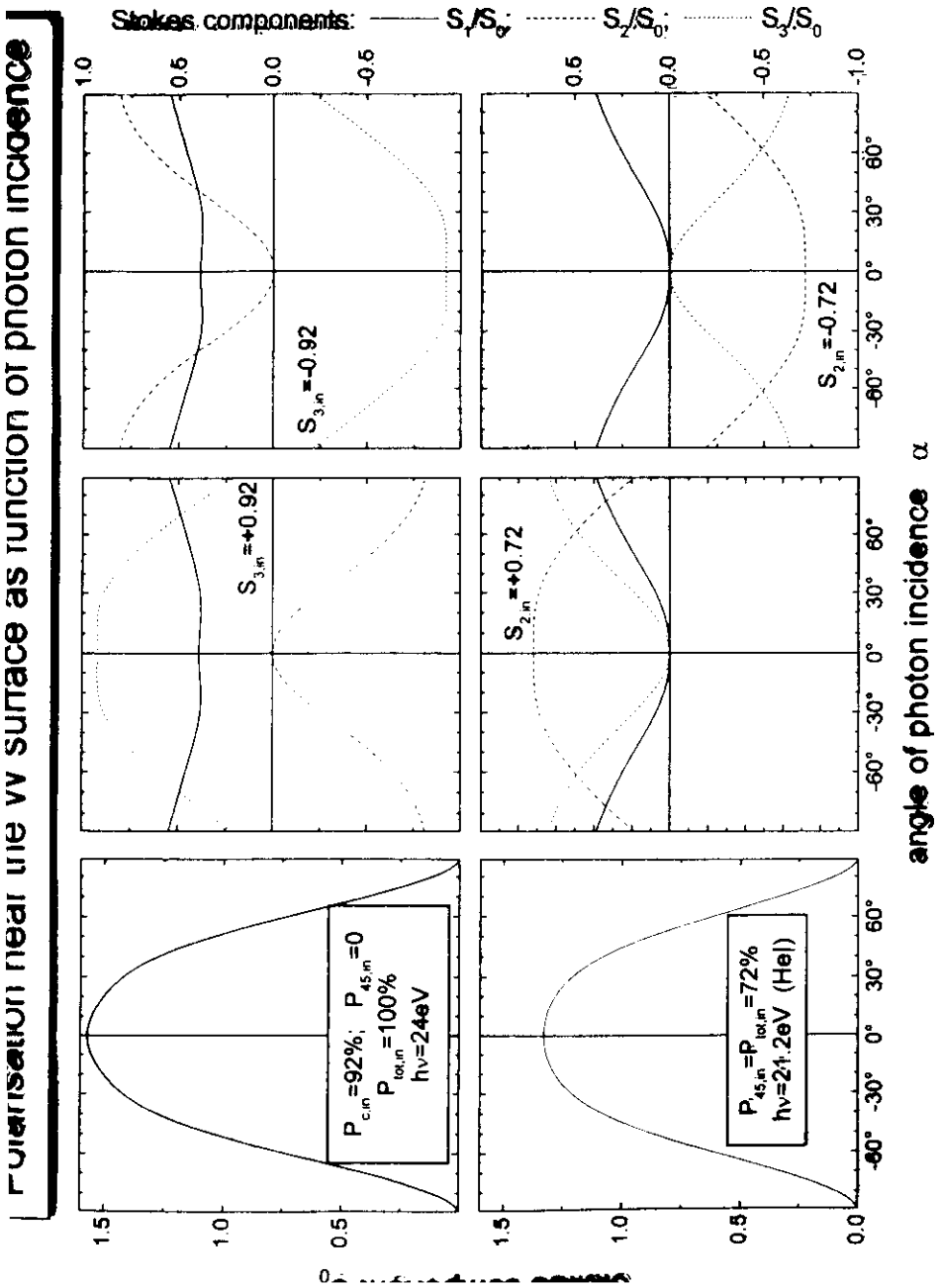

V The polarisation and orientation of the states

We will define now what is meant if we say an atom, orbital, or electronic state is polarised, aligned or oriented. There is no uniform definition of these terms. From a formal point of view we find in a rough characterisation that a free atom or a specific electronic level can be either of spherical symmetry in the case of filled shells or of cylindrical (axial) symmetry if an unfilled shell is not of s-like character. Here we made use that we describe the interaction of the electrons with the core by a central potential. To observe the cylindrical symmetry we need to assign properly a z-axis, what can be done by applying external fields like electric (Stark-effect), magnetic (Zeeman-effect), electromagnetic (photoemission) fields, or the interaction with the solid surface.

In principal, every physical quantity can be characterised by its expectation value (n=1) or its n-th statistical moment that is given by:

$$\langle X \rangle^{(n)} := \langle \Psi | X^n | \Psi \rangle = \int \Psi \cdot X^n \cdot \Psi^* \cdot dX$$

This can be used to define different quantities like orientation and alignment

V.1 Definitions

V.1.1 Orientation of the angular momentum

The orientation of the angular momentum can be characterised by the state multipoles, that are the expectation values for the total angular momentum operators. The degree of orientation O or alignment A of the total angular momentum for states$|j,m_j\rangle$ that are at least of cylindrical symmetry are given by:

$$O_0^{(1)}(j,m_j) = \frac{m_j}{\sqrt{j(j+1)}}$$

$$A_0^{(2)}(j,m_j) = \frac{3m_j^2 - j(j+1)}{\sqrt{j(j+1)}}$$

The same equations can be used for any angular momentum and especially for the orbital angular momentum if simply replacing j by ℓ.

The orientation and alignment of states $\Psi=n(m_j)\ |j,m_j\rangle$ build from pure states $|j,m_j\rangle$ are given by the mean value of the individual states weighted by their occupation probabilities $n(m_j)$:

$$\overline{O}(j) = \sum_{m_j} n(m_j) O_0^{(1)}(j,m_j)$$

$$\overline{A}(j) = \sum_{m_j} n(m_j) A_0^{(2)}(j,m_j)$$

It is seen that both vanish for a filled shell where all m_j are distributed equally. For s- and p- states we find for the degrees of orientation and alignment:

state $\|j,m_j\rangle$	$O^{(1)}$	$A^{(2)}$
$\|1/2,-1/2\rangle$	$-1/\sqrt{3}$	0

|1/2,+1/2>	+1/√3	0
|3/2,−3/2>	-3/√15	6/√15
|3/2,−1/2>	-1/√15	-6/√15
|3/2,+1/2>	+1/√15	-6/√15
|3/2,+3/2>	+3/√15	6/√15

For filled $s_{1/2}$ or $p_{1/2}$ shells we find that both the mean orientation and the mean alignment of the total angular momentum vanish.

V.1.2 Orientation of the electron spin

The spinpolarisation vector of an electronic state $\Psi=\alpha|\uparrow>+\beta|\downarrow>$ build from two spinors is given by:

$$\vec{P} = \frac{1}{|\alpha|^2+|\beta|^2}\cdot\begin{Bmatrix} \alpha\beta^* + \alpha^*\beta \\ i(\alpha\beta^* - \alpha^*\beta) \\ |\alpha|^2 - |\beta|^2 \end{Bmatrix} = \frac{1}{|\alpha|^2+|\beta|^2}\cdot\begin{Bmatrix} 2\Re e(\alpha^*\beta) = 2\Re e(\alpha\beta^*) \\ 2\Im m(\alpha^*\beta) = -2\Im m(\alpha\beta^*) \\ |\alpha|^2 - |\beta|^2 \end{Bmatrix}$$

The denominator is the total intensity. In close analogy to photons we can define a 4-component spin-vector to describe the spin-polarised electrons:

$$\vec{S} = \begin{Bmatrix} |\alpha|^2+|\beta|^2 \\ \alpha\beta^* + \alpha^*\beta \\ i(\alpha\beta^* - \alpha^*\beta) \\ |\alpha|^2 - |\beta|^2 \end{Bmatrix}$$

The polarisation vector becomes simple in all cases where $|m_j|=j=\ell+1/2$, in this case the spin is purely z-oriented:

$$\vec{P}(l, j=l+1/2, m_j=\pm j) = \pm\begin{Bmatrix} 0 \\ 0 \\ 1 \end{Bmatrix}$$

The spinpolarisation vectors of the remainingp-states of an atom are given by:

$$\vec{P}(p_{1/2,\pm 1/2}) = \pm\begin{Bmatrix} \sin(2\vartheta)\cos(\varphi) \\ \sin(2\vartheta)\sin(\varphi) \\ \cos^2(\vartheta) - \sin^2(\vartheta) \end{Bmatrix}$$

$$\vec{P}(p_{3/2,\pm 1/2}) = \pm\frac{1}{3\cos^2(\vartheta)+1}\begin{Bmatrix} 4\sin(2\vartheta)\cos(\varphi) \\ 4\sin(2\vartheta)\sin(\varphi) \\ 5\cos^2(\vartheta) - 1 \end{Bmatrix}$$

If we add the intensities incoherently, than the spinpolarisation vanishes for any closed shell and additionally for any filled subshell, as can be seen from the double sign. The absolute value of the polarisation is $\left|\vec{P}\right| = \pm 1$ for any of the states, in agreement with the Pauli exclusion principle.

In photoemission we have to account for the final (free electron) states that are given by a mixture of pure spinors, what will give surely a different answer than the case of the pure spinors.

V.1.3 Orientation, polarisation and alignment of the charge distribution

The angular dependency of the charge distribution of an atom or specific orbital is given by the square of the electron wavefunction:

$$\rho(\vartheta,\varphi) = \left|\Psi_{n,l,j,m}(\vartheta,\varphi)\right|^2$$

The overall charge density depends on the radial part $R_{n,\ell,j}$ of the wavefunction, too. If the number of electrons in a particular subshell is N, then we normalise thewavefunctionby:

$$N = \langle r^0\rangle \cdot \sum_{i=1}^{N}\iint \rho_i(\vartheta,\varphi)d\vartheta d\varphi$$

The equations to calculate then-th moment of the position are given below.

Atoms that are adsorbed at a solid surface become polarised. Here „polarised" has a different meaning compared to free atoms. It denotes the effect that the charge distribution is altered in such a way that it results in a net dipole moment. The effective dipole moment (at a surface) is proportional to the Cosine of the angle measured with respect to the z-axis that is $\cos(\vartheta)$. From this we can define the polarisation or better orientation of the atom or a specific electronic state by the expectation value of the first Legendre Polynomial:

$$O_1 \equiv \langle\cos(\vartheta)\rangle = \langle z\rangle = \int_{-1}^{+1}\Psi\cdot z\cdot\Psi^*\cdot dz = \int_{-1}^{+1}|\Psi(z)|^2 z\cdot dz$$

The dipole momentum is given by the orientation multiplied by the first statistical moment of the position vector, that is the mean distance between the electron and the core:

$$p_0 = O_1\cdot\langle r^1\rangle$$

For $O_1>0$ the dipole moment points in the direction of the z-axis. In analogy the alignment of the charge distribution is given by the expectation value of the second Legendre Polynomial:

$$A_2 \equiv \langle P_2(z=\cos(\vartheta))\rangle = \int_{-1}^{+1}|\Psi(z)|^2\frac{(3z^2-1)}{2}\cdot dz$$

For $A_2>0$ we have a z-alignment of the charge distribution and it is of xy-type for $A_2<0$. Due to the cylindrical or spherical symmetry free atoms or orbitals of free atoms cannot be oriented but are only aligned. We call an atom or orbital as *„really oriented" if the degree of orientation does not vanish* $O_1\neq 0$. In this case not only its angular momentum or spin is oriented but also its charge distribution.

From the probability distribution of the pure spinor spherical harmonics it is seen that such states cannot be truly oriented because only even potencies occur in $W_{j,m}$.

Note 1: In both cases it is assumed that the radial part of the wavefunction depends only on r but not on ϑ or φ.

Note 2: The statistical moments of the position weighted by the square of the radial part of the wavefunction are given by the following integrals:

$$\frac{\langle r^n \rangle}{\langle r^0 \rangle} = \frac{\int R^2_{n,l,j} \cdot r^{n+1} dr}{\int R^2_{n,l,j} \cdot r \cdot dr}$$

r^0 is used for normalisation and r^1 is the expectation value of the mean distance between the electron and the core.

Note 3: It is also possible to define the orientation with respect to other directions than z by replacing the integral on zdz by integrals on xdx or ydy.

V.2 The case of LSJ coupling for ferromagneticmetals

In the case of rare earth metals the orientation of the different angular momenta (spin, orbital, and total) is given most oftenly for LSJ coupling assuming that in the magnetised case $<J_z>=-J$, meaning that only $M_J=-J$ is occupied. The expectation values for the spin and orbital angular momenta of the coupled wave functions are then given by:

$$\begin{aligned} < J_z > &= -J \\ < L_z > &= < J_z > \frac{J(J+1)+L(L+1)-S(S+1)}{2J(J+1)} \\ < S_z > &= < J_z > \frac{J(J+1)+S(S+1)-L(L+1)}{2J(J+1)} \end{aligned}$$

The z-component expectation values of the spin (S), orbital (L), and total (J) angular momentum for completely polarised states are given in the table below for open shell ions of some ferromagnetic materials with partially filled d- or f- shells:

Ion	open shell	Ground-state	S	$<S_z>$	L	$<L_z>$	J	$<J_z>$
Fe^{3+}	$3d^5$	$^6S_{5/2}$	5/2	-5/2	0	0	5/2	-5/2
Fe^{2+}	$3d^6$	$^5D_4$	2	-2	2	-2	4	-4
Co^{2+}	$3d^7$	$^4F_{9/2}$	3/2	-45/22	3	-27/11	9/2	-9/2
Ni^{2+}	$3d^8$	$^3F_4$	1	-1	3	-3	4	-4
Gd^{3+}	$4f^7$	$^8S_{7/2}$	7/2	-7/2	0	0	7/2	-7/2
Tb^{3+}	$4f^8$	$^7F_6$	3	-3	3	-3	6	-6
Dy^{3+}	$4f^9$	$^6H_{15/2}$	5/2	-115/34	5	-70/51	15/2	-15/2

V.3 Disturbed states

Here we will deal with some effects that arise if the angular part of the initial state is described not only by a single orbital angular momentum quantum number, but by a mixture of different orbital angular momenta.

If only one orbital angular momentum ℓ contributes we find from the cylindrical symmetry of the spherical harmonics, that any sum of the type

$$\sum_m n_m Y_{l,m}$$

will be of cylindrical symmetry, too, meaning that we cannot observe an orientation of the charge cloud, but only an alignment

In the following we will treat some wavefunctions of the type:

$$\Psi = \sqrt{1-x}\, Y_{l1,m1} R_{n1,l1} + \sqrt{x}\, Y_{l2,m2} R_{n2,l2}$$

where x gives the partition of the second type of wavefunction. Such types of wavefunctions typically appear in MO or LCAO theory or for the so called surface molecules. The later are in the simplest case a atom adsorbed on top of a surface-atom.

The normalisation integrals forz-alligned states ($m_1=m_2=0$) is then given for any l by:

$$I_0 = 2\pi \int |\Psi|^2 = (1-x)\langle r^0_{l1} \rangle + x\langle r^0_{l2} \rangle$$

The integrals giving the statistical moments are given by:

$$I_1 = 2\pi \int |\Psi|^2 z dz = 2\pi \sqrt{x(1-x)}\, \langle R_{n1,l1} R_{n2,l2} r \rangle \int Y_{l1,0} Y_{l2,0} \cdot z dz$$

$$I_2 = 2\pi \int |\Psi|^2 z^2 dz = 2\pi \left\{ (1-x)\langle r^2_{l1} \rangle \int Y_{l1,0} \cdot z^2 dz + x\langle r^2_{l2} \rangle \int Y_{l2,0} \cdot z^2 dz \right\}$$

$<R_{n1,l1}R_{n2,l2}r>$ is called the overlap integral. Furthermore, we made use of the symmetry properties of the spherical harmonics $Y_{l,0}$ that are functions of z only. We will see later, that the various integrals including the radial parts will not be needed to describe the dichroism but only the angular parts, therefore it is convenient to define the orientation and alignment of the angular parts of the wavefunctions only:

$$\frac{o^0_1}{2\pi} = \sqrt{x(1-x)} \int Y_{l1,0} Y_{l2,0} \cdot z dz$$

$$\frac{a^0_2}{2\pi} = 3\left\{ (1-x) \int Y_{l1,0} \cdot z^2 dz + x \int Y_{l2,0} \cdot z^2 dz \right\} - 1$$

V.3.1 Mixing of s and p states

We start with an somewhat academically case. Firstly we assume that the initial state wavefunction is given by a coherent superposition of the not perturbed p_z-wave with small amount of an s-wave:

$$\Psi_i = \sqrt{1-n} \cdot p_z \pm \sqrt{n} \cdot s = \sqrt{1-n} \cdot Y_{10} R_1 \pm \sqrt{n} \cdot Y_{00} R_0$$

0<n<1 is the part describing the s-like wave. We omitted the main quantum number assigning the radial part R of the wave function, to avoid confusion. Such a wavefunction has an oriented charge distribution as can be seen if we calculate the statistical moments with respect to the z-axis. The normalisation and the degree of orientation or alignment connected to this state are given by:

$$2\pi\langle|\Psi_i|^2\rangle = (1-n)\cdot\langle R_1^2\rangle + n\cdot\langle R_0^2\rangle$$

$$O_1^{sp} = \frac{2}{\sqrt{3}}\frac{\pm\sqrt{n(1-n)}\cdot\langle R_1 R_0 r\rangle}{(1-n)\cdot\langle R_1^2\rangle + n\cdot\langle R_0^2\rangle}$$

$$A_2^{sp} = \frac{1}{5}\frac{5(1-n)\cdot\langle R_1^2 r^2\rangle + 9n\cdot\langle R_1^2 r^2\rangle}{(1-n)\cdot\langle R_1^2\rangle + n\cdot\langle R_1^2\rangle} - 1$$

$\langle R_1 R_0 r\rangle$ is the overlap integral.

The equations become simple, if we neglect the dependency on the radial parts:

$$o_1^{sp} = \pm\frac{2}{\sqrt{3}}\sqrt{n-n^2}$$
$$a_2^{sp} = 4n$$

V.3.2 Mixing of z-allignedstates

An interesting case is the coupling of p- to d- states as can be observed in adsorption of light atoms like C, N or O on d-band transition metals. The binding energy of the 2p-states of these atoms is comparable to that of the metal d-states, so that hybrids can be formed by an overlap of the wavefunctions.

The most simple is the coupling of z-aligned states. Assuming that the initial state wavefunction is given by a coherent superposition of the not perturbed p_z-wave with a small amount of a d_{z2}-wave one finds for the resulting wave function (0<n<1):

$$\Psi_i = \sqrt{1-n}\cdot p_z \pm \sqrt{n}\cdot d_{z^2} = \sqrt{1-n}\cdot Y_{10}R_1 \pm \sqrt{n}\cdot Y_{20}R_2$$

so that we have to solve the following integrals to determine the properties of the charge orientation:

$$I_1 = 2\pi\int|\Psi_i|^2 z\,dz = \pm 4\sqrt{\frac{1}{15}}\sqrt{n-n^2}\cdot\langle R_1 R_2 r\rangle$$

$$I_2 = 2\pi\int|\Psi_i|^2 z^2\,dz = \frac{1}{105}\{63(1-n)\cdot\langle R_1^2 r^2\rangle + 55n\cdot\langle R_2^2 r^2\rangle\}$$

From this integrals we find the orientation and the alignment of the mixed state to be given by:

$$O_1 = \pm 4\sqrt{\frac{1}{15}}\frac{\sqrt{n-n^2}\cdot\langle R_1 R_2 r\rangle}{(1-n)\cdot\langle R_1^2\rangle + n\cdot\langle R_2^2\rangle}$$

$$A_2 = \frac{1}{35}\frac{63(1-n)\cdot\langle R_1^2 r^2\rangle + 55n\cdot\langle R_2^2 r^2\rangle}{(1-n)\cdot\langle R_1^2\rangle + n\cdot\langle R_2^2\rangle} - 1$$

Again neclectingthe radial parts, we find simplified:

$$o_1 = \pm 4\sqrt{\frac{1}{15}}\sqrt{n-n^2}$$

$$a_2 = \frac{28-8n}{35}$$

The alignment is always bigger than 1 and therefore in z-direction, whereas the sign of the orientation depends how we add or subtract the two states from each other.

Another interesting case is the d_{z2} surface state of the hcp rare earth metals observed at the (0001) surfaces. A shift of the charge distribution towards the bulk can be modelled assuming a mixing with an f_{z3} state (note: mixing with p_z does not describe the complete charge distribution in the surface plane, such a coupling will shift this part towards the vacuum). The initial state is then (0<n<1):

$$\Psi_i = \sqrt{1-n}\cdot d_{z^2} \pm \sqrt{n}\cdot f_{z^3} = \sqrt{1-n}\cdot Y_{20}R_2 \pm \sqrt{n}\cdot Y_{30}R_3$$

Its charge distribution and orientation can be calculated from the following equations if we make use that for the z-directionparallel to the surface normal one has to subtract (use negative sign).

$$I_1 = 2\pi\int|\Psi_i|^2 z\,dz = \frac{-6}{\sqrt{35}}\sqrt{n-n^2}\int R_2 R_3 r\,dr$$

$$O_1 = \frac{-6}{\sqrt{35}}\frac{\sqrt{n-n^2}\cdot\langle R_2 R_3 r\rangle}{(1-n)\cdot\langle R_2^2\rangle + n\cdot\langle R_3^2\rangle}$$

If we neglect again the radial parts we find:

$$o_1 = \frac{-6}{\sqrt{35}}\sqrt{n-n^2}$$

having a maximum for n=1/2.

More general, the orientation has its maximum value of

$$O_{1,\max} = \frac{-3}{\sqrt{35}}\cdot\langle R_2 R_3 r\rangle\sqrt{\frac{\langle R_2^2\rangle + \langle R_3^2\rangle}{\langle R_2^2\rangle\cdot\langle R_3^2\rangle}}$$

at $n_{\max} = \frac{\langle R_2^2\rangle}{\langle R_2^2\rangle + \langle R_3^2\rangle}$

VI Photoelectron cross sections and Pleochroism

Usually the photoemission differential cross sections are calculated in terms of spherical harmonics, or the orbital angular momentum. To make it easier to compare the different PIPE effects like CDAD, LDAD and spDAD, we will give a description in terms of the polarisation of light.

To calculate the photoemission cross section for electrons excited by a photon with energy hν we start with Fermi's golden rule that describes the transition probability from an initial state Ψ_i to a final state Ψ_f if the Hamiltonian $\underline{H}$ is effective. The Hamiltonian in question is the dipole operator $\underline{H} = \vec{\varepsilon} \cdot \vec{r}$, where $\vec{\varepsilon}$ is the polarisation vector and $\vec{r}$ is the position vector.

$$\frac{d\sigma}{d\Omega}(E_{kin}) = \left|\left\langle \Psi_f \middle| \underline{H} \middle| \Psi_i \right\rangle\right|^2 = \tfrac{4\pi}{3} a_0 a_0^2 \cdot h\nu \cdot \left|\left\langle \phi_{E_{kin},\vec{k}} \middle| \vec{\varepsilon} \cdot \vec{r} \middle| \phi_{n,l,m} \right\rangle\right|^2$$

As was shown in the first section this equation can be rewritten in the following way:

$$\frac{d\sigma}{d\Omega}(E_{kin}) = c_\sigma \cdot \left|\vec{\varepsilon} \cdot \left\langle \phi_{E_{kin},\vec{k}} \middle| \vec{r} \middle| \phi_{n,l,m} \right\rangle\right|^2 = c_\sigma \left|\vec{\varepsilon} \cdot \vec{\xi}\right|^2$$

so that is divided in the polarisation dependent part and the general photoemission part. The position vector is given in spherical co-ordinates by:

$$\vec{r} = r \begin{Bmatrix} \sin(\vartheta)\cos(\varphi) \\ \sin(\vartheta)\sin(\varphi) \\ \cos(\vartheta) \end{Bmatrix} = r \cdot \hat{r}$$

Firstly, we will examine this equation for reel orbitals.

VI.1 The cross section for real orbitals

We start with the matrix elements, that are calculated by expanding the wave functions of the initial and final state.

VI.1.1 The initial states

The initial state wave functions are solutions of the Schrödinger equation for bound states and given by:

$$\phi_{n,l,m} = R_{n,l} \sum_m n(m) Y_{l,m}(\vartheta,\varphi)$$

$R_{n,\ell}=R_\ell$ is the radial part of the wave function depending on the main quantum number n, the orbital quantum number ℓ and the magnetic quantum number m. The Radial-parts have to be determined numerically from the Schrödinger equation using a Hartree-Fock (HF) or Hartree-Fock-Slater (HFS) method. The n(m)'s are coefficients to form real orbitals from the spherical harmonics $Y_{\ell,m}=Y_{\ell,m}(\vartheta,\varphi)$. Both are given in tables, below in Appendix.

VI.1.2 The final states

The final state wave function depending on the kinetic energy E_{kin} of an emitted electron is written using a partial wave expansion:

$$\phi_{E_{kin},\vec{k}} = 4\pi \sum_{l',m'} i^{l'} \exp\{-i\delta_{l'}\} Y^*_{l',m'}(\hat{k}) Y_{l',m'}(\hat{r}) R_{k,l'}(E_{kin}, r)$$

$\hat{k}$ and $\hat{r}$ are unit vectors of the momentum and position. The radial parts $R_{k,\ell'}(E_{kin},r)$ of the final state wave functions have to be determined numerically. From the dipole selection rules we have $\Delta\ell=1$ and $\ell'=\ell-1,\ell+1$. The dipole selection must not be used as a priori condition as will be shown below.

VI.1.3 The cross section

We insert initial and final state wavefunctions (ϕ_i and ϕ_f) into the equation for the cross section. Furthermore we integrate the r-dependent part of the matrix element (k marks the dependence of $Y_{\ell,m}$ on the angles of emission ϑ_k, φ_k):

$$\left\langle \phi_f \middle| \underline{H} \middle| \phi_i \right\rangle = 4\pi \vec{\varepsilon} \cdot \sum_{m,m'} n(m) \begin{cases} (-i)^{l-1} \left\langle Y_{l-1,m'} \middle| \hat{r} \middle| Y_{l,m} \right\rangle \cdot \exp(i\delta_{l-1}) R_{l-1} Y_{l-1,m'}(\hat{k}) + \dots \\ \dots + (-i)^{l+1} \left\langle Y_{l+1,m'} \middle| \hat{r} \middle| Y_{l,m} \right\rangle \cdot \exp(i\delta_{l+1}) R_{l+1} Y_{l+1,m'}(\hat{k}) \end{cases}$$

$$R_{l\pm1} = \int_0^\infty R_{k,l\pm1}(E_{kin}, r) \cdot r \cdot R_{n,l}(r) \cdot r^2 dr$$

The radial matrixelements $R_{\ell\pm1}$ are named by the final states but nevertheless they are depending on the initial state, too. In the following we will use the abbreviation $\rho_{\ell\pm1}$ for the complex radial matrix element:

$$\rho_{l\pm1} = (-i)^{l\pm1} \cdot R_{l\pm1} \cdot \exp\{i\delta_{l\pm1}\}$$

The angular distribution of the photoelectron amplitude is then given by:

$$\left\langle \phi_f \middle| \underline{H} \middle| \phi_i \right\rangle = 4\pi \vec{\varepsilon} \cdot \sum_{l',m'} \left\langle Y_{l',m'} \middle| \hat{r} \middle| Y_{l,m} \right\rangle \cdot Y_{l',m'}(\hat{k}) \cdot \rho_{l'}$$

$$\rho_{l\pm1} = (-i)^{l\pm1} \cdot \exp\{i\delta_{l\pm1}\} \cdot \int_0^\infty R_{k,l\pm1}(E_{kin}, r) \cdot r \cdot R_{n,l}(r) \cdot r^2 dr$$

To determine the cross section for transitions between reel atomic orbitals we have to calculate the following transition probabilities:

$$T_{l'm'} = \left\langle Y_{l\pm1,m'} \middle| \hat{r} \middle| Y_{l,m} \right\rangle$$

Bearing in mind the selection rules $\Delta m=0,\pm1 \Rightarrow m'=m,m\pm1$. Note, that now the unit position vector appears, due to the integration on r. The dipole-operator can be written expanding the unit position vector in terms of spherical harmonics:

$$\begin{aligned}\vec{\varepsilon}\cdot\hat{r} &= \varepsilon_x\cdot\sin(\vartheta)\cos(\varphi)+\varepsilon_y\cdot\sin(\vartheta)\sin(\varphi)+\varepsilon_z\cdot\cos(\vartheta)\\ &= -\varepsilon_x\cdot\sqrt{\tfrac{2\pi}{3}}\,(Y_{11}-Y_{1-1})+(\varepsilon_{yr}+i\varepsilon_{yi})\cdot i\sqrt{\tfrac{2\pi}{3}}\,(Y_{11}+Y_{1-1})+\varepsilon_z\cdot 2\sqrt{\tfrac{\pi}{3}}\,Y_{10}\end{aligned}$$

Using the first form of the dipole operator we can determine the trace of the diagonal transition matrix from the following integrals:

$$sp(T_{l',m'})=\begin{pmatrix} 4\pi\cdot\int_0^{+\pi}\left\{\int_0^{2\pi} Y^*_{l\pm1,m'}\cdot\sin(\vartheta)\cos(\varphi)\cdot Y_{l,m}d\varphi\right\}\sin(\vartheta)d\vartheta \\ 4\pi\cdot\int_0^{+\pi}\left\{\int_0^{2\pi} Y^*_{l\pm1,m'}\cdot\sin(\vartheta)\sin(\varphi)\cdot Y_{l,m}d\varphi\right\}\sin(\vartheta)d\vartheta \\ 4\pi\cdot\int_0^{+\pi}\left\{\int_0^{2\pi} Y^*_{l\pm1,m'}\cdot\cos(\vartheta)\cdot Y_{l,m}d\varphi\right\}\sin(\vartheta)d\vartheta \end{pmatrix}$$

and the ξ-functions can be calculated from the following equations:

$$\begin{aligned}\xi_{x,l\pm1} &= \sum_{m,m'} n(m)\cdot T^x_{l\pm1,m'}\cdot Y_{l\pm1,m'}\rho_{l\pm1}\\ \xi_{y,l\pm1} &= \sum_{m,m'} n(m)\cdot T^y_{l\pm1,m'}\cdot Y_{l\pm1,m'}\rho_{l\pm1}\\ \xi_{z,l\pm1} &= \sum_{m,m'} n(m)\cdot T^z_{l\pm1,m'}\cdot Y_{l\pm1,m'}\rho_{l\pm1}\end{aligned}$$

leading to the X-functions used byGoldberg et al.:

$$X_{l\pm1,m}=\vec{\varepsilon}\cdot\vec{\Xi}\;;\;\vec{\Xi}=\begin{pmatrix}\xi_x\\ \xi_y\\ \xi_z\end{pmatrix}$$

Besides the work of Goldberg we have included here the case of circularly polarised light. The calculation of the cross section for linearly polarised light in terms of X_{l-1},X_{l+1} functions is given in the paper of Goldberg. The polarisation dependence of the cross section is not directly seen using the X-functions:

$$\frac{d\sigma}{d\Omega}=c_\sigma\cdot\begin{Bmatrix} X^2_{r,l-1}+X^2_{r,l+1}+X^2_{i,l-1}+X^2_{i,l+1}+\dots \\ \dots+2\cdot(X_{r,l-1}\cdot X_{r,l+1}+X_{i,l-1}\cdot X_{i,l+1})\cos(\delta_{l+1}-\delta_{l-1})+\dots \\ \dots+2\cdot(X_{i,l-1}\cdot X_{r,l+1}-X_{r,l-1}\cdot X_{i,l+1})\sin(\delta_{l+1}-\delta_{l-1}) \end{Bmatrix}$$

The polarisation dependence of the cross section is not directly seen using the X-functions.

To show the influence arising from the different polarisation-vector components of the exciting radiation we will use the explicit form involving the ξ-functions. We expand the dipole operator in terms of spherical harmonics:

$$\vec{\varepsilon}\cdot\hat{r}=\sqrt{\frac{2\pi}{3}}\cdot\{-(Y_{11}-Y_{1-1})\varepsilon_x+i\cdot(Y_{11}+Y_{1-1})(\varepsilon_{yr}+i\varepsilon_{yi})+\sqrt{2}\cdot Y_{10}\varepsilon_z\}$$

to continue the calculation of the transition matrix. We use eithe6j-symbols ($\beta=\Delta m$)

$$\begin{aligned}\int_0^{\pi}\left\{\int_0^{2\pi} Y^*_{l\pm1,m+\beta}Y_{1\beta}Y_{lm}d\varphi\right\}\sin(\vartheta)d\vartheta &= \sqrt{\frac{(2(l\pm1)+1)3(2l+1)}{4\pi}}\begin{pmatrix} l\pm1 & 1 & l\\ 0 & 0 & 0\end{pmatrix}\begin{pmatrix} l\pm1 & 1 & l\\ m' & 0,\pm1 & m\end{pmatrix}\\ &= (-1)^{l\pm1-l}\sqrt{\frac{(2(l\pm1)+1)3}{4\pi}}\,C^{l,0}_{l\pm1,0,1,0}\begin{pmatrix} l\pm1 & 1 & l\\ m' & 0,\pm1 & m\end{pmatrix}\end{aligned}$$

or Clebsch-Gordan $C^{l_3,m_3}_{l_1,m_1,l_2,m_2}$ to solve the integrals, resulting in the Gaunt coefficienic $^{\Delta l}(l',m',l,m)$:

$$\begin{aligned}\sqrt{\tfrac{2\pi}{3}}\int_0^{\pi}\left\{\int_0^{2\pi} Y^*_{l\pm1,m'}Y_{1,\beta}Y_{lm}d\varphi\right\}\sin(\vartheta)d\vartheta &= \sqrt{\tfrac{2\pi}{3}}\sqrt{\tfrac{3}{4\pi}}\sqrt{\tfrac{(2l+1)\cdot3}{2(l\pm1)+1}}\cdot C^{l\pm1,0}_{l,0,1,0}\cdot C^{l\pm1,m+\beta}_{l,m,1,\beta}\\ &= c_{l\pm1}\cdot C^{l\pm1,m+\beta}_{l,m,1,\beta}\\ &= \sqrt{\tfrac{3}{2}}\,c^1(l\pm1,m+\beta,l,m)=g(l\pm1,m+\beta,l,m)\\ &\beta=\Delta m=0,\pm1\end{aligned}$$

The modified Gaunt-coefficients $g(\ell\pm1,m+\beta,\ell,m)$ are tabulated below in the appendix. The first C-G coefficient $C^{l',0}_{l,0,1,0}$ vanishes for $\ell+1+\ell'$=odd, that is the selection rule $\ell'=\ell\pm1$ or $\Delta\ell=\pm1$. The second vanishes for $m'\neq m+\beta$ including the selection rule $\Delta m=m'-m=\beta=0,\pm1$ resulting in the following ξ-functions:

$$\begin{aligned}\xi_{x,l\pm1} &= -4\pi\cdot\sum_m n_m\{g(l\pm1,m+1,l,m)Y_{l\pm1,m+1}-g(l\pm1,m-1,l,m)Y_{l\pm1,m-1}\}\rho_{l\pm1}\\ \xi_{y,l\pm1} &= i\cdot4\pi\cdot\sum_m n_m\{g(l\pm1,m+1,l,m)Y_{l\pm1,m+1}+g(l\pm1,m-1,l,m)Y_{l\pm1,m-1}\}\rho_{l\pm1}\\ \xi_{z,l\pm1} &= 4\pi\sqrt{2}\cdot\sum_m n_m g(l\pm1,m,l,m)Y_{l\pm1,m}\rho_{l\pm1}\end{aligned}$$

Finally, the trace of the transition matrix for emission from a state ℓ,m to a final state $\ell'=\ell\pm1$,m'=m,m±1 is given by:

$$sp(T_{l',m'})=4\pi\cdot\begin{pmatrix}-g(l\pm1,m\pm1,l,m)\\ i\cdot g(l\pm1,m\pm1,l,m)\\ \sqrt{2}\cdot g(l\pm1,m,l,m)\end{pmatrix}$$

and the equation for the Ξ-function for the emission from a state with definite orbital angular momentum reads:

$$\Xi=\left\{\sum_m n_m\sum_{l'}\sum_{m'}[T_{l',m'}\cdot Y_{l',m'}\rho_{l'}]\right\}$$

VI.1.4 Result: The G-functions

We are now able to calculate in more general the G-functions from the real and imaginary parts of the ξ-functions using the equations derived above:

$$G_{\parallel} = \tfrac{1}{2}\cos^2(\vartheta_q)\cdot|\xi_x|^2 + \tfrac{1}{2}\sin^2(\vartheta_q)\cdot|\xi_z|^2 - \sin(2\vartheta_q)\cdot\Re(\xi_z\xi_z^*)$$

$$G_{\perp} = \tfrac{1}{2}|\xi_y|^2$$

$$G_0 = \tfrac{1}{2}\left\{\cos^2(\vartheta_q)\cdot|\xi_x|^2 + |\xi_y|^2 + \sin^2(\vartheta_q)\cdot|\xi_z|^2\right\} - \sin(2\vartheta_q)\cdot\Re(\xi_z\xi_z^*)$$

$$G_1 = \tfrac{1}{2}\left\{\cos^2(\vartheta_q)\cdot|\xi_x|^2 - |\xi_y|^2 + \sin^2(\vartheta_q)\cdot|\xi_z|^2\right\} - \sin(2\vartheta_q)\cdot\Re(\xi_z\xi_z^*)$$

$$G_{45} = G_2 = 2\cdot\left\{\cos(\vartheta_q)\cdot\Re(\xi_x\xi_y^*) - \sin(\vartheta_q)\cdot\Re(\xi_y^*\xi_z)\right\}$$

$$G_{circ} = G_3 = 2\cdot\left\{\cos(\vartheta_q)\cdot\Im(\xi_x\xi_y^*) - \sin(\vartheta_q)\cdot\Im(\xi_y^*\xi_z)\right\}$$

In the following we will give some applications of the equations derived above, namely the emission and PIPE from initial s- and p-states.

VI.1.5 Ξ-functions for pure spherical harmonics

We start with the Ξ-functions for pure spherical harmonics. From these we can build the X-functions for real orbitals, later. We start with the Ξ-function for initial Y_{00} that is s-states.

$$\Xi(Y_{00}) = \begin{Bmatrix} \xi_x(Y_{00}) = \\ \xi_y(Y_{00}) = \\ \xi_z(Y_{00}) = \end{Bmatrix} = 4\pi\cdot\begin{Bmatrix} -\frac{1}{\sqrt{2}}\{Y_{11} - Y_{1-1}\} \\ \frac{i}{\sqrt{2}}(Y_{11} + Y_{1-1}) \\ Y_{10} \end{Bmatrix}\cdot\rho_1$$

Now we calculate the Ξ-functions the pure spherical harmonics $Y_{\ell=1,m}$ that contribute to the initial p-states:

a) Y_{11}

$$\Xi(Y_{11}) = 4\pi\cdot\begin{Bmatrix} -\left\{\left\{\sqrt{\frac{3}{5}}\,Y_{22} - \sqrt{\frac{1}{10}}\,Y_{20}\right\}\rho_2 + \sqrt{\frac{1}{2}}\,Y_{00}\rho_0\right\} \\ i\cdot\left\{\left\{\sqrt{\frac{3}{5}}\,Y_{22} + \sqrt{\frac{1}{10}}\,Y_{20}\right\}\rho_2 - \sqrt{\frac{1}{2}}\,Y_{00}\rho_0\right\} \\ \sqrt{\frac{3}{5}}\,Y_{21}\rho_2 \end{Bmatrix}$$

b) Y_{1-1}

$$\Xi(Y_{1-1}) = 4\pi\cdot\begin{Bmatrix} -\left\{\left\{\sqrt{\frac{1}{10}}\,Y_{20} - \sqrt{\frac{3}{5}}\,Y_{2-2}\right\}\rho_2 - \sqrt{\frac{1}{2}}\,Y_{00}\rho_0\right\} \\ i\cdot\left\{\left\{\sqrt{\frac{1}{10}}\,Y_{20} + \sqrt{\frac{3}{5}}\,Y_{2-2}\right\}\rho_2 - \sqrt{\frac{1}{2}}\,Y_{00}\rho_0\right\} \\ \sqrt{\frac{3}{5}}\,Y_{2-1}\rho_2 \end{Bmatrix}$$

c) Y_{10}

$$\Xi(Y_{10}) = 4\pi\cdot\begin{Bmatrix} -\sqrt{\frac{3}{10}}\{Y_{21} - Y_{2-1}\}\rho_2 \\ i\cdot\sqrt{\frac{3}{10}}\{Y_{21} + Y_{2-1}\}\rho_2 \\ \left\{\sqrt{\frac{4}{5}}\,Y_{20}\rho_2 + Y_{00}\rho_0\right\} \end{Bmatrix}$$

The Ξ-functions for real orbitals can be build from the Ξ-functions for spherical harmonics writing the initial state as:

$$|i\rangle = \sum_m n(m)Y_{i,m}$$

First we find for an initial s-state having only m=0:

$$\Xi(s) = \begin{Bmatrix} \xi_x(s) = \\ \xi_y(s) = \\ \xi_z(s) = \end{Bmatrix} = 4\pi\cdot\begin{Bmatrix} p_x \\ p_y \\ p_z \end{Bmatrix}\cdot\rho_s$$

For the 3 real p-states that are p_x, p_y, p_z we have:

$n(m)$	$m=+1$	$m=-1$	$m=0$
p_x	$-\frac{1}{\sqrt{2}}$	$\frac{1}{\sqrt{2}}$	0
p_y	$\frac{i}{\sqrt{2}}$	$\frac{-i}{\sqrt{2}}$	0
p_z	0	0	1

from this we can find the Ξ-functions from:

a) p_x

$$\Xi(p_x) = 4\pi \cdot \begin{Bmatrix} -\left\{\sqrt{\frac{1}{5}}\, d_{z^2} - \sqrt{\frac{3}{5}}\, d_{x^2-y^2}\right\} \cdot \rho_d + s \cdot \rho_s \\ \sqrt{\frac{3}{5}}\, d_{xy} \cdot \rho_d \\ \sqrt{\frac{3}{5}}\, d_{xz} \cdot \rho_d \end{Bmatrix}$$

b) p_y

$$\Xi(p_y) = 4\pi \cdot \begin{Bmatrix} \sqrt{\frac{3}{5}}\, d_{xy} \cdot \rho_d \\ -\left\{\sqrt{\frac{1}{5}}\, d_{z^2} + \sqrt{\frac{3}{5}}\, d_{x^2-y^2}\right\} \cdot \rho_d + s \cdot \rho_s \\ \sqrt{\frac{3}{5}}\, d_{yz} \cdot \rho_d \end{Bmatrix}$$

c) p_z

$$\Xi(p_z) = 4\pi \cdot \begin{Bmatrix} \sqrt{\frac{3}{5}}\, d_{xz} \cdot \rho_d \\ \sqrt{\frac{3}{5}}\, d_{yz} \cdot \rho_d \\ \sqrt{\frac{4}{5}}\, d_{z^2} \cdot \rho_d + s \cdot \rho_s \end{Bmatrix}$$

VI.1.6 CDAD and LDAD from s and p orbitals

To show the influence arising from the different polarisation-vector components of the exciting radiation we will use the explicit form involving the Ξ-functions that are given above for different initial states.

For initial s-states we see, that there is no difference in the phases of the final state ξ-functions, therefore the imaginary part of the xy and yz mixed products vanishes and therefore no CDAD can be observed. On the other hand the real part of the mixed products leads to the occurrence of LDAD. The LDAD can be found from the equations:

$$\frac{I_{LDAD}}{c_\sigma} = 2 \cdot P_{45} \cdot \left\{\cos(\vartheta_q) \cdot \Re(\xi_x \xi_y^*) + \sin(\vartheta_q) \cdot \Re(\xi_y^* \xi_z)\right\}$$

$$\Re(\xi_x \xi_y^*) = 16\pi^2 \cdot p_x p_y \cdot R_p^2 = \frac{3}{8} \cdot \sin^2(\vartheta)\sin(2\varphi) \cdot R_p^2$$

$$\Re(\xi_y^* \xi_z) = 16\pi^2 \cdot p_y p_z \cdot R_p^2 = \frac{3}{4} \cdot \sin(2\vartheta)\sin(\varphi) \cdot R_p^2$$

so that the LDAD for an initial s-state is given by (setting P=1):

$$\frac{I_{LDAD}^s}{c_\sigma \cdot R_p^2} = \frac{3}{2} \cdot \{\cos(\vartheta_q) \cdot \sin^2(\vartheta)\sin(2\varphi) + \sin(\vartheta_q) \cdot 2\sin(2\vartheta)\sin(\varphi)\}$$

For initial p-states the mixed products are given by:

a) p_x

$$\xi_x \xi_y^* = -16\pi^2 \left(\frac{3}{5} d_{xy} \cdot \left\{\sqrt{\frac{1}{3}}\, d_{z^2} - d_{x^2-y^2}\right\} \cdot R_d^2 + \sqrt{\frac{3}{5}} \cdot s d_{xy} \cdot \rho_s \rho_d^*\right)$$

$$\xi_y^* \xi_z = 16\pi^2 \frac{3}{5} \cdot d_{xz} d_{xy} \cdot R_d^2$$

b) p_y

$$\xi_x \xi_y^* = 16\pi^2 \cdot \left(\frac{3}{5} d_{yz} \left\{\sqrt{\frac{1}{3}}\, d_{z^2} + d_{x^2-y^2}\right\} \cdot R_d^2 - \sqrt{\frac{3}{5}}\, s d_{xy} \cdot \rho_s^* \rho_d\right)$$

$$\xi_y^* \xi_z = -16\pi^2 \cdot \left(\frac{3}{5} d_{yz} \left\{\sqrt{\frac{1}{3}}\, d_{z^2} + d_{x^2-y^2}\right\} \cdot R_d^2 - \sqrt{\frac{3}{5}}\, s d_{yz} \cdot \rho_s^* \rho_d\right)$$

c) p_z

$$\xi_x \xi_y^* = 16\pi^2 \frac{3}{5} \cdot d_{xz} d_{yz} \cdot R_d^2$$

$$\xi_y^* \xi_z = 16\pi^2 \left(\frac{2}{5}\sqrt{3}\, d_{xz} d_{z^2} \cdot R_d^2 + \sqrt{\frac{3}{5}}\, s d_{yz} \cdot \rho_s \rho_d^*\right)$$

The CDAD can be found from the equation:

$$\frac{I_{CDAD}}{c_\sigma} = 2 \cdot P_c \cdot \left\{\cos(\vartheta_q) \cdot \Im(\xi_x \xi_y^*) - \sin(\vartheta_q) \cdot \Im(\xi_y^* \xi_z)\right\}$$

The angular dependent functions are all real, and one has to take the Real and Imaginary part only of the part arising from the combination of different complex matrix elements. The products of the radial matrix elements are given by:

$$\rho_s \rho_d^* = (-i)^0 \cdot R_s \exp(i\delta_s) \cdot (i)^2 \cdot R_d \exp(-i\delta_d) = -R_s R_d \exp(-i(\delta_d - \delta_s)$$

$$\rho_s^* \rho_d = (i)^0 \cdot R_s \exp(-i\delta_s) \cdot (-i)^2 \cdot R_d \exp(i\delta_d) = -R_s R_d \exp(i(\delta_d - \delta_s)$$

so that their real and imaginary parts are described by:

$$\Re(\rho_s \rho_d^*) = -R_s R_d \cos(\delta_d - \delta_s)$$
$$\Im(\rho_s \rho_d^*) = +R_s R_d \sin(\delta_d - \delta_s)$$

$$\Re(\rho_s^* \rho_d) = -R_s R_d \cos(\delta_d - \delta_s)$$
$$\Im(\rho_s^* \rho_d) = -R_s R_d \sin(\delta_d - \delta_s)$$

Inserting these imaginary parts we finally find for theCDAD of initial real p-orbitals:

a) p_x

$$\frac{I_{CDAD}^{p_x}}{16\pi^2 c_\sigma} = -2 \cdot \sqrt{\frac{3}{5}} \cdot \cos(\vartheta_q) \cdot s d_{xy} \cdot R_s R_d \cdot \sin(\delta_d - \delta_s)$$

$$-\frac{3}{4\pi} \cdot \cos(\vartheta_q) \cdot \sin^2(\vartheta)\sin(2\varphi) \cdot R_s R_d \cdot \sin(\delta_d - \delta_s)$$

b) p_y

$$\frac{I^{p_y}_{CDAD}}{16\pi^2 c_\sigma} = 2\cdot\sqrt{\frac{3}{5}}\cdot\left[\cos(\vartheta_q)\cdot sd_{xy} + \sin(\vartheta_q)\cdot sd_{yz}\right]\cdot R_s R_d\cdot\sin(\delta_d-\delta_s)$$

$$\frac{3}{4\pi}\cdot\left[\cos(\vartheta_q)\cdot\sin^2(\vartheta)\sin(2\varphi) + \sin(\vartheta_q)\cdot\sin(2\vartheta)\sin(\varphi)\right]\cdot R_s R_d\cdot\sin(\delta_d-\delta_s)$$

c) p_z

$$\frac{I^{p_z}_{CDAD}}{16\pi^2 c_\sigma} = -2\cdot\sqrt{\frac{3}{5}}\sin(\vartheta_q)\cdot sd_{yz}\cdot R_s R_d\cdot\sin(\delta_d-\delta_s)$$

$$-\frac{3}{4\pi}\cdot\sin(\vartheta_q)\cdot\sin(2\vartheta)\sin(\varphi)\cdot R_s R_d\cdot\sin(\delta_d-\delta_s)$$

Adding all three terms theCDAD vanishes as expected.

The LDAD is more complicated because we have more terms remaining from the real parts of the equations given above.

VI.2 The case of spin-orbit interaction

VI.2.1 Including the electron spin

We have measured a non vanishing CDAD for Rubidium 4p-states adsorbed at platinum. The 4p shell of Rb is filled by 6 electrons and therefore they may be equally distributed to p_x, p_y and p_z like states. In this case no CDAD is expected as shown above, and is seen also from the spherical symmetry of a filled p-shell. On the other hand the p-states are split into $p_{1/2}$ and $p_{3/2}$ due to spin-orbit interaction that can be resolved easily.

The states are described by the three quantum numbers ℓ, j=$\ell\pm$s and m_j corresponding to the orbital, the total angular momentum and its projection on the z-axis.

The initial state wave functions are described by spinor spherical harmonics that are tensor spherical harmonics for spin ½ particles as given by Varshalovich et al.[5.1]:

$$\begin{aligned}\Omega^{l}_{jm_j}(\vartheta,\varphi) \equiv Y^{l,s=1/2}_{jm_j} &= \sum_{m_l,m_s} C^{j,m_j}_{l,m_l,\frac{1}{2},m_s} Y_{lm_l}(\vartheta,\varphi)\chi_{\frac{1}{2}m_s} \\ &= C^{j,m_j}_{l,m_l=m_j-\frac{1}{2},\frac{1}{2},+\frac{1}{2}} Y_{lm_l}(\vartheta,\varphi)|\uparrow\rangle + C^{j,m_j}_{l,m_l=m_j+\frac{1}{2},\frac{1}{2},-\frac{1}{2}} Y_{lm_l}(\vartheta,\varphi)|\downarrow\rangle \\ &= \begin{pmatrix} a_l(j,m_j)Y_{l,m_j-1/2} \\ b_l(j,m_j)Y_{l,m_j+1/2}\end{pmatrix}\end{aligned}$$

m_ℓ and m_s are the projection quantum numbers of the orbital angular momentum and the electron spin and c are the basis spin functions. The Clebsch-Gordan coefficients C^{j,m_j}_{l,m_l,s,m_s} can be interpreted as probability that the state |l, s, m_l, m_s> contributes to the coupled state|j,m_j>.

The quadratic forms of the spherical harmonics describing the angular distribution of electrons show that the angular distribution of electrons in spin-orbit split states is independent on the orbital angular momentum ℓ and the angle φ meaning it is of rotational symmetry with respect to the z-axis (cylindrical symmetry).

For a filled initial p-state we have 6 different wave functions that differ at least in one quantum number: j=1/2, m_j=±1/2 and j=3/2, m_j=±3/2,±1/2. From $W_{1/2,1/2}=|Y_{00}|^2$ we see that the distribution of electrons in the $p_{1/2}$- or $s_{1/2}$- states are spherical symmetric and do not expect that CDAD occurs. Moreover for all filled shells a spherical symmetric charge distribution is obtained in averaging over all m_j substates for given total angular momentum j, therefore *no* CDAD is expected for emission from unperturbed filled shells.

By applying the equations to determine the photoelectron cross sections as described above we get the spin resolved intensities. In our PIPE experiments the electron spin is not measured and therefore we obtain the intensities from an incoherent superposition of the cross sections for spin up and spin down electrons.

In our experiments we observed CDAD for initial states with spherical symmetry as well for C-1s as for Rb-$4p_{1/2}$ states that cannot explained by the formalism described above where we assumed emission from free atoms. In the following we will discuss the influence of the surface showing that this is the origin of the measured effects.

Three spherical harmonics are contributing to the spin orbit resolved $p_{1/2,3/2}$ states, namely Y_{10}, Y_{11}, and Y_{1-1}. The G functions connected to these three spherical harmonics are given in the Appendix. From the equations for G_{circ} it is seen that for truly oriented states the CDAD does not vanish if z,k and

q are parallel (or antiparallel, respectively), that is for Φ_q=0, ϑ=0. How such a state can be prepared is discussed in connection with magnetic effects.

As shown above, I_{CDAD} is given by $2G_{circ}$, applying this relation to the $p_{\pm 1/2}$ states we have:

$$\frac{I_{CDAD}^{m_j=+1/2}}{4c_\sigma \pi R_d^2} = \{\sin(\Phi_q)\sin(2\vartheta)\cdot\sin(\delta_d-\delta_s)\cdot r_s + \ldots$$
$$\ldots + \tfrac{2}{3}\cos(\Phi_q)\{[3\cdot\sin^2(\vartheta)-1]-[3\cos^2(\vartheta)-1]\cos(\delta_d-\delta_s)\cdot r_s - r_s^2\} + \ldots$$
$$\ldots + \sin(\Phi_q)\sin(2\vartheta)\cdot\sin(\delta_d-\delta_s)\cdot r_s\}$$

$$\frac{I_{CDAD}^{m_j=-1/2}}{4c_\sigma \pi R_d^2} = \{-\tfrac{2}{3}\cos(\Phi_q)\{[3\cdot\sin^2(\vartheta)-1]-[3\cos^2(\vartheta)-1]\cos(\delta_d-\delta_s)\cdot r_s - r_s^2\} - \ldots$$
$$\ldots - \sin(\Phi_q)\sin(2\vartheta)\cdot\sin(\delta_d-\delta_s)\cdot r_s\}$$

In the case of an incoherent superposition of the intensities we have spin resolved:

$$\frac{I_{CDAD}^{\uparrow\downarrow}}{4c_\sigma \pi R_d^2} = \{+\sin(\Phi_q)\sin(2\vartheta)\cdot\sin(\delta_d-\delta_s)\cdot r_s - \ldots$$
$$\ldots - \sin(\Phi_q)\sin(2\vartheta)\cdot\sin(\delta_d-\delta_s)\cdot r_s\}$$

Without resolution of the electron spin I_{CDAD} vanishes as expected for a state with spherical symmetry. On the other hand if the two states are split by a magnetic field then we have without spin resolution a CDAD of opposite sign for both states:

$$\frac{I_{CDAD}^{m_j=\pm 1/2}}{8c_\sigma \pi R_d^2} = \pm\ \{\tfrac{1}{3}\cos(\Phi_q)\{[3\sin^2(\vartheta)-1]-[3\cos^2(\vartheta)-1]\cos(\delta_d-\delta_s)\cdot r_s - r_s^2\}\} + \ldots$$
$$\ldots + \sin(\Phi_q)\sin(2\vartheta)\cdot\sin(\delta_d-\delta_s)\cdot r_s\}$$

Note that a magnetic field to produce the splitting (similar to Zeeman-effect) must be applied parallel or antiparallel to the surface normal, that may be inconvenient to be prepared in experiments.

VI.2.2 · Spin-orbit interaction in the final state

In the description above we have omitted the possibility of spinflip as well as the j-dependency of the phases and radial matrix elements of the final states.

The S-O-split states are described by the wave functions:

$$|\ell, s, j, m_j> = |\ell, m_\ell, s, m_s, j=\ell+s, m_j=m_\ell+m_s>$$

Where m_ℓ and m_s are not good quantum numbers. From the dipole selection rules we have for the final state $\Delta\ell$=1 and Δm=0,±1. Now we have to consider the conservation of the total angular momentum leading to the selection ruleΔj=0,±1 in addition. Thus the final states are given by:

$|\ell', s=1/2, j', m_j'> = |\ell'=\ell\pm1, s=1/2, j'=j,j\pm1, m_j'=m_j,m_j\pm1>$

making use that m_j is a good quantum number. The dipole-operator does not act directly on the spin, but a specific fixed $m_j'=m_\ell'+m_s'=m_j\pm1$ can be reached by $\Delta m_\ell=\pm1$, $\Delta m_s=0$ as well as $\Delta m_\ell=0$, $\Delta m_s=\pm1$, bearing in mind that the m's cannot exceedℓ, s, or j.

Two new features are shown, firstly the final state wave functions now depend on j rather than ℓ and therefore we have to use j-dependent phases δ_j and matrix elements R_j. These quantities can be computed by solving numerically the Dirac-equation for bound and free states using either a suitable potential or directly a Hartree-Fock method. Secondly, even in transitions from states with pure spin orientation (say $Y_{00}|\uparrow>$ like $s_{1/2,1/2}$) the final states can be build partly by a mixture of $|\uparrow>$ and $|\downarrow>$ states showing the possibility of spinflip

The initial states are given by the spinor spherical harmonics described above:

$$\phi_i = \Omega_{j,m_j}^l(\hat{r})\cdot R_{n,l,j} = \begin{pmatrix} a_l(j,m_j)\ Y_{l,m_j-1/2}(\hat{r}) \\ b_l(j,m_j)\ Y_{l,m_j+1/2}(\hat{r}) \end{pmatrix} R_{n,l,j}$$

Where a and b are the Clebsch-Gordan coefficients for m_s=+1/2 and -1/2, and $\hat{r}$ is the unit position vector describing the angular dependence. The final states are expanded in a sum of spinor spherical harmonics given by:

$$\phi_f = 4\pi \sum_{l',j',m_j'} (-i)^{l'}\Omega_{j',m_j'}^{l'+}(\hat{k})\Omega_{j',m_j'}^{l'}(\hat{r})R_{f'}\exp\{i\delta_{f'}\}$$

Inserting both states we find that the differential cross-section for a state with given magnetic quantum number m_j is given by:

$$\langle\phi_f|H|\phi_i\rangle = 4\pi \sum_{l',j',m_j'} \left\langle (-i)^{l'}\Omega_{j',m_j'}^{l'+}(\hat{k})\Omega_{j',m_j'}^{l'}(\hat{r})R_{j'}\exp\{i\delta_{j'}\}\middle|\vec{\varepsilon}\cdot\vec{r}\middle|\Omega_{j,m_j}^{l}(\hat{r})\cdot R_{n,l,j}\right\rangle$$
$$= 4\pi\cdot\vec{\varepsilon}\cdot\sum_{l',j',m_j'}\left\langle\Omega_{j',m_j'}^{l'}(\hat{r})|\hat{r}|\Omega_{j,m_j}^{l}(\hat{r})\right\rangle\cdot\Omega_{j',m_j'}^{l'}(\hat{k})\cdot\rho_{n,l,j}^{l',j'}$$

$$\rho_{n,l,j}^{l',j'} = i^{l'}\exp\{i\delta_{f'}\}\int R_{f'}\cdot r\cdot R_{n,l,j}\cdot r^2 dr$$

The final state radial-function and phase depend on the kinetic energy of the electrons ($\varepsilon=E_{kin}$). The radial integrals depend on the initial and final state radial-functions but are assigned here only by the final state total angular momentum for short:

$$R_{j'} = R_{n,l,j}^{\varepsilon,l',j'} = \int_0^\infty R_{n,l,j}\cdot R_{\varepsilon,l',j'}\cdot r^3 dr$$

From the radial integrals we define the complex radial matrix-element as:

$$\rho_{f'} = i^{l'}R_{f'}\exp\{i\delta_{f'}\} = \rho_{n,l,j}^{\varepsilon,l',j'}$$

To find the angular distribution of the photoelectrons we make use that the angular dependent parts of interest can be written as:

$$\langle f| = \sum_{l'j'm'} \Omega^{l'}_{j'm'_j} = \sum_{l'j'm'} \begin{pmatrix} a_{l'}(j',m'_j)Y_{l\pm1,m'_j-1/2} \\ b_{l'}(j',m'_j)Y_{l\pm1,m'_j+1/2} \end{pmatrix}$$

According to the $\Delta\ell=\pm1$ selection rule this sum can be divided into two parts:

$$\langle f| = \sum_{\substack{j'=l-3/2,\,l-1/2 \\ m'_j=m_j,\,m_j\pm1}} \begin{pmatrix} a_{l-1}(j',m'_j)Y_{l-1,m'_j-1/2} \\ b_{l-1}(j',m'_j)Y_{l-1,m'_j+1/2} \end{pmatrix} + \sum_{\substack{j'=l+3/2,\,l+1/2 \\ m'_j=m_j,\,m_j\pm1}} \begin{pmatrix} a_{l+1}(j',m'_j)Y_{l+1,m'_j-1/2} \\ b_{l+1}(j',m'_j)Y_{l+1,m'_j+1/2} \end{pmatrix}$$

Note that the selection rules must be fulfilled, limiting the number of possible final states. For initial s-states only final p-states are possible. For initial p-states one has two (j=1/2) or three (j=3/2) final j'-states depending on j, whereas in all other cases with $\ell>1$ a maximum of three j'-states are reachable. It is worthwhile to note that the selection rules are superfluous to be used a priory because they are included in the properties of the Clebsch-Gordan coefficients that occur during the various steps in the calculations. On the other hand they prevent doing some unnecessary work.

Finally the transition probability matrix elements M_{if} can be calculated as in the case of reel orbitals and from these the ξ-functions needed to determine the polarisation dependent differential cross sections.

$$M_{if} = \langle f|\underline{H}|i\rangle = \left\langle \Omega^{l'}_{j'm'_j}\middle|\,\vec{\varepsilon}\cdot\hat{r}\,\middle|\Omega^{l}_{jm_j}\right\rangle$$
$$\vec{\varepsilon}\cdot M_{if} = \langle f|\underline{H}|i\rangle = \vec{\varepsilon}\cdot\left\langle \Omega^{l'}_{j'm'_j}\middle|\hat{r}\middle|\Omega^{l}_{jm_j}\right\rangle$$

To calculate the transition probability matrix elements one makes use of the orthonormality of the spin functions, that is $\langle\uparrow|\downarrow\rangle=0$ and $\langle\uparrow|\uparrow\rangle=1$. Inserting the initial and final state wavefunction in matrix representation we have:

$$M_{if} = \int_0^{\pi}\left\{\int_0^{2\pi}\Omega^{l'+}_{j'm'_j}\sqrt{\tfrac{2\pi}{3}}\,Y_{k=1,\beta=0,\pm1}\Omega^{l}_{jm_j}d\varphi\right\}\sin(\vartheta)d\vartheta$$

$$= \sqrt{\tfrac{2\pi}{3}}\iint\begin{pmatrix} a'Y^*_{l',m'_j-1/2} & b'Y^*_{l',m'_j+1/2}\end{pmatrix}Y_{k=1,\beta=0,\pm1}\begin{pmatrix} aY_{l,m_j-1/2} \\ bY_{l,m_j+1/2}\end{pmatrix}d\varphi\sin(\vartheta)d\vartheta$$

$$= \{a'a\cdot g(l\pm1,m_j+\beta-1/2,l,m_j-1/2)+b'b\cdot g(l\pm1,m_j+\beta+1/2,l,m_j+1/2)\}$$

$$= \gamma^l_\beta(j',m'_j,j,m_j)$$

The abbreviations $a=a_\ell(j,m_j)$ and $b=b_\ell(j,m_j)$ and similar for the primed coefficients are used. The modified Spinor-Gaunt-coefficients $\gamma^l_\beta(j',m'_j,j,m_j)$ for spinflip emission are shown in the appendix.

Using the modified Gaunt-coefficients γ_j, the ξ-functions for initial s- and p- states are given by the following equations. Thereby we use the complex radial matrix element as given above, but take 2j as index for abbreviation:

$$\rho^l_{2j} = i^l R_{n,l,j}\exp\{i\delta_{l,j}\}$$

a1) $s_{1/2,+1/2} \rightarrow p$

$$\Xi(s_{1/2,+1/2}) = \begin{Bmatrix} \left\{\left(\sqrt{\frac{1}{6}}\, p_{3/2,3/2} - \sqrt{\frac{1}{18}}\, p_{3/2,-1/2}\right)\cdot \rho_3^1 + \frac{1}{3} p_{1/2,-1/2}\cdot \rho_1^1\right\} \\ -i\left\{\left(\sqrt{\frac{1}{6}}\, p_{3/2,3/2} + \sqrt{\frac{1}{18}}\, p_{3/2,-1/2}\right)\cdot \rho_3^1 - \frac{1}{3} p_{1/2,-1/2}\cdot \rho_1^1\right\} \\ -\sqrt{2}\left\{\frac{1}{3} p_{3/2,1/2}\cdot \rho_3^1 - \sqrt{\frac{1}{18}}\, p_{1/2,1/2}\cdot \rho_1^1\right\} \end{Bmatrix}$$

a2) $s_{1/2,-1/2} \rightarrow p$

$$\Xi(s_{1/2,-1/2}) = \begin{Bmatrix} -\left\{\left(\sqrt{\frac{1}{6}}\, p_{3/2,-3/2} - \sqrt{\frac{1}{18}}\, p_{3/2,1/2}\right)\cdot \rho_3^1 - \frac{1}{3} p_{1/2,1/2}\cdot \rho_1^1\right\} \\ -i\left\{\left(\sqrt{\frac{1}{6}}\, p_{3/2,-3/2} + \sqrt{\frac{1}{18}}\, p_{3/2,1/2}\right)\cdot \rho_3^1 + \frac{1}{3} p_{1/2,1/2}\cdot \rho_1^1\right\} \\ -\sqrt{2}\left\{\frac{1}{3} p_{3/2,-1/2}\cdot \rho_3^1 + \sqrt{\frac{1}{18}}\, p_{1/2,-1/2}\cdot \rho_1^1\right\} \end{Bmatrix}$$

b1) $p_{1/2,+1/2} \rightarrow s,d$

$$\Xi(p_{1/2,+1/2}) = \begin{Bmatrix} \left\{\left(\sqrt{\frac{1}{6}}\, d_{3/2,3/2} - \sqrt{\frac{1}{18}}\, d_{3/2,-1/2}\right)\cdot \rho_3^2 - \frac{1}{3} s_{1/2,-1/2}\cdot \rho_1^0\right\} \\ -i\left\{\left(\sqrt{\frac{1}{6}}\, d_{3/2,3/2} + \sqrt{\frac{1}{18}}\, d_{3/2,-1/2}\right)\cdot \rho_3^2 + \frac{1}{3} s_{1/2,-1/2}\cdot \rho_1^0\right\} \\ -\sqrt{2}\left\{\frac{1}{3} d_{3/2,1/2}\cdot \rho_3^2 + \sqrt{\frac{1}{18}}\, s_{1/2,1/2}\cdot \rho_1^0\right\} \end{Bmatrix}$$

b2) $p_{1/2,-1/2} \rightarrow s,d$

$$\Xi(p_{1/2,-1/2}) = \begin{Bmatrix} -\left\{\left(\sqrt{\frac{1}{6}}\, d_{3/2,-3/2} - \sqrt{\frac{1}{18}}\, d_{3/2,1/2}\right)\cdot \rho_3^2 + \frac{1}{3} s_{1/2,1/2}\cdot \rho_1^0\right\} \\ -i\left\{\left(\sqrt{\frac{1}{6}}\, d_{3/2,-3/2} + \sqrt{\frac{1}{18}}\, d_{3/2,1/2}\right)\cdot \rho_3^2 - \frac{1}{3} s_{1/2,1/2}\cdot \rho_1^0\right\} \\ -\sqrt{2}\left\{\frac{1}{3} d_{3/2,-1/2}\cdot \rho_3^2 - \sqrt{\frac{1}{18}}\, s_{1/2,-1/2}\cdot \rho_1^0\right\} \end{Bmatrix}$$

c1) $p_{3/2,3/2} \rightarrow s,d$

$$\Xi(p_{3/2,+3/2}) = \begin{Bmatrix} \left\{\left(\sqrt{\frac{1}{5}}\, d_{5/2,5/2} - \sqrt{\frac{1}{50}}\, d_{5/2,1/2}\right)\cdot \rho_5^2 + \sqrt{\frac{1}{75}}\, d_{3/2,1/2}\cdot \rho_3^2 - \sqrt{\frac{1}{6}}\, s_{1/2,1/2}\cdot \rho_1^0\right\} \\ -i\left\{\left(\sqrt{\frac{1}{5}}\, d_{5/2,5/2} + \sqrt{\frac{1}{50}}\, d_{5/2,1/2}\right)\cdot \rho_5^2 - \sqrt{\frac{1}{75}}\, d_{3/2,1/2}\cdot \rho_3^2 + \sqrt{\frac{1}{6}}\, s_{1/2,1/2}\cdot \rho_1^0\right\} \\ -\sqrt{2}\left\{\sqrt{\frac{2}{25}}\, d_{5/2,3/2}\cdot \rho_5^2 - \sqrt{\frac{1}{50}}\, d_{3/2,3/2}\cdot \rho_3^2\right\} \end{Bmatrix}$$

c2) $p_{3/2,1/2} \rightarrow s,d$

$$\Xi(p_{3/2,1/2}) = \begin{Bmatrix} \left\{\left(\sqrt{\frac{3}{25}}\, d_{5,3} - \sqrt{\frac{3}{50}}\, d_{5,-1}\right)\cdot \rho_5^2 + \left(\sqrt{\frac{1}{75}}\, d_{3,3} + \frac{2}{15} d_{3,-1}\right)\cdot \rho_3^2 - \sqrt{\frac{1}{18}}\, s_{1,-1}\cdot \rho_1^0\right\} \\ -i\left\{\left(\sqrt{\frac{3}{25}}\, d_{5,3} + \sqrt{\frac{3}{50}}\, d_{5,-1}\right)\cdot \rho_5^2 + \left(\sqrt{\frac{1}{75}}\, d_{3,3} - \frac{2}{15} d_{3,-1}\right)\cdot \rho_3^2 + \sqrt{\frac{1}{18}}\, s_{1,-1}\cdot \rho_1^0\right\} \\ -\sqrt{2}\left\{\sqrt{\frac{3}{25}}\, d_{5,1}\cdot \rho_5^2 - \sqrt{\frac{1}{450}}\, d_{3,1}\cdot \rho_3^2 - \frac{1}{3} s_{1,1}\cdot \rho_1^0\right\} \end{Bmatrix}$$

c3) $p_{3/2,-1/2} \rightarrow s,d$

$$\Xi(p_{3/2,-1/2}) = \begin{Bmatrix} -\left\{\left(\sqrt{\frac{3}{25}}\, d_{5,-3} - \sqrt{\frac{3}{50}}\, d_{5,1}\right)\cdot \rho_5^2 - \left(\sqrt{\frac{1}{75}}\, d_{3,-3} + \frac{2}{15} d_{3,1}\right)\cdot \rho_3^2 - \sqrt{\frac{1}{18}}\, s_{1,1}\cdot \rho_1^0\right\} \\ -i\left\{\left(\sqrt{\frac{3}{25}}\, d_{5,-3} + \sqrt{\frac{3}{50}}\, d_{5,1}\right)\cdot \rho_5^2 - \left(\sqrt{\frac{1}{75}}\, d_{3,-3} - \frac{2}{15} d_{3,1}\right)\cdot \rho_3^2 + \sqrt{\frac{1}{18}}\, s_{1,1}\cdot \rho_1^0\right\} \\ -\sqrt{2}\left\{\sqrt{\frac{3}{25}}\, d_{5,-1}\cdot \rho_5^2 + \sqrt{\frac{1}{450}}\, d_{3,-1}\cdot \rho_3^2 - \frac{1}{3} s_{1,-1}\cdot \rho_1^0\right\} \end{Bmatrix}$$

c4) $p_{3/2,-3/2} \rightarrow s,d$

$$\Xi(p_{3/2,-3/2}) = \begin{Bmatrix} -\left\{\left(\sqrt{\frac{1}{5}}\, d_{5/2,-5/2} - \sqrt{\frac{1}{50}}\, d_{5/2,-1/2}\right)\cdot \rho_5^2 - \sqrt{\frac{1}{75}}\, d_{3/2,-1/2}\cdot \rho_3^2 - \sqrt{\frac{1}{6}}\, s_{1/2,-1/2}\cdot \rho_1^0\right\} \\ -i\left\{\left(\sqrt{\frac{1}{5}}\, d_{5/2,-5/2} + \sqrt{\frac{1}{50}}\, d_{5/2,-1/2}\right)\cdot \rho_5^2 + \sqrt{\frac{1}{75}}\, d_{3/2,-1/2}\cdot \rho_3^2 + \sqrt{\frac{1}{6}}\, s_{1/2,-1/2}\cdot \rho_1^0\right\} \\ -\sqrt{2}\left\{\sqrt{\frac{2}{25}}\, d_{5/2,-3/2}\cdot \rho_3^2 + \sqrt{\frac{1}{50}}\, d_{3/2,-3/2}\cdot \rho_3^2\right\} \end{Bmatrix}$$

We write the spin-up and spin down parts of the Ξ-functions using spherical harmonics to calculate the CDAD of the spin-orbit split initial states.

For $s_{1/2}$ states we find:

a) $s_{1/2,+1/2} \rightarrow p$

$$\begin{aligned} \xi\uparrow_x &= \sqrt{\tfrac{1}{6}}\, Y_{11}\cdot \rho_3^1 - \tfrac{1}{6}\sqrt{\tfrac{2}{3}}\, Y_{1-1}\cdot(\rho_3^1 + 2\cdot\rho_1^1) \\ \xi\downarrow_x &= -\tfrac{1}{3}\sqrt{\tfrac{1}{3}}\, Y_{10}\cdot(\rho_3^1 - \rho_1^1) \\ \xi\uparrow_y &= -i\cdot\left\{\sqrt{\tfrac{1}{2}}\, Y_{11}\cdot\rho_3^1 + \tfrac{1}{3}\sqrt{\tfrac{1}{2}}\, Y_{1-1}\cdot(\rho_{3/2}^1 + 2\cdot\rho_1^1)\right\} \\ \xi\downarrow_y &= -i\cdot\left\{\tfrac{1}{3}\sqrt{\tfrac{1}{3}}\, Y_{10}\cdot(\rho_3^1 - \rho_1^1)\right\} \\ \xi\uparrow_z &= -\tfrac{1}{3}\sqrt{\tfrac{1}{3}}\, Y_{10}\cdot(2\cdot\rho_3^1 + \rho_1^1) \\ \xi\downarrow_z &= -\tfrac{2}{3}\sqrt{\tfrac{1}{3}}\, Y_{11}\cdot(\rho_3^1 - \rho_1^1) \end{aligned}$$

b) $s_{1/2,-1/2} \rightarrow p$

$$\begin{aligned} \xi\uparrow_x &= \tfrac{1}{3}\sqrt{\tfrac{1}{3}}\, Y_{10}\cdot(\rho_3^1 - \rho_1^1) \\ \xi\downarrow_x &= -\sqrt{\tfrac{1}{6}}\, Y_{1-1}\rho_3^1 + \tfrac{1}{6}\sqrt{\tfrac{2}{3}}\, Y_{11}\cdot(\rho_3^1 + 2\cdot\rho_1^1) \\ \xi\uparrow_y &= -i\cdot\tfrac{1}{3}\sqrt{\tfrac{1}{3}}\, Y_{10}\cdot(\rho_3^1 - \rho_1^1) \\ \xi\downarrow_y &= -i\cdot\left\{\sqrt{\tfrac{1}{6}}\, Y_{1-1}\rho_3^1 + \tfrac{1}{6}\sqrt{\tfrac{2}{3}}\, Y_{11}\cdot(\rho_3^1 + 2\cdot\rho_1^1)\right\} \\ \xi\uparrow_z &= -\tfrac{1}{3}\sqrt{\tfrac{2}{3}}\, Y_{1-1}\cdot(\rho_3^1 - \rho_1^1) \\ \xi\downarrow_z &= -\tfrac{1}{3}\sqrt{\tfrac{1}{3}}\, Y_{10}\cdot(2\cdot\rho_3^1 + \rho_1^1) \end{aligned}$$

The influence of spin-orbit interaction to the final state is seen clearly. It leads to a spin flip if there is a difference in the complex final state radial matrix elements, that is if $\rho_{3/2} - \rho_{1/2} \neq 0$.

To calculate the CDAD we have to determine the contributions of the both spin channels and the two m_j substates.

For the $p_{1/2}$ states we find:

a) $p_{1/2,+1/2} \rightarrow$ s,d

$$\xi\uparrow_x = -\sqrt{\tfrac{1}{30}}\,(Y_{21} - Y_{2-1})\cdot\rho_3^2$$
$$\xi\downarrow_x = \left(\sqrt{\tfrac{2}{15}}\,Y_{22} - \tfrac{1}{3}\sqrt{\tfrac{1}{5}}\,Y_{20}\right)\cdot\rho_3^2 - \tfrac{1}{3}Y_{00}\cdot\rho_1^0$$
$$\xi\uparrow_y = i\cdot\sqrt{\tfrac{1}{30}}\,(Y_{21} + Y_{2-1})\cdot\rho_3^2$$
$$\xi\downarrow_y = -i\cdot\left\{\left(\sqrt{\tfrac{2}{15}}\,Y_{22} + \tfrac{1}{3}\sqrt{\tfrac{1}{5}}\,Y_{20}\right)\cdot\rho_3^2 + \tfrac{1}{3}Y_{00}\cdot\rho_1^0\right\}$$
$$\xi\uparrow_z = -\tfrac{2}{3}\sqrt{\tfrac{1}{5}}\,Y_{20}\cdot\rho_3^2 + \tfrac{1}{3}Y_{00}\cdot\rho_1^0$$
$$\xi\downarrow_z = -\sqrt{\tfrac{2}{15}}\,Y_{21}\cdot\rho_3^2$$

b) $p_{1/2,-1/2} \rightarrow$ s,d

$$\xi\uparrow_x = \left(\sqrt{\tfrac{2}{15}}\,Y_{2-2} - \tfrac{1}{3}\sqrt{\tfrac{1}{5}}\,Y_{20}\right)\cdot\rho_3^2 - \tfrac{1}{3}Y_{00}\cdot\rho_1^0$$
$$\xi\downarrow_x = \sqrt{\tfrac{1}{30}}\,(Y_{2-1} - Y_{21})\cdot\rho_3^2$$
$$\xi\uparrow_y = i\cdot\left\{\left(\sqrt{\tfrac{2}{15}}\,Y_{2-2} + \tfrac{1}{3}\sqrt{\tfrac{1}{5}}\,Y_{20}\right)\cdot\rho_3^2 + \tfrac{1}{3}Y_{00}\cdot\rho_1^0\right\}$$
$$\xi\downarrow_y = -i\cdot\sqrt{\tfrac{1}{30}}\,(Y_{2-1} + Y_{21})\cdot\rho_3^2$$
$$\xi\uparrow_z = \sqrt{\tfrac{2}{15}}\,Y_{2-1}\cdot\rho_3^2$$
$$\xi\downarrow_z = -\tfrac{1}{3}\sqrt{\tfrac{2}{5}}\,Y_{20}\cdot\rho_3^2 + \tfrac{1}{3}Y_{00}\cdot\rho_1^0$$

VI.3 References:

[5.1] D.A.Varshalovich, A.N.Moskalev and V.K.Khersonskii; *„Quantum theory of Angular Momentum"*; World Scientific; Singapore (1988)

see also:

U.Fano; Phys.Rev. 178 (1969) 131

T.E.H.Walker, J.T.Waber; J.Phys. B: At.Mol.Phys. 6 (1973) 1165

T.E.H.Walker, J.T.Waber; J.Phys. B: At.Mol.Phys. 7 (1974) 674

S.M.Goldberg, C.S.Fadley, S.Kono; J.Elec.Spec.Rel.Phen. 21 (1981) 285

H.Klar, H.Kleinpoppen; J.Phys. B: At.Mol.Phys. 15 (1982) 933

G.v.d.Laan; Phys.Rev. B51 (1995) 240

N.A.Cherepkov, V.V.Kusnetsov, V.A.Verbitskii; J.Phys. B: At.Mol.Opt.Phys. 28 (1995) 1221

PHYSICAL REVIEW LETTERS

2-3

EXPERIMENTAL VERIFICATION OF THE FANO EFFECT

J. Kessler and J. Lorenz
Physikalisches Institut der Universität Karlsruhe, Karlsruhe, Germany

(Received 8 December 1969)

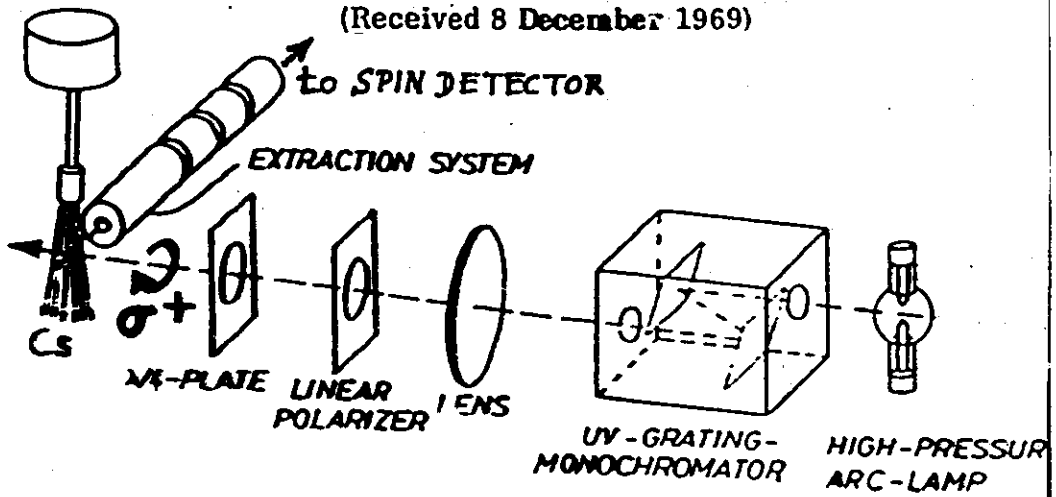

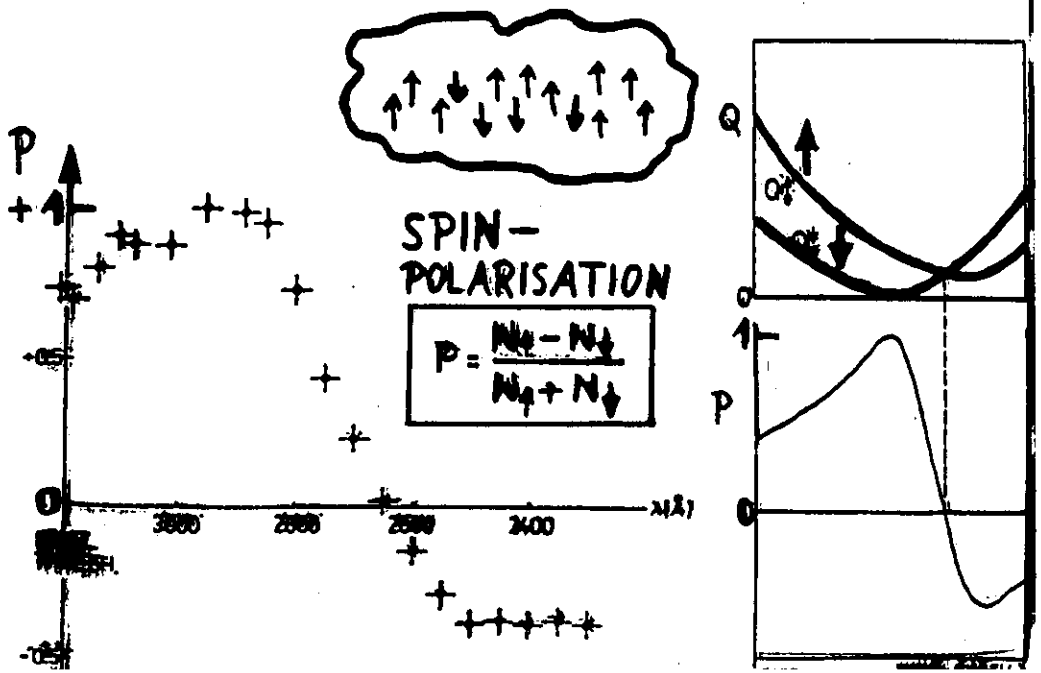

Fano-Effekt an s-Zuständen

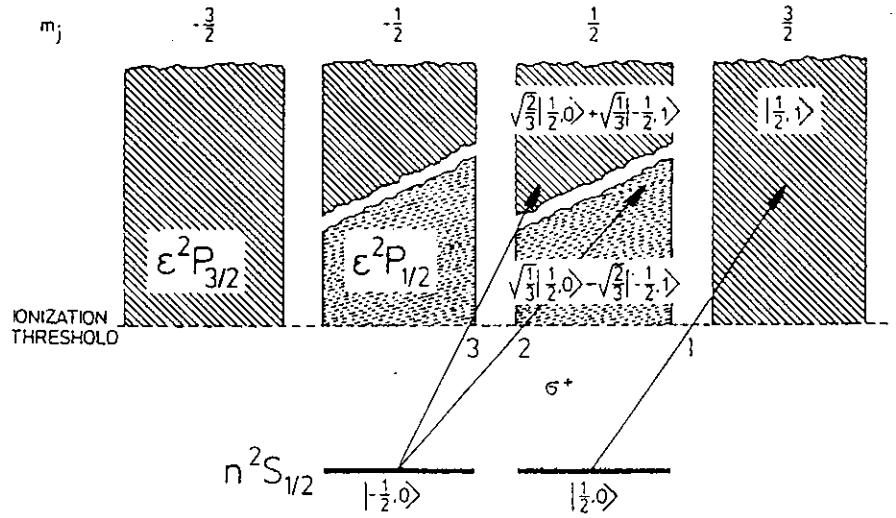

Fig. 5.2. Level diagram for the discussion of the photoionization of alkali atoms. The angular-momentum properties of the states are characterized by combinations of the kets $|m_s, m_l\rangle$

Ke

Alkali-Atome: $ns(^2S_{1/2})$

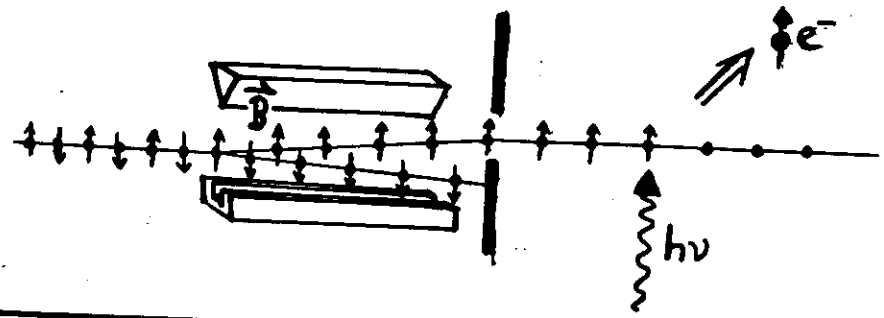

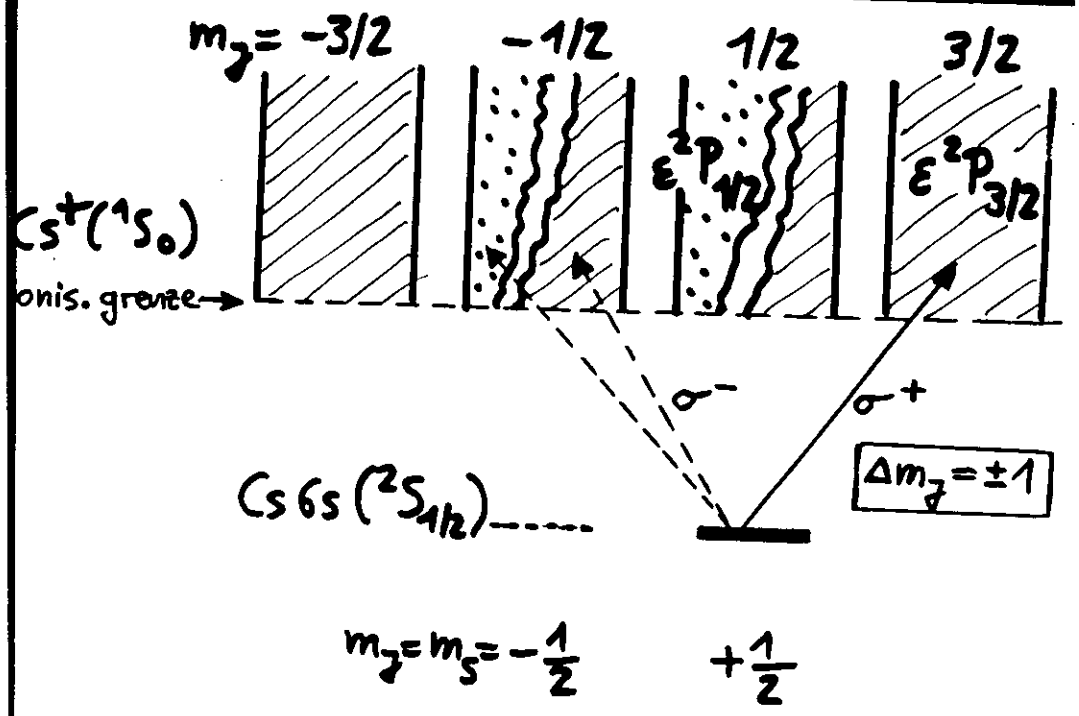

$m_j = m_s = -\frac{1}{2}$ $+\frac{1}{2}$

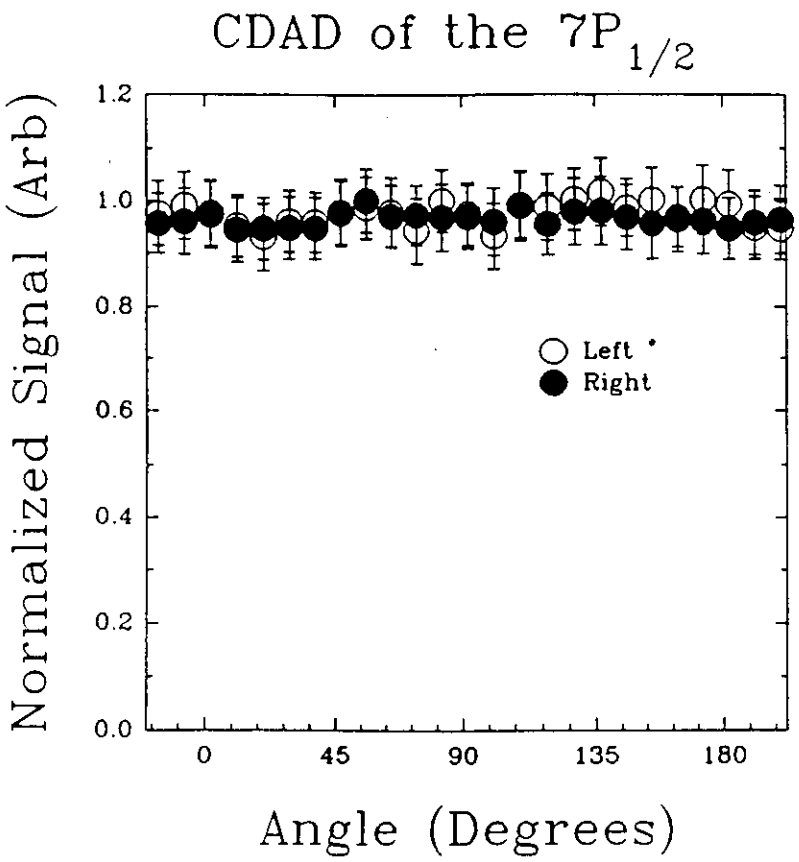

Fig. 4.40. Photoelectron angular distributions from the $7^2P_{1/2}$ state of cesium using both left and right circular polarized light.

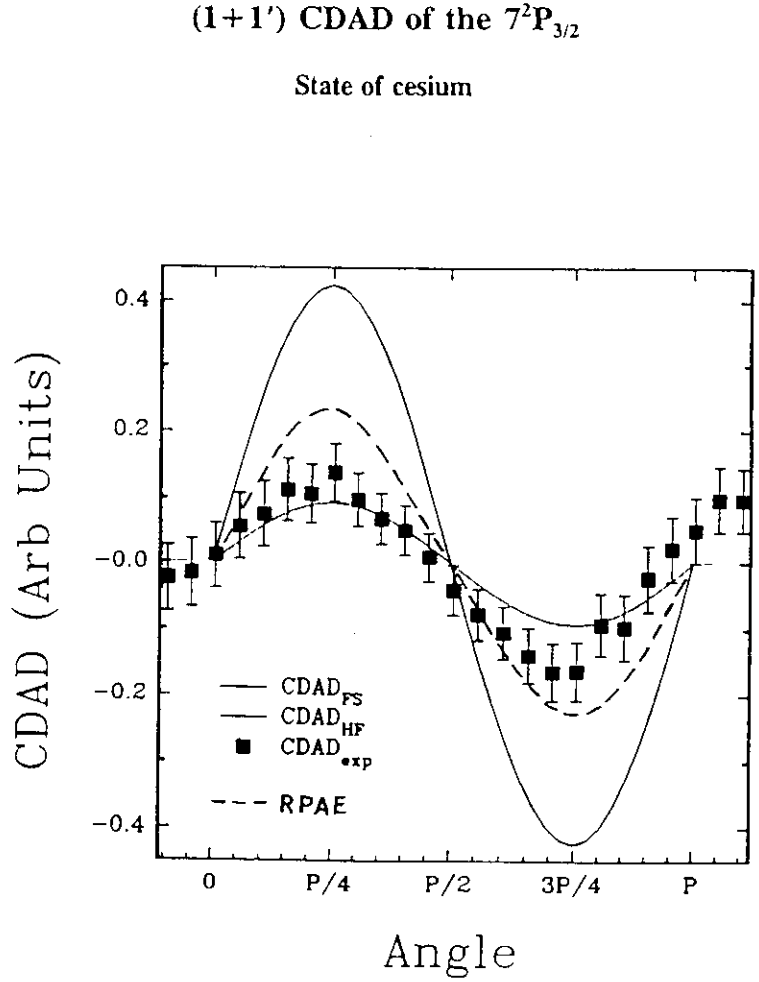

Fig. 4.37. Observed CDAD of the $7^2P_{3/2}$ state of cesium. Theoretical calculations by Dubs, *et al.*[74] Dashed curve is the long time limit using the model of Greene and Zare.[5]

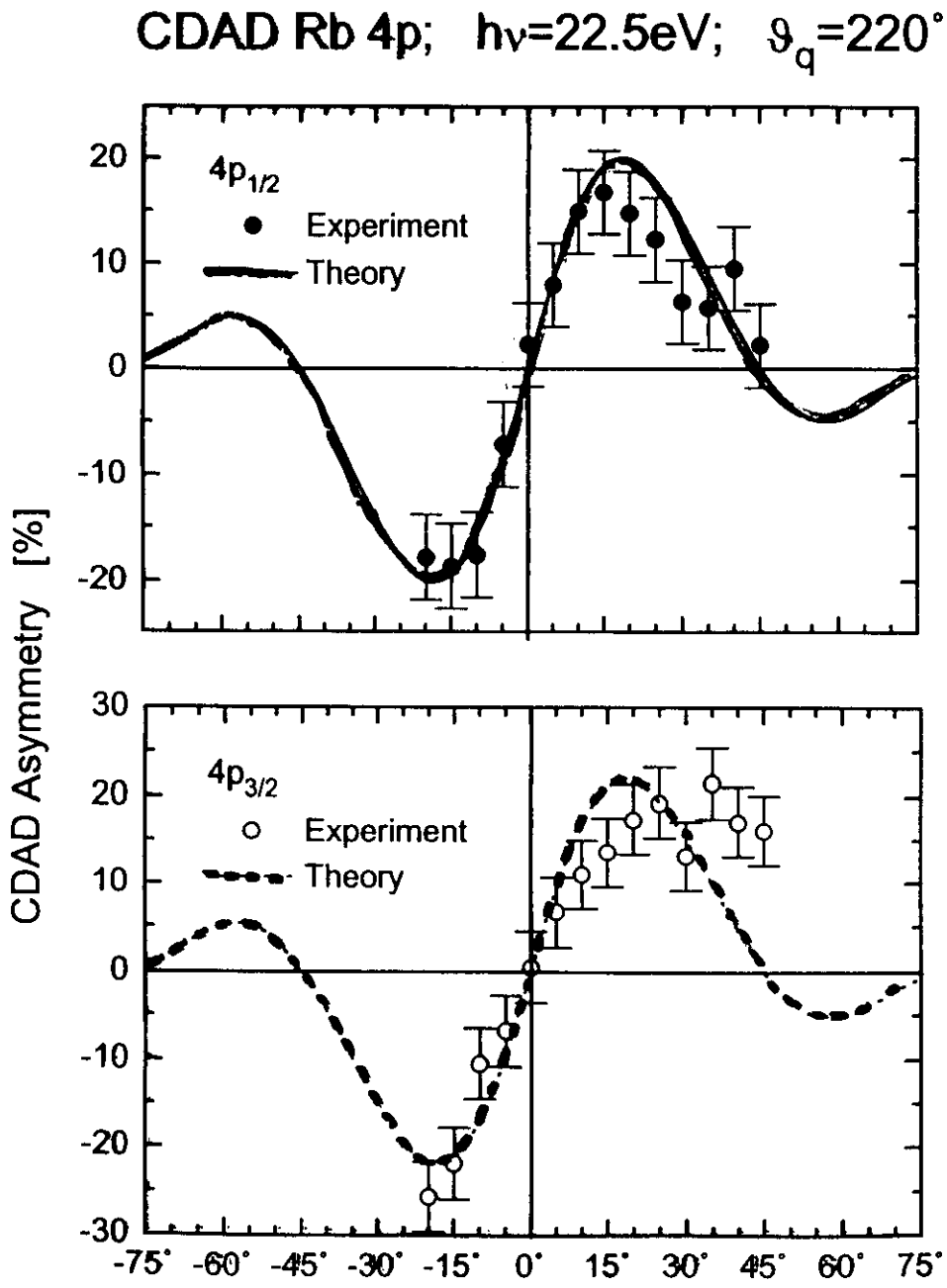

VIII Initial state effects: Perturbation of states at surfaces

Initial state effects occur in photoemission due to a perturbation of the initial state wave functions.

VIII.1 Initial state effects in emission from real orbitals

Gadzuk [7.1] has first discussed the influence of initial state effects on the photoemission angular distribution from real orbitals of adsorbed atoms. He explains initial state effects as initial state interference of the adsorbate valence orbitals with such from a d-band substrate. He used the tight binding approximation to find for the initial state wavefunction $|i_l\rangle$ that is build by coupling of the pure initial state $|l\rangle$ to the metal orbital $|\varphi_g\rangle$ of symmetry g:

$$|i_l\rangle = |l\rangle + \sum_j a_j \cdot \beta_g |\varphi_g\rangle$$

$$\beta_g = \frac{1}{N_g} \sum_{j=1}^{N_g} a_j \frac{\langle \varphi_g | H | i \rangle}{\varepsilon_l - \bar{\varepsilon}}$$

Where the sum is taken on all N_g nearest neighbours in the substrate. $a_j=\pm 1$ are geometry dependent phase factors matching the sign of the coupledwavefunction:

$$a_j = sign\left(\langle l(\hat{R}_j)\rangle \cdot \langle \varphi_g(-\hat{R}_j)\rangle\right)$$

β_g measures the coupling strength if the interaction energy is given by H. The sum can be expressed as a bond site structure factor depending on the momentum k of the emitted electron:

$$S(i,g,k) = \sum_j \frac{a_j}{N_g} \exp\left\{-i\vec{k}\cdot\vec{R}_j\right\} = \sum_j \frac{a_j}{N_g} \exp\{-i\left[k_x r_{xj} + k_y r_{yj} + k_z r_{zj}\right]\}$$
$$= \sum_j \frac{a_j}{N_g} \exp\{-i\cdot|k|\cdot\left[x_j \sin(\vartheta)\cos(\varphi) + y_j \sin(\vartheta)\sin(\varphi) + z_j \cos(\vartheta)\right]\}$$

The final state is then of the form:

$$|f_{\pm 1}\rangle = |l \pm 1\rangle + |\varphi_{g,l\pm 1}\rangle$$

Gadzuk has discussed only pdσ and sdσ like coupling of the states. But in general one has to take idπ and idδ (i=s,p) like bonding into account, too.

The tables for the structure factors for On-Top, 2-fold bridge, and 4-fold hollow sites are given in the appendix.

In the work of Gadzuk the wave functions as given above are not normalised, and the interaction strength is not seen directly. In the LCAO approximation, the initial state wave functions are described by:

$$|i_p\rangle = u_1 \Psi_p + u_2 \Psi_d$$

$$|i_d\rangle = u_2 \Psi_p - u_1 \Psi_d$$

We apply first order perturbation theory to this state. From the secular equation we calculate for the energy dependencyE(k) of the coupled state:

$$\varepsilon = \frac{W_i + W_d}{2} \pm \sqrt{\left(\frac{W_i - W_d}{2}\right)^2 + |W_{id}(k)|^2}$$

To estimate the coupling coefficients we choose the phase of the first coupling coefficient such that it becomes real and calculate the second according to the structure factor above, so that the initial state reads:

$$|i\rangle = c\left\{\left(1 + \sqrt{1+|a|^2}\right)\cdot|i_i\rangle + a\cdot|\varphi_g\rangle\right\}$$

$$a = \frac{|W_{id}|}{\Delta\varepsilon} S(i,g,k) \qquad c^2 = \frac{1}{2\left(1+|a|^2+\sqrt{1+|a|^2}\right)}$$

Here W_{id} is the exchange energy and $\Delta\varepsilon=|W_i-W_d|/2$ the difference of the binding energies of the adsorbate valence orbital and the substrate d-band, both taken at k=0. W_{id} can be calculated from the bandwitdth E_{BW} of the coupled state:

$$\frac{W_{id}}{\Delta\varepsilon} = \sqrt{\left(\frac{E_{BW}}{\Delta\varepsilon}\right)^2 + \left|\frac{2\cdot E_{BW}}{\Delta\varepsilon}\right|}$$

From the initial state we find theξ-functions describing the photoemission matrix elementM_{if} to be:

$$\vec{\xi} = \frac{1+\sqrt{1+|a|^2}}{c}\cdot\vec{\xi}_i + \frac{a}{c}\cdot\vec{\xi}_g$$

VIII.1.1 Special case of Oxygen adsorbed onCu(110)

In oxygen adsorption on copper a Cu(111)-p(2x1)-O superstructure is observed. The substrate has a twofold symmetry and only one kind of bridge sites occur. Different kinds of adsorption sites have been discussed like missing row or buckled row models, both in flat and out of plane bridges. Alternatively one may discuss an On-Top adsorption site. We assume an orientation of the adsorbate in rows along the y-axis, the coupling to the copper d-electrons in the different cases can then be established like follows:

adsorption site	initial states		coupling function S(p,d,k)
	coupled state	d-state symmetry	
On-Top	p_z	d_{z2}	$-exp\{i\,k\,h\cos(\vartheta)\}$
Flat bridge	p_y	d_{x2-y2}	$i\,sin(k\,d/2\,sin(\vartheta)sin(\varphi))$

Out of plane Bridge	p_x	d_{xz}	$-exp\{i\,k\,h\,cos(\vartheta)\}\,cos(k_x d_x/2\,sin(\vartheta)cos(\varphi))$
	p_y	d_{yz}	$-exp\{i\,k\,h\,cos(\vartheta)\}\,cos(k\,d_y/2\,sin(\vartheta)sin(\varphi))$
	p_z	d_{yz}	$-i\,exp\{i\,k\,h\,cos(\vartheta)\}\,sin(k\,d_y/2\,sin(\vartheta)sin(\varphi))$

Where k is the electron momentum and h, d are the height above the substrate or the distance between the neighbouring Cu atoms: $d_x=d_{NN}$, $d_y=a$. As shown above, the initial state can be expressed by a coherent superposition of theO-2p and Cu-3d states:

$$c\cdot|i\rangle = a\cdot|O\text{-}2p\rangle + \beta\cdot S(p,d,k)\cdot|Cu\text{-}3d\rangle$$

$$a = \left(1+\sqrt{1+\beta^2|S(k)|^2}\right) \;;\; \beta = \frac{W_{pd}}{\Delta\varepsilon}$$

$$c = \sqrt{2\left(1+\beta^2|S(k)|^2+\sqrt{1+\beta^2|S(k)|^2}\right)}$$

Where β_i is a parameter describing the coupling strength between the oxygen 2p and the Cu 3d electrons. This parameter depends on the energy dispersion of the bands observed for the different symmetries of theCu-2p states [7.2].

Making use of the dipole selection rules $\Delta\ell=\pm1$) the final state can be written as:

$$|f\rangle = \{s\cdot\rho_{O2p-s} - d\cdot\rho_{O2p-d}\} + i\cdot\{p\cdot\rho_{Cu3d-p} - f\cdot\rho_{Cu3d-f}\}$$

$$\rho_i = e^{-i\delta_\ell} R_\ell$$

Here complex radial functions ρ are used. The indices assign the atom and the initial and final state orbital angular momentum.

For the On-Top adsorption we find that the O-$2p_z$ state is mixed with the Cu-$3d_{z2}$. The coupled p_z state is given by:

$$|i\rangle \propto a\cdot|O\text{-}2p_z\rangle + \beta\cdot\exp\{i\cdot k_z h\}\cdot|Cu\text{-}3d_{z^2}\rangle$$

From $|S|^2=1$ we find that this state shows <u>no</u> dispersion in contradiction to the experiment, where all states show dispersion, therefore we can exclude this case of the adsorption site.

Inserting the final state wave function we find the Ξ-function. If the electrons are collected in the y-z-plane at $\varphi=\pi/2$ the equations become simpler:

$$\vec{\Xi}_{OT} = c_p \begin{Bmatrix} 0 \\ 3\sin(\vartheta)\cos(\vartheta) \\ \frac{\rho_s}{\rho_d} - [3\cos^2(\vartheta)-1] \end{Bmatrix} + c_d \cdot \begin{Bmatrix} 0 \\ \sin(\vartheta)\left[2\frac{\rho_p}{\rho_f} - 3(5\cos^2(\vartheta)-1)\right] \\ \cos(\vartheta)\left[4\frac{\rho_p}{\rho_f} - 3(5\cos^2(\vartheta)-3)\right] \end{Bmatrix}$$

$$c_p = a \cdot \frac{\rho_d}{\sqrt{4\pi}} \cdot \frac{1}{\sqrt{3}}$$

$$c_d = i \cdot \beta \cdot \exp\{i \cdot kh\cos(\vartheta)\} \cdot \frac{\rho_f}{\sqrt{4\pi}} \cdot \sqrt{\frac{1}{20}}$$

Here ρ_f denotes the complex radial matrix element. Collecting the photoelectrons in the y-z-plane, the CDAD from the unperturbed O-$2p_z$ state is given by:

$$I^{p_z}_{CDAD} \propto \sin(\vartheta)\cos(\vartheta)R_sR_d\sin(\delta_d-\delta_s)$$

Whereas we find for the coupled case:

$$\begin{aligned} I^{OT}_{CDAD} \propto\ & \sin(\vartheta)\cos(\vartheta)R_sR_d\sin(\delta_d-\delta_s) \\ & + \sqrt{\tfrac{3}{20}}\,\frac{\beta}{a}\sin(\vartheta)\ \{2R_sR_p\cos[kh\cos(\vartheta)+\delta_p-\delta_s] + .. \\ & \quad ... + [5\cos^2(\vartheta)-1]R_sR_f\cos[kh\cos(\vartheta)+\delta_f-\delta_s] - .. \\ & \quad ... - 2[9\cos^2(\vartheta)-1]R_pR_d\cos[kh\cos(\vartheta)+\delta_p-\delta_d] - .. \\ & \quad .. - [\cos^2(\vartheta)+1]R_dR_f\cos[kh\cos(\vartheta)+\delta_f-\delta_d]\} \\ & + \frac{3}{2}\left(\frac{\beta}{a}\right)^2\sin(\vartheta)\cos(\vartheta)[3\cos(\vartheta)-1]R_pR_f\sin(\delta_f-\delta_p) \end{aligned}$$

In the bridge adsorption site the O-$2p_y$ state is coupled to the Cu-3d states. We find for the CDAD for electrons collected in they-z-plane of the uncoupled case:

$$I^{p_y}_{CDAD} \propto -\sin(\vartheta)\cos(\vartheta)R_sR_d\sin(\delta_d-\delta_s)$$

That is the negative of the p_z-CDAD, whereas for the coupled cases it is changed in the following way.

In the case of adsorption in the flat bridge site the oxygen $2p_y$-state is coupled to the copper $3d_{x2-y2}$-state and in the case of the out of plane bridge site we find from the coupling of the $2p_y$ state to the $3d_{yz}$ state. The CDAD of the coupled p_y-states is given by the following equations:

a) For the Flat Bridge site:

$$\begin{aligned} I^{FB}_{CDAD} \propto\ & -\sin(\vartheta)\cos(\vartheta)R_sR_d\sin(\delta_d-\delta_s) \\ & -\sqrt{\tfrac{1}{20}}\,\frac{\beta}{a}\sin^2(\vartheta)\cos(\vartheta)\ \{5\cdot R_sR_f\sin[\delta_f-\delta_s] + .. \\ & \quad ... + 6\cdot R_pR_d\sin[\delta_d-\delta_p] + .. \\ & \quad .. + R_dR_f\sin[\delta_f-\delta_d]\}\cdot\sin(k\tfrac{d}{2}\sin(\vartheta)) \\ & -\frac{3}{2}\left(\frac{\beta}{a}\right)^2\sin^3(\vartheta)\cos(\vartheta)R_pR_f\sin(\delta_f-\delta_p)\cdot\sin^2(k\tfrac{d}{2}\sin(\vartheta)) \end{aligned}$$

a) For the Out of Plane Bridge site:

$$\begin{aligned} I^{OB}_{CDAD} \propto\ & -\sin(\vartheta)\cos(\vartheta)R_sR_d\sin(\delta_d-\delta_s) \\ & + \sqrt{\tfrac{1}{5}}\,\frac{\beta}{a}\sin(\vartheta)\ \{R_sR_p\cos[kh\cos(\vartheta)+\delta_p-\delta_s] - .. \\ & \quad ... - [5\cos^2(\vartheta)-1]R_sR_f\cos[kh\cos(\vartheta)+\delta_f-\delta_s] + .. \\ & \quad ... + 2[3\cos^2(\vartheta)-1]R_pR_d\cos[kh\cos(\vartheta)+\delta_p-\delta_d] + .. \\ & \quad .. + [\cos^2(\vartheta)-2]R_dR_f\cos[kh\cos(\vartheta)+\delta_f-\delta_d]\}\cdot\sin(k\tfrac{d}{2}\sin(\vartheta)) \\ & -3\left(\frac{\beta}{a}\right)^2\sin(\vartheta)\cos(\vartheta)[\cos^2(\vartheta)-2]R_pR_f\sin(\delta_f-\delta_p)\sin^2(k\tfrac{d}{2}\sin(\vartheta)) \end{aligned}$$

VIII.2 References

[7.1] J.W.Gadzuk; Phys.Rev. **B10** (1974) 5030

[7.2] S.Hüfner, „Electronic structure of NiO and related 3-d-transition-metal compounds"; Advances in Physics **43**(2) (1994) 183-356

see also:

J.C.Slater, G.F.Koster; Phys.Rev. **94** (1954) 1498

J.W.Gadzuk; Surf.Sci. **43** (1974) 44

J.W.Gadzuk; Solid State Comm. **15** (1974) 1011

J.W.Gadzuk; Surf.Sci. **53** (1975) 143

J.W.Gadzuk; Phys.Rev. **B12** (1975) 5608

J.F.Herbst; Phys.Rev. **B15** (1977) 3720

S.Froyen, W.A.Harrison; Phys.Rev. **B20** (1979) 2420

R.R.Sharma; Phys.Rev. **B19** (1979) 2813

Y.Boudeville, J.Rosseau-Violet, F.Cyrot-Lackmann, S.N.Khanna; J.Physique **44** (1983) 433

X Photoelectron diffraction

X.1 Scattering and pleochroic effects

One has to involve scattering theory into the photoemission process, if the electron wavelength[2] λ_e is of the order of the interatomic distances. As in the case of reflection, the overall wavefunction is build from the direct wave ϕ_0 and all scattered waves ϕ_j. We neglect multiple scattering and write the wavefunction (or say better: its complex amplitude) in single scattering approximation as:

$$\Psi\left(\vec{r},\vec{k}\right)=\phi_0\left(\vec{r},\vec{k}\right)+\sum_j \phi_j\left(\vec{r},\vec{r}_j,\vec{k}\right)$$

In experiments the detector is situated far away from the emitting centre and all waves 0,j can be taken to have a limiting spherical wave form. Nevertheless, the effective amplitudes and phases are dependent on the photoexcitation matrix element.

The amplitudes of the scattered waves depend on the amplitude of the initial wave and the distance between the emitting and the scattering atom r_j. From the limiting spherical waveform the decay is proportional to $1/r_j$. The scattering excitation probability of thej-th wave is then given by:

$$A_j(r_j,\vartheta_j,\varphi_j)=\frac{\phi_0(\hat{k}=\hat{r}_j)}{r_j}$$

As usual, the scattering angle θ_j is measured with respect to the momentum $\vec{k}_j$ of the primary emitted electron and the momentum of the observed electrons is $\vec{k}_0$. The scattering angle can be calculated from the scalar-product of the unit momentum vectors:

$$\begin{aligned}\cos(\theta_j) &= \hat{k}_0\cdot\hat{k}_j\\ &= \sin(\vartheta)\sin(\vartheta_j)\left[\cos(\varphi)\cos(\varphi_j)+\sin(\varphi)\sin(\varphi_j)\right]+\cos(\vartheta)\cos(\vartheta_j)\\ &= \sin(\vartheta)\sin(\vartheta_j)\cos(\varphi-\varphi_j)+\cos(\vartheta)\cos(\vartheta_j)\end{aligned}$$

If the observation angle is ϑ and the scatterer is situated at a distance r_j and an angle ϑ_j regarding the emitter, where both ϑ and ϑ_j are measured with respect to the surface normal. In the special geometry we use in our experiments we have$\varphi=\pi/2$ and therefore:

$$\theta\left(\varphi=\tfrac{\pi}{2}\right)=\arccos\{\sin(\vartheta)\sin(\vartheta_j)\sin(\varphi_j)+\cos(\vartheta)\cos(\vartheta_j)\}$$

The final state waves ϕ_j are produced by electron atom scattering that is described usually by a complex plane wave scattering factor$f_j(\theta_j)$ including the scattering phaseshiftη_j:

$$f_j(\theta_j)=\left|f_j(\theta_j)\right|\cdot\exp\{i\eta_j(\theta_j)\}$$

The scattering factor is calculated from a partial-wave analysis in terms of the orbital angular momentum ℓ:

$$f(\theta)=\frac{i}{2k}\sum_{l=0}^{\infty}(2l+1)\cdot\{1-\exp\{2i\delta_l\}\}\cdot P_l(\cos(\theta))=\left|f(\theta)\right|\cdot\exp\{i\eta(\theta)\}$$

1 The de-Broglie wavelength of the electrons is given by: $\lambda=2\pi/k$

Where δ_ℓ are the partial-wave phaseshifts and P_ℓ are Legendre polynomials. θ is measured with respect to the momentum of the primary electron.

The overall difference in the path between the primary and the scattered wave is $r_j[1-\cos(\theta_j)]$ and therefore the total phaseshiftα_j of the j-th scattered wave is given by:

$$\begin{aligned}a_j(\theta_j)&=kr_j\left[1-\cos(\theta_j)\right]+\eta_j(\theta_j)\\ kr_j&=2\pi\cdot\frac{r_j}{\lambda}\end{aligned}$$

If we neglect thermal effects and inelastic scattering, the photoelectron intensity can be written in single scattering plane wave(ssc-pw) approximation:

$$\frac{d\sigma}{d\Omega}\propto\left|\phi_0(\vartheta,\phi)+\sum_j\left\{\frac{\phi_0(\vartheta_j,\varphi_j)}{r_j}\cdot\left|f_j(\theta_j)\right|\cdot\exp ia_j(\theta_j)\right\}\right|^2$$

Due to inelastic processes the initial and the scattered waves are damped during their propagation inside the crystal-surface-adsorbate system. The inelastic attenuation length Λ_e or the electron mean free path has to be determined experimentally and the amplitude is expected phenomenologically to fall off by an exponential law $\exp(-L/2\Lambda_e)=\exp(-\gamma L)$. Each wave ϕ_0 and ϕ_j has to be multiplied by such an exponential factor involving the path length L_0 and L_j. Furthermore the amplitude of the scattered wave decreases due to vibrational effects that can be included simply by multiplying each ϕ_j by an associated temperature-dependent Debye-Waller factorW_j.

We assume that the emitting atom is located in the topmost layer and that the shortest path length (parallel to the surface normal) to the vacuum is r_0. The path lengths L_0,L_j depending on the emitting angle for the emitting and thej-th scattering atom are given by:

$$L_0=\frac{r_0}{\cos(\vartheta)}\text{ and }L_j=r_j+\frac{r_0+z_0}{\cos(\vartheta)}$$

The perpendicular distances $z_{j,0}$ can be calculated from r_j and the difference in the path lengths are given by:

$$\Delta L_j=L_j-L_0=r_j\cdot\left\{1-\frac{\cos(\vartheta)}{\cos(\vartheta_j)}\right\}$$

If the overall wavefunction is normalised by$\exp\{-\gamma L_0\}$, than the scattered wave can be written as:

$$\sum_j\phi_0(\vartheta_j,\varphi_j)\cdot\Gamma_j\cdot\left|f(\theta_j(\vartheta,\vartheta_j))\right|\cdot\exp\{ia_j(\theta_j(\vartheta,\vartheta_j))\}$$

$$\Gamma_j=\frac{\exp\{-\gamma\Delta L_j\}\cdot W_j}{r_j}$$

We have to pay attention on two points calculating the damping of the electrons. Firstly, the mean free path and therefore $\gamma=\gamma(E_{kin})$ depends on the kinetic energy of the electrons. Secondly, the mean free path inside the adsorbate layer can differ strongly from that inside of the substrate because it is material specific.

Finally, the overall wave function including scattering is given by:

$$\Psi(\vec{k}) = \left[\phi_0(\vartheta,\phi) + \sum_j \{\phi_0(\vartheta_j,\varphi_j)\cdot\Gamma_j\cdot|f_j(\theta_j)|\cdot\exp ia_j(\theta_j)\}\right]\Gamma_o$$

Where Γ_0 includes the influence from the refraction and damping of the primary wave as described in the previous chapters. The cross section has to be corrected due to the influence of the Debye-Waller factor to Γ_j as described by Fadley. We will discuss it later (see below). Γ_0 influences the PIPE intensity but not the asymmetries. The influence of the scattering to PIPE will be discussed first in general and later for some special examples.

X.2 Dichroism Estimated for Single Scattering Photoelectron diffraction

Before giving examples, we will estimate a more general case of the dichroic signals. We can write the CDAD (and LDAD) equations for the cases of 100% polarisation as:

$$I^{LDAD} = 2c_\sigma\cdot\left\{\cos(\vartheta_q)\Re(\xi_x\xi_y^*) - \sin(\vartheta_q)\Re(\xi_y^*\xi_z)\right\}$$
$$I^{CDAD} = 2c_\sigma\cdot\left\{\cos(\vartheta_q)\Im(\xi_x\xi_y^*) - \sin(\vartheta_q)\Im(\xi_y^*\xi_z)\right\}$$
$$I^s = c_\sigma\cdot|\xi_y|^2$$
$$I^p = c_\sigma\cdot\{\cos^2(\vartheta_q)|\xi_x|^2 - \sin(2\vartheta_q)\Re(\xi_x\xi_z^*) + \sin^2(\vartheta_q)|\xi_z|^2\}$$

From these equations we have to determine the Ξ-functions. As above, we divide those into two parts:

$$\Xi = \Xi_0 + \Xi_r = \begin{Bmatrix}\xi_{x0}\\ \xi_{y0}\\ \xi_{z0}\end{Bmatrix} + \sum_j \begin{Bmatrix}\xi_x(\vartheta_j,\varphi_j)\\ \xi_y(\vartheta_j,\varphi_j)\\ \xi_z(\vartheta_j,\varphi_j)\end{Bmatrix}\frac{f(\theta_j)}{r_j}\exp\{ikr_j(1-\cos(\theta_j))\}$$

For LDAD and CDAD we need the mixed products:

$$\xi_x\xi_y^* = \left[\xi_{x0} + \sum_j \xi_x(\vartheta_j,\varphi_j)\frac{f(\theta_j)}{r_j}\exp i\{kr_j(1-\cos(\theta_j))\}\right]\cdot\left[\xi_{y0}^* + \sum_j \xi_y^*(\vartheta_j,\varphi_j)\frac{f^*(\theta_j)}{r_j}\exp -i\{kr_j(1-\cos(\theta_j))\}\right]$$
$$\xi_y^*\xi_z = \left[\xi_{z0} + \sum_j \xi_z(\vartheta_j,\varphi_j)\frac{f(\theta_j)}{r_j}\exp i\{kr_j(1-\cos(\theta_j))\}\right]\cdot\left[\xi_{y0}^* + \sum_j \xi_y^*(\vartheta_j,\varphi_j)\frac{f^*(\theta_j)}{r_j}\exp -i\{kr_j(1-\cos(\theta_j))\}\right]$$

In the case of filled shells, the direct terms do show neither LDAD nor CDAD and the differences between the direct and the cross terms can be written as inEXAFS theory.

$$\chi_{xy} = \xi_x\xi_y^* - \xi_{x0}\xi_{y0}^* = \xi_{y0}^*\sum\xi_x(\vartheta_j,\varphi_j)\frac{f(\theta_j)}{r_j}\exp i\{kr_j(1-\cos(\theta_j))\} + \xi_{x0}\sum\xi_y^*(\vartheta_j,\varphi_j)\frac{f^*(\theta_j)}{r_j}\exp -i\{kr_j(1-\cos(\theta_j))\}$$
$$\chi_{yz} = \xi_y^*\xi_z - \xi_{y0}^*\xi_{z0} = \xi_{y0}^*\sum\xi_z(\vartheta_j,\varphi_j)\frac{f(\theta_j)}{r_j}\exp i\{kr_j(1-\cos(\theta_j))\} + \xi_{z0}\sum\xi_y^*(\vartheta_j,\varphi_j)\frac{f^*(\theta_j)}{r_j}\exp -i\{kr_j(1-\cos(\theta_j))\}$$

We neglected the sum over the i-j combinations of the kind $\frac{f(\theta_i)f(\theta_j)}{r_i r_j}$. Combining the phase-factors arising from the scattering and path difference LDAD and CDAD are given from the real or imaginary parts of:

$$\chi_{xy} = \xi_{y0}^*\sum\xi_x(\vartheta_j,\varphi_j)\frac{|f(\theta_j)|}{r_j}\exp\{ia_j\} + \xi_{x0}\sum\xi_y^*(\vartheta_j,\varphi_j)\frac{|f(\theta_j)|}{r_j}\exp\{-ia_j\}$$
$$\chi_{yz} = \xi_{y0}^*\sum\xi_z(\vartheta_j,\varphi_j)\frac{|f(\theta_j)|}{r_j}\exp\{ia_j\} + \xi_{z0}\sum\xi_y^*(\vartheta_j,\varphi_j)\frac{|f(\theta_j)|}{r_j}\exp\{-ia_j\}$$
$$a_j = kr_j(1-\cos(\theta_j)) + \eta(\theta_j)$$

The first (xy) term is connected through the polarisation vector to $\cos(\vartheta_q)$ and the second (yz) to $\sin(\vartheta_q)$. To show that there is a possibility to have CDAD even at normal photon incidence one has to proof that the first term does not vanish for a particular initial state independent on the crystal symmetry.

For initial s-states we have:

$$\vec{\xi}_0 \propto \begin{Bmatrix}p_x\\ p_y\\ p_z\end{Bmatrix}p_p = \begin{Bmatrix}\sin(\vartheta)\cos(\varphi)\\ \sin(\vartheta)\sin(\varphi)\\ \cos(\vartheta)\end{Bmatrix}R_p\exp(i\delta_p)$$

leading to:

$$\chi_{xy} = \sin(\vartheta)\sin(\varphi)\sum\sin(\vartheta_j)\cos(\varphi_j)\frac{|f(\theta_j)|}{r_j}\exp ia_j + \sin(\vartheta)\cos(\varphi)\sum\sin(\vartheta_j)\sin(\varphi_j)\frac{|f(\theta_j)|}{r_j}\exp -ia_j$$
$$\chi_{yz} = \sin(\vartheta)\sin(\varphi)\sum\cos(\vartheta_j)\frac{|f(\theta_j)|}{r_j}\exp ia_j + \cos(\vartheta)\sum\sin(\vartheta_j)\sin(\varphi_j)\frac{|f(\theta_j)|}{r_j}\exp -ia_j$$

finally CDAD is given by the equations:

$$\chi_{xy}^{CDAD} = \sin(\vartheta)\sin(\varphi)\sum\sin(\vartheta_j)\cos(\varphi_j)\frac{|f(\theta_j)|}{r_j}\sin\{kr_j(1-\cos(\theta_j)+\eta(\theta_j)\}$$
$$-\sin(\vartheta)\cos(\varphi)\sum\sin(\vartheta_j)\sin(\varphi_j)\frac{|f(\theta_j)|}{r_j}\sin\{kr_j(1-\cos(\theta_j)+\eta(\theta_j)\}$$
$$\chi_{yz}^{CDAD} = \sin(\vartheta)\sin(\varphi)\sum\cos(\vartheta_j)\frac{|f(\theta_j)|}{r_j}\sin\{kr_j(1-\cos(\theta_j)+\eta(\theta_j)\}$$
$$-\cos(\vartheta)\sum\sin(\vartheta_j)\sin(\varphi_j)\frac{|f(\theta_j)|}{r_j}\sin\{kr_j(1-\cos(\theta_j)+\eta(\theta_j)\}$$

Both terms depend only on the phaseshift introduced by the scattering and not on the photoemission phases, therefore CDAD from s-states can be used to determine the geometrical properties of an adsorbate system directly. The first term gives the possibility to observe CDAD even for normal photon incidence here we have:

$$I_{NI}^{CDAD} \propto \sin(\vartheta)\sin(\varphi)\sum\sin(\vartheta_j)\cos(\varphi_j)\frac{|f(\theta_j)|}{r_j}\sin\{kr_j(1-\cos(\theta_j)+\eta(\theta_j)\}$$
$$-\sin(\vartheta)\cos(\varphi)\sum\sin(\vartheta_j)\sin(\varphi_j)\frac{|f(\theta_j)|}{r_j}\sin\{kr_j(1-\cos(\theta_j)+\eta(\theta_j)\}$$
$$I_{NI}^{CDAD} \propto \sin(\vartheta)\sum\sin(\vartheta_j)[\sin(\varphi-\varphi_j)]\frac{|f(\theta_j)|}{r_j}\sin\{kr_j(1-\cos(\theta_j)+\eta(\theta_j)\}$$

vorsicht mit dieser argumentation !!!! --> Both terms are symmetric in the emission angle ϑ, therefore the CDAD at normal photon incidence shows indirectly the symmetries of the crystal system and characteristic Zeros occur if the plane of electron emission coincides with a plane of symmetry $\varphi=\varphi_j$.

In an symmetric arrangement we have the same angle $\vartheta_j=\vartheta_s$ for all neighbouring atoms (or atoms in equivalent shells around the emitter having all the same distance to the emitter) leading to:

$$I_{NI,sym}^{CDAD} \propto \sin(\vartheta)\sum_s\left\{\sin(\vartheta_s)\sum_j\sin(\varphi-\varphi_{j,s})\frac{|f(\theta_{j,s})|}{r_{j,s}}\sin\{kr_{j,s}(1-\cos(\theta_{j,s})+\eta(\theta_{j,s})\}\right\}$$
$$\cos(\theta_{j,s}) = \sin(\vartheta)\sin(\vartheta_s)\cos(\varphi-\varphi_{j,s})+\cos(\vartheta)\cos(\vartheta_s)$$

The sum has to be taken over all equivalent shells containing atoms of the same distance to the emitter. In every shell with n-fold symmetry we can write the angle $\varphi_{j,s}$ as $\varphi_s+(j-1)\frac{2\pi}{n}$ for j=1..n leading to:

$$I_{NI,sym}^{CDAD} \propto \sin(\vartheta)\sum_s\sin(\vartheta_s)\sum_{j=1}^{n}[\sin(\varphi-\varphi_s-(j-1)\tfrac{2\pi}{n})]\frac{|f(\theta_s)|}{r_s}\sin\{kr_s(1-\cos(\theta_s)+\eta(\theta_s)\}$$
$$\cos(\theta_s) = \sin(\vartheta)\sin(\vartheta_s)\cos(\varphi-\varphi_s-(j-1)\tfrac{2\pi}{n})+\cos(\vartheta)\cos(\vartheta_s)$$

If the symmetry is odd like n=2,4,6 we find at every angle φ_j one atom at ϑ_j and one at $-\vartheta_j$ and we can rearrange the equation to be:

$$I_{NI,2n-fold}^{CDAD} \propto \sin(\vartheta)\sum_s\left\{\sin(\vartheta_s)\sum_{j=1}^{n/2}[F_{j+}-F_{j-}]\sin(\varphi-\varphi_s-2(j-1)\tfrac{2\pi}{n})\right\}$$
$$F_{j\pm} = \frac{|f(\theta_\pm)|}{r_s}\sin\{kr_s(1-\cos(\theta_\pm)+\eta(\theta_\pm)\}$$
$$\cos(\theta_\pm) = \pm\sin(\vartheta)\sin(\vartheta_s)\cos(\varphi-\varphi_s-2(j-1)\tfrac{2\pi}{n})+\cos(\vartheta)\cos(\vartheta_s)$$

and the sums over j in different symmetric arrangements are

for n=2:

$$I_{NI,2-fold}^{CDAD} \propto \sin(\vartheta)\sum_s\sin(\vartheta_s)\sin(\varphi-\varphi_s)[F_{j+}-F_{j-}]$$
$$F_{j\pm} = \frac{|f(\theta_\pm)|}{r_s}\sin\{kr_s[1-\cos(\theta_\pm)]+\eta(\theta_\pm)\}$$
$$\cos(\theta_\pm) = \pm\sin(\vartheta)\sin(\vartheta_s)\cos(\varphi-\varphi_s)+\cos(\vartheta)\cos(\vartheta_s)$$

for n=4:

$$I_{NI,4-fold}^{CDAD} \propto \sin(\vartheta)\sum_s\sin(\vartheta_s)\sin(\varphi-\varphi_s)\{[F_{1+}-F_{1-}]-[F_{2+}-F_{2-}]\}$$

$$F_{j\pm} = \frac{|f(\theta_{j\pm})|}{r_s}\sin\{kr_s[1-\cos(\theta_{j\pm})]+\eta(\theta_{j\pm})\}$$
$$\cos(\theta_{1\pm}) = \pm\sin(\vartheta)\sin(\vartheta_s)\cos(\varphi-\varphi_s)+\cos(\vartheta)\cos(\vartheta_s)$$
$$\cos(\theta_{2\pm}) = -\pm\sin(\vartheta)\sin(\vartheta_s)\cos(\varphi-\varphi_s)+\cos(\vartheta)\cos(\vartheta_s)$$

The χ_{yz}-term connected to the Sine of photon incidence shows the possibility to have CDAD in normal emission where we have $\vartheta_j=\vartheta_j$ and therefore:

$$I_{NE}^{CDAD} \propto \sin(\vartheta_q)\sum_j\sin(\vartheta_j)\sin(\varphi_j)\frac{|f(\vartheta_j)|}{r_j}\sin\{kr_j[1-\cos(\vartheta_j)]+\eta(\vartheta_j)\}$$

In any symmetric arrangement we have the same angle $\vartheta_j=\vartheta_s$ for all neighbouring atoms (or atoms in equivalent shells around the emitter) leading to:

$$I_{NE,sym}^{CDAD} \propto \sin(\vartheta_q)\sum_s\left\{\sin(\vartheta_s)\frac{|f(\vartheta_s)|}{r_s}\sin\{kr_s[1-\cos(\vartheta_s)]+\eta(\vartheta_s)\}\sum_j\sin(\varphi_{j,s})\right\}$$

where the sum has to be taken over all equivalent shells around the emitter. The sum over the Sine-terms vanishes in any n-fold adsorption site (or symmetric arrangement) because we have for n from 2 to 6 independent of an rotation φ_0 of the system:

$$\sum_j^n\sin[\varphi_0+(j-1)\tfrac{2\pi}{n}] = \sin(\varphi_0)\sum_j^n\cos[(j-1)\tfrac{2\pi}{n}]+\cos(\varphi_0)\sum_j^n\sin[(j-1)\tfrac{2\pi}{n}] = 0$$

So for symmetric adsorption sites no CDAD can be observed in Normal emission, at least for initial s-states and 100% circular polarisation.

In one of the previous chapters we had mentioned that there can be a slight misalignment of the photon beam. In that case we had to take the $\xi_x\xi_z$ combination into account. The additional term in the CDAD was given by:

$$I_{CDAD}^{oop} \simeq -2P_{circ}\sin(2\vartheta_q)\sin(\varphi_q)\cdot\Im(\xi_x^*\xi_z)$$

The scattering contribution to the dichroism from the imaginary part of the $\xi_x\xi_z$ combination for an initial s-state is given by:

$$\chi_{xz}^{CDAD} = R_p^2 \sin(\vartheta)\cos(\varphi)\sum \cos(\vartheta_j)\frac{|f(\theta_j)|}{r_j}\sin\{kr_j[1-\cos(\theta_j]+\eta(\theta_j)\}$$
$$-R_p^2\cos(\vartheta)\sum \sin(\vartheta_j)\cos(\varphi_j)\frac{|f(\theta_j)|}{r_j}\sin\{kr_j[1-\cos(\theta_j]+\eta(\theta_j)\}$$

Depending on the geometrical arrangement, this term is as big as the yz-term. The complete CDAD is given by:

$$\frac{\chi^{CDAD}}{R_p^2 P_{circ}} = \cos(\vartheta_q)\cos(\varphi_q)\left\{\sin(\vartheta)\sin(\varphi)\sum \sin(\vartheta_j)\cos(\varphi_j)\frac{|f(\theta_j)|}{r_j}\sin\{a(\theta_j)\}\right.$$
$$\left.-\sin(\vartheta)\cos(\varphi)\sum \sin(\vartheta_j)\sin(\varphi_j)\frac{|f(\theta_j)|}{r_j}\sin\{a(\theta_j)\}\right\}$$
$$-\sin(\vartheta_q)\cos(\varphi_q)\left\{\sin(\vartheta)\sin(\varphi)\sum \cos(\vartheta_j)\frac{|f(\theta_j)|}{r_j}\sin\{a(\theta_j)\}\right.$$
$$\left.-\cos(\vartheta)\sum \sin(\vartheta_j)\sin(\varphi_j)\frac{|f(\theta_j)|}{r_j}\sin\{a(\theta_j)\}\right\}$$
$$-2\sin(2\vartheta_q)\sin(\varphi_q)\left\{\sin(\vartheta)\cos(\varphi)\sum \cos(\vartheta_j)\frac{|f(\theta_j)|}{r_j}\sin\{a(\theta_j)\}\right.$$
$$\left.\cos(\vartheta)\sum \sin(\vartheta_j)\cos(\varphi_j)\frac{|f(\theta_j)|}{r_j}\sin\{a(\theta_j)\}\right\}$$

If we take the geometry most often used in the experiments with $\varphi=\pi/2$ and $\alpha=\pi/4$, then we have:

$$\frac{\chi^{CDAD}}{R_p^2 P_{circ}} \simeq -\sqrt{\tfrac{1}{2}}\cos(\varphi_q)\left\{\sin(\vartheta)\sum[\sin(\vartheta_j)\cos(\varphi_j)-\cos(\vartheta_j)]\frac{|f(\theta_j)|}{r_j}\sin\{a(\theta_j)\}\right.$$
$$\left.+\cos(\vartheta)\sum \sin(\vartheta_j)\sin(\varphi_j)\frac{|f(\theta_j)|}{r_j}\sin\{a(\theta_j)\}\right\}$$
$$-\tfrac{1}{2}\sin(\varphi_q)\left\{\cos(\vartheta)\sum \sin(\vartheta_j)\cos(\varphi_j)\frac{|f(\theta_j)|}{r_j}\sin\{a(\theta_j)\}\right\}$$

The scattering contribution can be easily calculated if we take only the next nearest neighbours in an adsorbate into account. In this case we have $\vartheta_j=\pi/2$ and assuming a misalignment of 5° we find for the CDAD:

$$\chi_{NNAdsorbat}^{CDAD} \propto -\sum \sin(\vartheta+\varphi_j)|f(\theta_j)|\sin\{a(\theta_j)\}$$
$$\mp 0.06\cos(\vartheta)\sum \cos(\varphi_j)|f(\theta_j)|\sin\{a(\theta_j)\}$$

$$\cos(\theta_j) = \sin(\vartheta)\sin(\varphi_j)$$

It is seen, that the out of plane component is only of influence if $\cos(\vartheta)$ becomes not too small, and that it is negligible at large emission angles.

The situation becomes more difficult if one likes to calculate the dichroism for initial states with angular momentum higher than Zero, because one has to average on all m-substates of degenerated initial states. We will give here a short description of initial real-orbitals.

For an p_x-state the CDAD is given by:

$$\frac{\chi_{xy}^{CDAD}(p_x)}{16\pi^2 c_\sigma \frac{3}{5}R_d^2} = -\sum\Big(d_{xy}^0\Big\{\sqrt{\tfrac{1}{3}}\,d_{z^2}^{j'} - d_{x^2-y^2}^{j'}\Big\} - \Big\{\sqrt{\tfrac{1}{3}}\,d_{z^2}^0 - d_{x^2-y^2}^0\Big\}d_{xy}^{j'}\Big)F_j\sin\{a_j\}$$
$$+\sqrt{\tfrac{2}{3}}\frac{R_1}{R_d}\sum\Big\{d_{xy}^0 s^j\sin\{a_j+(\delta_1-\delta_d)\} - s^0 d_{xy}^{j'}\sin\{a_j-(\delta_1-\delta_d)\}\Big\}F_j$$
$$\frac{\chi_{yz}^{CDAD}(p_x)}{16\pi^2 c_\sigma \frac{1}{5}R_d^2} = \sum\big(d_{xy}^0 d_{xz}^{j'} - d_{xz}^0 d_{xy}^{j'}\big)F_j\sin\{a_j\}$$
$$F_j = \frac{|f(\theta_j)|}{r_j}$$
$$a_j = kr_j(1-\cos(\theta_j)+\eta(\theta_j)$$

For an initial p_y-state we find for the CDAD:

$$\frac{\chi_{xy}^{CDAD}(p_y)}{16\pi^2 c_\sigma \frac{1}{5}R_d^2} = \sum\Big\{d_{xy}^{j'}\Big\{\sqrt{\tfrac{1}{3}}\,d_{z^2}^0 + d_{x^2-y^2}^0\Big\} - d_{xy}^0\Big\{\sqrt{\tfrac{1}{3}}\,d_{z^2}^{j'} + d_{x^2-y^2}^{j'}\Big\}\Big\}F_j\sin\{a_j\}$$
$$+\sqrt{\tfrac{2}{3}}\frac{R_1}{R_d}\sum\Big\{s^0 d_{xy}^{j'}\sin\{a_j-(\delta_1-\delta_d)\} - d_{xy}^0 s^j\sin\{a_j+(\delta_1-\delta_d)\}\Big\}F_j$$
$$\frac{\chi_{yz}^{CDAD}(p_y)}{16\pi^2 c_\sigma \frac{3}{5}R_d^2} = -\sum\Big\{d_{yz}^{j'}\Big\{\sqrt{\tfrac{1}{3}}\,d_{z^2}^0 + d_{x^2-y^2}^0\Big\} - d_{yz}^0\Big\{\sqrt{\tfrac{1}{3}}\,d_{z^2}^{j'} + d_{x^2-y^2}^{j'}\Big\}\Big\}F_j\sin\{a_j\}$$
$$+\sqrt{\tfrac{2}{3}}\frac{R_1}{R_d}\sum\big(s^0 d_{yz}^{j'}\sin\{a_j-(\delta_1-\delta_d)\} - d_{yz}^0 s^j\sin\{a_j+(\delta_1-\delta_d)\}\big)F_j$$

For an initial p_z-state we find for the CDAD:

$$\frac{\chi_{xy}^{CDAD}(p_z)}{16\pi^2 c_\sigma \frac{3}{5}R_d^2} = \sum\big(d_{yz}^0 d_{xz}^{j'} - d_{xz}^0 d_{yz}^{j'}\big)F_j\sin\{a_j\}$$
$$\frac{\chi_{yz}^{CDAD}(p_z)}{16\pi^2 c_\sigma \frac{3}{5}R_d^2} = \sum\sqrt{\tfrac{4}{3}}\big(d_{yz}^0 d_{z^2}^{j'} - d_{z^2}^0 d_{yz}^{j'}\big)F_j\sin\{a_j\}$$
$$+\sum\sqrt{\tfrac{2}{3}}\Big\{d_{yz}^0 s^j\sin\{a_j+(\delta_1-\delta_d)\} - s^0 d_{yz}^{j'}\sin\{a_j-(\delta_1-\delta_d)\}\Big\}F_j$$

The CDAD for the complete (a filled degenerated state) p-state is given by the sum of the values calculated above:

$$\frac{\chi_{xy}^{CDAD}(p)}{16\pi^2 c_\sigma \frac{3}{5}R_d^2} = \sum\left(d_{yz}^0 d_{xz}^j - d_{xz}^0 d_{yz}^j\right)F_j \sin\{a_j\}$$

$$\frac{\chi_{yz}^{CDAD}(p)}{16\pi^2 c_\sigma \frac{3}{5}R_d^2} = \sum\left(d_{xy}^0 d_{xz}^j - d_{xz}^0 d_{xy}^j\right)F_j \sin\{a_j\}$$
$$-\sum\left\{\left\{\sqrt{3}\,d_{z^2}^0 + d_{x^2-y^2}^0\right\}d_{yz}^j - d_{yz}^0\left\{\sqrt{3}\,d_{z^2}^j + d_{x^2-y^2}^j\right\}\right\}F_j \sin\{a_j\}$$

It is seen that final state s-waves do not contribute to the CDAD, but we have interference between the direct and scattered final state d-waves only, at least in the approximation neglecting ij-cross-terms and multiple scattering.

In terms of the angles we find:

$$\frac{\chi_{xy}^{CDAD}(p)}{9\pi c_\sigma R_d^2} = \sum \sin(2\vartheta)\sin(\varphi)\cdot\sin(2\vartheta_j)\cos(\varphi_j)F_j \sin\{a_j\}$$
$$-\sum \sin(2\vartheta)\cos(\varphi)\cdot\sin(2\vartheta_j)\sin(\varphi_j)F_j \sin\{a_j\}$$

$$\frac{\chi_{yz}^{CDAD}(p)}{9\pi c_\sigma R_d^2} = \sum \sin^2(\vartheta)\sin(2\varphi)\cdot\sin(2\vartheta_j)\cos(\varphi_j)F_j \sin\{a_j\}$$
$$-\sum \sin(2\vartheta)\cos(\varphi)\cdot\sin^2(\vartheta_j)\sin(2\varphi_j)F_j \sin\{a_j\}$$
$$-\sum\{3\cos^2(\vartheta)+\sin^2(\vartheta)\cos(2\varphi)-1\}\cdot\sin(2\vartheta_j)\sin(\varphi_j)F_j \sin\{a_j\}$$
$$+\sum \sin(2\vartheta)\sin(\varphi)\cdot\{3\cos^2(\vartheta_j)+\sin^2(\vartheta_j)\cos(2\varphi_j)-1\}F_j \sin\{a_j\}$$

As in the case of initial s-states there is one term remaining in normal emission:

$$\frac{I_{NE}^{CDAD}(p)}{9\pi c_\sigma R_d^2} = -2\sin(\vartheta_q)\sum \sin(2\vartheta_j)\sin(\varphi_j)\frac{|f(\vartheta_j)|}{r_j}\sin\{kr_j[1-\cos(\vartheta_j)]+\eta(\vartheta_j)\}$$

that vanishes for the symmetric adsorption sites.

The Normal incidence case is given by:

$$\frac{\chi_{NI}^{CDAD}(p)}{9\pi c_\sigma R_d^2} = \sin(2\vartheta)\sum \sin(2\vartheta_j)\sin(\varphi-\varphi_j)\frac{|f(\theta_j)|}{r_j}\sin\{kr_j[1-\cos(\theta_j)]+\eta(\theta_j)\}$$

This is similar to the case of NI-CDAD from an initial s-state, but here 2ϑ-terms occur rather than ϑ-terms.

For not degenerated p-states, where we can distinguish between p_x, p_y and p_z states we find in the special geometry where the electrons are collected in the y-z-plane ($\varphi=\pi/2$):

a) p_x

$$\frac{\chi_{xy}^{CDAD}(p_x)}{6\pi c_\sigma R_d^2} = \cos(\vartheta_q)\ \sum \sin^2(\vartheta_j)\sin(2\varphi_j)\left\{\sin\{a_j\} - \frac{R_s}{R_d}\sin\{a_j+(\delta_d-\delta_s)\}\right\}F_j$$

$$F_j = \frac{|f(\theta_j)|}{r_j}$$
$$a_j = kr_j[1-\cos(\theta_j)+\eta(\theta_j)]$$

b) p_y

$$\frac{\chi_{xy}^{CDAD}(p_y)}{6\pi c_\sigma R_d^2} = \sum \sin^2(\vartheta_j)\sin(2\varphi_j)\left\{\{3\sin^2(\vartheta)-1\}\sin\{a_j\} + \frac{R_s}{R_d}\sin\{a_j-(\delta_s-\delta_d)\}\right\}F_j$$

$$\frac{\chi_{yz}^{CDAD}(p_y)}{6\pi c R_d^2} = \sum\{\sin(2\vartheta_j)\sin(\varphi_j)\{3\sin^2(\vartheta)-1\} - \sin(2\vartheta)\{3\sin^2(\vartheta_j)-1\}\}F_j \sin\{a_j\}$$
$$+\frac{R_s}{R_d}\sum(\sin(2\vartheta_j)\sin(\varphi_j)\sin\{a_j-(\delta_s-\delta_d)\} - \sin(2\vartheta)\sin\{a_j+(\delta_s-\delta_d)\})F_j$$

c) p_z

$$\frac{\chi_{xy}^{CDAD}(p_z)}{9\pi c_\sigma R_d^2} = \sin(2\vartheta)\sum \sin(2\vartheta_j)\sin(\varphi_j)F_j \sin\{a_j\}$$

$$\frac{\chi_{yz}^{CDAD}(p_z)}{6\pi^2 c_\sigma R_d^2} = \sum(\sin(2\vartheta)[3\cos^2(\vartheta_j)-1] - [3\cos^2(\vartheta)-1]\sin(2\vartheta_j)\sin(\varphi_j))F_j \sin\{a_j\}$$
$$+\frac{R_s}{R_d}\sum\{\sin(2\vartheta)\sin\{a_j+(\delta_s-\delta_d)\} - \sin(2\vartheta_j)\sin(\varphi_j)\sin\{a_j-(\delta_s-\delta_d)\}\}F_j$$

X.3 Spindependent scattering

As in the case of scattering independent of the electron spin we write the amplitude of the wavefunction as sum of the initially emitted wave Ψ_0 and all scattered waves Ψ_j. The spin-dependence is introduced via the spinflip amplitude and the spin dependent transition probabilities.

$$\Psi = \Psi_0 + \sum_j S_j \cdot \Psi_j \cdot \Gamma_j$$

The wave function of directly emitted electrons is given by $\Psi_0(\vartheta,\varphi) = \vec{\varepsilon}\bullet\vec{\xi}$ as calculated in the previous chapter. The j-th scattered wave has the complex amplitude $\Psi_j = \Psi_0(\vec{r}_j)$ given by the amplitude of the primary wave at the location of the scattering atom.

The spin dependent scattering matrix

$$S_j = f_j \cdot 1 - ig_j \cdot \vec{\sigma}\bullet\hat{n}_j$$

connected to the j-th scattering atom depends on the spin vector composed from the Pauli spin matrices and furthermore on,

the non flip amplitude: $f_j = f(\theta_j) = |f(\theta_j)|\exp\{ia_j\}$ and

the spin flip amplitude: $g_j = f(\theta_j) = |g(\theta_j)| \exp\{i\beta_j\}$

where the difference in the path of the scattered and direct wave is included:

$$a_j = kr_j(1-\cos(\theta_j)+\eta_f(\theta_j)\ ;\ \beta_j = kr_j(1-\cos(\theta_j)+\eta_g(\theta_j)$$

The scattering geometry is defined by two quantities, the scattering angle and the normal vector to the scattering plane, that are given by:

$$\cos(\theta_j) = \frac{\vec{r}_j \bullet \vec{k}}{|\vec{r}_j| \cdot |\vec{k}|}\ ;\ \hat{n}_j = \begin{pmatrix} n_{jx} \\ n_{jy} \\ n_{jz} \end{pmatrix} = \frac{\vec{r}_j \times \vec{k}}{|\vec{r}_j \times \vec{k}|}$$

Finally we have the completed complex scattering matrix given by:

$$S_j = \begin{pmatrix} f_j - i \cdot g_j n_{jz} & -g_j(i \cdot n_{jx} + n_{jy}) \\ -g_j(i \cdot n_{jx} - n_{jy}) & f_j + i \cdot g_j n_{jz} \end{pmatrix} = \begin{pmatrix} S^j_{11} & S^j_{21} \\ S^j_{12} & S^j_{22} \end{pmatrix}$$

The damping factor Γ_j includes the 1/r decrease of the spherical wave, the inelastic processes and thermal effects:

$$\Gamma_j = \frac{\exp\left\{-\frac{L_j}{2\cdot\lambda_e}\right\}}{r_j} \cdot W_j$$

The direct wave Ψ_0 and the amplitude Ψ_j of the primary wave at the location of the j-th scattering atom can be written as spinor:

$$\Psi_0 = \begin{pmatrix} a_0 \\ \beta_0 \end{pmatrix}\ ;\ \Psi_i = \begin{pmatrix} a(\vec{r}_j) \\ \beta(\vec{r}_j) \end{pmatrix} = \begin{pmatrix} a_j \\ \beta_j \end{pmatrix}$$

Inserting these spinor into the equation given above the total amplitude of the wave is given by a coherent superposition of the spin components of the wave functions:

$$\Psi_{ges} = \begin{pmatrix} a \\ \beta \end{pmatrix} = \begin{pmatrix} a_0 \\ \beta_0 \end{pmatrix}\Gamma_0 + \sum_j \begin{pmatrix} a_j \cdot (f_j - i \cdot g_j n_{jz}) - \beta_j \cdot g_j(i \cdot n_{jx} + n_{jy}) \\ \beta_j \cdot (f_j + i \cdot g_j n_{jz}) - a_j \cdot g_j(i \cdot n_{jx} - n_{jy}) \end{pmatrix}\Gamma_j$$
$$= \begin{pmatrix} a_0 \\ \beta_0 \end{pmatrix}\Gamma_0 + \sum_j \begin{pmatrix} a_j \cdot S^j_{11} + \beta_j \cdot S^j_{21} \\ \beta_j \cdot S^j_{22} + a_j \cdot S^j_{12} \end{pmatrix}\Gamma_j$$

The total intensity of the photoelectron current is then given by:

$$I(\vartheta,\varphi) = aa^* + \beta\beta^* = |a|^2 + |\beta|^2$$

If the spin of the photoelectrons is resolved, then the electron spin polarisation can be calculated from the relations:

$$\vec{P} = \begin{Bmatrix} P_x \\ P_y \\ P_z \end{Bmatrix} = \frac{1}{aa^* + \beta\beta^*} \begin{Bmatrix} a\beta^* + a^*\beta \\ i \cdot [a\beta^* - a^*\beta] \\ aa^* - \beta\beta^* \end{Bmatrix}$$

Note that from quantum mechanics the polarisation components cannot be measured at once in a single measurement, but they can be determined in independent experiments.

We will here examine only the CDAD. To do so we have first to calculate the CDAD observed in both spin channels independently and than we have to add the results.

For the spin-up component we have after subtracting the direct part neglecting terms with $1/r_i r_j$:

$$\chi^{\alpha}_{xy} = a_{0y} \sum\left(a_{jx} \cdot S^j_{11} + \beta_{jx} \cdot S^j_{21}\right) + a_{0x} \sum\left(a^*_{jy} \cdot S^{j*}_{11} + \beta^*_{jy} \cdot S^{j*}_{21}\right)$$
$$\chi^{\alpha}_{yx} = a_{0z} \sum\left(a^*_{jy} \cdot S^{j*}_{11} + \beta^*_{jy} \cdot S^{j*}_{21}\right) + a^*_{0y} \sum\left(a_{jx} \cdot S^j_{11} + \beta_{jx} \cdot S^j_{21}\right)$$

and for the spin down component:

$$\chi^{\beta}_{yz} = \beta^*_{0y} \sum\left(\beta_{jx} \cdot S^j_{22} + a_{jx} \cdot S^j_{12}\right) + \beta_{0x} \sum\left(\beta^*_{jy} \cdot S^{j*}_{22} + a^*_{jy} \cdot S^{j*}_{12}\right)$$
$$\chi^{\beta}_{yz} = \beta_{0z} \sum\left(\beta^*_{jy} \cdot S^{j*}_{22} + a^*_{jy} \cdot S^{j*}_{12}\right) + \beta^*_{0y} \sum\left(\beta_{jx} \cdot S^j_{22} + a_{jx} \cdot S^j_{12}\right)$$

We will analyse at this point only the CDAD from initial $s_{1/2}$ and $p_{1/2}$ states, that are easiest to handle. because one has only two m_j substates.

X.3.1 Intensity and Spinpolarisation in Spindependent Scattering

We like to show some properties of the spindependent scattering. If we apply the scattering matrix to an wavefunction Ψ_0 we find after the scattering event the wavefunction:

$$\Psi_S = \underline{S} \cdot \Psi_0 = \underline{S} \cdot \begin{pmatrix} a \\ \beta \end{pmatrix} = \begin{pmatrix} a \cdot (f(\theta) - i \cdot g \cdot n_z) - \beta \cdot g(\theta) \cdot (i \cdot n_x + n_y) \\ \beta \cdot (f(\theta) + i \cdot g \cdot n_z) - a \cdot g(\theta) \cdot (i \cdot n_x - n_y) \end{pmatrix}$$

The intensity and spinpolarisation of this wave are given by:

$$I_S = I_0\left\{S_0(\theta) + S_2(\theta)\vec{P} \bullet \vec{n}\right\}$$

$$\vec{P}_S = \frac{\left[(S_0(\theta) - S_3(\theta))\vec{P} \bullet \vec{n} + S_2(\theta)\right]\vec{n} + S_3(\theta)\vec{P} - S_1(\theta)\left(\vec{P} \times \vec{n}\right)}{S_0(\theta) \cdot \left(1 + S_2(\theta)\vec{P} \bullet \vec{n}\right)}$$

$I_0=|\alpha|^2+|\beta|^2$ is the intensity and P is the spinpolarisation of the wave before scattering. We used the following 4-component vector for abbreviation:

$$\vec{S}(\theta)=\begin{pmatrix} S_0(\theta) \\ S_1(\theta) \\ S_2(\theta) \\ S_3(\theta) \end{pmatrix}=\begin{pmatrix} |f|^2+|g|^2 \\ fg^*+f^*g \\ i\cdot(fg^*-f^*g) \\ |f|^2-|g|^2 \end{pmatrix}$$

This vector is similar to the Stokes-vector describing the polarisation of photons. The component $S_2(\theta)/S_0(\theta)$ is usually called the Sherman-function.

X.4 References

[1] A.Liebsch; Phys.Rev.Lett. 32 (1974) 1203

[2] A.Liebsch; Phys.Rev. B13 (1976) 544

[3] K.A.Thompson, C.S.Fadley; J.Elec.Spec.Rel.Phen. 33 (1984) 29

[4] R.Trehan, J.Osterwalder, C.S.Fadley; J.Elec.Spec.Rel.Phen. 42 (1987) 187

[5] D.J.Friedman, C.S.Fadley; J.Elec.Spec.Rel.Phen. 51 (1990) 689

[6] B.Sinkovic, D.J.Friedman, C.S.Fadley; J.Magn.Magn.Mat. 92 (1991) 301

[7] C.S.Fadley, Surf.Sci.Rep. 19 (1993) 231

[8] F.Salvat, R.Mayol; Comp.Phys.Comm. 74 (1993) 358

[9] D.P.Woodruff, A.M.Bradshaw; Rep.Prog.Phys. 57 (1994) 1029

[10] D.P.Woodruff; Surf.Sci. 299/300 (1994) 183

[11] C.S.Fadley, M.A.vanHove, Z.Hussain, A.P.Kaduwela; J.Elec.Spec.Rel.Phen. 75 (1995) 273

Fig. 2.1. Universal curve of electron mean free path: experiment (Rhodin & Gadzuk, 1979; Somorjai, 1981); theory (Penn, 1976).

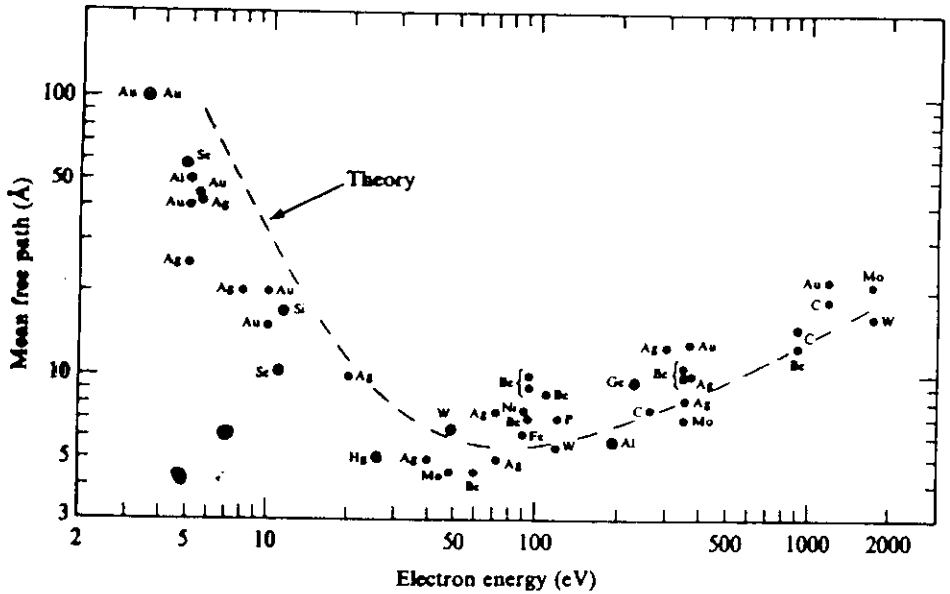

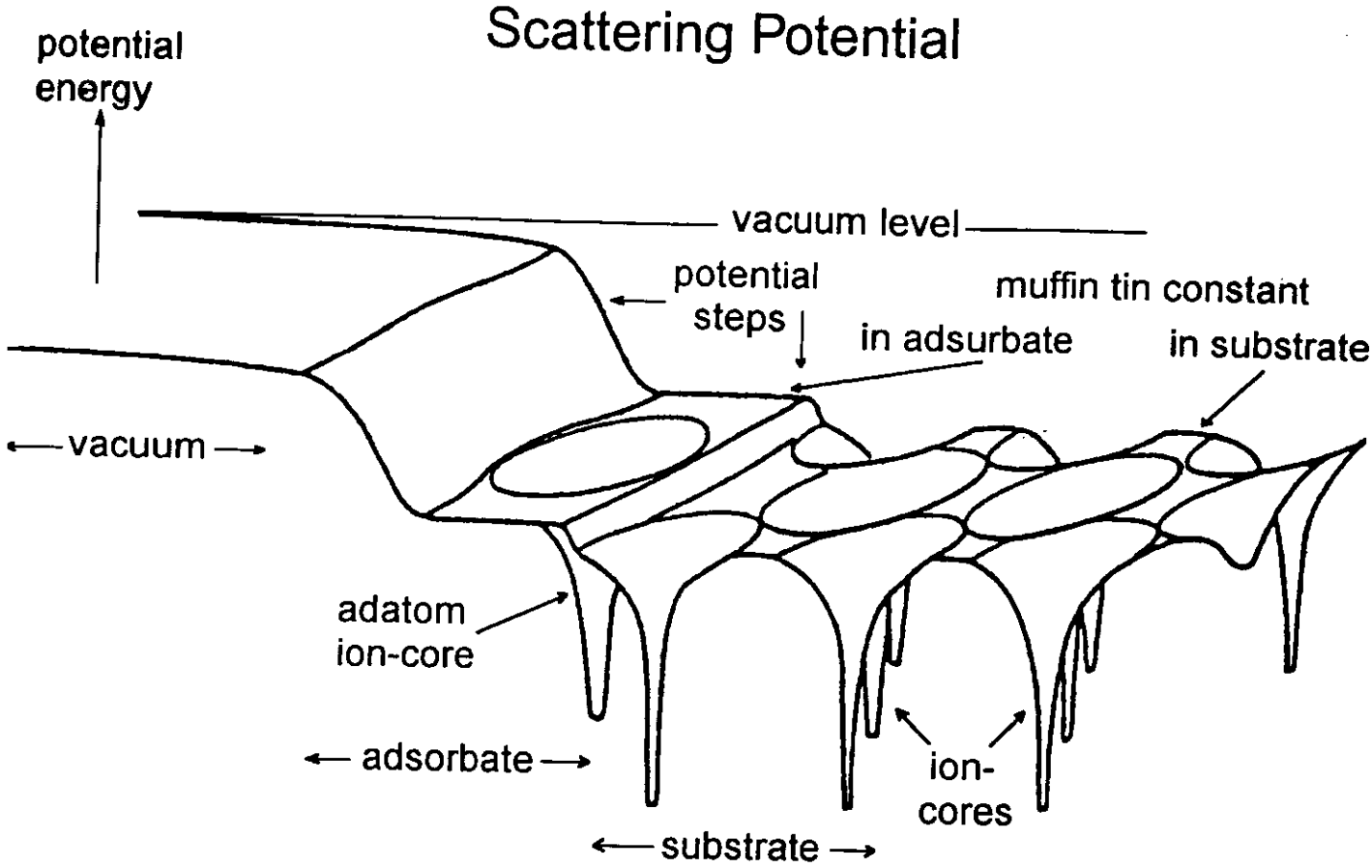

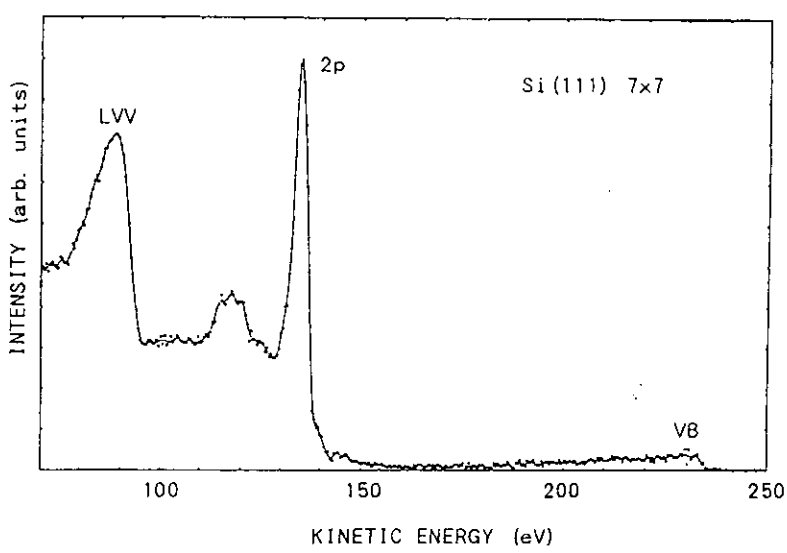

Fig. 1. Photoelectron spectrum from Si(111)7 × 7 surface at the photon energy of about 240 eV.

CDAD from Si 2p, Si(001) normal incidence; Ekin = 250eV

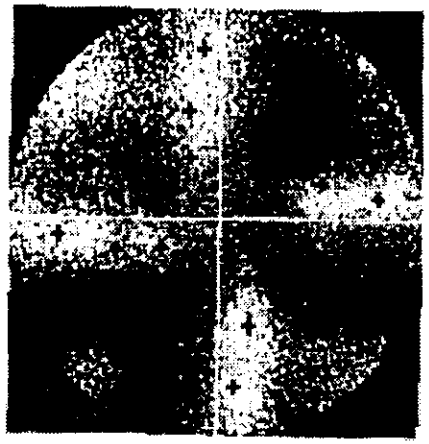

RCP light

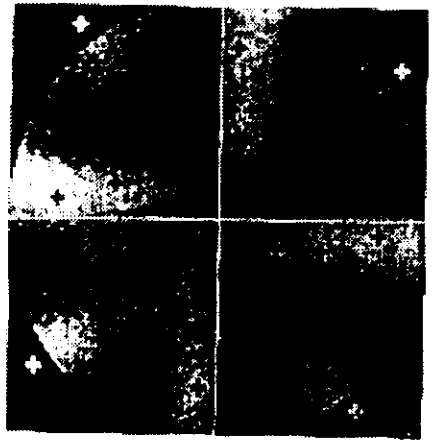

LCP light

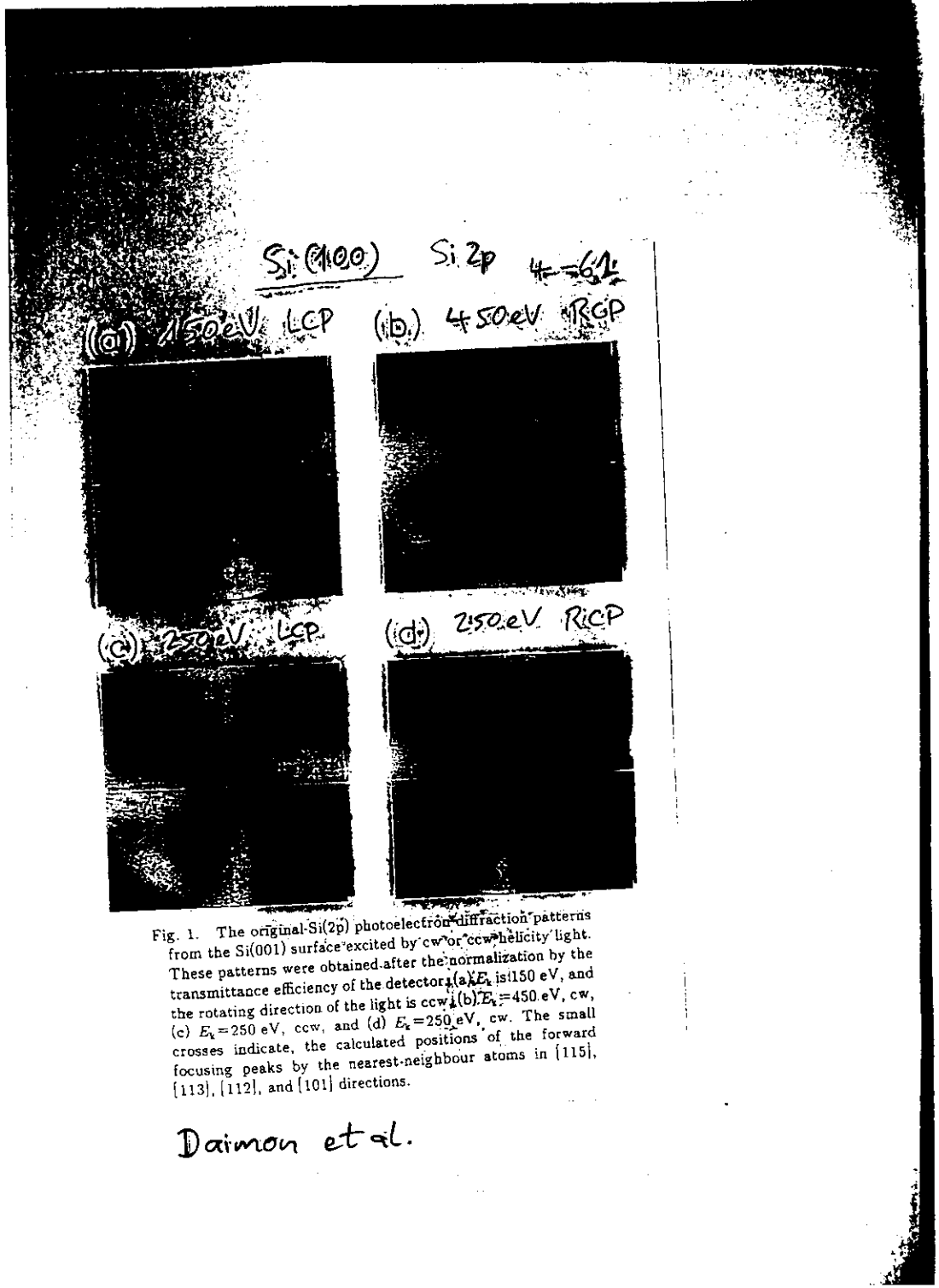

Fig. 1. The original Si(2p) photoelectron diffraction patterns from the Si(001) surface excited by cw or ccw helicity light. These patterns were obtained after the normalization by the transmittance efficiency of the detector. (a) E_k is 150 eV, and the rotating direction of the light is ccw, (b) E_k=450 eV, cw, (c) E_k=250 eV, ccw, and (d) E_k=250 eV, cw. The small crosses indicate the calculated positions of the forward focusing peaks by the nearest-neighbour atoms in [115], [113], [112], and [101] directions.

Daimon et al.

I.Daimon et al, Jpn.J.ApplPhys. 32(1993)1480

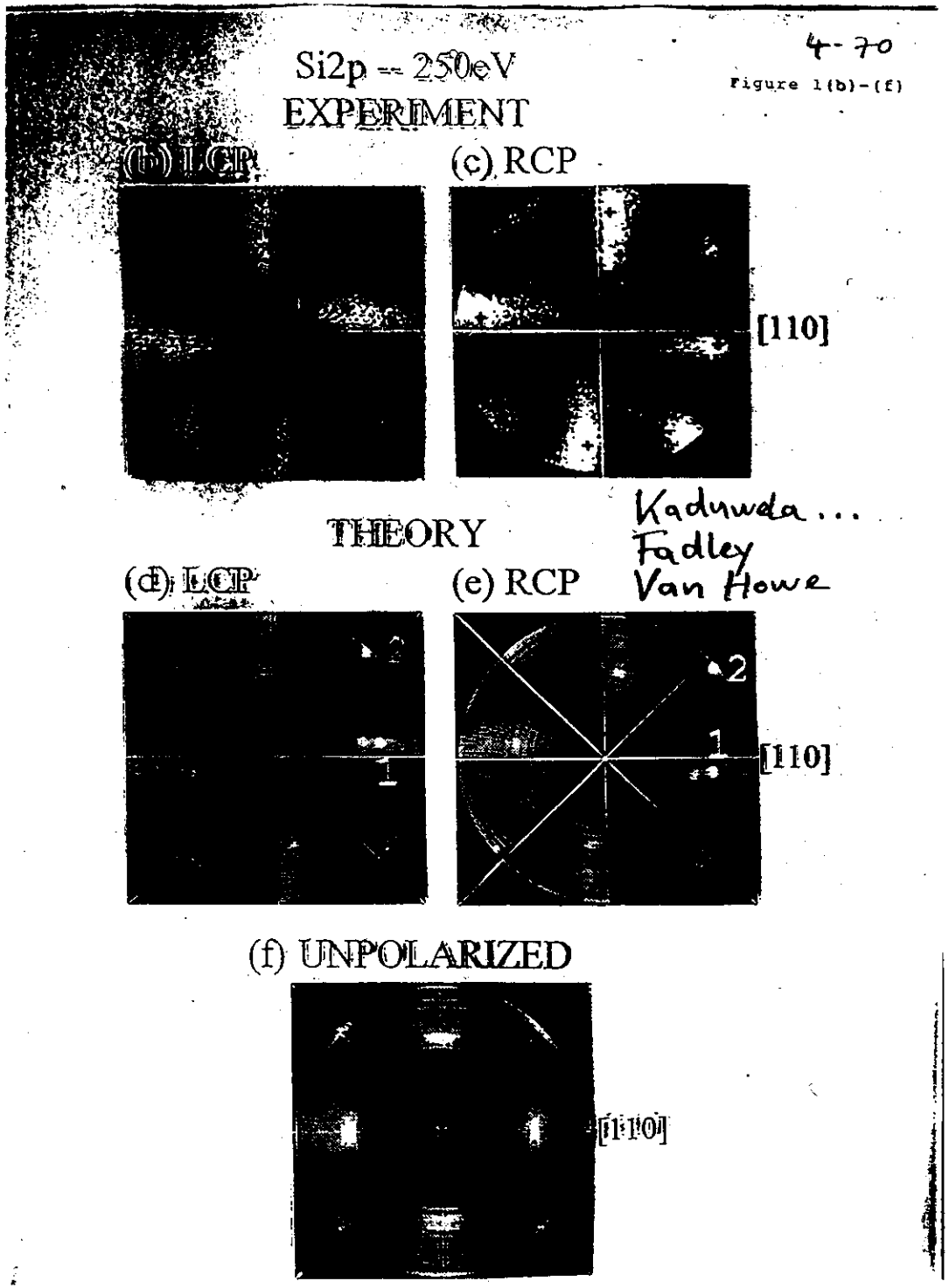

XI Examples and remarks on Photoelectron Diffraction

XI.1 Examples for real orbitals

XI.1.1 Example scattering in emission from s- initial states

We will show now som examples how the scattering at surface atoms leads to a CDAD even in the case of s-emission, although one has no m-dependence of the phases. We restrict ourselves on symmetric nearest neighbour sites meaning $\vartheta_j=\vartheta'$ and $r_j=r$ for all j neighbouring atoms and examine the geometry with $\varphi=\pi/2$.

XI.1.1.1 s-state CDAD from On-Top site adsorption or a free Diatomic

This is the simplest possibility to include the scattering. The adsorbed atom is located at a distance r in z-direction above the substrate. The emission from the substrate atom ($\vartheta'=0$; $\varphi'=\pi/2$; $\theta=\vartheta$) is called ↑-orientation, and that from the adsorbate ($\vartheta'=\pi$; $\varphi'=\pi/2$; $\theta=\pi-\vartheta$) ↓-orientation. An oriented diatomic molecule may be described by the same equations. The amplitudes of the primary wave are that of the p-waves:

$$\Xi_0 = \left\{ \begin{array}{c} \sin(\vartheta)\cos(\varphi) \\ \sin(\vartheta)\sin(\varphi) \\ \cos(\vartheta) \end{array} \right\} \exp\{i\delta\} R_p$$

Inserting the position vector to the primary wave the amplitudes of the scattered waves are:

$$\Xi_1^{\uparrow} = \left\{ \begin{array}{c} 0 \\ 0 \\ \frac{|f(\vartheta)|}{r} \exp i\{kr[1-\cos(\vartheta)]+\eta(\vartheta)\} \end{array} \right\} \exp\{i\delta\} R_p$$

for the up-orientation or for the down orientation:

$$\Xi_1^{\downarrow} = \left\{ \begin{array}{c} 0 \\ 0 \\ \frac{|f(\pi-\vartheta)|}{r} \exp i\{kr[1-\cos(\pi-\vartheta)]+\eta(\pi-\vartheta)\} \end{array} \right\} \exp\{i\delta\} R_p$$

In the geometry of measurements that is observation in the plane with $\varphi=\pi/2$ we have

$$\phi_0 = \left[(\varepsilon_{yr}+i\varepsilon_{yi})\sin(\vartheta)+\varepsilon_z\cos(\vartheta)\right]\exp\{i\delta\}R_p$$

$$\phi_1^{\uparrow} = \varepsilon_z \frac{|f(\vartheta)|}{r} \exp i\{kr[1-\cos(\vartheta)]+\eta(\vartheta)+\delta\}R_p$$

$$\phi_1^{\downarrow} = -\varepsilon_z \frac{|f(\pi-\vartheta)|}{r} \exp i\{kr[1-\cos(\pi-\vartheta)]+\eta(\pi-\vartheta)+\delta\}R_p$$

and from this the CDAD is given by:

$$\frac{I^{\uparrow}_{CDAD}}{c_\sigma \cdot R^2_{pS}} = -2\sin(\vartheta_q)\frac{|f(\vartheta)|}{r}\sin(\vartheta)\sin\{kr[1-\cos(\vartheta)]+\eta(\vartheta)\}$$

$$\frac{I^{\downarrow}_{CDAD}}{c_\sigma \cdot R^2_{pA}} = 2\sin(\vartheta_q)\frac{|f(\pi-\vartheta)|}{r}\sin(\vartheta)\sin\{kr[1+\cos(\vartheta)]+\eta(\pi-\vartheta)\}$$

that shows that a CDAD occurs for a free oriented molecule even if the initial state is assumed to be spherical (e.g.: s core-level of one of the atoms). Moreover the CDAD depends for heteronuclear molecules on the orientation of the axis and not only on the alignment.

The cross sections for unpolarised light are given by:

$$\frac{2I^{\uparrow}_0}{c_\sigma R^2_{pS}} = \sin^2(\vartheta)+\sin^2(\vartheta_q)\left[\cos^2(\vartheta)+\frac{2|f(\vartheta)|}{r}\cos(\vartheta)\cos\{kr[1-\cos(\vartheta)]+\eta\}+\frac{|f(\vartheta)|^2}{r^2}\right]$$

$$\frac{I^{\downarrow}_0}{c_\sigma R^2_{pA}} = \sin^2(\vartheta)+\sin^2(\vartheta_q)\left[\cos^2(\vartheta)-\frac{2|f(\pi-\vartheta)|}{r}\cos(\vartheta)\cos\{kr[1+\cos(\vartheta)]+\eta\}+\frac{|f(\pi-\vartheta)|^2}{r^2}\right]$$

The dependence on the emission angle is much more complicated than in the case of I_{CDAD}. Moreover the contribution from scattering to the observed intensity may be much smaller than that from the direct emission. Therefore it is much easier to extract the information about the adsorbate structure from I_{CDAD} than from I_0.

a) a strongly simplified estimation of On-Top CDAD

We will simplify the CDAD-equations by setting $|f(\vartheta)|=1/k$, $\beta=0$ to obtain simply a spherical wave outgoing from the scattering centre and furthermore we expand the Sine of the phases for small values of kr, then we have:

$$I^{\uparrow}_{CDAD} = \sin(\vartheta_q)c_\sigma R^2_{pS}[\sin(2\vartheta)-2\sin(\vartheta)]$$

$$I^{\downarrow}_{CDAD} = \sin(\vartheta_q)c_\sigma R^2_{pA}[\sin(2\vartheta)+2\sin(\vartheta)]$$

The differences between ↑- and ↓-orientation is clearly shown.

b) The sign of CDAD in 1s-emission from an oriented CO molecule.

We will estimate the sign of the CDAD for emission from the 1s-orbitals of CO molecules for near normal emission. For comparison with adsorbed molecules we assume the molecular axis pointing from

C to O to be oriented along the positive z-axis. In this case the Ξ-functions for emission from the s-states of the C- or the O-atom are given by (inelastic and thermal effects are neglected):

$$\Xi_{C-1s} = \left\{\begin{array}{c} 0 \\ \sin(\vartheta) \\ \cos(\vartheta)+\frac{|f_O(\vartheta)|}{r_{CO}}\exp i\{kr_{CO}[1-\cos(\vartheta)]+\eta_O(\vartheta)\} \end{array}\right\} R_{Cp}\exp\{i\delta_{Cp}\}$$

$$\Xi_{O-1s} = \left\{\begin{array}{c} 0 \\ \sin(\vartheta) \\ \cos(\vartheta)-\frac{|f_C(\pi-\vartheta)|}{r_{CO}}\exp i\{kr_{CO}[1+\cos(\vartheta)]+\eta_C(\pi-\vartheta)\} \end{array}\right\} R_{Op}\exp\{i\delta_{Op}\}$$

and the corresponding CDAD is given by:

$$I^{C-1s}_{CDAD} = -2\sin(\vartheta_q)\frac{c_\sigma|f_O(\vartheta)|R^2_{Cp}}{r_{CO}}\sin(\vartheta)\sin\{kr_{CO}[1-\cos(\vartheta)]+\eta_O(\vartheta)\}$$

$$I^{O-1s}_{CDAD} = 2\sin(\vartheta_q)\frac{c_\sigma|f_C(\pi-\vartheta)|R^2_{Op}}{r_{CO}}\sin(\vartheta)\sin\{kr_{CO}[1+\cos(\vartheta)]+\eta_C(\pi-\vartheta)\}$$

For near normal emission ($\vartheta=0$) we find $\sin(\vartheta)\approx\vartheta$, $\cos(\vartheta)\approx1$ and moreover in the geometry used in the experiments it was $\sin(\vartheta_q=130°)>0$ leading to:

$$I^{C-1s}_{CDAD}(\vartheta\approx0) \propto -\vartheta\cdot|f_O(0)|\cdot\sin\{\eta_O(0)\}$$

$$I^{O-1s}_{CDAD}(\vartheta\approx0) \propto \vartheta\cdot|f_C(\pi)|\cdot\sin\{2\cdot k\cdot r_{CO}+\eta_C(\pi)\}$$

For kinetic energies of around 100eV we find for the scattering parameters [Fink]: $\eta_O(0)\approx0.82$, $\eta_C(\pi)\approx-1.1$, $kr_{CO}\approx1.2$ and $2kr_{CO}+\eta C(\pi)\approx1.3$ leading to $\sin(\eta_O(0))\approx0.73>0$ and $\sin(2kr_{CO}+\eta_C(\pi))\approx0.97>0$. Both phase-factors are positive. From these values it is seen that the C-1s-CDAD for free oriented molecules has to be negative for positive observation angles $\vartheta>0$ in the case of near normal emission.

c) more diatomics

The case of a diatomic molecule and a single atom in an On-Top site adsorption place are very similar. From this point of view we will examine two other surface dimers. One aligned along the x-axis and another aligned along the z-axis.

The direct wave is the same as before, to calculate the scattering part we need the scattering angles. We take two geometries, the emitting atom is placed in the origin.

i) x-aligned atom ($\Leftrightarrow$) with the scattering atom at the positive $\Rightarrow$+x ($\vartheta_i=\pi/2$, $\varphi_i=0$), or the negative $\Leftarrow$−x ($\vartheta_i=\pi/2$, $\varphi_i=\pi$) side of the origin. For this case the Ξ-function is given by (upper sign corresponds to +x orientation):

$$\Xi^{\pm x} = \left\{ \begin{array}{c} \sin(\vartheta)\cos(\varphi) \pm \frac{|f(\theta)|}{r} \exp i\{kr[1 - \pm\sin(\vartheta)\cos(\varphi)] + \eta(\theta)\} \\ \sin(\vartheta)\sin(\varphi) \\ \cos(\vartheta) \end{array} \right\} \exp\{i\delta\} R_p$$

$$\cos(\theta) = \pm\sin(\vartheta)\cos(\varphi)$$

ii) y-aligned atom with the scattering atom at the positive ⇑+y ($\vartheta_i=\pi/2$, $\varphi_i=\pi/2$), or the negative ⇓−y ($\vartheta_i=\pi/2$, $\varphi_i=-\pi/2$) side of the origin. Here the Ξ-function is given by (upper sign corresponds to +y orientation):

$$\Xi^{\pm y} = \left\{ \begin{array}{c} \sin(\vartheta)\cos(\varphi) \\ \sin(\vartheta)\sin(\varphi) \pm \frac{|f(\theta)|}{r} \exp i\{kr[1 - \pm\sin(\vartheta)\sin(\varphi)] + \eta(\theta)\} \\ \cos(\vartheta) \end{array} \right\} \exp\{i\delta\} R_p$$

$$\cos(\theta) = \pm\sin(\vartheta)\sin(\varphi)$$

The CDAD is described by the imaginary parts of the xy or yz products of the Ξ-function components. The first scales with the Cosine of the angle of photon incidence, whereas the second scales with the Sine. In the case of the z-orientation, as given at the beginning, there is no xy combination, and therefore CDAD vanishes at normal photon incidence. Now, for x- and y-orientation we have a non-vanishing imaginary part of the xy type. This means, that there is a non vanishing CDAD at normal incidence from the atoms in the surface plane.

If we are taking the signal in the yz-plane at $\varphi=\pi/2$ we find for the imaginary parts in question in the case of x-orientation:

$$\frac{\Im(\xi_x \xi_y^*)}{R_p^2} = \pm\sin(\vartheta)\frac{\left|f(\frac{\pi}{2})\right|}{r} \sin\{kr + \eta(\tfrac{\pi}{2})\}$$

and in the case of y-orientation (here the upper sign corresponds to y-orientation at negative y axis):

$$\frac{\Im(\xi_y^* \xi_z)}{R_p^2} = \pm\cos(\vartheta)\frac{\left|f(\frac{\pi}{2} \pm \vartheta)\right|}{r} \sin\{kr[1 \pm \sin(\vartheta)] + \eta(\tfrac{\pi}{2} \pm \vartheta)\}$$

Now, for the y-orientation the CDAD does not vanish in normal emission.

From the examination of surface dimers we found two interesting things:

1. CDAD is possible at normal photon incidence
2. CDAD is possible in normal electron emission.

A remaining thing is, to show for real surfaces consisting of more atoms, that the different contributions from scattering at the neighbouring atoms do not cancel out.

XI.2 Influences arising from multiple scattering (s-state, diatomic molecule)

In the case of a diatomic molecule the influence of multiple scattering can be determined very easy. As example we use CO. We start with the electron emitted from the C-atom with the amplitude $\Psi_0^C(\vartheta,\varphi)$ and scattered at the oxygen atom with a probability as given above. This scattered wave is scattered again at the carbon atom and so on. The amplitude of the wave in the double scattering event is given by:

$$\begin{aligned} \frac{\Psi_{2R}^C}{\Psi_0^C(0,\frac{\pi}{2})} = {} & |f_O(\vartheta)| \exp\{i[kr(1-\cos(\vartheta)) + \eta_O(\vartheta)]\} \frac{\exp(-\gamma \cdot r)}{r} + \ldots \\ & \ldots + |f_C(\pi-\vartheta)| \exp\{i[kr(1+\cos(\vartheta)) + \eta_C(\pi-\vartheta)]\} \cdot \ldots \\ & \ldots \cdot |f_O(\pi)| \exp\{i[2kr + \eta_O(\pi)]\} \frac{\exp(-2\cdot\gamma\cdot r)}{r^2} \end{aligned}$$

or expressed as multiple of the single scattering amplitude given above:

$$\begin{aligned} \frac{\Psi_{2R}^C}{\Psi_{SSc}^C} &= 1 + \frac{|f_C(\pi-\vartheta)||f_O(\pi)|}{|f_O(\vartheta)|} \exp\{i[2kr(1+\cos(\vartheta)) + \eta_C(\pi-\vartheta) + \eta_O(\pi) - \eta_O(\vartheta)]\} \frac{\exp(-\gamma\cdot r)}{r} \\ \frac{\Psi_{SSc}^C}{\Psi_0^C(0,\frac{\pi}{2})} &= |f_O(\vartheta)| \exp\{i[kr(1-\cos(\vartheta)) + \eta_O(\vartheta)]\} \frac{\exp(-\gamma\cdot r)}{r} \end{aligned}$$

Here and in the following we use r=r_{CO} for abbreviation. Starting with this double scattered wave that is the wave scattered one time at each of the both atoms we find for then-th scattered wave:

$$\Psi_{n,R}^C = \Psi_{2R}^C \cdot \left[|f_O(\pi)|^n |f_C(\pi)|^n \cdot \exp\{i[2nkr + n(\eta_O(\pi) + \eta_C(\pi))]\} \frac{\exp\{-2n\gamma r\}}{r^{2n}} \right]$$

The complete scattered wave is given by a summation over an infinite number of scattering events:

$$\Psi_R^C = \Psi_{2R}^C \cdot \sum_{n=0}^{\infty} |f_O(\pi)|^n |f_C(\pi)|^n \cdot \frac{\exp\{-2n\gamma r\}}{r^{2n}} \exp\{i[2nkr + n(\eta_O(\pi) + \eta_C(\pi))]\}$$

$$\sum_{n=0}^{\infty} \Psi_{n,R}^C = \frac{1}{1 - |f_O(\pi)||f_C(\pi)| \cdot \frac{\exp\{-2\gamma r\}}{r^2} \exp\{i[2kr + \eta_O(\pi) + \eta_C(\pi)]\}}$$

and expressed as multiple of the single scattering amplitude we have:

$$\frac{\Psi_R^C}{\Psi_{SSc}^C} = \frac{1 + \frac{|f_C(\pi-\vartheta)||f_O(\pi)|}{|f_O(\vartheta)|} \exp\{i[2kr(1+\cos(\vartheta)) + \eta_C(\pi-\vartheta) + \eta_O(\pi) - \eta_O(\vartheta)]\} \frac{\exp(-\gamma\cdot r)}{r}}{1 - |f_O(\pi)||f_C(\pi)| \cdot \frac{\exp\{-2\gamma r\}}{r^2} \exp\{i[2kr + \eta_O(\pi) + \eta_C(\pi)]\}}$$

$$\frac{\Psi_{SSc}^C}{\Psi_0^C(0,\frac{\pi}{2})} = |f_O(\vartheta)| \exp\{i[kr(1-\cos(\vartheta)) + \eta_O(\vartheta)]\} \frac{\exp(-\gamma\cdot r)}{r}$$

The multiple scattering amplitudes are complex numbers and can be recalculated to have the same appearance as the single scattering amplitudes: $f=|f|\exp\{i\alpha\}$.

We will again estimate the reflected wave for near normal emission. Neglecting the inelastic processes (γ=0) we find:

$$\Psi_R^C(\vartheta = 0, E_{kin} = 100eV) \approx \Psi_{SSc}^C(0) \cdot 1.1 \exp\{0.08 \cdot i\}$$

showing that the influence of multiple scattering is small in this case. Moreover the sign of the CDAD for near normal emission is not effected.

Starting with emission from the oxygen atom we find that the double scattering amplitudes differ but that the multiple scattering parts are the same as in the case of emission from the carbon atom:

$$\frac{\Psi_{2R}^O}{\Psi_0^O(\pi, \frac{\pi}{2})} = |f_C(\pi - \vartheta)| \exp\{i[kr(1+\cos(\vartheta)) + \eta_C(\pi - \vartheta)]\} \frac{\exp(-\gamma \cdot r)}{r} + \ldots$$
$$\ldots + |f_O(\vartheta)| \exp\{i[kr(1-\cos(\vartheta)) + \eta_O(\vartheta)]\} \cdot \ldots$$
$$\ldots \cdot |f_C(\pi)| \exp\{i[2kr + \eta_C(\pi)]\} \frac{\exp(-2 \cdot \gamma \cdot r)}{r^2}$$

$$\Psi_R^O = \frac{\Psi_{2R}^O}{1 - |f_O(\pi)||f_C(\pi)| \cdot \frac{\exp\{-2\gamma r\}}{r^2} \exp\{i[2kr + \eta_O(\pi) + \eta_C(\pi)]\}}$$

The examples given above may be strongly oversimplified but they show the influence of the surface to the PIPE in principle. For systems of physical reality the cross sections have to be calculated numerically taking into account more complete final state wave functions, that will be part of future work.

XI.3 Further Remarks on Scattering

Refraction, Reflection, Temperature effects etc.

XI.3.1 Incommensurate Adsorbates

A problem occurs in using the cluster formalism to describe the scattering effects in emission from surfaces, that are incommensurate adsorbate structures. In the description of commensurable adsorbate structures one has only a restricted number of possibilities how to arrange the adsorbate atoms with respect to the substrate. If we have an incommensurate overlayer than the ratio of the lattice constants of adsorbate and substrate r_{Ad}/r_{Sub} is a real number and we have to take an infinite number of clusters to describe the problem. To estimate the influence of photoelectron diffraction on the dichroism in this case, we divide the scattering part of the amplitude into two parts, one describing the wave scattered at adsorbate atoms (A), and the other describing the wave scattered at the substrate atoms (S):

$$\Psi = \Psi_0 + \sum_{\mu}^{nA} S_{\mu A} \Psi_{\mu A} + \sum_{\mu S}^{nS} S_{\mu S} \Psi_{\mu S}$$

Here Ψ_0, Ψ_{jA}, and Ψ_{jS} are the direct amplitude and the amplitudes of the emitted electron at the j-th adsorbate or substrate atom, respectively, and S are the scattering matrices at the adsorbate and substrate atoms. If we neglect spin dependent scattering these are simply given by:

$$S_j = f(\theta)\Gamma_j \;;\; \Gamma_j = \frac{1}{r_j} \exp\left\{-\frac{\Delta L_j}{2\lambda_e}\right\}$$

Here we have included the damping part to the scattering function S for abbreviation and the complex scattering amplitude $f(\theta)$ includes the scattering phaseshift as well as the phaseshift depending on the path of the electrons from the emitter to the scatterer. If we like to include spin dependent scattering than we use the 2x2 scattering matrix like it was given in the previous chapter including the spinflip amplitude. The intensity of the scattered wave can be found from the square absolute of the amplitude:

$$I \propto \Psi\Psi^* = |\Psi_0|^2 + 2\Re e(\Psi_0 \sum S_{jA}^* \Psi_{jA}^*) + \sum S_{jA}\Psi_{jA} \sum S_{jA}^* \Psi_{jA}^*$$
$$+2\Re e(\Psi_0 \sum S_{jS}^* \Psi_{jS}^*) + \sum S_{jS}\Psi_{jS} \sum S_{jS}^* \Psi_{jS}^*$$
$$+2\Re e\left(\sum S_{jA}\Psi_{jA} \sum S_{jS}^* \Psi_{jS}^*\right)$$

If we have nSD possible orientations of the substrate with respect to the adsorbate (or vice versa), than we find the total intensity by averaging over all possible clusters.

$$I_{tot} = \frac{1}{nSD} \sum I_i \propto \frac{1}{nSD} \sum \Psi_i \Psi_i^*$$

Inserting the equation with the scattering part divided in adsorbate and substrate we find that the direct and adsorbate part are unchanged and we have to average only the parts including scattering from the substrate:

$$I_{tot} \propto \frac{1}{nSD} \sum \Psi_i \Psi_i^* = |\Psi_0|^2 + 2\Re e(\Psi_0 \sum S_{jA}^* \Psi_{jA}^*) + \sum S_{jA}\Psi_{jA} \sum S_{jA}^* \Psi_{jA}^*$$
$$+\frac{1}{nSD} \sum\left\{2\Re e(\Psi_0 \sum S_{ijS}^* \Psi_{ijS}^*) + \sum S_{ijS}\Psi_{ijS} \sum S_{ijS}^* \Psi_{jS}^*\right\}$$
$$+\frac{1}{nSD} \sum\left\{2\Re e\left(\sum S_{jA}\Psi_{jA} \sum S_{ijS}^* \Psi_{ijS}^*\right)\right\}$$

As mentioned above, nSD becomes infinite for an incommensurate adsorbate layer. In the following we concentrate on the emission from an adsorbate atom. In this case we have to average over all possible orientations of the emitting adsorbate atom with respect to the unit cell of the substrate lattice, meaning that the discrete summation in the equation above has to be replaced by an integration:

$$I_{tot} = I_0 + I_A + I_S$$
$$I_S \propto \int\left\{2\Re e(\Psi_0 \sum S_{ijS}^* \Psi_{ijS}^*) + \sum S_{ijS}\Psi_{ijS} \sum S_{ijS}^* \Psi_{jS}^* + 2\Re e\left(\sum S_{jA}\Psi_{jA} \sum S_{ijS}^* \Psi_{ijS}^*\right)\right\} d\vec{r}_i$$
$$S_{ijS}\Psi_{ijS} = S\left(\vec{r}_{jS} - \vec{r}_i\right)\Psi\left(\vec{r}_{jS} - \vec{r}_i\right)$$

For a further analysis we neglect all terms containing products of the form S_iS_j being of the order of double scattering events. The substrate part is then described by the first term. the direct amplitude does not depend on the integration variable, therefore we can perform the integration before calculating the real part, and we find the approximated substrate part to be given by:

$$I_S \propto 2\Re e\left(\Psi_0 \int_{SWSC} \left\{\sum S\left(\vec{r}_{jS} - \vec{r}_i\right)\Psi\left(\vec{r}_{jS} - \vec{r}_i\right)\right\}^* d\vec{r}_i\right)$$

The integration has to take place on one Wigner-Seitz cell of the substrate surface. $\vec{r_i}$ is the vector describing all locations of the emitting adsorbate atom within the boundary of this cell, and $\vec{r_{jS}}$ is the vector pointing from the emitting adsorbate atom (being located in the middle of the cell) to the substrate atoms. Note: We have to average on all possible substrate clusters that cannot be described by a translation within the surface unit cell. That is the case if we have to take into account different stacking order of the substrate layer, for example when we are dealing with (111)fcc or (0001)hcp surfaces.

We can proceed in the same way to estimate the influence of the substrate on CDAD and LDAD in the case of incommensurate adsorbate structures. We start with the χ expressions given in the previous chapter. Again the adsorbate part remains unchanged and the remaining terms have to be integrated to describe the influence of the substrate:

$$\chi_{xyA} = \xi^*_{y0} \sum \xi_{xjA} S(\theta_{jA}) + \xi_{x0} \sum \xi^*_{yjA} S^*(\theta_{jA})$$
$$\chi_{yzA} = \xi^*_{y0} \sum \xi_{zjA} S(\theta_{jA}) + \xi_{z0} \sum \xi^*_{yjA} S^*(\theta_{jA})$$

$$\chi_{xyS} = \xi^*_{y0} \int \sum \xi_x(\vec{r}_{jS} - \vec{r}_i) S(\vec{r}_{jS} - \vec{r}_i) d\vec{r}_i + \xi_{x0} \int \sum \xi^*_y(\vec{r}_{jS} - \vec{r}_i) S^*(\vec{r}_{jS} - \vec{r}_i) d\vec{r}_i$$
$$\chi_{yzS} = \xi^*_{y0} \int \sum \xi_z(\vec{r}_{jS} - \vec{r}_i) S(\vec{r}_{jS} - \vec{r}_i) d\vec{r}_i + \xi_{z0} \int \sum \xi_y(\vec{r}_{jS} - \vec{r}_i) S^*(\vec{r}_{jS} - \vec{r}_i) d\vec{r}_i$$

a) Initial s-state

For an initial s-state we find that the adsorbate induced part of the dichroism is given by:

$$\frac{\chi_{xyA}}{R_\beta^2} = \sin(\vartheta)\sin(\varphi) \sum \cos(\varphi_{jA}) S(\theta_{jA}) + \sin(\vartheta)\cos(\varphi) \sum \sin(\varphi_{jA}) S^*(\theta_{jA})$$
$$= \sin(\vartheta) \sum \sin(\varphi - \varphi_{jA}) \, \mathrm{Im}\{S(\theta_{jA})\}$$
$$= \sin(\vartheta) \sum \cos(\varphi - \varphi_{jA}) \, \mathrm{Re}\{S(\theta_{jA})\}$$

$$\frac{\chi_{yzA}}{R_\beta^2} = \cos(\vartheta) \sum \sin(\varphi_{jA}) S^*(\theta_{jA})$$

$$\theta_{jA} = \sin(\vartheta)\cos(\varphi - \varphi_{jA})$$

The equation in the second and third line are given for CDAD or LDAD, respectively.

XI.3.2 Temperature Effects

Temperature effects in electron scattering are described by Pendry in his work on LEED[1].

Two possibilities to include temperature effects in scattering are described by Pendry. The first is introducing a Debye-Waller factor associating thermal fluctuations with the scattering factor:

$$f_{DW} = \exp\{-w_a\} = W_j$$

1 Pendry '*LEED*'

w_a depends on the momentum transfer and compressibility of the solid. The latter is measured by the Debye-temperature T_D. It can be is approximated by the formula:

$$w_a = \frac{3|\Delta k|^2 T}{2 m_j k_B T_D^2} = \frac{3}{2} \cdot \frac{2 E_{kin} T}{m_{a.Z} \frac{m_p}{m_e} k_B T_D^2}$$

The mass m_a of the atom is written in multiples of the proton to electron mass ratio. And the kinetic energy is measured with respect to the Zero of the Muffin-Tin Potential.

Another way is to describe the temperature dependent damping of the scattering amplitudes by temperature dependent phases.

The temperature dependent phases can be found from the Zero Kelvin phases solving the following equation:

$$\exp\{i\delta_l(T)\} \sin(\delta_l(T)) = \sum_{Ll'} i^L \exp\{-2i\alpha\} j_L(-2i\alpha) \exp\{i\delta_{l'}\} \sin(\delta_{l'}) A_{Ll,l'}$$

$$A_{Ll,l'} = \sqrt{\frac{4\pi(2L+1)(l'+1)}{(2l+1)}} B^{l'}(L0, l0) = \sqrt{\frac{4\pi(2L+1)(l'+1)}{(2l+1)}} \int_\Omega Y^*_{l'0} Y_{L0} Y_{l0} \cdot d\Omega$$

α is approximated by w_a. The integrals can be found from Gaunt's coefficients and j_L is the Bessel-function of first kind with complex argument.

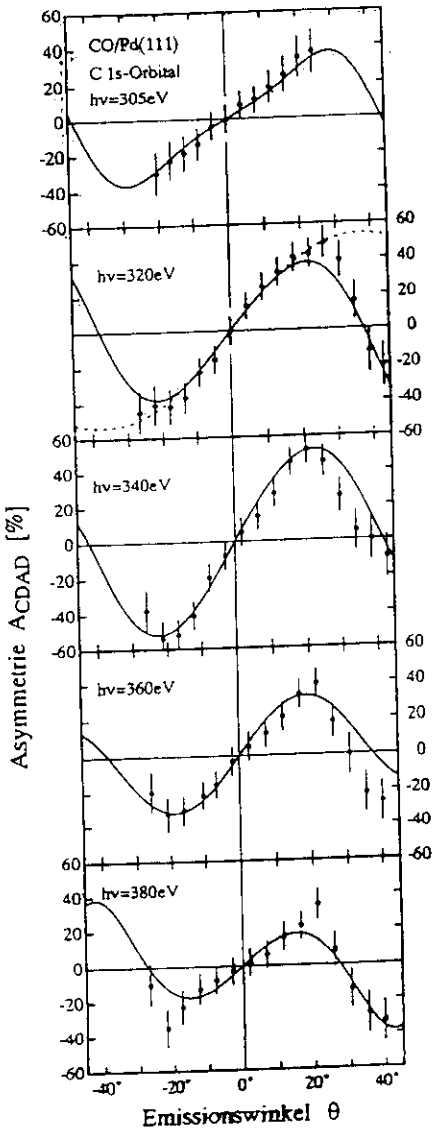

3. Baumann
.... "s" → "p"

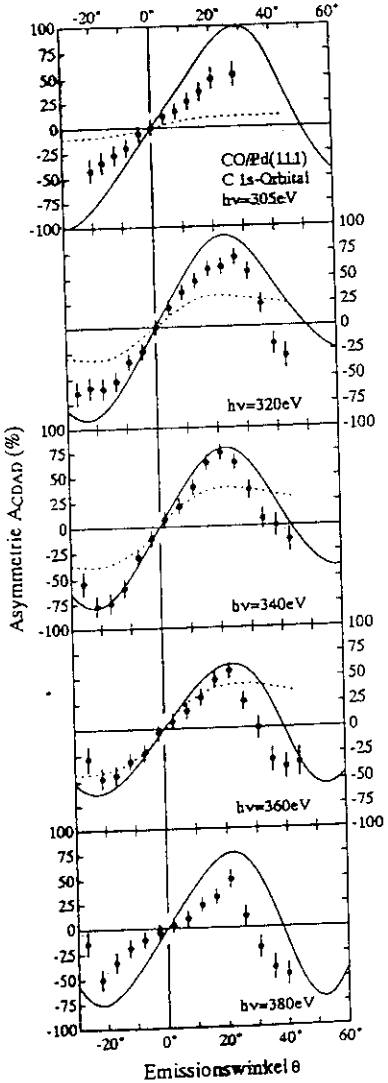

— McKoy N:CO
.... Cherepkov

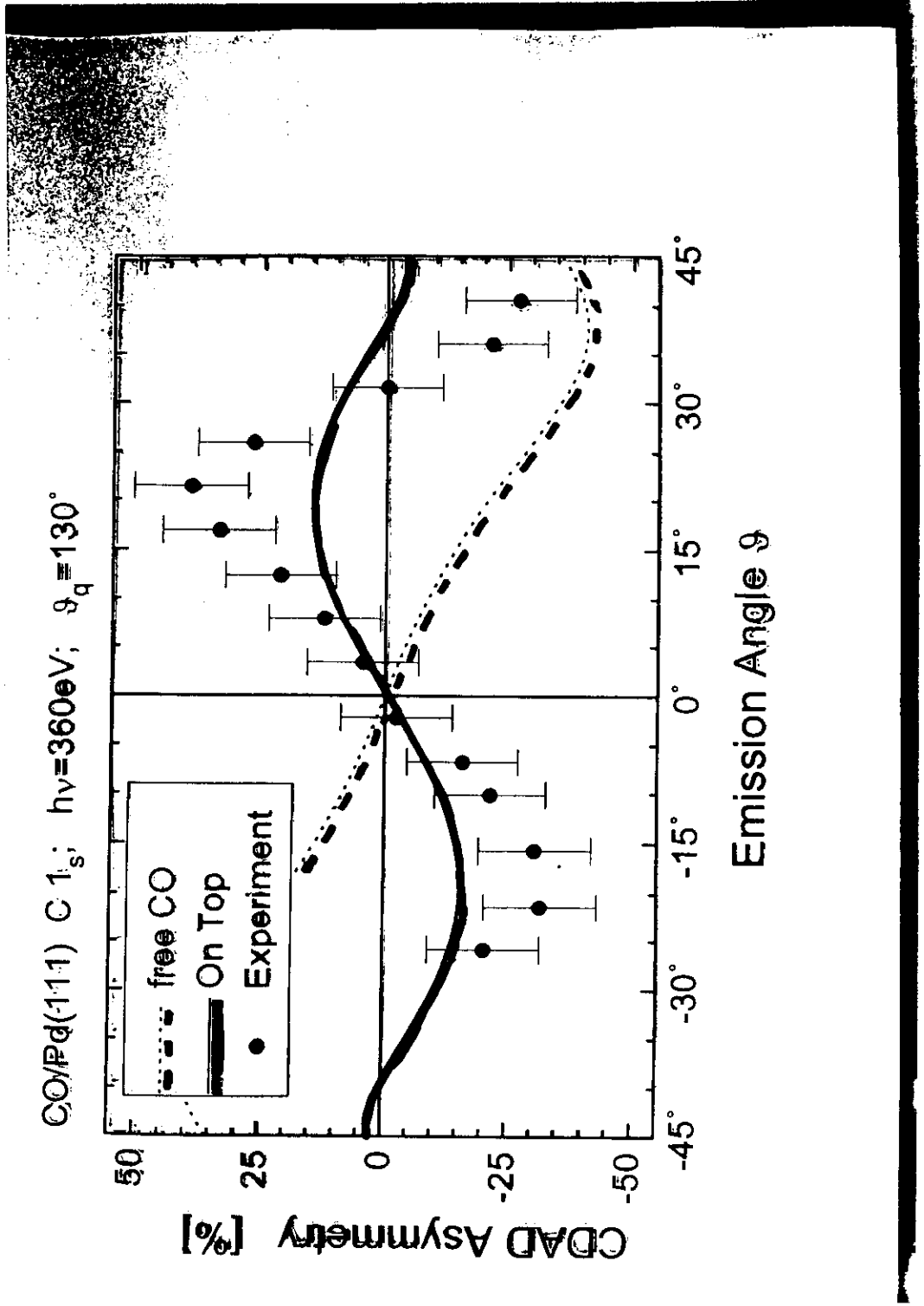

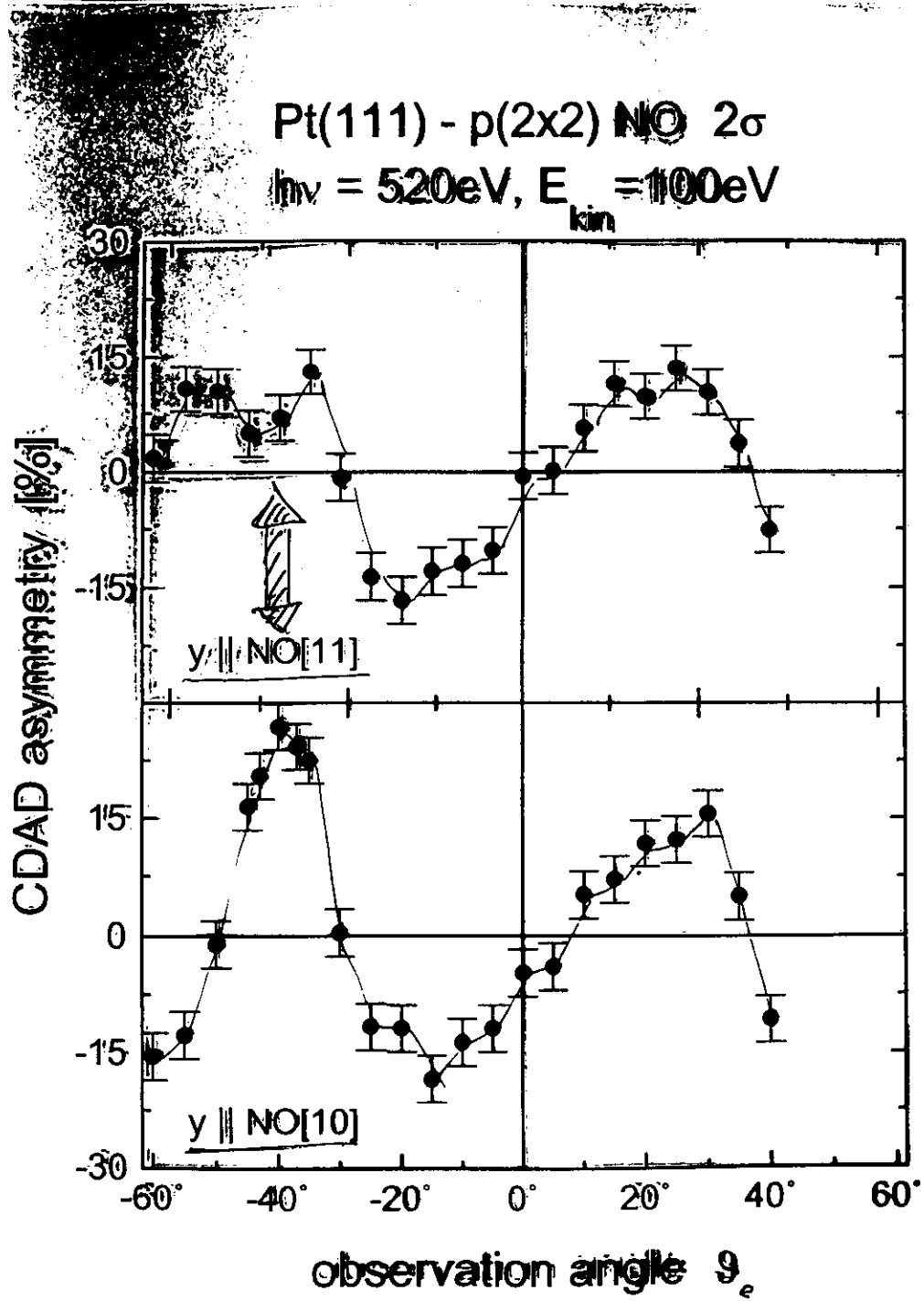
Pt(111) - p(2x2) NO 2σ
hν = 520eV, E_kin = 100eV
CDAD asymmetry [%]
y || NO[11]
y || NO[10]
observation angle ϑ_e

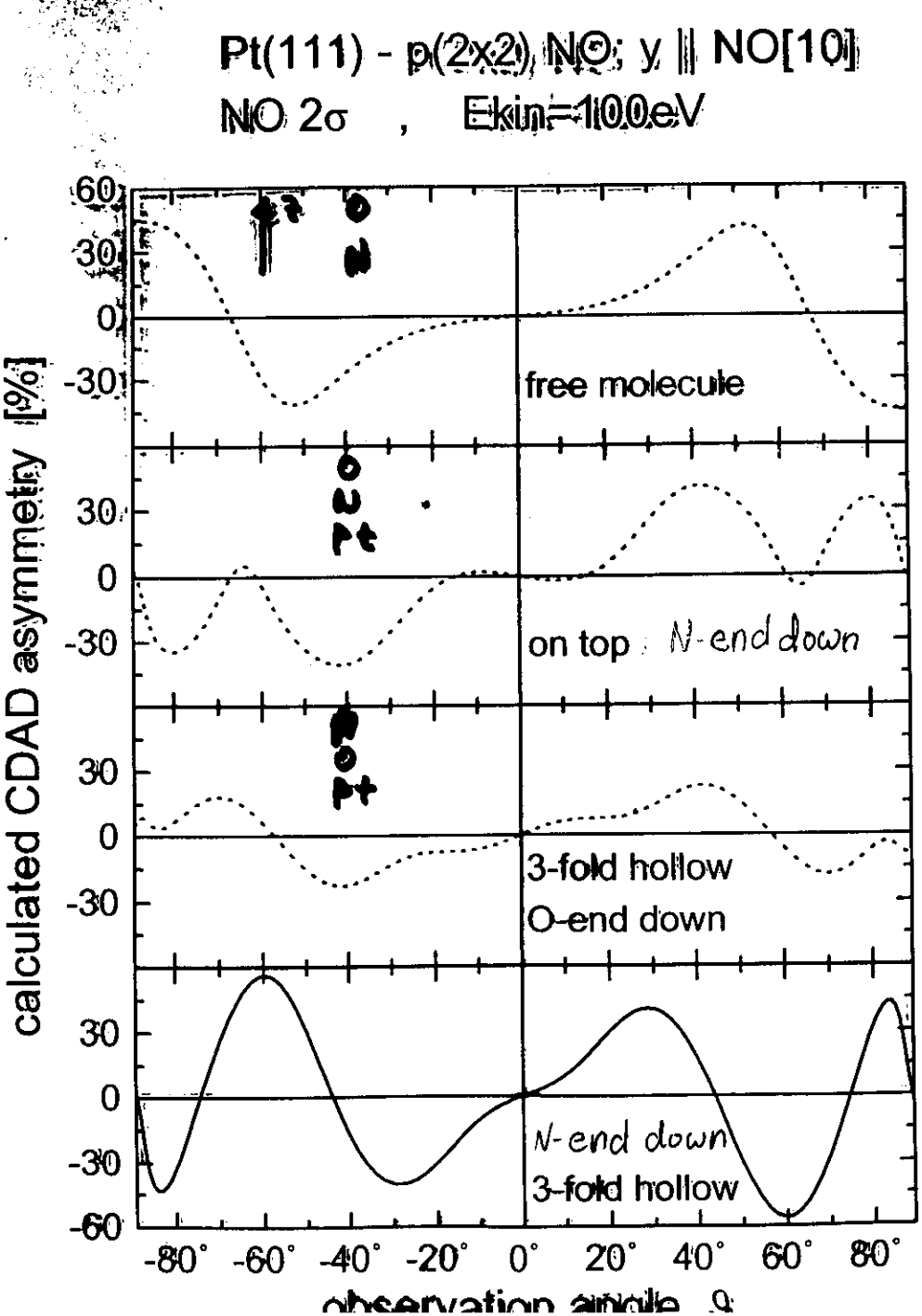
Pt(111) - p(2x2) NO; y || NO[10]
NO 2σ , Ekin=100eV
calculated CDAD asymmetry [%]
free molecule
on top N-end down
3-fold hollow
O-end down
N-end down
3-fold hollow
observation angle ϑ

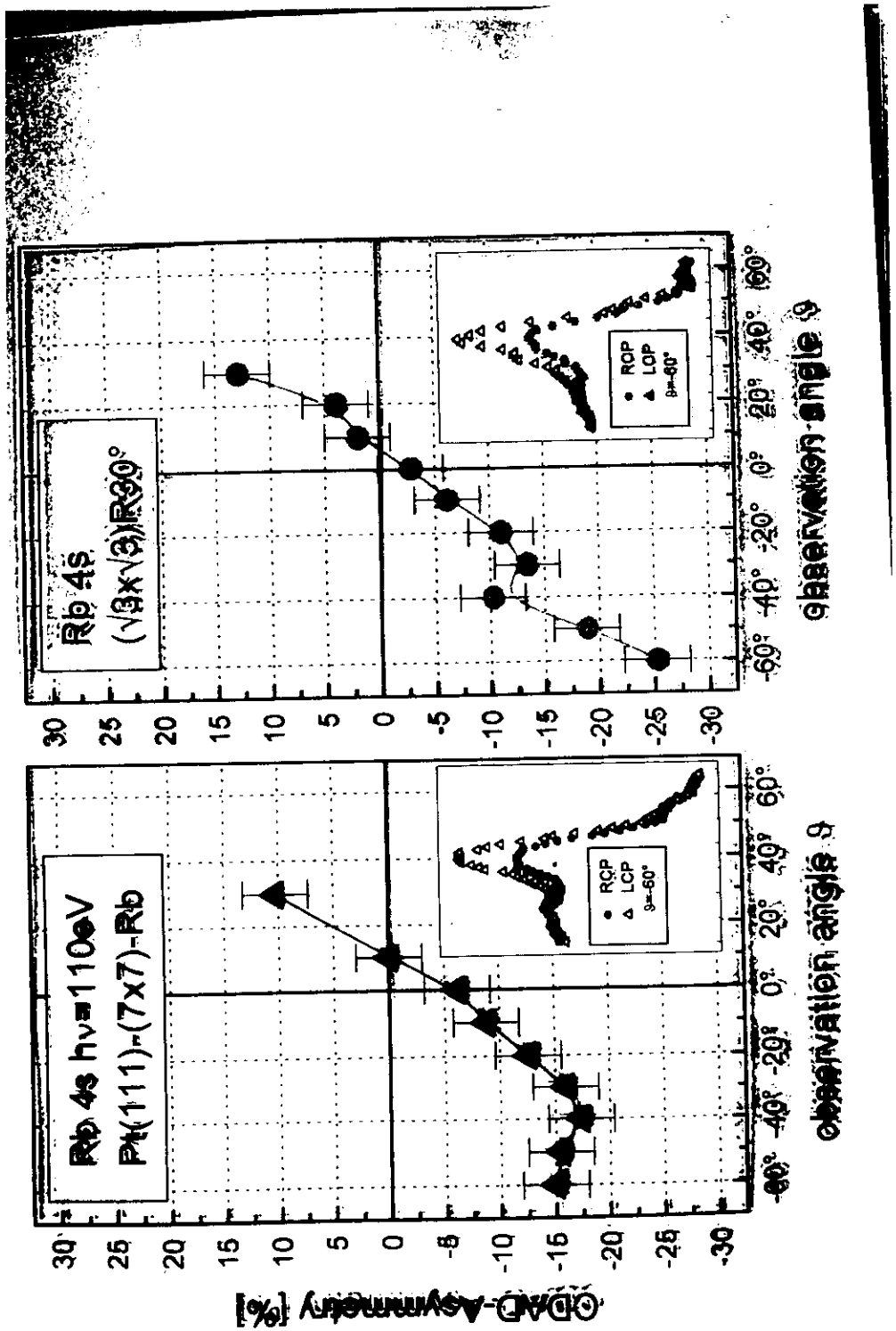

XII Rotation and Magnetic effects

Magnetic effects occur if the orientation of the initial state is changed. Orientation means that the occupation probability n(m) differs at least for two states with different signs of their magnetic quantum number: $n(m) \neq n(-m)$, whereas alignment means that the occupation numbers differ for two states with different magnetic quantum numbers: $n(m_1) \neq n(m_2)$ but are equal for the opposite sign: $n(m_i) = n(-m_i)$. Rotations, mirror-operations, and magnetic effects can be introduced to the equations above by applying the Wigner D-functions to the initial state. Until now, we had assumed that the surface normal is the natural axis of alignment namely the z-axis. In the case of magnetic measurements the direction of the applied magnetisation $\vec{M}$ is most often in plane with the surface that are the x- and y-axes and defines a new quantisation axis z' for the initial states. This new x'y'z'-frame has to be transformed by a rotation or mirror operation into the original xyz-frame, to describe the photoemission in the same frame where the photon polarisation and electron momentum is defined.

XII.1 The equivalence of MCDAD and CMDAD

Before using the rotation and mirror operations, we will show that magnetic dichroism in the angular distribution MDAD is a special case of CDAD for oriented states. This follows directly from the properties of the spherical harmonics and the dipole operator.

We describe first the dipole operator for circularly polarised photons travelling along the z-axis. We find for the polarisation and position vector:

$$\vec{\varepsilon}_{CP} = \frac{1}{\sqrt{2}} \begin{Bmatrix} 1 \\ \pm i \\ 0 \end{Bmatrix} \qquad \vec{r} = \sqrt{\frac{2\pi}{3}} \begin{Bmatrix} -(Y_{11} - Y_{1-1}) \\ i(Y_{11} + Y_{1-1}) \\ \sqrt{2}\, Y_{10} \end{Bmatrix} r$$

where the upper sign stands for RCP. The dot product results in the dipole operator $\underline{D}_{CP}$ for circularly polarised light:

$$\vec{\varepsilon} \bullet \vec{r} = \underline{D}_{CP} = -\sqrt{\frac{\pi}{3}} \left[(Y_{11} - Y_{1-1}) \pm (Y_{11} + Y_{1-1}) \right] r$$

or if we split the position from the angular dependent part:

$$\vec{\varepsilon} \bullet \hat{r} = \underline{d}_{CP} = \sqrt{\frac{\pi}{3}} \begin{cases} -2Y_{11} & RCP \\ 2Y_{1-1} & LCP \end{cases}$$

We neglect the spin, because the dipole operator does not interact directly with the spin. We assume furthermore that we have an oriented initial state described by a single spherical harmonic Y_{lm} ($l>0$, $m<>0$). The orbital angular momentum has to be higher than 0, because s states can neither be oriented nor aligned. The projection of the orbital angular momentum may not be 0, because these states are only aligned along the z-axis.

Inserting such an initial state into the golden rule expression we find for the matrix elements for RCP or LCP, respectively:

$$\frac{M^{+}_{RCP}}{-8\pi\sqrt{\frac{\pi}{3}}} = \langle Y_{lm}|Y_{11}|Y_{l+1m+1}\rangle\rho_{l+1}Y_{l+1m+1}(\hat{k}) + \langle Y_{lm}|Y_{11}|Y_{l-1m+1}\rangle\rho_{l-1}Y_{l-1m+1}(\hat{k})$$

$$\frac{M^{+}_{LCP}}{8\pi\sqrt{\frac{\pi}{3}}} = \langle Y_{lm}|Y_{1-1}|Y_{l+1m-1}\rangle\rho_{l+1}Y_{l+1m-1}(\hat{k}) + \langle Y_{lm}|Y_{1-1}|Y_{l-1m-1}\rangle\rho_{l-1}Y_{l-1m-1}(\hat{k})$$

Where we used the index + to assign that we used +z to define the orientation. $\rho_{l\pm1}$ are complex radial matrix elements. TheCDAD is given by the difference of the square absolute of the matrix elements:

$$I_{CDAD} = I_{RCP} - I_{LCP} = |M_{RCP}|^2 - |M_{LCP}|^2 = M_{RCP}M^{*}_{RCP} - M_{LCP}M^{*}_{LCP}$$

Now we change the orientation of the initial state to be parallel to -z. In that case we have simply to replace the projection quantum number m by -m. The matrix element foRCP is than given by:

$$M^{-}_{RCP} \propto \langle Y_{l-m}|Y_{11}|Y_{l+1-(m-1)}\rangle\rho_{l+1}Y_{l+1-(m-1)}(\hat{k}) + \langle Y_{l-m}|Y_{11}|Y_{l-1-(m-1)}\rangle\rho_{l-1}Y_{l-1-(m-1)}(\hat{k})$$

Now we make use of the properties of the spherical harmonics and their conjugate complex: $Y^{*}_{lm} = (-1)^{|m|}Y_{l-m}$ to calculate the conjugate of the matrix element and find:

$$M^{-*}_{RCP} \propto \langle Y_{lm}|Y_{1-1}|Y_{l+1m-1}\rangle\rho^{*}_{l+1}Y_{l+1m-1}(\hat{k}) + \langle Y_{lm}|Y_{1-1}|Y_{l-1m-1}\rangle\rho^{*}_{l-1}Y_{l-1m-1}(\hat{k})$$

Making use that Y_{1-1} describes LCP, it follows for the difference of the intensities by switching the orientation that:

$$I^{+z}_{RCP} - I^{-z}_{RCP} = |M^{+}_{RCP}|^2 - |M^{-}_{RCP}|^2 = |M^{+}_{RCP}|^2 - |M^{+}_{LCP}|^2 = I^{+}_{CDAD}$$

This shows clearly that there is no difference between switching the helicity at fixed orientation and switching the orientation at fixed helicity in the case of initial states with oriented orbital angular momentum.

Nevertheless, we have to show finally that we did not calculate for a trivial case meaning we have to show that I_{CDAD} does not vanish. We will show this for l=1, m=1, because the equations for the general case are too long to be derived here:

$$\frac{M^{+}_{RCP}}{-8\pi\sqrt{\frac{\pi}{3}}} = \langle Y_{11}|Y_{11}|Y_{22}\rangle\rho_{2}Y_{22}(\hat{k})$$

$$\frac{M^{+}_{LCP}}{8\pi\sqrt{\frac{\pi}{3}}} = \langle Y_{11}|Y_{1-1}|Y_{20}\rangle\rho_{2}Y_{20}(\hat{k}) + \langle Y_{11}|Y_{1-1}|Y_{00}\rangle\rho_{0}Y_{00}(\hat{k})$$

Obviously from the dipole selection rule, we cannot have an s partial wave in the final state for RCP but for LCP.

In the case of an true orientation we are not only interested in the differential but also in the total cross-section and whether there is a circular dichroism. The equations for the total cross-section and the CD are given by:

$$\sigma = \int|M_{if}|^2 d\Omega$$

$$I_{CD} = \int I_{CDAD}d\Omega$$

Inserting the matrix elements leads to:

$$I_{CD} = \int(M_{RCP}M^{*}_{RCP} - M_{LCP}M^{*}_{LCP})d\Omega$$

$$\frac{I_{CD}}{\frac{64}{9}\pi^3} = \int\Big|\langle Y_{lm}|Y_{11}|Y_{l+1m+1}\rangle\rho_{l+1}Y_{l+1m+1}(\hat{k}) + \langle Y_{lm}|Y_{11}|Y_{l-1m+1}\rangle\rho_{l-1}Y_{l-1m+1}(\hat{k})\Big|^2 - \Big|\langle Y_{lm}|Y_{1-1}|Y_{l+1m-1}\rangle\rho_{l+1}Y_{l+1m-1}(\hat{k}) + \langle Y_{lm}|Y_{1-1}|Y_{l-1m-1}\rangle\rho_{l-1}Y_{l-1m-1}(\hat{k})\Big|^2 d^3\hat{k}$$

On the other hand we can take the general equation derived for the CDAD and apply it to the case of photons travelling along the z-axis. This leads to:

$$I_{CD} = 2c_{\sigma}\int\Im(\xi_x\xi^{*}_y)d\Omega$$

The ξ-functions we need are:

$$\frac{\xi_x}{-4\pi} = \{g(l+1,m+1,l,m)Y_{l+1,m+1} - g(l+1,m-1,l,m)Y_{l+1,m-1}\}\rho_{l+1} + \{g(l-1,m+1,l,m)Y_{l-,m+1} - g(l-1,m-1,l,m)Y_{l-1,m-1}\}\rho_{-1}$$

$$\frac{\xi^{*}_y}{-i\cdot 4\pi} = \{g(l+1,m+1,l,m)Y^{*}_{l+1,m+1} + g(l+1,m-1,l,m)Y^{*}_{l+1,m-1}\}\rho^{*}_{l+1} + \{g(l-1,m+1,l,m)Y^{*}_{l-1,m+1} + g(l-1,m-1,l,m)Y^{*}_{l-1,m-1}\}\rho^{*}_{l-1}$$

läßt sich eventuell vereinfachen, wenn man Produkt und Imaginärteil davon ausrechnet, probieren und in 5a verwenden

In the case of an Y_{11} state we have for example:

$$\frac{\xi_x\xi^{*}_y(Y_{11})}{16\pi^2} = i\cdot\Big\{\Big\{\sqrt{\tfrac{3}{5}}\,Y_{22} - \sqrt{\tfrac{1}{10}}\,Y_{20}\Big\}\rho_2 + \sqrt{\tfrac{1}{2}}\,Y_{00}\rho_0\Big\}\Big\{\Big\{\sqrt{\tfrac{3}{5}}\,Y^{*}_{22} + \sqrt{\tfrac{1}{10}}\,Y^{*}_{20}\Big\}\rho^{*}_2 - \sqrt{\tfrac{1}{2}}\,Y^{*}_{00}\rho^{*}_0\Big\}$$

he other question is, what happens if we have an aligned state. This case was already shown before !!! We will use first $ap_z \propto Y_{10}$ state as an example:

$$\frac{M^+_{RCP}}{-8\pi\sqrt{\frac{\pi}{3}}} = \langle Y_{10}|Y_{11}|Y_{21}\rangle \rho_2 Y_{21}(\hat{k})$$

$$\frac{M^+_{LCP}}{8\pi\sqrt{\frac{\pi}{3}}} = \langle Y_{10}|Y_{1-1}|Y_{2-1}\rangle \rho_2 Y_{2-1}(\hat{k})$$

eneral case of z-aligned states (Y_{l0}):

$$M^+_{RCP} \propto -\langle Y_{l0}|Y_{11}|Y_{l+1+1}\rangle \rho_{l+1} Y_{l+1+1}(\hat{k}) + \langle Y_{l0}|Y_{11}|Y_{l-1+1}\rangle \rho_{l-1} Y_{l-1+1}(\hat{k})$$

$$M^+_{LCP} \propto \langle Y_{l0}|Y_{1-1}|Y_{l+1-1}\rangle \rho_{l+1} Y_{l+1-1}(\hat{k}) + \langle Y_{l0}|Y_{1-1}|Y_{l-1-1}\rangle \rho_{l-1} Y_{l-1-1}(\hat{k})$$

XI.2 Magnetic dichroism described by Rotations

Applying a rotation about the Euler angles $\underline{\omega}=(\alpha,\beta,\gamma)$ to the spherical harmonics or the spinor spherical armonics has the result:

$$\hat{D}(\underline{\omega})Y_{lm}(\vartheta,\varphi) = Y_{lm'}(\vartheta',\varphi') = \sum_{m=-l}^{l} Y_{lm}(\vartheta,\varphi)D^l_{mm'}(\alpha,\beta,\gamma)$$

$$\hat{D}(\underline{\omega})\Omega^j_{jm}(\vartheta,\varphi) = \Omega^j_{jm'}(\vartheta',\varphi') = \sum_{m=-j}^{j} \Omega^j_{jm}(\vartheta,\varphi)D^j_{mm'}(\alpha,\beta,\gamma)$$

The rotational D-functions using Wigner d-functions are given by:

$$D^l_{m,m'} = \exp(-im\alpha)\cdot d^l_{m,m'}(\beta)\cdot\exp(-im'\gamma)$$

Where m' is the projection of ℓ or j on the rotated z'-axis .The rotation follows the scheme:

a) rotation about the initial z-axis through α ($0\le\alpha<2\pi$)

b) rotation about the new y'-axis through β ($0\le\beta\le\pi$)

c) rotation about the new z'-axis through γ ($0\le\gamma<2\pi$)

or equivalently:

a') rotation about the initial z-axis through γ ($0\le\gamma<2\pi$)

b') rotation about the initial y-axis through β ($0\le\beta\le\pi$)

c') rotation about the initial z-axis through α ($0\le\alpha<2\pi$)

or:

a") rotation about the initial z-axis through $\alpha+\pi/2$

b") rotation about the new x'-axis through β

c") rotation about the new z'-axis through $\gamma-\pi/2$

In all cases (α,β,γ) give the relative orientation of the final frame S'(x',y',z') with respect to the initial co-ordinates S(x,y,z).

Note that we need the inverse of the rotation to transform x'y'z' back to xyz. If the Euler angles $\underline{\omega}=(\alpha,\beta,\gamma)$ describe the Z'-system with respect to the original frame than it is transformed into Z by the inverse rotation through $\underline{\omega}^{-1}=(-\gamma,-\beta,-\alpha)=(\pi-\gamma,\beta,\pi-\alpha)$. The rotation operator $D(\underline{\omega}^{-1}{}_{\perp,\parallel})$ transforms the co-ordinates with the magnetisation as quantisation axis z' back to the xyz-coordinates as defined in the previous chapters.

We will distinguish special cases of rotation that depend whether the x'-z' or the y'-z'-planes are corresponding to the surface:

a) For the x'-z'-plane in the surface and the z'-axis of the atomic frame coincidences with the x-axis of the laboratory frame. If the quantisation axis due to the magnetisation is parallel to the x-axis we have $\underline{\omega}_\parallel=(0,\pi/2,\pi/2)$ and $\underline{\omega}^{-1}{}_\parallel=(\pi/2,\pi/2,\pi)$,this is called ||-orientation.

b) For the y'-z'-plane in the surface and the z'-axis of the atomic frame coincidences with the y-axis of the laboratory frame. For this $\perp$-orientation the magnetisation is parallel to the y-axis with $\underline{\omega}_\perp=(\pi/2,\pi/2,\pi)$ and $\underline{\omega}^{-1}{}_\perp=(0,\pi/2,\pi/2)$.

Switching the sign of the magnetisation is due to a mirror operation at the y-z or x-z-plane depending whether the initial magnetisation has parallel or perpendicular orientation. Reflections with respect to the meridian planes result in:

$$\hat{M}^{\parallel}_{y-z}Y_{lm}(\vartheta,\varphi) = i\cdot(-1)^m Y_{l-m}(\vartheta,\varphi)$$

$$\hat{M}^{\perp}_{x-z}Y_{lm}(\vartheta,\varphi) = (-1)^m Y_{l-m}(\vartheta,\varphi)$$

and reflection with respect to the equatorial plane results in:

$$\hat{M}_{x-y}Y_{lm}(\vartheta,\varphi) = (-1)^{l+m}Y_{lm}$$

Examples of rotational matrices for real states with $\ell=1$:

$\ell=1$		m'		
	$D_\perp$	1	0	-1
m	1	-i/2	$+i/\sqrt{2}$	+i/2
	0	$-i/\sqrt{2}$	0	$-i/\sqrt{2}$
	-1	+i/2	$+i/\sqrt{2}$	-i/2

ℓ=1		m'		
	$D_{\parallel}$	1	0	-1
m	1	-i/2	-i/√2	+i/2
	0	-i/√2	0	-i/√2
	-1	-i/2	+i/√2	+i/2

Example: We assume Y_{11} in ||-orientation, that is the z'-axis being aligned along the x-axis. Applying the rotation we have in the laboratory system:

$$\hat{D}(\underline{\omega}_{\parallel})Y_{11} = \frac{-i}{\sqrt{2}}\left\{Y_{10} + \frac{1}{\sqrt{2}}(Y_{11} + Y_{1-1})\right\} = \frac{-i}{\sqrt{2}}\{i \cdot p_z + p_y\}$$

and a mirror operation leads finally to:

$$\hat{M}^{\parallel}\left[\hat{D}^{\parallel}(Y_{11})\right] = \hat{M}^{\parallel}\left[\frac{-i}{\sqrt{2}}\left\{Y_{10} + \frac{1}{\sqrt{2}}(Y_{11} + Y_{1-1})\right\}\right] = \frac{1}{\sqrt{2}}\left\{Y_{10} + \frac{-1}{\sqrt{2}}(Y_{1-1} + Y_{11})\right\}$$

$$= \frac{1}{\sqrt{2}}(p_z + i \cdot p_y) \qquad = \hat{D}^{\parallel}(i \cdot Y_{1-1})$$

The latter shows that the sequence of rotation and mirror operations can be interchanged.

In most magnetic surface science experiments the magnetisation is in the x-y plane and we have to apply the rotation to this case. The angle μ of the magnetisation is measured with respect to the x-axis, so that $M^{\parallel}=M_x=M\cos(\mu)$ and $M^{\perp}=M_y=M\sin(\mu)$. The magnetic field rotates the states by $\underline{\omega}_{\perp,xz}=(\mu,\pi/2,\pi/2)$ (x'z'-plane in surface). The set of Euler angles that converts the $M_{z'}$-axis from the x'-z'-plane back into the laboratory x-y-plane is given by the inverted rotation $(\underline{\omega}_{\perp,xz})^{-1}=(\pi/2,\pi/2,\pi-\mu)$. Applying this relation we find the rotational matrix as follows:

$$D_{\mu}^{-1} = e^{-i m\frac{\pi}{2}} \cdot d^{l}_{m'm}\left(\frac{\pi}{2}\right) \cdot e^{-i m'(\pi-\mu)} = e^{-i\left(m\frac{\pi}{2}+m'\pi\right)} \cdot d^{l}_{m'm}\left(\frac{\pi}{2}\right) \cdot e^{i m'\mu}$$

that reads for $p_{1/2}$-states (ℓ=1,j=1/2):

$$D^{-1}_{\mu,j=1/2} = \begin{pmatrix} \frac{(1-i)}{2}\exp\left\{-i\frac{\pi-\mu}{2}\right\} & -\frac{(1-i)}{2}\exp\left\{i\frac{\pi-\mu}{2}\right\} \\ \frac{(1+i)}{2}\exp\left\{-i\frac{\pi-\mu}{2}\right\} & \frac{(1+i)}{2}\exp\left\{i\frac{\pi-\mu}{2}\right\} \end{pmatrix}$$

Further rotational matrices for the states with higher total angular momentum are given in the appendix. Applying the rotational matrix we find that the $p'_{1/2}$ states with the z'-axis (of the x'z'-plane) in the xy-plane are given by:

$$p'_{1/2,+1/2} = -\frac{(1+i)}{2}\exp\left\{i\frac{\mu}{2}\right\}p_{1/2,+1/2} \qquad -\frac{(1+i)}{2}\exp\left\{-i\frac{\mu}{2}\right\}p_{1/2,-1/2}$$

$$p'_{1/2,-1/2} = \frac{(1-i)}{2}\exp\left\{i\frac{\mu}{2}\right\}p_{1/2,+1/2} \qquad -\frac{(1-i)}{2}\exp\left\{-i\frac{\mu}{2}\right\}p_{1/2,-1/2}$$

From the rotational matrix we find the scheme to build the rotated states in the perpendicular or parallel orientation by inserting $\mu_{\perp}=90°$ or $\mu_{\parallel}=0°$, respectively.

$D_{\perp}$		m'	
		½	-1/2
m	½	-i/√2	-1/√2
	-1/2	1/√2	i/√2

$D_{\parallel}$		m'	
		½	-1/2
m	½	-(1+i)/2	-(1+i)/2
	-1/2	(1-i)/2	-(1-i)/2

meaning that if a magnetic field is applied either along the x- or the y-axis, than for the parallel and perpendicular orientations of the magnetic field in the x-y laboratory co-ordinates the two magnetised $p'_{1/2,m}$-substates are described by:

$M_{\perp} \rightarrow D^{-1}{}_{\perp}$	
$p'_{1/2,+1/2}=$	$-[i\,p_{1/2,+1/2}+p_{1/2,-1/2}]/\sqrt{2}$
$p'_{1/2,-1/2}=$	$[p_{1/2,+1/2}+i\,p_{1/2,-1/2}]/\sqrt{2}$

$M_{\parallel} \rightarrow D^{-1}{}_{\parallel}$	
$p'_{1/2,+1/2}=$	$-[p_{1/2,+1/2}+p_{1/2,-1/2}](1+i)/2$
$p'_{1/2,-1/2}=$	$[p_{1/2,+1/2}-p_{1/2,-1/2}](1-i)/2$

The magnetic field removes the degeneracy of the m_j-sublevels, so that they appear at different energies. If the sign of the magnetic field is reversed than the energetically order of the sublevels is reversed, too. The dichroic signal is then given by the difference of the intensities of the sublevels corresponding to the same energy.

$$I^{MD} = I^{M+} - I^{M-}$$

that becomes easy in the case of the $p_{1/2}$ 2-level system:

For a fixed polarisation and the magnetic field M parallel to the surface normal, or $M_{\perp}$ parallel to the y-axis, or $M_{\parallel}$ parallel to the x-axis we find using the Ξ-functions:

$$I^{MD} = |\,\Xi(p_{1/2,1/2})\,|^2 - |\,\Xi(p_{1/2,-1/2})\,|^2$$

$$I^{M\perp D} = 4\,\Re e\{\, e^{i\mu}\,\Xi(p_{1/2,1/2})\,\Xi^*(p_{1/2,-1/2})\}$$

$$I^{M\perp D} = -4\,\Im m\{\,\Xi(p_{1/2,1/2})\,\Xi^*(p_{1/2,-1/2})\}$$

$$I^{M\parallel D} = 4\,\Re e\{\,\Xi(p_{1/2,1/2})\,\Xi^*(p_{1/2,-1/2})\}$$

Note that we have to handle the spin up and spin down intensities separately.

The easiest case is that of pure s-polarisation because we have to take into account only the component ξ_y.

$$\xi_y(p_{1/2,+1/2}) = i \cdot \sqrt{\tfrac{1}{6}} \left\{ \left(\sqrt{3}\,\Omega^2_{3/2,3/2} + \Omega^2_{3/2,-1/2} \right) \cdot \rho^2_{3/2} + \sqrt{2}\,\Omega^0_{1/2,-1/2} \cdot \rho^0_{1/2} \right\}$$
$$\xi_y(p_{1/2,-1/2}) = i \cdot \sqrt{\tfrac{1}{6}} \left\{ \left(\sqrt{3}\,\Omega^2_{3/2,-3/2} + \Omega^2_{3/2,1/2} \right) \cdot \rho^2_{3/2} - \sqrt{2}\,\Omega^0_{1/2,1/2} \cdot \rho^0_{1/2} \right\}$$

or spin resolved:

$$\xi \uparrow_y (p_{1/2,+1/2}) = -i \cdot \sqrt{\tfrac{1}{10}} \left(Y_{21} + Y_{2-1} \right) \cdot \rho^2_{3/2}$$
$$\xi \downarrow_y (p_{1/2,+1/2}) = i \cdot \left\{ \sqrt{\tfrac{1}{15}} \left(\sqrt{6}\, Y_{22} + Y_{20} \right) \cdot \rho^2_{3/2} + \sqrt{\tfrac{1}{3}}\, Y_{00} \cdot \rho^0_{1/2} \right\}$$

$$\xi \uparrow_y (p_{1/2,-1/2}) = -i \cdot \left\{ \sqrt{\tfrac{1}{15}} \left(\sqrt{6}\, Y_{2-2} + Y_{20} \right) \cdot \rho^2_{3/2} + \sqrt{\tfrac{1}{3}}\, Y_{00} \cdot \rho^0_{1/2} \right\}$$
$$\xi \downarrow_y (p_{1/2,-1/2}) = i \cdot \sqrt{\tfrac{1}{10}} \left(Y_{2-1} + Y_{21} \right) \cdot \rho^2_{3/2}$$

First we calculate the case for the magnetisation being parallel to the surface normal. To simplify the equations we make use that $Y^*_{\ell,m}=(-1)^m Y_{\ell,-m}$ and find for the intensities of both substates excited by linearly s-polarised light:

$$\xi\xi^* \uparrow_y (p_{1/2,+1/2}) = \tfrac{1}{10}(2|Y_{21}|^2 - (Y_{21}Y_{21} + Y_{2-1}Y_{2-1})) \cdot R_d^2$$

$$\begin{aligned} \xi\xi^* \downarrow_y (p_{1/2,+1/2}) = {} & \tfrac{1}{15}(6|Y_{22}|^2 + |Y_{20}|^2 + Y_{20}\sqrt{6}\,(Y_{22} + Y_{2-2})) \cdot R_d^2 \\ & + \tfrac{1}{3}|Y_{00}|^2 \cdot R_s^2 \\ & + 2\sqrt{\tfrac{1}{45}}\, Y_{20} Y_{00} \cdot \cos\{\delta_d - \delta_s\} \cdot R_s R_d \\ & + \sqrt{\tfrac{2}{15}}\, Y_{00} \cdot [Y_{22} \exp\{i(\delta_d - \delta_s)\} + Y_{2-2} \exp\{-i(\delta_d - \delta_s)\}] R_s R_d \end{aligned}$$

$$\begin{aligned} \xi\xi^* \uparrow_y (p_{1/2,-1/2}) = {} & \tfrac{1}{15}(6|Y_{22}|^2 + |Y_{20}|^2 + Y_{20}\sqrt{6}\,(Y_{22} + Y_{2-2})) \cdot R_d^2 \\ & + \tfrac{1}{3}|Y_{00}|^2 \cdot R_s^2 \\ & 2\sqrt{\tfrac{1}{45}}\, Y_{20} Y_{00} \cdot \cos\{(\delta_d - \delta_s)\} \cdot R_s R_d \\ & + \sqrt{\tfrac{2}{15}}\, Y_{00} \cdot [Y_{22} \exp\{-i(\delta_d - \delta_s)\} + Y^*_{22} \exp\{i(\delta_d - \delta_s)\}] R_s R_d \end{aligned}$$
$$\xi\xi^* \downarrow_y (p_{1/2,-1/2}) = \tfrac{1}{10}(2|Y_{21}|^2 - (Y_{21}Y_{21} + Y_{2-1}Y_{2-1})) \cdot R_d^2$$

Inserting real orbitals and the angular dependence the equations simplify to be:

$$\begin{aligned} \frac{\xi\xi^* \uparrow_y (p_{1/2,+1/2})}{1/4\pi} = {} & \tfrac{3}{4}(\sin^2(2\vartheta)[2 - \cos(2\varphi)]) \cdot R_d^2 \\ \frac{\xi\xi^* \downarrow_y (p_{1/2,+1/2})}{1/4\pi} = {} & \left(3\sin^4(\vartheta) + 2\sin^2(\vartheta) + \tfrac{2}{3} \right) \cdot R_d^2 \\ & + \tfrac{1}{2}[3\cos^2(\vartheta) - 1]\sin^2(\vartheta)\cos(2\varphi) \cdot R_d^2 \\ & + \tfrac{1}{3} \cdot R_s^2 \\ & + \tfrac{1}{3} \cdot [3\cos^2(\vartheta) - 1] \cdot \cos\{\delta_d - \delta_s\} \cdot R_s R_d \\ & + \sin 2(\vartheta)[\cos(2\varphi)\cos(\delta_d - \delta_s) - \sin(2\varphi)\sin(\delta_d - \delta_s)] R_s R_d \end{aligned}$$

$$\begin{aligned} \frac{\xi\xi^* \uparrow_y (p_{1/2,-1/2})}{1/4\pi} = {} & \left(6\sin^4(\vartheta) + \tfrac{1}{3}[3\cos^2(\vartheta) - 1]^2 \right) \cdot R_d^2 \\ & + \tfrac{1}{2}[3\cos^2(\vartheta) - 1] \cdot \sin^2(\vartheta)\cos(2\varphi) \cdot R_d^2 \\ & + \tfrac{1}{3} \cdot R_s^2 \\ & + \tfrac{1}{3}[3\cos^2(\vartheta) - 1] \cdot \cos\{(\delta_d - \delta_s)\} \cdot R_s R_d \\ & + \sin 2(\vartheta)\{\cos(2\varphi)\cos(\delta_d - \delta_s) + \sin(2\varphi)\sin(\delta_d - \delta_s)\} R_s R_d \\ \frac{\xi\xi^* \downarrow_y (p_{1/2,-1/2})}{1/4\pi} = {} & \tfrac{3}{4}\sin^2(2\vartheta)\{2 - \cos(2\varphi)\} \cdot R_d^2 \end{aligned}$$

There are only two terms differing and we find for the magnetic dichroism:

$$I^{MDs} = -\frac{c_\sigma}{4\pi} \cdot 2\sin^2(\vartheta)\sin(2\varphi)\sin(\delta_d - \delta_s) R_s R_d$$

It vanishes in normal emission (ϑ=0°) and in the x-z (φ=0°) and y-z (φ=90°) planes

For in-plane magnetisation we need the mixed product $\xi_{1/2}\xi^*_{-1/2}$ (index for m_j) that give:

$$\begin{aligned} \xi_{+1/2}\xi^*_{-1/2} \uparrow_y = {} & \sqrt{\tfrac{1}{150}}\,(\sqrt{6}\, Y_{22} + Y_{20})(Y_{21} + Y_{2-1}) \cdot R_d^2 \\ & + \sqrt{\tfrac{1}{30}}\,(Y_{21} + Y_{2-1}) \cdot Y_{00} \cdot R_s R_d \exp\{i(\delta_d - \delta_s)\} \end{aligned}$$

$$\begin{aligned} \xi_{+1/2}\xi^*_{-1/2} \downarrow_y = {} & -\sqrt{\tfrac{1}{150}}\,(\sqrt{6}\, Y_{22} + Y_{20})(Y_{21} + Y_{2-1}) \cdot R_d^2 \\ & - \sqrt{\tfrac{1}{30}}\,(Y_{21} + Y_{2-1}) \cdot Y_{00} \cdot R_s R_d \exp\{-i(\delta_d - \delta_s)\} \end{aligned}$$

resulting in:

$$\Re e(\xi\xi^* \uparrow) + \Re e(\xi\xi^* \downarrow) = \frac{1}{4\pi} \sin(2\vartheta)\sin(\varphi) \cdot R_s R_d \cdot \sin(\delta_d - \delta_s)$$
$$\Im m(\xi\xi^* \uparrow) + \Im m(\xi\xi^* \downarrow) = 0$$

and we have finally the magnetic dichroism for s-polarised light and in-plane magnetisation given by:

$$I^{M\parallel D,s} = \frac{c_\sigma}{4\pi} \cdot 4\sin(2\vartheta)\sin(\varphi) \cdot R_s R_d \cdot \sin(\delta_d - \delta_s)$$

$$I^{M\perp D,s} = 0$$

The dichroism $I^{M\perp D,s}$ for the magnetic field parallel to the photon polarisation vanishes. The dichroism $I^{M\parallel D,s}$ for the magnetic field perpendicular to the photon polarisation can be observed in the yz-plane (φ=90°) but not in the special case of normal emission (ϑ=0°) or in the xz-plane (φ=0°).

For the case of p-polarisation we find for the magnetisation parallel to the surface normal (angle of incidence α is measured with respect to surface normal inx-z-plane):

$$\frac{I^{MD,s}}{\frac{8\pi}{3}c_\sigma R_s R_d \sin(\delta_d - \delta_s)} = -\sin^2(\vartheta)\sin(2\varphi)$$

$$\frac{I^{MD,p}}{\frac{8\pi}{3}c_\sigma R_s R_d \sin(\delta_d - \delta_s)} = \cos^2(\alpha)\sin^2(\vartheta)\sin(2\varphi) - \frac{1}{4}\sin(2\alpha)\sin(2\vartheta)\sin(\varphi)$$

Unpolarised light can be described by the incoherent superposition of linearly s- and p-polarised light. From the difference in the MD signals we see the evidence for a magnetic dichroism excited by unpolarised light.

$$\frac{I^{MD,0}}{\frac{4\pi}{3}c_\sigma R_s R_d \sin(\delta_d - \delta_s)} = -\sin^2(\alpha)\sin^2(\vartheta)\sin(2\varphi) - \frac{1}{4}\sin(2\alpha)\sin(2\vartheta)\sin(\varphi)$$

The complete angular distributions for the magnetic dichroism excited by circularly or S_2-linearly polarised light are to complicated to be reproduced here. We give them only for spectroscopy in the y-z-plane (φ=90°):

$$\frac{I^{MD,\ RLP}_{\ \ LLP}}{\frac{16\pi}{3}c_\sigma} = -\left[\cos(\alpha)\cdot\sin^2(\vartheta) + \tfrac{1}{16}\sin(2\alpha)\cdot\sin(2\vartheta)\right]R_s R_d \sin(\delta_d - \delta_s)$$

$$\frac{I^{MD,\ RCP}_{\ \ LCP}}{\frac{16\pi}{3}c_\sigma} = \pm\cos(\alpha)\cdot\{(3\cos^2(\vartheta)-1)[R_d^2 + R_s R_d\cos(\delta_d - \delta_s)] + \left[\tfrac{1}{3}R_s^2 - R_d^2\right]\}$$
$$-\tfrac{1}{16}\sin(2\alpha)\cdot\sin(2\vartheta)\cdot R_s R_d \sin(\delta_d - \delta_s)$$

The LMDAD excited by the S_2-polarised photons is the same independent of the sign of polarisation. If applying circularly polarised light of opposite helicity the term connected to cos(α) switches sign,

whereas the term connected to sin(2α) stays in sign. Obviously we find for circularly polarised light a magnetic dichroism in normal emission:

$$\frac{I^{MD.\ RCP}_{\ \ LCP}(\vartheta = 0°)}{\frac{16\pi}{3}c_\sigma} = \pm\cos(\alpha)\cdot\{R_d^2 + 2R_s R_d\cos(\delta_d - \delta_s) + \tfrac{1}{3}R_s^2\}$$

Additionally, we find a circular magnetic dichroism given by:

$$I^{CMD.\ RCP}_{\ \ LCP} = \pm(\tfrac{8\pi}{3})^2 c_\sigma \cdot \cos(\alpha)(R_d^2 - R_s^2)$$

It means that there is a difference in the total cross section if the sign of the magnetisation is switched at fixed photon polarisation. This CMD is independent on the final state phases δ_s,δ_d. The meaning of R_s, R_d in absorption spectroscopy is discussed elsewhere.

XII.3 References

[1] B.T.Thole, G.v.d.Laan; Phys.Rev. **B44** (1991) 12424

[2] G.v.d.Laan, B.T.Thole; Phys.Rev. **B48** (1993) 210

[3] B.T.Thole, G.v.d.Laan; Phys.Rev. **B49** (1994) 9613

[4] D.Venus; Phys.Rev. **B49** (1994) 8821

[5] N.A.Cherepkov; Phys.Rev. **B50** (1994) 13813

[6] T.Scheunemann, S.V.Haliiov, J.Henk, R.Feder; Solid State Comm. **91** (1994) 487

[7] G.v.d.Laan, B.T.Thole; Phys.Rev. **B52** (1995) 15355

[8] N.A.Cherepkov, V.V.Kusnetzov, V.A.Verbitskii; J.Phys. B: At.Mol.Opt.Phys. **28** (1995) 1221

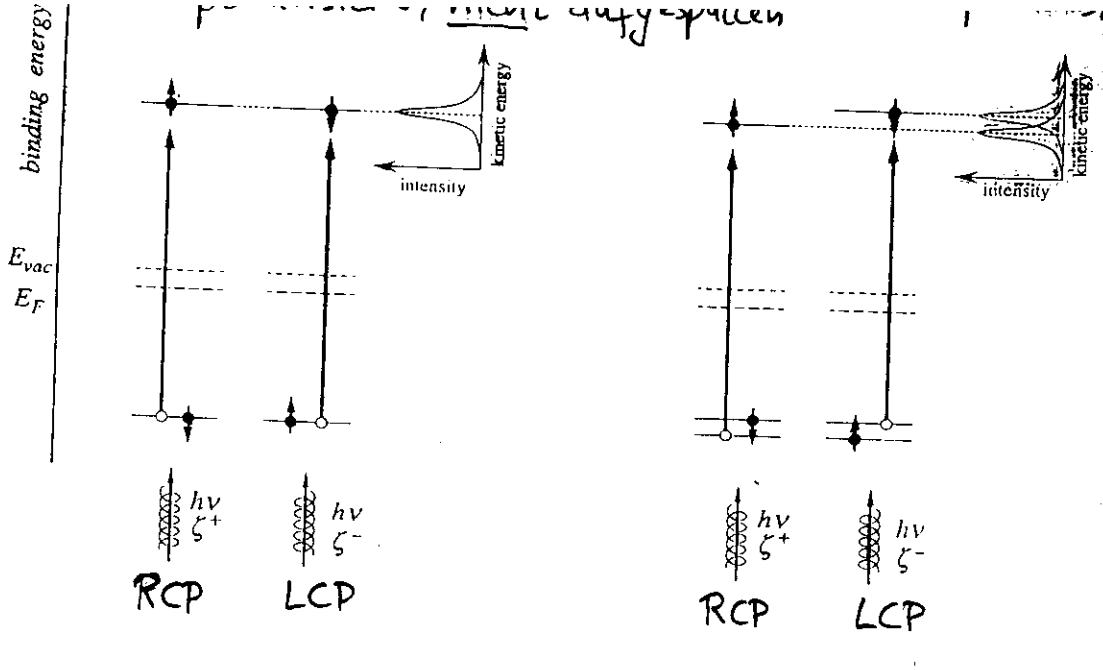

a) Optical orientation from non-magnets

b) Optical orientation from ferromagnets

FIGURE 37. Schematic representation of the principle of optical orientation from ferromagnets (b) when compared with nonmagnetic materials (a).

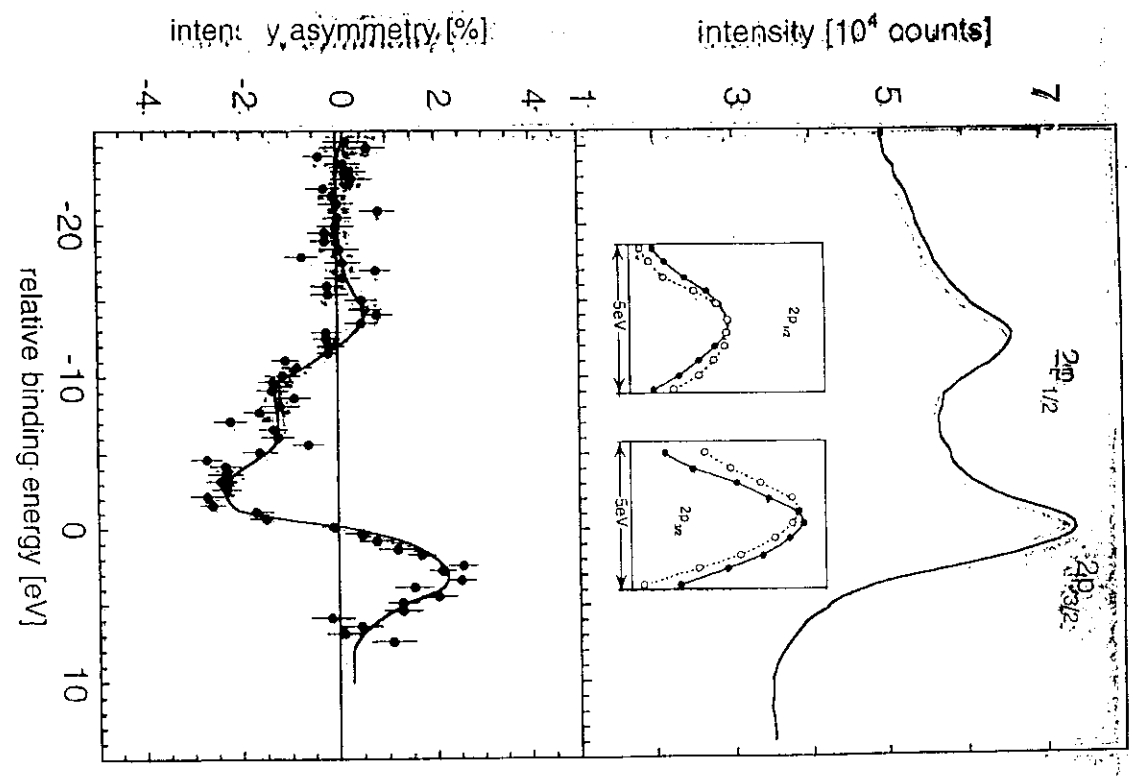

FIGURE 38. Magnetic circular dichroism in soft X-ray core-level photoemission. Intensity distribution averaged over two magnetization directions (top panel) and corresponding intensity asymmetry calculated according to Equation 23 (bottom panel). The inset gives the region of the peaks on an enlarged energy scale in order to show the change in the peak position with the magnetization direction more clearly. (From Baumgarten, L., Schneider, C. M., Schäfers, F., Petersen, H., and Kirschner, J., Rev. Sci. Instrum.,

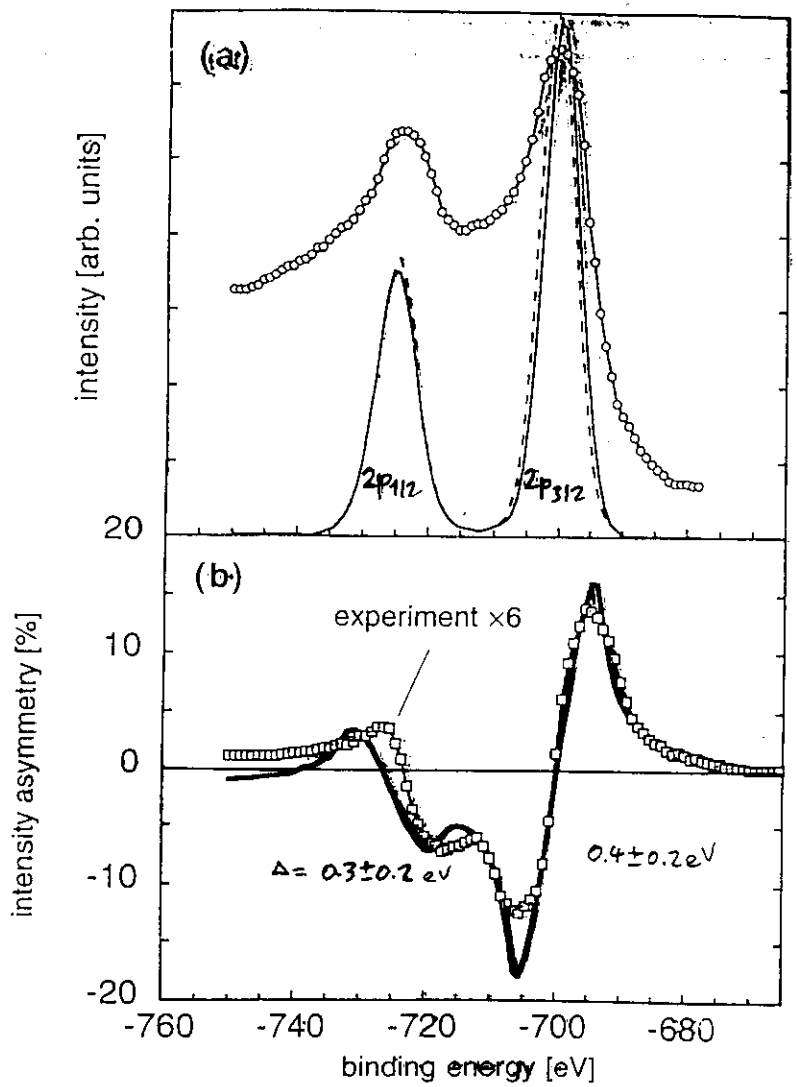

FIGURE 39. Calculated MCDAD spectra for the experimental situation shown in Figure 38. The intensity spectra (solid and broken line) for both magnetization directions are compared with the experimental result (circles) (a). (b) Comparison of the theoretical (solid) and experimental (squares) results, the latter having been scaled up by a factor of six. (From Ebert, H., Baumgarten, L., Schneider, C. M., and Kirschner, J., *Phys. Rev. B*, 44, 4406, 1991. With permission.)

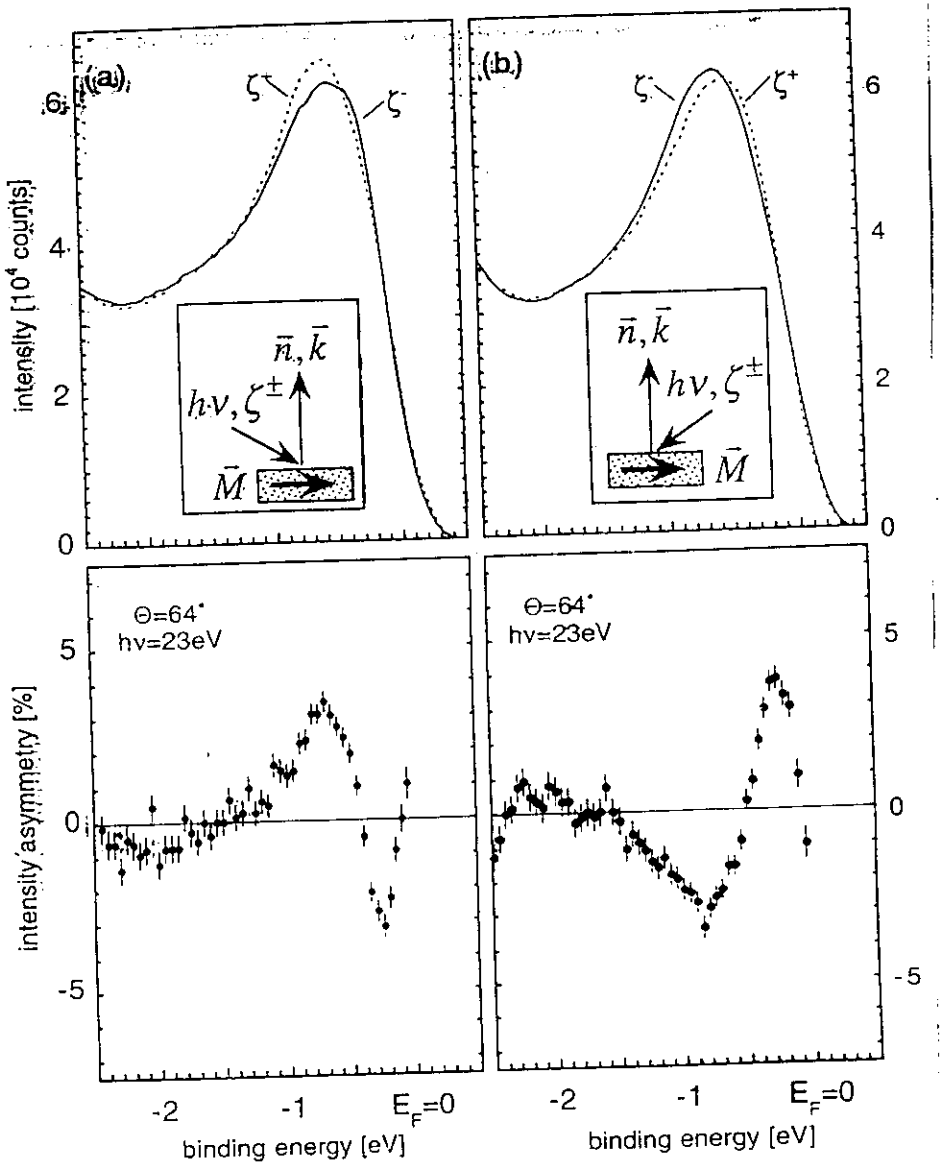

FIGURE 42. MCDAD in the 3d valence bands of Co. Top panels: intensity spectra for light of positive and negative helicity, respectively. Bottom panels: corresponding intensity asymmetry. (a) and (b) refer to different experimental geometries, as shown in the inset. (From Schneider, C. M., Hammond, M. S., Schuster, P., Cebollada, A., Miranda, R., and Kirschner, J., *Phys. Rev. B*, 44, 12066, 1991. With permission.)

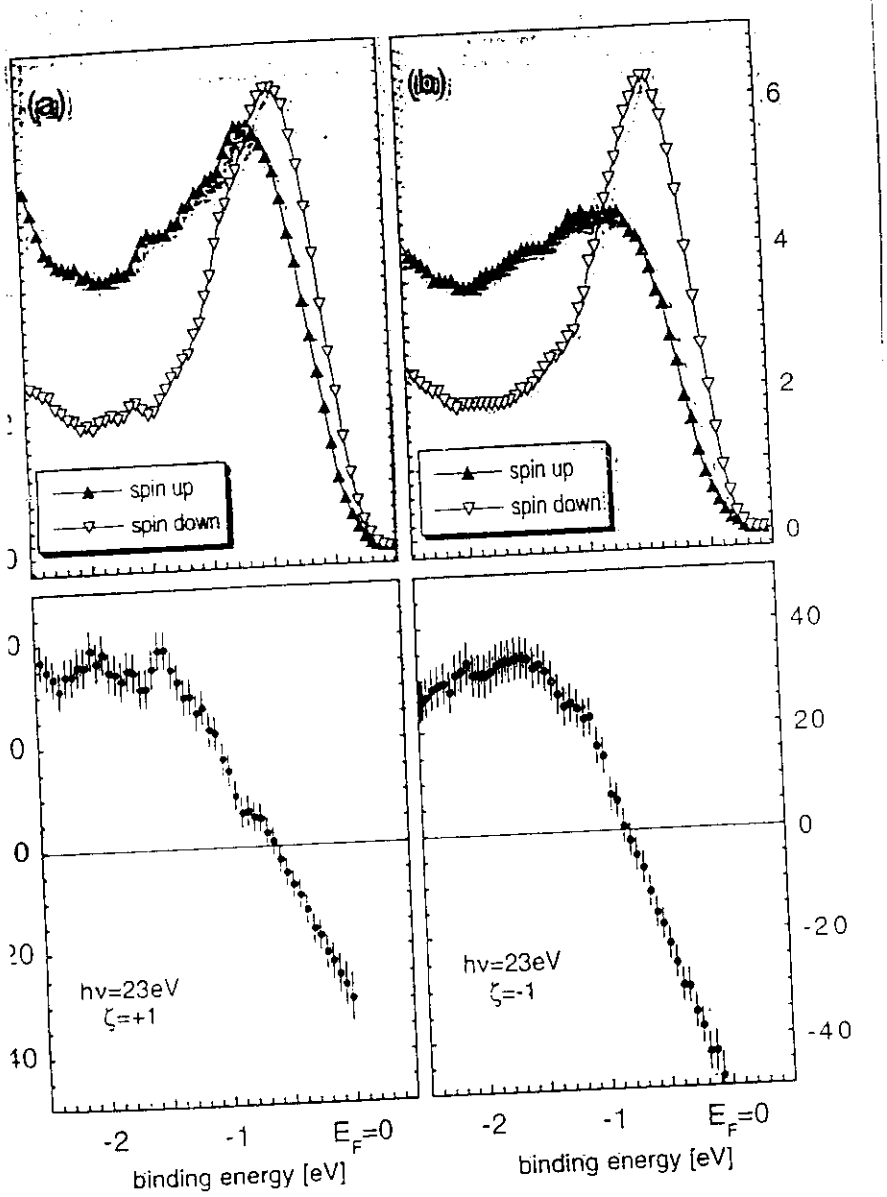

RE 43. Spin-resolved MCDAD in the Co 3d bands. Data set in (a) and (b) taken with : light, respectively. Upper panels: partial intensities with majority (▲) and minority :aracter (▼). Bottom panels: corresponding spin polarization component parallel to urface along the direction of the sample magnetization. (From Schneider, C. M., a. D., and Kirschner, J., in *Vacuum Ultraviolet Radiation Physics*, Wuilleumier, F. J., With permission.)

Hopster et al., Phys. Rev. Lett. 51, 829 (1983)

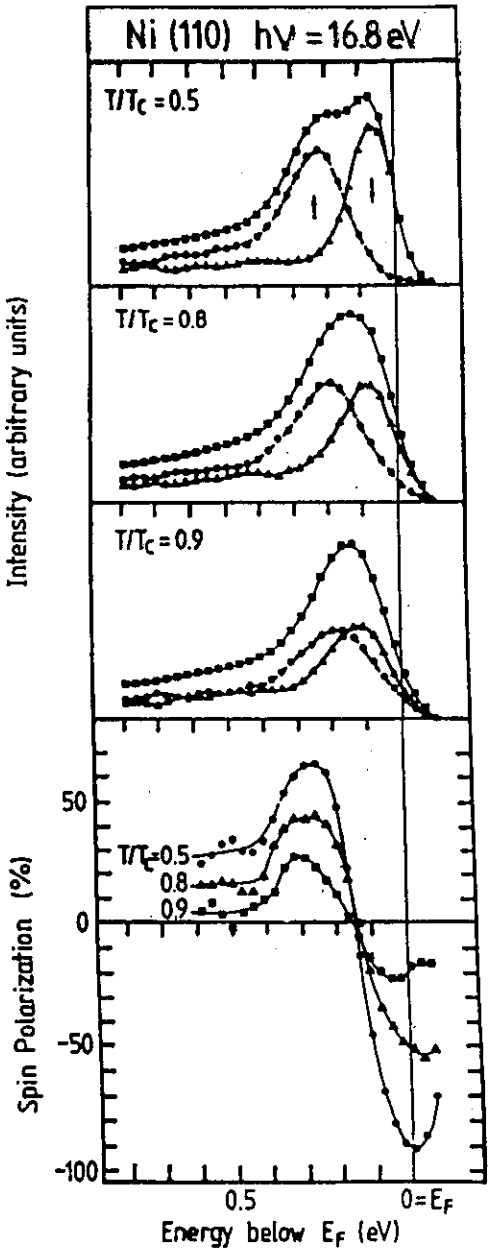

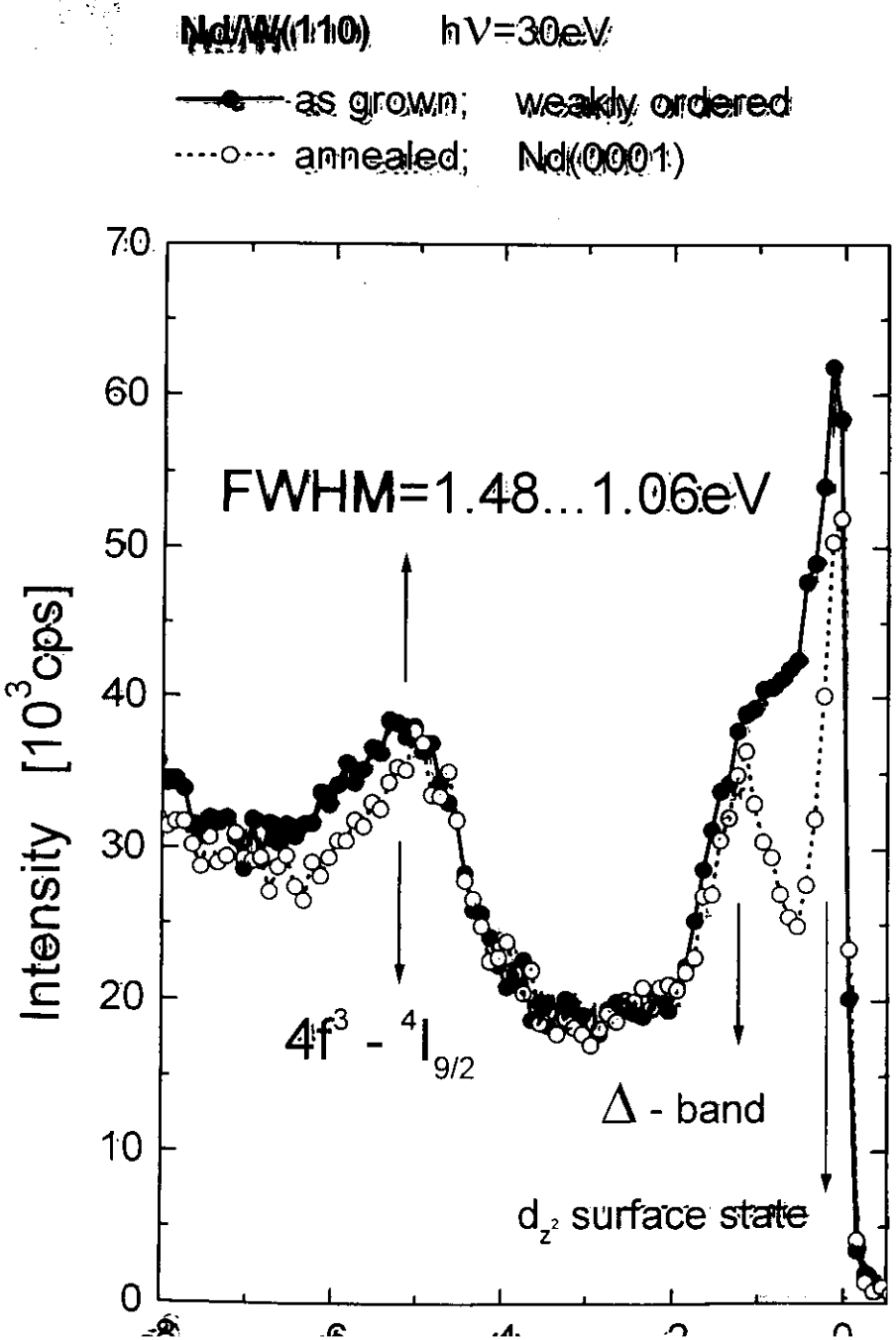
Nd/W(110) hν=30eV
as grown; weakly ordered
annealed; Nd(0001)
FWHM=1.48...1.06eV
Intensity [10^3 cps]
4f^3 - ^4I_9/2
Δ - band
d_z² surface state

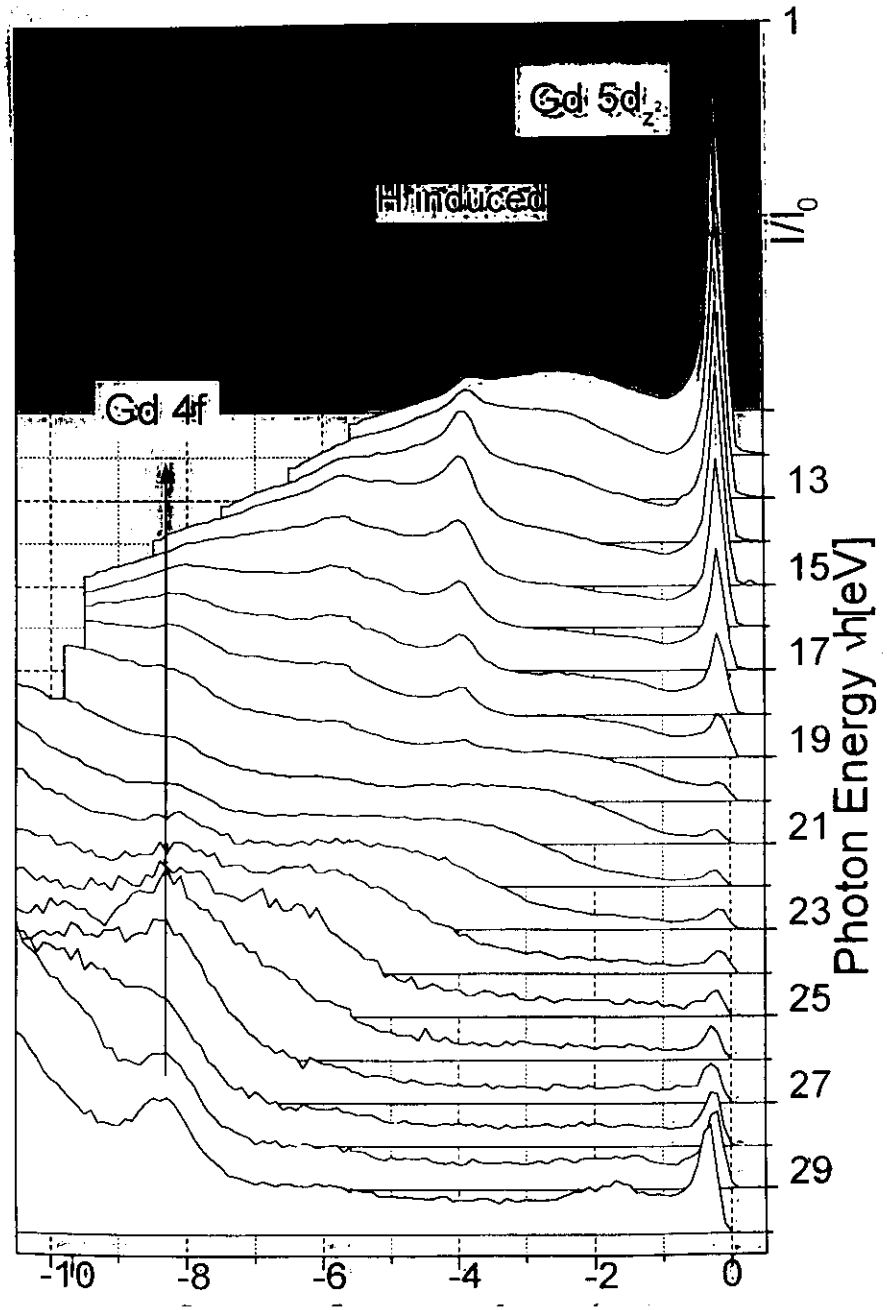
Gd 5d_z²
E_F induced
Gd 4f
I/I_0
Photon Energy hν[eV]

Tb(0001) / Gd(0001) / W(110)

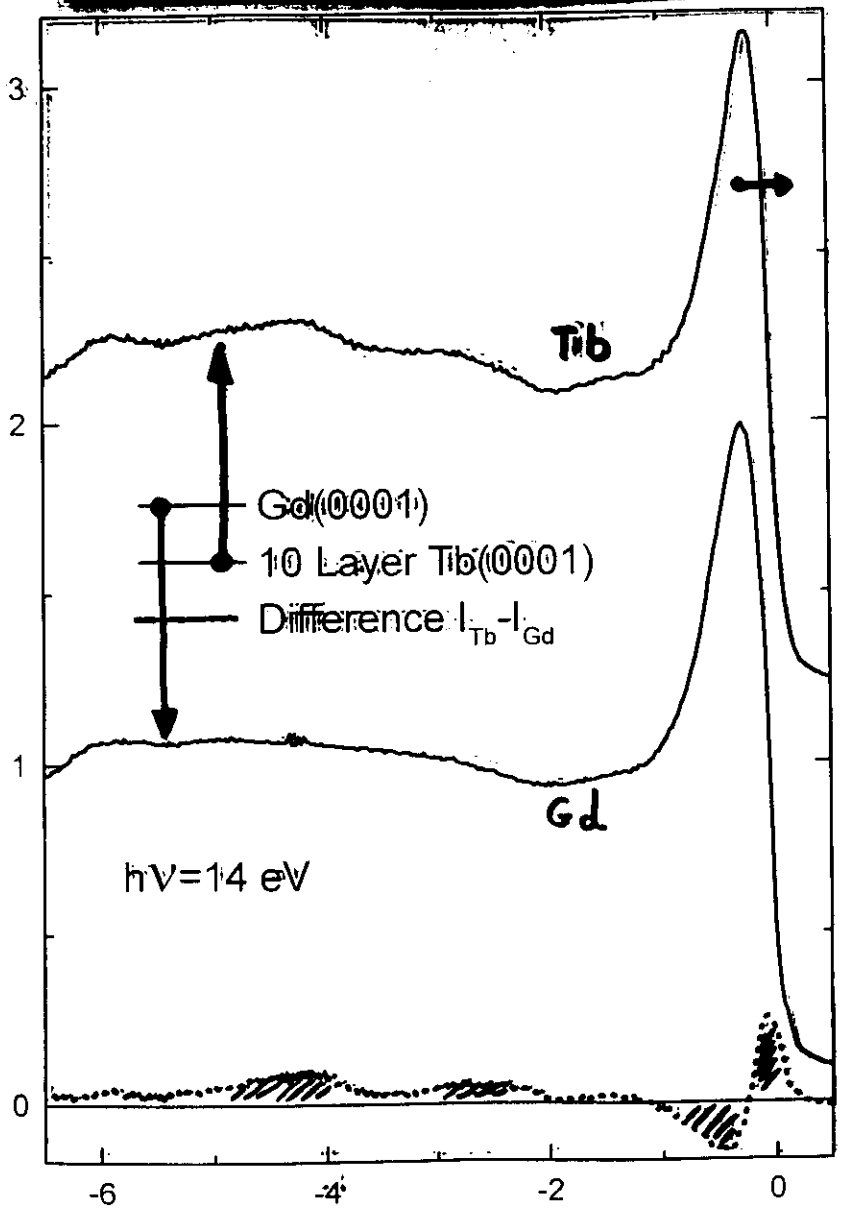

Dependence of UPS-cross sections on photon energy for 5d$_{z^2}$ -surface-state

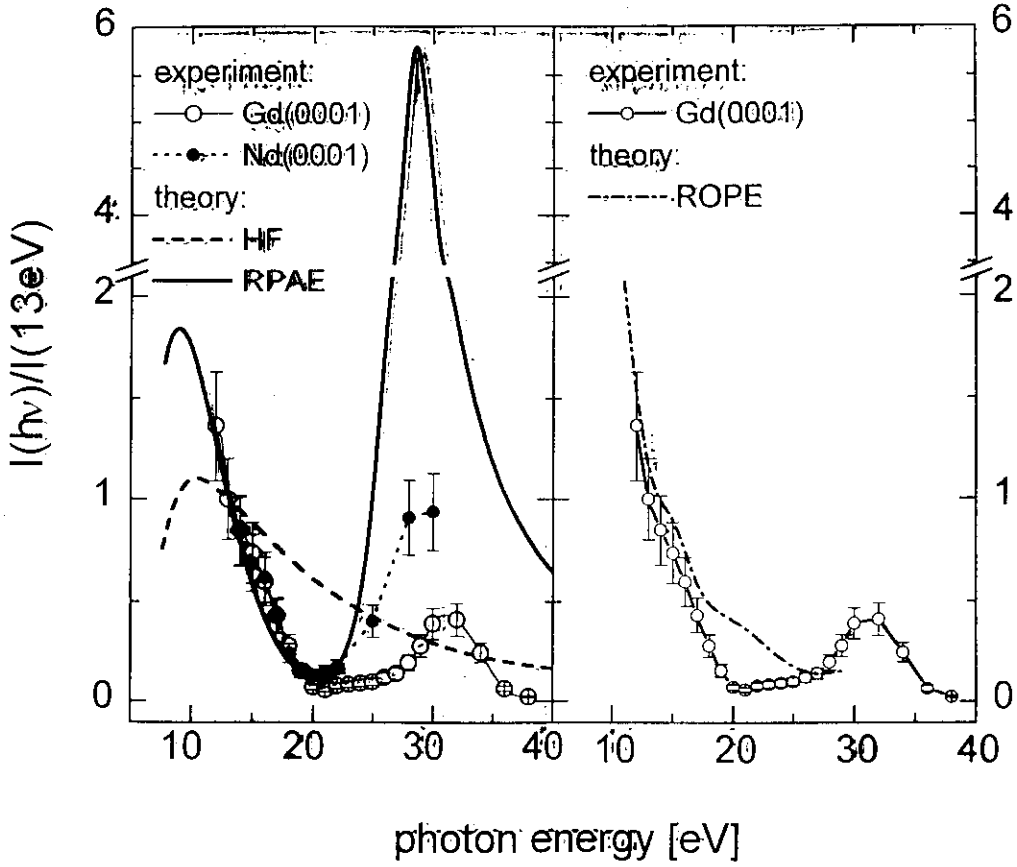

left: Atomic calculations
HF = Hartree-Fock
RPAE = Random phase approximation with exchange (N.A. Cherepkov et al.) including resonance 5p -> 5d
right: Calculation for solid Gd
ROPE = relativistic one-step photoemission (J. Braun et al.)

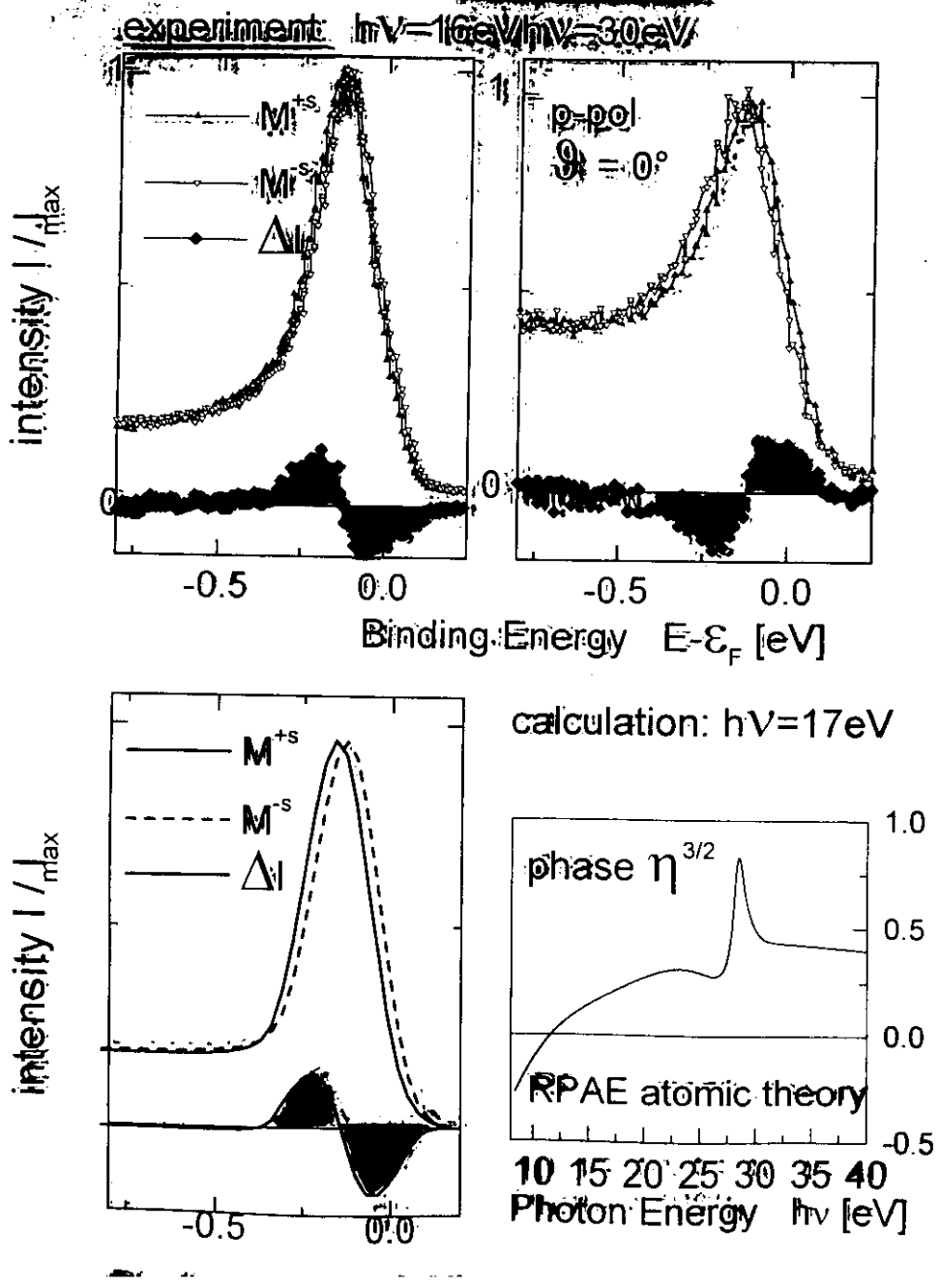
experiment hν=16eV/hν=30eV
M+s
M-s
ΔI
p-pol
ϑ = 0°
intensity I / I max
-0.5
0.0
Binding Energy E-ε_F [eV]
M+s
M-s
ΔI
calculation: hν=17eV
phase η 3/2
RPAE atomic theory
1.0
0.5
0.0
-0.5
10 15 20 25 30 35 40
Photon Energy hν [eV]

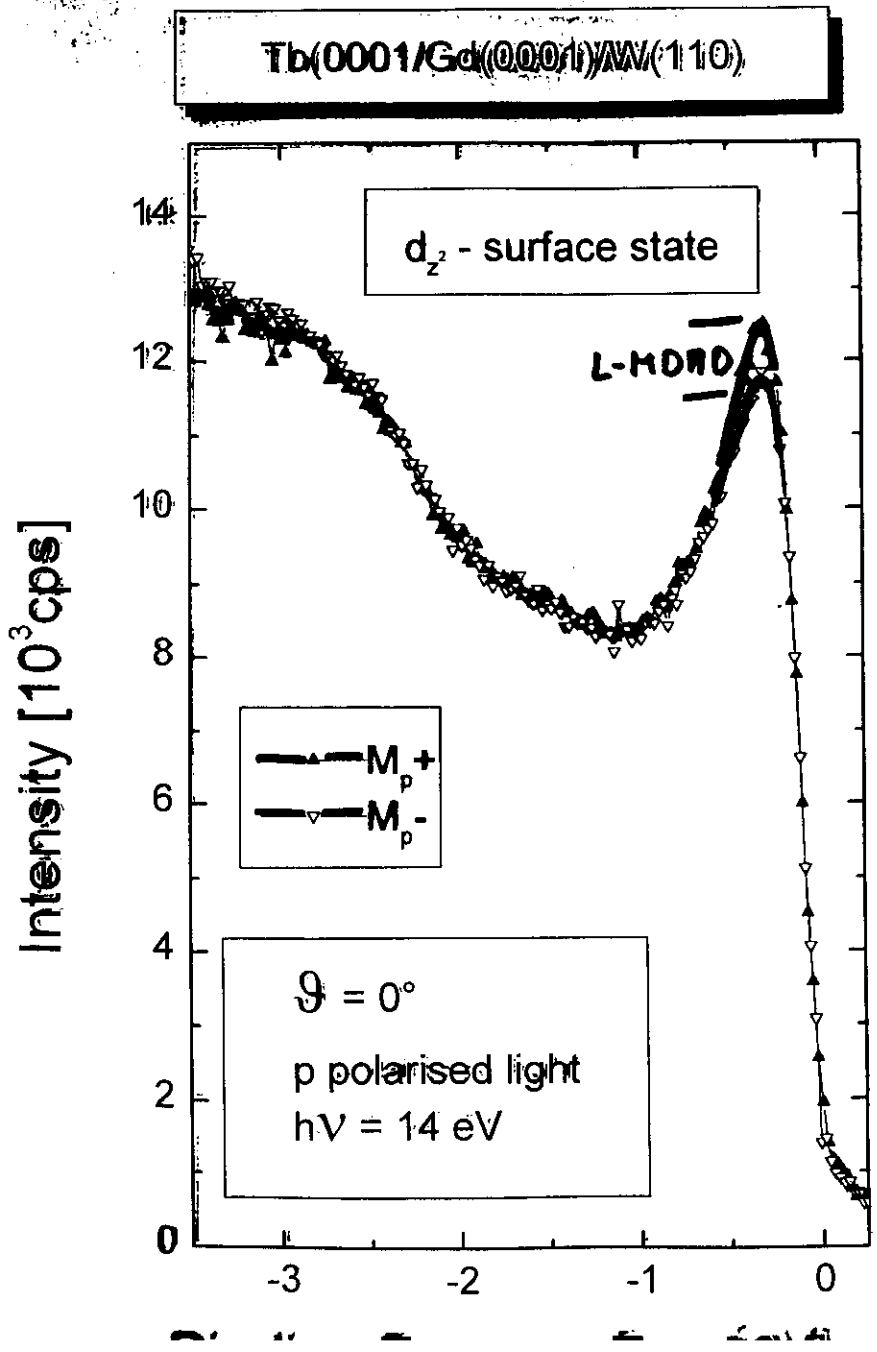
Tb(0001/Gd(0001)/W(110)
d_z² - surface state
L-HOMO
M_p+
M_p-
ϑ = 0°
p polarised light
hν = 14 eV
Intensity [10³cps]
14
12
10
8
6
4
2
0
-3
-2
-1
0

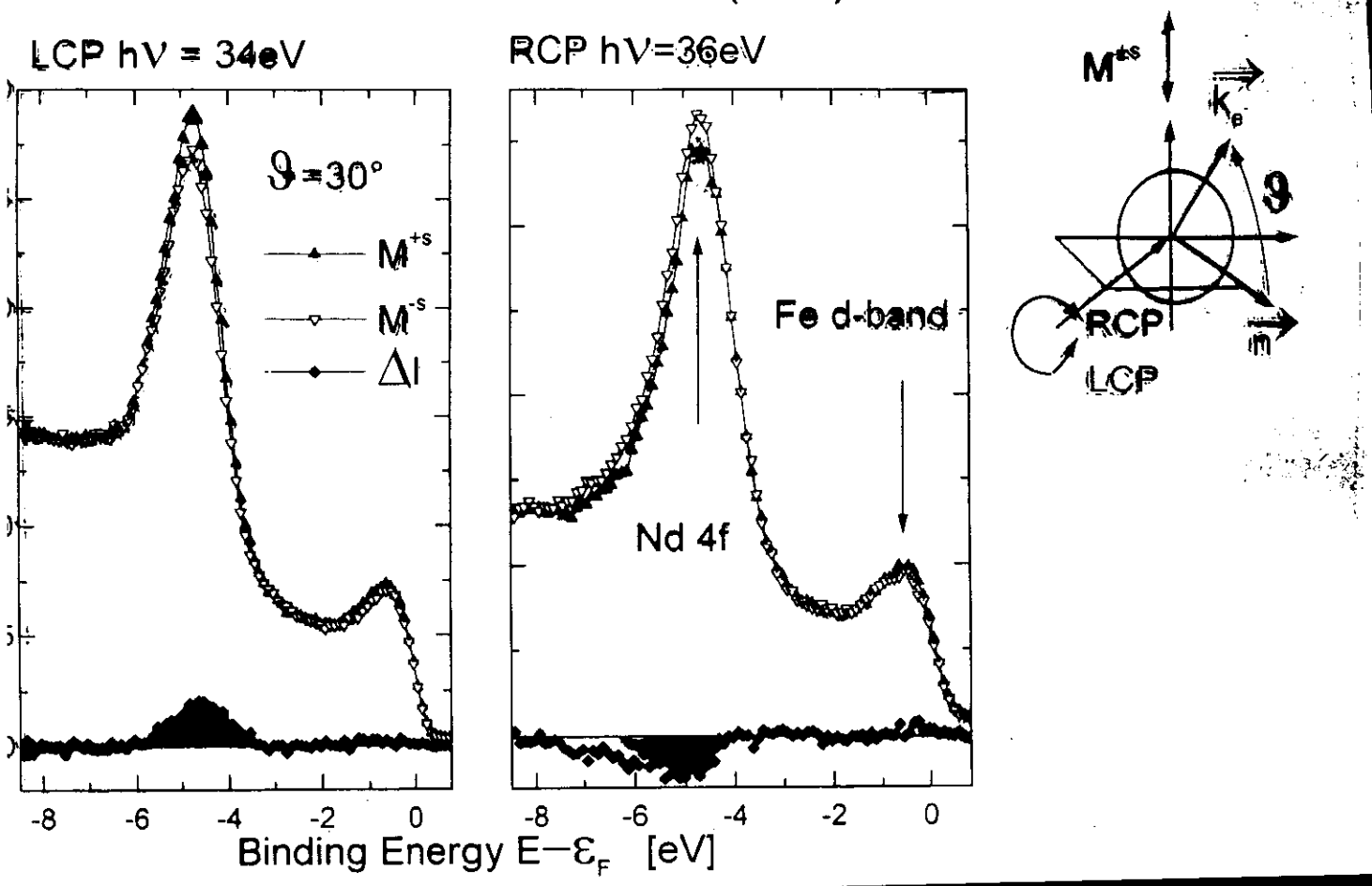
C-MDAD 1ML Nd at Fe/W(110)
LCP hν = 34eV
RCP hν=36eV
ϑ=30°
M+s
M-s
ΔI
Fe d-band
Nd 4f
RCP
LCP
-8
-6
-4
-2
0
Binding Energy E−ε_F [eV]

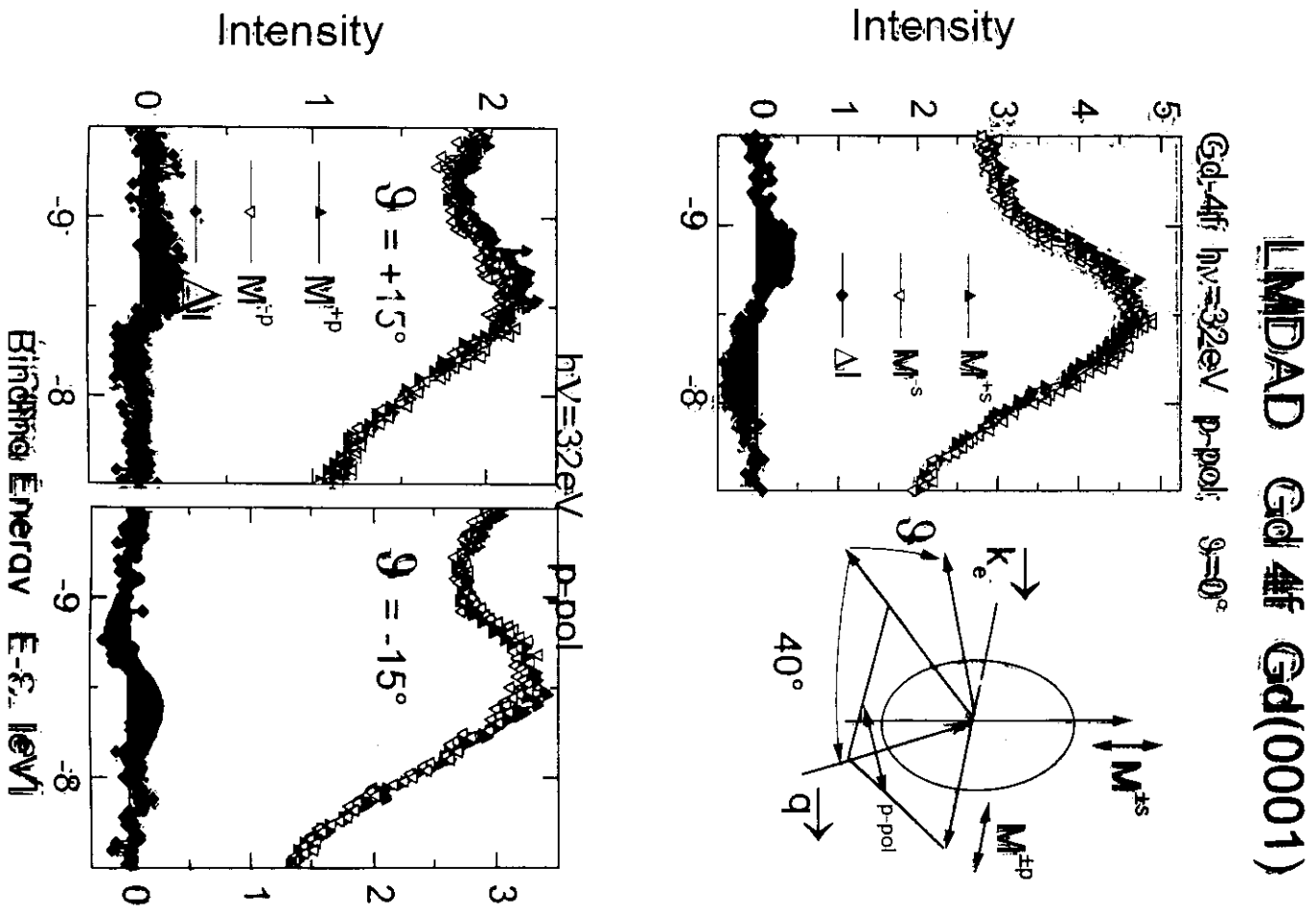
LMDAD Gd 4f Gd(0001)
Gd-4f hν=32eV p-pol ϑ=0°
Intensity
M+s
M-s
ΔI
40°
p-pol
hν=32eV p-pol
ϑ = +15°
ϑ = -15°
M+p
M-p
Binding Energy E-ε_F level

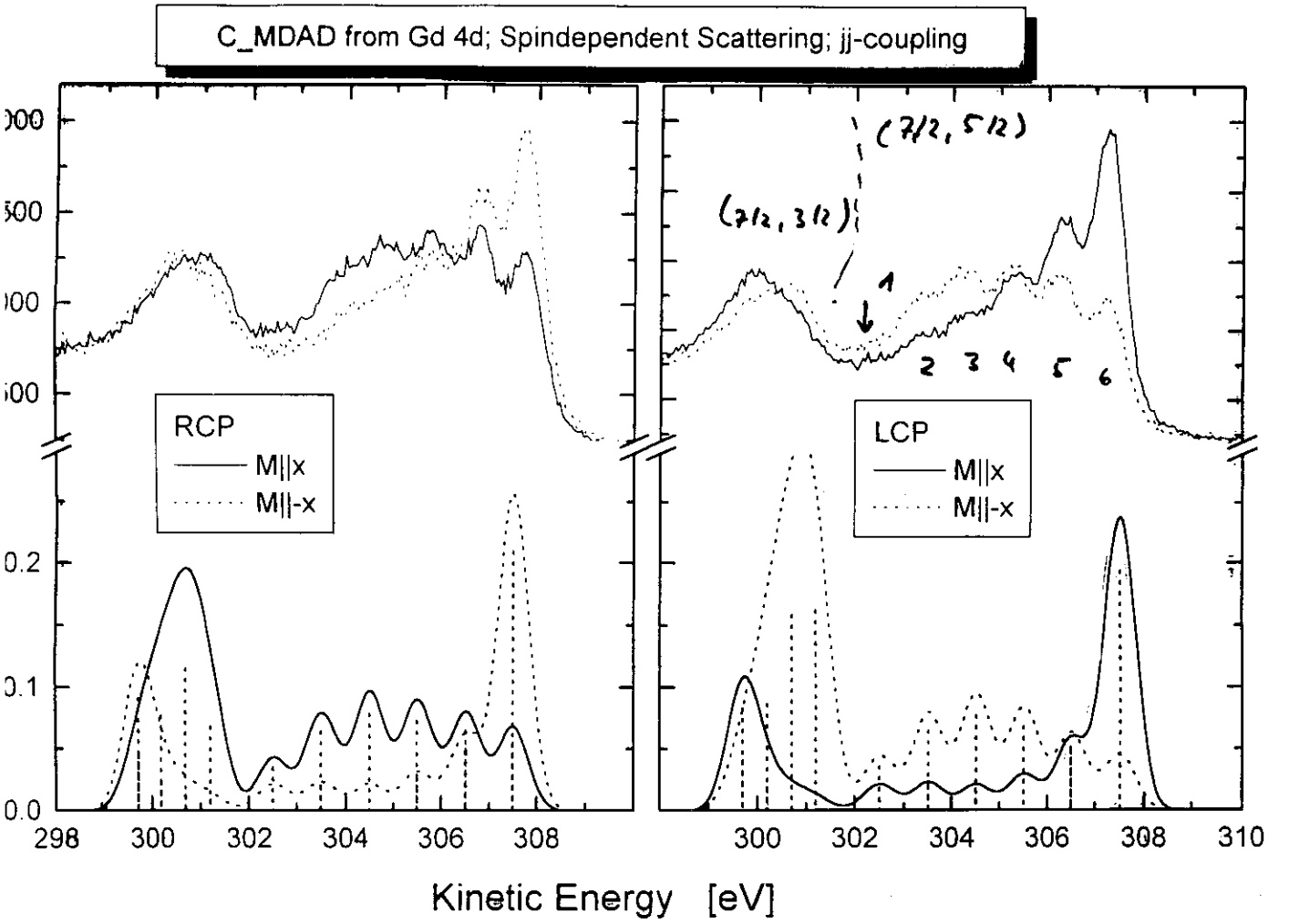
C_MDAD from Gd 4d; Spindependent Scattering; jj-coupling
(7/2, 5/2)
(7/2, 3/2)
1
2 3 4 5 6
RCP
M||x
M||-x
LCP
M||x
M||-x
0.2
0.1
0.0
298 300 302 304 306 308
300 302 304 306 308 310
Kinetic Energy [eV]

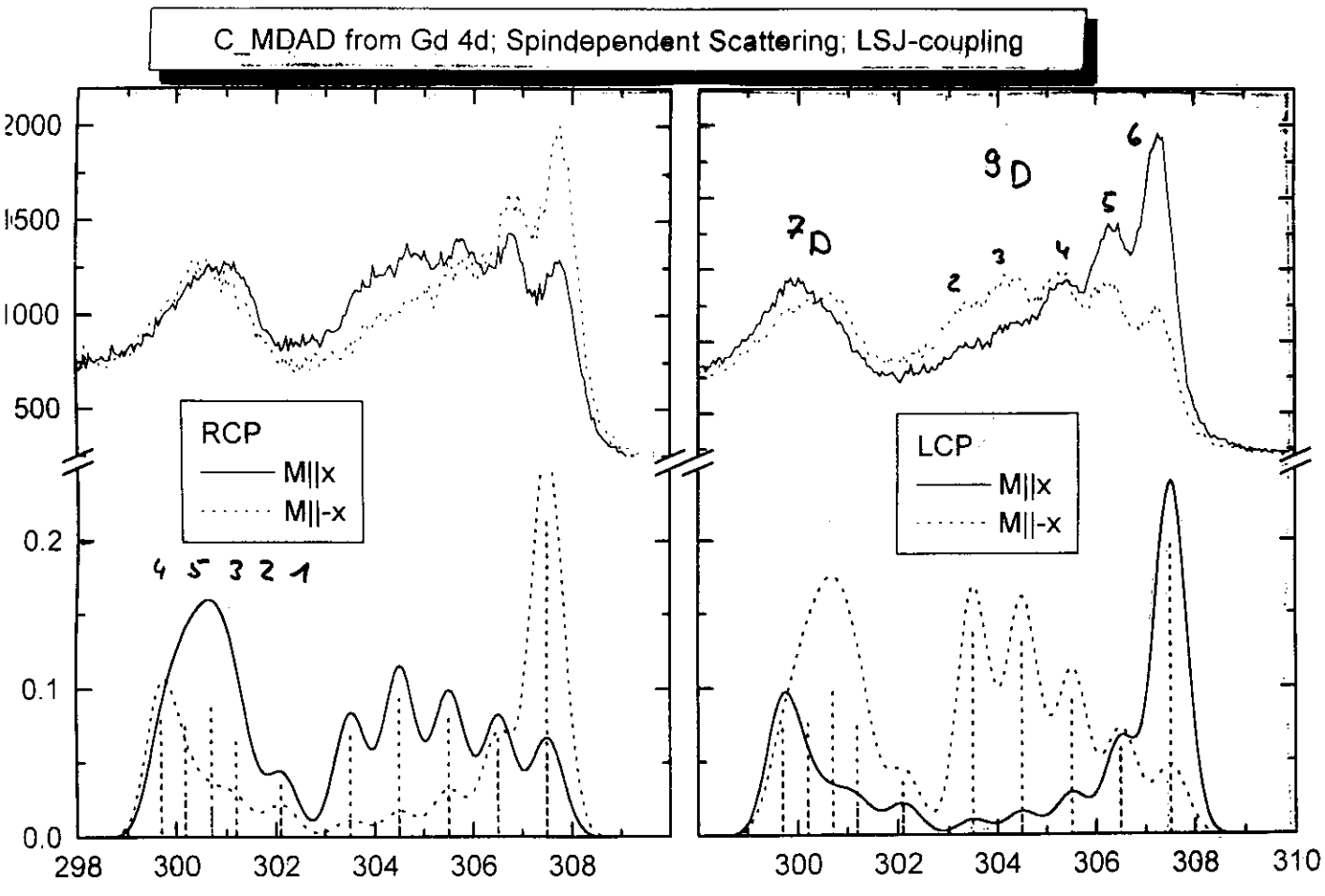
C_MDAD from Gd 4d; Spindependent Scattering; LSJ-coupling
3D
7D
6
5
4
3
2
RCP
M||x
M||-x
4 5 3 2 1
LCP
M||x
M||-x
0.2
0.1
0.0
298 300 302 304 306 308
300 302 304 306 308 310
Kinetic Energy [eV]

CDAD Nd(0001)/W(110)

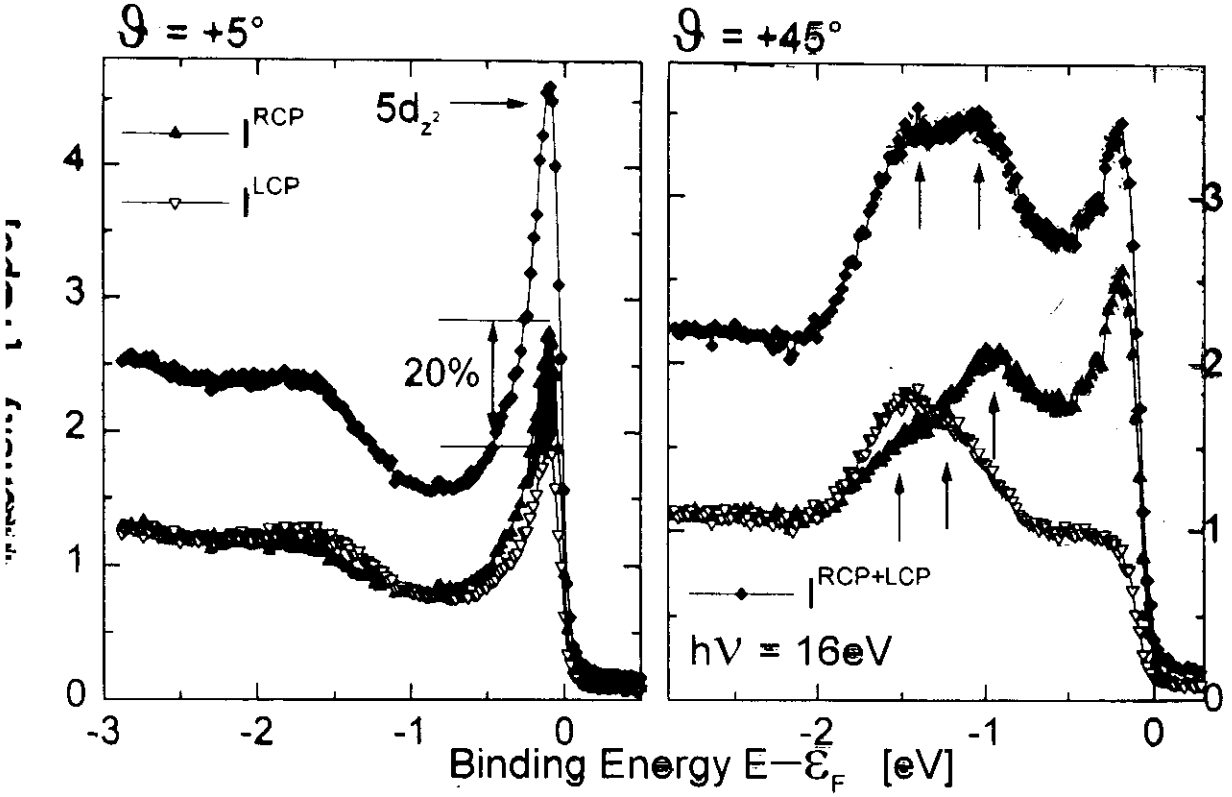

- *huge CDAD in surface state*
- *better effective resolution by CDAD*

Surface Bandstructure

Nd(0001)

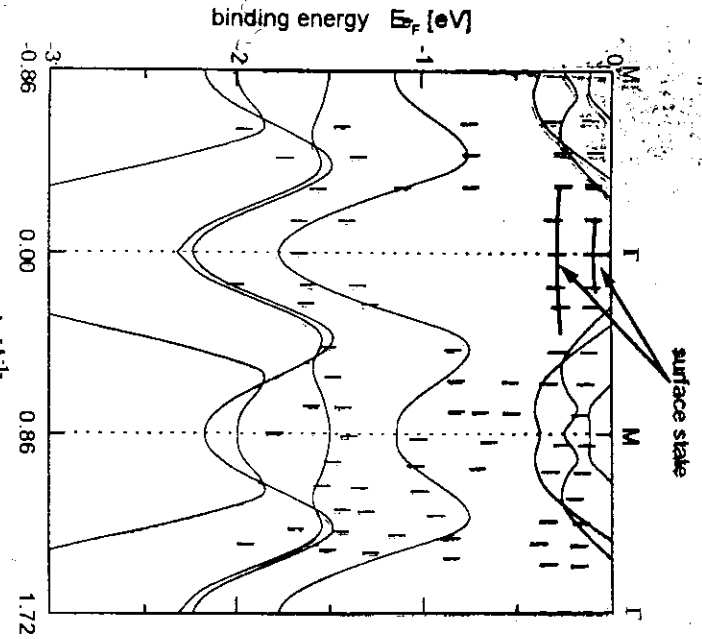

Johannes Gutenberg -Universität, Institut für Physik, D-55099 Mainz, Germany

XIII Some general references

[1] C.R.Brundle and A.D.Baker; Eds.: *Electron Spectroscopy: Theory, Techniques and Applications*; Academic Press, London, New York, San Francisco (1977)

[2] M.C.Desjonqueres and D.Spanjaard; *Concepts in Surface Physics*; Springer Verlag, Berlin (1995) 2nd Edition

[2] R.Feder; Ed.: *Polarized Electrons in Surface Physics*; World Scientific Publishing Co., Singapore (1985)

[3] B.Feuerbacher, B.Fitton, and R.F.Willis; Eds.: *Photoemission and the Electronic Properties of Surfaces*; John Wiley & Sons, Chichester, New York, Brisbane, Toronto (1978)

[4] J.Kessler; *Polarized Electrons*; Springer Verlag, Berlin, Heidelberg, New York, Tokyo (1985) 2nd Edition

XIV Acknowledgement

I gratefully acknowledge the help of many colleques:

J.Bansmann, N.A.Cherepkov, R.Deneke, C.S.Fadley, M.Getzlaff, Ch.Grünewald, Y.Hwu, Th.Jentzsch, H.J.Jüpner, M.Merkel, J.Morais, A.Oelsner, Ch.Ostertag, J.Paul, M.Schicketanz, O.Schmidt, C.M.Schneider, G.Schönhense, W.Swiech, Ch.Winde, C.Westphal, and last not least the beamline crews of the synchrotron facilities ALS (Brkeley, USA), BESSY (Berlin, Germany), ESRF (Grenoble, France), and SRRC (Hsinchu, Taiwan ROC).

This work is financially supported by the BMBF, DIG and DAAD.

XIV.1 Spherical Harmonics and Real Orbitals

The spherical harmonics $Y_{\ell,m}(\vartheta,\varphi)$ can be divided in ϑ and φ depending parts using Legendre polynomials $P_{\ell,m}(\vartheta)$:

$$Y_{l,m} = N_{l,m} P_{l,m}(\vartheta) \frac{1}{\sqrt{2\pi}} \{\cos(m\varphi) + i\sin(m\varphi)\}$$

$$N_{l,m} = \sqrt{\frac{(l-|m|)!\cdot(2l+1)}{2\cdot(l+|m|)!}} \cdot \begin{cases} (-1)^m & \text{for } m>0 \\ 1 & \text{for } m\le 0 \end{cases}$$

$$P_{l,m}(\xi=\cos(\vartheta)) = \frac{(1-\xi^2)^{\frac{|m|}{2}}}{2^l\cdot l!} \cdot \frac{d^{l+|m|}}{d\xi^{l+|m|}}(\xi^2-1)^l$$

From this definition we see that the conjugated spherical harmonics are given by:

$$Y^*_{l,m} = (-1)^{|m|} Y_{l,-m} = \exp\{i2m\varphi\} Y_{l,m}$$

and

$$Y_{l,-m} = (-1)^{|m|} Y^*_{l,m} = (-1)^{|m|} \exp\{i2m\varphi\} Y_{l,m}$$

XIV.1.1 Table of Spherical Harmonics and real orbitals

The spherical harmonics and some real orbitals with low ℓ up to 4 are given in the following tables:

i) ℓ=0, the s-orbital:

$$Y_{00} = \frac{1}{\sqrt{4\pi}}$$
$$s = Y_{00} = \frac{1}{\sqrt{4\pi}}$$

ii) ℓ=1:

$$Y_{11} = -\tfrac{1}{2}\sqrt{\tfrac{3}{2\pi}}\sin(\vartheta)\{\cos(\varphi)+i\sin(\varphi)\}$$
$$Y_{10} = \sqrt{\tfrac{3}{4\pi}}\cos(\vartheta)$$
$$Y_{1-1} = \tfrac{1}{2}\sqrt{\tfrac{3}{2\pi}}\sin(\vartheta)\{\cos(\varphi)-i\sin(\varphi)\}$$

the p-orbitals:

$$p_x = \tfrac{-1}{\sqrt{2}}(Y_{11}-Y_{1-1}) = \sqrt{\tfrac{3}{4\pi}}\sin(\vartheta)\cos(\varphi)$$
$$p_y = \tfrac{i}{\sqrt{2}}(Y_{11}+Y_{1-1}) = \sqrt{\tfrac{3}{4\pi}}\sin(\vartheta)\sin(\varphi)$$
$$p_z = Y_{10} = \sqrt{\tfrac{3}{4\pi}}\cos(\vartheta)$$

iii) ℓ=2:

$$
\begin{aligned}
Y_{22} &= \tfrac{1}{4}\sqrt{\tfrac{15}{2\pi}}\,\sin^2(\vartheta)\{\cos(2\varphi)+i\sin(2\varphi)\}\\
Y_{21} &= -\tfrac{1}{4}\sqrt{\tfrac{15}{2\pi}}\,\sin(2\vartheta)\{\cos(\varphi)+i\sin(\varphi)\}\\
Y_{20} &= \tfrac{1}{4}\sqrt{\tfrac{5}{\pi}}\,[3\cos^2(\vartheta)-1]\\
Y_{2-1} &= \tfrac{1}{4}\sqrt{\tfrac{15}{2\pi}}\,\sin(2\vartheta)\{\cos(\varphi)-i\sin(\varphi)\}\\
Y_{2-2} &= \tfrac{1}{4}\sqrt{\tfrac{15}{2\pi}}\,\sin^2(\vartheta)\{\cos(2\varphi)-i\sin(2\varphi)\}
\end{aligned}
$$

the d-orbitals:

$$
\begin{aligned}
d_{xy} &= \tfrac{-i}{\sqrt{2}}(Y_{22}-Y_{2-2}) &&= \tfrac{1}{4}\sqrt{\tfrac{15}{\pi}}\,\sin^2(\vartheta)\sin(2\varphi)\\
d_{xz} &= \tfrac{-1}{\sqrt{2}}(Y_{21}-Y_{2-1}) &&= \tfrac{1}{4}\sqrt{\tfrac{15}{\pi}}\,\sin(2\vartheta)\cos(\varphi)\\
d_{yz} &= \tfrac{i}{\sqrt{2}}(Y_{21}+Y_{2-1}) &&= \tfrac{1}{4}\sqrt{\tfrac{15}{\pi}}\,\sin(2\vartheta)\sin(\varphi)\\
d_{x^2-y^2} &= \tfrac{1}{\sqrt{2}}(Y_{22}+Y_{2-2}) &&= \tfrac{1}{4}\sqrt{\tfrac{15}{\pi}}\,\sin^2(\vartheta)\cos(2\varphi)\\
d_{z^2} &= Y_{20} &&= \tfrac{1}{4}\sqrt{\tfrac{5}{\pi}}\,[3\cos^2(\vartheta)-1]
\end{aligned}
$$

iv) ℓ=3:

$$
\begin{aligned}
Y_{30} &= \tfrac{1}{4}\sqrt{\tfrac{7}{\pi}}\,[5\cos^2(\vartheta)-3]\cdot\cos(\vartheta)\\
Y_{3\pm1} &= -\pm\tfrac{1}{8}\sqrt{\tfrac{21}{\pi}}\,[5\cos^2(\vartheta)-1]\sin(\vartheta)\{\cos(\varphi)\pm i\sin(\varphi)\}\\
Y_{3\pm2} &= \tfrac{1}{4}\sqrt{\tfrac{105}{2\pi}}\,\cos(\vartheta)\sin^2(\vartheta)\{\cos(2\varphi)\pm i\sin(2\varphi)\}\\
Y_{3\pm3} &= -\pm\tfrac{1}{8}\sqrt{\tfrac{35}{\pi}}\,\sin^3(\vartheta)\{\cos(3\varphi)\pm i\sin(3\varphi)\}
\end{aligned}
$$

the f-orbitals:

$$f_{z^3} = Y_{30}$$

$$f_{yz^2} = \tfrac{i}{\sqrt{2}}(Y_{31}+Y_{3-1}) \quad ; \quad f_{xz^2} = \tfrac{-1}{\sqrt{2}}(Y_{31}-Y_{3-1})$$

$$f_{(x^2-y^2)z} = \tfrac{1}{\sqrt{2}}(Y_{32}+Y_{3-2}) \quad ; \quad f_{xyz} = \tfrac{-i}{\sqrt{2}}(Y_{32}-Y_{3-2})$$

$$f_{xy^2} = \tfrac{i}{\sqrt{2}}(Y_{33}+Y_{3-3}) \quad ; \quad f_{x^3y} = \tfrac{-1}{\sqrt{2}}(Y_{33}-Y_{3-3})$$

v) ℓ=4:

$$
\begin{aligned}
Y_{40} &= \tfrac{3}{16}\sqrt{\tfrac{1}{\pi}}\,[35\cos^4(\vartheta)-30\cos^3(\vartheta)+3]\\
Y_{4\pm1} &= -\pm\tfrac{3}{8}\sqrt{\tfrac{5}{\pi}}\,\sin(\vartheta)[7\cos^3(\vartheta)-3\cos(\vartheta)]\{\cos(\varphi)\pm i\sin(\varphi)\}\\
Y_{4\pm2} &= \tfrac{3}{8}\sqrt{\tfrac{5}{2\pi}}\,\sin^2(\vartheta)[7\cos^2(\vartheta)-1]\{\cos(2\varphi)\pm i\sin(2\varphi)\}\\
Y_{4\pm3} &= -\pm\tfrac{3}{8}\sqrt{\tfrac{35}{\pi}}\,\sin^3(\vartheta)\cos(\vartheta)\{\cos(3\varphi)\pm i\sin(3\varphi)\}\\
Y_{4\pm4} &= \tfrac{3}{16}\sqrt{\tfrac{35}{2\pi}}\,\sin^4(\vartheta)\{\cos(4\varphi)\pm i\sin(4\varphi)\}
\end{aligned}
$$

the g-orbitals:

$$g_{z^4} = Y_{40}$$

$$g_{yz^3} = \tfrac{i}{\sqrt{2}}(Y_{41}+Y_{4-1}) \quad ; \quad g_{xz^3} = \tfrac{-1}{\sqrt{2}}(Y_{41}-Y_{4-1})$$

$$g_{(x^2-y^2)z^2} = \tfrac{1}{\sqrt{2}}(Y_{42}+Y_{4-2}) \quad ; \quad g_{xyz^2} = \tfrac{-i}{\sqrt{2}}(Y_{42}-Y_{4-2})$$

$$g_{xy^2z} = \tfrac{i}{\sqrt{2}}(Y_{43}+Y_{4-3}) \quad ; \quad g_{x^3yz} = \tfrac{-1}{\sqrt{2}}(Y_{43}-Y_{4-3})$$

$$g_{xy^3} = \tfrac{-1}{\sqrt{2}}(Y_{44}+Y_{4-4}) \quad ; \quad g_{x^4y} = \tfrac{-i}{\sqrt{2}}(Y_{44}-Y_{4-4})$$

XIV.2 The final states for initial state real orbitals

Here we give the possible final states for real orbitals as initial states:

initial state	q	final state	
		ℓ-1	ℓ+1
s	ε_x	-	p_x
	ε_y	-	p_y
	ε_z	-	p_z

initial state	q	final state	
		ℓ-1	ℓ+1
p_x	ε_x	s	d_{z2} , $d_{x2\text{-}y2}$
	ε_y	-	d_{xy}
	ε_z	-	d_{xz}

p_z	ε_x	-	d_{xz}
	ε_y	-	d_{yz}
	ε_z	s	d_{z2}
p_y	ε_x	-	d_{xy}
	ε_y	s	d_{z2} , d_{x2y2}
	ε_z	-	d_{yz}

initial state	q	final state	
		ℓ-1	ℓ+1
d_{xy}	ε_x	p_y	f_{xy2} , f_{yz2}
	ε_y	p_x	f_{x2y} , f_{xz2}
	ε_z	-	f_{xyz}
d_{xz}	ε_x	p_z	f_{z3} , $f_{(x2-y2)z}$
	ε_y	-	f_{xyz}
	ε_z	p_x	f_{xz2}
d_{z2}	ε_x	p_x	f_{xz2}
	ε_y	p_y	f_{yz2}
	ε_z	p_z	f_{z3}
d_{yz}	ε_x	-	f_{xyz}
	ε_y	p_z	f_{z3} , $f_{(x2-y2)z}$
	ε_z	p_y	f_{yz2}
d_{x2-y2}	ε_x	p_x	f_{x2y} , f_{xz2}
	ε_y	p_y	f_{xy2} , f_{yz2}
	ε_z	-	$f_{(x2-y2)z}$

initial state	q	final state	
		ℓ-1	ℓ+1
f_{x2y}	ε_x	d_{x2-y2}	g_{x3y} , $g_{(x2-y2)z2}$
	ε_y	d_{xy}	g_{xy3} , g_{xyz2}
	ε_z	-	g_{x3yz}

f_{xyz}	ε_x	d_{yz}	g_{xy2z} , g_{yz3}
	ε_y	d_{xz}	g_{x3yz} , g_{xz3}
	ε_z	d_{xy}	g_{xyz2}
f_{xz2}	ε_x	d_{z2} , d_{x2-y2}	g_{z4} , $g_{(x2-y2)z2}$
	ε_y	d_{xy}	g_{xyz2}
	ε_z	d_{xz}	g_{xz3}
f_{z3}	ε_x	d_{xz}	g_{xz3}
	ε_y	d_{yz}	g_{yz3}
	ε_z	d_{z2}	g_{z4}
f_{yz2}	ε_x	d_{xy}	g_{xyz2}
	ε_y	d_{z2} , d_{x2-y2}	g_{z4} , $g_{(x2-y2)z2}$
	ε_z	d_{xz}	g_{yz3}
$f_{(x2-y2)z}$	ε_x	d_{xz}	g_{x3yz} , g_{xz3}
	ε_y	d_{yz}	g_{xy2z} , g_{yz3}
	ε_z	d_{x2-y2}	$g_{(x2-y2)z2}$
f_{xy2}	ε_x	d_{xy}	g_{x3y} , g_{xyz2}
	ε_y	d_{x2-y2}	g_{xy3} , $g_{(x2-y2)z2}$
	ε_z	-	g_{xy2z}

XIV.3 The Gaunt-coefficients for real orbitals

The transition matrix is calculated from:

$$\int_0^{\pi}\left\{\int_0^{2\pi} Y^*_{l\pm1,m+\beta}Y_{1\beta}Y_{lm}d\varphi\right\}\sin(\vartheta)d\vartheta = \sqrt{\frac{(2(l\pm1)+1)3(2l+1)}{4\pi}}\begin{pmatrix} l\pm1 & 1 & l \\ 0 & 0 & 0\end{pmatrix}\begin{pmatrix} l\pm1 & 1 & l \\ m' & 0,\pm1 & m\end{pmatrix}$$

$$= (-1)^{l\pm1-l}\sqrt{\frac{(2(l\pm1)+1)3}{4\pi}}\,C^{l,0}_{l\pm1,0,1,0}\begin{pmatrix} l\pm1 & 1 & l \\ m' & 0,\pm1 & m\end{pmatrix}$$

or Clebsch-Gordan $C^{l_3,m_3}_{l_1,m_1,l_2,m_2}$ to solve the integrals, resulting in the Gaunt coefficient $c^{\Delta l}(l',m',l,m)$:

$$\sqrt{\tfrac{2\pi}{3}}\int_0^{\pi}\left\{\int_0^{2\pi} Y^*_{l\pm1,m'}Y_{1,\beta}Y_{lm}d\varphi\right\}\sin(\vartheta)d\vartheta = \sqrt{\tfrac{2\pi}{3}}\sqrt{\tfrac{3}{4\pi}}\sqrt{\tfrac{(2l+1)\cdot3}{2(l\pm1)+1}}\cdot C^{l\pm1,0}_{l0,1,0}\cdot C^{l\pm1,m+\beta}_{l,m,1,\beta}$$

$$= c_{l\pm1}\cdot C^{l\pm1,m+\beta}_{l,m,1,\beta}$$

$$= \sqrt{\tfrac{3}{2}}\,c^1(l\pm1,m+\beta,l,m) = g(l\pm1,m+\beta,l,m)$$

$$\beta = \Delta m = 0,\pm1$$

The modified Gaunt-coefficients g(ℓ±1,m+β,ℓ,m) are tabulated below. The first C-G coefficient $C^{l',0}_{l,0,1,0}$ vanishes for ℓ+1+ℓ'=odd, that is the selection rule ℓ'=ℓ±1 or Δℓ=±1. The second vanishes for m'≠m+β including the selection rule Δm=m'-m=β=0,±1

The non-Zero Gaunt-coefficients c^k as tabulated by Condon and Shortley and the modified coefficients g for initial s- and p-states are given by:

(ℓ'm'→ℓm)	c^1(ℓ'm'→ℓm)	c^1(ℓm→ℓ'm')	g(ℓ'm'→ℓm)	g(ℓm→ℓ'm')
(00,1±1)	1/√3	−1/√3	1/√2	−1/√2
(00,10)	1/√3	1/√3	1/√2	1/√2
(1±1,2±2)	√2/√5	−√2/√5	√3/√5	−√3/√5
(1±1,2±1)	1/√5	1/√5	√3/√10	√3/√10
(1±1,20)	1/√15	−1/√15	1/√10	−1/√10
(10,2±2)	0	0	0	0
(10,2±1)	1/√5	−1/√5	√3/√10	−√3/√10
(10,20)	2/√15	2/√15	√2/√5	√2/√5

Note: The arrows indicate the transition from initial to final state. It is used that $c^k(\ell m,\ell' m') = (-1)^{m-m'}c^k(\ell' m',\ell m)$, k=|Δℓ|=1 and:

$$\int_0^{\pi}\left\{\int_0^{2\pi} Y^*_{l',m'}Y_{k=1,\beta=0,\pm1}Y_{lm}d\varphi\right\}\sin(\vartheta)d\vartheta = \sqrt{\frac{2k+1}{2}}\,c^k(lm,l'm') = \sqrt{\frac{3}{2}}\,c^1(lm,l'm')$$

and

$$g(lm,l'm') = \sqrt{\tfrac{1}{2}}\,c^1(lm,l'm')$$

XIV.4 The G-functions for ℓ=1 spherical harmonics

Three spherical harmonics are contributing to the spin orbit resolved $p_{1/2}$ and $p_{3/2}$ initial states, namely Y_{10}, Y_{11}, and Y_{1-1}. The G functions connected to these three spherical harmonics are given in the experimental geometry by (for abbreviation the functions are divided by $\sigma_\kappa R_d^2$ and we use $r_s=R_s/R_d$):

a) for Y_{10}:

$G_\parallel$	$1/2\cos^2(\Phi_q)$	0
	$1/2\sin^2(\Phi_q)$	$4\{(3\cos(\vartheta)^2-1)^2-2(3\cos(\vartheta)^2-1)\cos(\delta_d-\delta_s)\,r_s+r_s^2\}$
	$-1/4\sin(2\Phi_q)$	0
$G_\perp$	½	$9\sin(2\vartheta)^2$
G_{45}	$1/2\cos(\Phi_q)$	0
	$-1/2\sin(\Phi_q)$	$12\sin(2\vartheta)\{(3\cos(\vartheta)^2-1)-\cos(\delta_d-\delta_s)\,r_s\}$
G_{circ}	$1/2\cos(\Phi_q)$	0
	$-1/2\sin(\Phi_q)$	$12\sin(2\vartheta)\sin(\delta_d-\delta_s)\,r_s$

b) for Y_{11}:

$G_\parallel$	$1/2\cos^2(\Phi_q)$	$2\{1+2\cos(\delta_d-\delta_s)\,r_s+r_s^2\}$
	$1/2\sin^2(\Phi_q)$	$9/2\sin(2\vartheta)^2$
	$-1/4\sin(2\Phi_q)$	$6\sin(2\vartheta)\sin(\delta_d-\delta_s)\,r_s$
$G_\perp$	½	$2\{(3\sin(\vartheta)^2-1)^2-2(3\sin(\vartheta)^2-1)\cos(\delta_d-\delta_s)\,r_s+r_s^2$
G_{45}	$1/2\cos(\Phi_q)$	$12\sin(\vartheta)^2\sin(\delta_d-\delta_s)\,r_s$
	$-1/2\sin(\Phi_q)$	$6\sin(2\vartheta)\{(3\sin(\vartheta)^2-1)-\cos(\delta_d-\delta_s)\,r_s\}$
G_{circ}	$1/2\cos(\Phi_q)$	$4\{(3\sin(\vartheta)^2-1)-(3\cos(\vartheta)^2-1)\cos(\delta_d-\delta_s)\,r_s-r_s^2\}$
	$-1/2\sin(\Phi_q)$	$-6\sin(2\vartheta)\sin(\delta_d-\delta_s)\,r_s$

c) for Y_{1-1}:

$G_\parallel$	$1/2\cos^2(\Phi_q)$	$2\{1+2\cos(\delta_d-\delta_s)\,r_s+r_s^2\}$
	$1/2\sin^2(\Phi_q)$	$9/2\sin(2\vartheta)^2$
	$-1/4\sin(2\Phi_q)$	$-6\sin(2\vartheta)\sin(\delta_d-\delta_s)\,r_s$
$G_\perp$	½	$2\{(3\sin(\vartheta)^2-1)^2-2(3\sin(\vartheta)^2-1)\cos(\delta_d-\delta_s)\,r_s+r_s^2$
G_{45}	$1/2\cos(\Phi_q)$	$-12\sin(\vartheta)^2\sin(\delta_d-\delta_s)\,r_s$
	$-1/2\sin(\Phi_q)$	$6\sin(2\vartheta)\{(3\sin(\vartheta)^2-1)-\cos(\delta_d-\delta_s)\,r_s\}$
G_{circ}	$1/2\cos(\Phi_q)$	$-4\{(3\sin(\vartheta)^2-1)-(3\cos(\vartheta)^2-1)\cos(\delta_d-\delta_s)\,r_s-r_s^2\}$
	$-1/2\sin(\Phi_q)$	$-6\sin(2\vartheta)\sin(\delta_d-\delta_s)\,r_s$

From the equations for G_{circ} it is seen that for truly oriented states the CDAD does not vanish if z,k and q are parallel (resp. antiparallel), that is for $\Phi_q=0$, $\vartheta=0$. How such a state can be prepared is discussed in connection with magnetic effects.

I.5 The Spinor Spherical Harmonics

The tensor spherical harmonics for spin ½ particles as given byVarshalovich are:

$$\Omega^{l}_{jm_j}(\vartheta,\varphi) \equiv Y^{j,s=1/2}_{jm_j} = \sum_{m_l,m_s} C^{jm_j}_{l,m_l,\frac{1}{2},m_s} Y_{lm_l}(\vartheta,\varphi)\chi_{\frac{1}{2}m_s}$$

$$= C^{j,m_j}_{l,m_l=m_j-\frac{1}{2},\frac{1}{2},+\frac{1}{2}} Y_{lm_l}(\vartheta,\varphi)|\uparrow\rangle + C^{j,m_j}_{l,m_l=m_j+\frac{1}{2},\frac{1}{2},-\frac{1}{2}} Y_{lm_l}(\vartheta,\varphi)|\downarrow\rangle$$

m_l and m_s are the projection quantum numbers of the orbital angular momentum and the electron spin and χ are the basis spin functions. The Clebsch-Gordan coefficients C^{j,m_j}_{l,m_l,s,m_s} can be interpreted as probability that the state $|\ell, s, m_l, m_s\rangle$ contributes to the coupled state $|j,m_j\rangle$. More explicitly the wave functions written as column matrix are given by:

$$\Omega^{l=j+1/2}_{jm_j} = \begin{pmatrix} -\sqrt{\dfrac{j-m+1}{2(j+1)}}\, Y_{j+1/2,m_j-1/2} \\ \sqrt{\dfrac{j+m+1}{2(j+1)}}\, Y_{j+1/2,m_j+1/2} \end{pmatrix}$$

$$\Omega^{l=j-1/2}_{jm_j} = \begin{pmatrix} \sqrt{\dfrac{j+m}{2j}}\, Y_{j-1/2,m_j-1/2} \\ \sqrt{\dfrac{j-m}{2j}}\, Y_{j-1/2,m_j+1/2} \end{pmatrix}$$

If not otherwise denoted in the following m will be used for m_j. Each spherical harmonic can be written as:

$$\Omega^{l}_{j,m} = \begin{pmatrix} a_l(j,m) Y_{l,m-1/2} \\ b_l(j,m) Y_{l,m+1/2} \end{pmatrix}$$

and the connected conjugate complex spherical harmonic is given by:

$$\Omega^{l*}_{j,m} = (-1)^{l+j-m}\begin{pmatrix} 0 & 1 \\ -1 & 0 \end{pmatrix}\Omega^{l}_{j,-m} = (-1)^{l+j-m}\begin{pmatrix} (-1)^{|m+1/2|}\cdot b_l \cdot Y^*_{l,m+1/2} \\ -(-1)^{|m-1/2|}\cdot a_l \cdot Y^*_{l,m-1/2} \end{pmatrix}$$

Ω für $-m_j$ einfügen

According to the orthonormality ($\langle\uparrow|\uparrow\rangle=1$, $\langle\uparrow|\downarrow\rangle=0$) of the basis spin functions one needs to use most oftenly the Hermitian conjugated spherical harmonics:

$$\Omega^{l+}_{j,m} = \begin{pmatrix} a_l \cdot Y^*_{l,m-1/2}, & b_l \cdot Y^*_{l,m+1/2} \end{pmatrix}$$

The quadratic forms of the spherical harmonics describing the angular distribution of electrons are given by:

$$W^l_{j,m}(\vartheta) \equiv \Omega^{l+}_{j,m}\Omega^l_{j,m} = a_l^2 \cdot \left|Y_{l,m-1/2}\right|^2 + b_l^2 \cdot \left|Y_{l,m+1/2}\right|^2$$

$$\equiv W_{j,m}(\vartheta) = \frac{1}{2(j+1)}\left\{(j+m+1)\left|Y_{j+1/2,m+1/2}\right|^2 + (j-m+1)\left|Y_{j+1/2,m-1/2}\right|^2\right\}$$
$$= \frac{1}{2j}\left\{(j+m)\left|Y_{j-1/2,m-1/2}\right|^2 + (j-m)\left|Y_{j-1/2,m+1/2}\right|^2\right\}$$

This shows that the angular distribution of electrons in spin-orbit split states is independent on the orbital angular momentum ℓ and the angle φ, meaning it is of rotational symmetry (cylindrically symmetric) with respect to the z-axis.

In some cases it is necessary to calculate for projection λ of the spin parallel to the electron linear momentum. Using Wigner rotation matrices and the helicity basis functions the spinor spherical harmonics for this case are given by:

$$\Omega^l_{jm_j}(\vartheta,\varphi) = \sqrt{\frac{2l+1}{4\pi}} \sum_\lambda C^{j,\lambda}_{l,0,\frac{1}{2},\lambda} \cdot D^j_{-\lambda,-m_j}(0,\vartheta,\varphi) \cdot \chi_{\frac{1}{2},\lambda}(\vartheta,\varphi)$$

I.5.1.1 The relativistic quantumnumber and the selection rules

The description of the initial states by $|j,m_j\rangle$ is ambiguous because for a given orbital angular momentum and spin we can have either $j=\ell-s$ or $j=\ell+s$ for the total angular momentum. Furthermore the selection rules $\Delta\ell=\pm1$ and $\Delta j=0,\pm1$ cannot answer the questions whether a final state with quantum number $\ell+\Delta\ell$, $j+\Delta j$ exists. It is convenient to define a relativistic angular momentum quantum number by:

$$k = (l-j)(2j+1) \qquad k \neq 0$$

It is seen that $k<0$ only for $j=\ell+1/2$, therefore the description is unambiguous and we can find ℓ and j from k by:

$$k<0 \qquad l = l(k) = |k+1| \qquad j = j(k) = |k+1/2|$$
$$k>0 \qquad l = l(k) = k \qquad\quad j = j(k) = k-1/2$$

This relativistic quantum number can take all values $-\infty<k<+\infty$ with $k\neq0$ and the projection of the total angular momentum j takes the values:

$$-\frac{|k|+1}{2} < m_j < \frac{|k|+1}{2}$$

To avoid half integer quantum numbers we use $m=2*m_j$, in addition:

$$m = \pm(2n+1) \qquad n = 0,1,\ldots$$

$$-|k|-1 < m < |k|+1$$

The Spinor Spherical harmonics are then given by:

$$\Omega_{k>0,m} = \sqrt{\frac{1}{2}}\begin{pmatrix} -\sqrt{1-\frac{m}{2k+1}}\,Y_{k,(m-1)/2} \\ \sqrt{1+\frac{m}{2k+1}}\,Y_{k,(m+1)/2} \end{pmatrix}$$

$$\Omega_{k<0,m} = \sqrt{\frac{1}{2}}\begin{pmatrix} \sqrt{1-\frac{m}{2k+1}}\,Y_{-(k+1),(m-1)/2} \\ \sqrt{1+\frac{m}{2k+1}}\,Y_{-(k+1),(m+1)/2} \end{pmatrix}$$

or

$$\Omega_{k,m} = \begin{pmatrix} a_{k,m}\cdot Y_{l(k),(m-1)/2} \\ b_{k,m}\cdot Y_{l(k),(m+1)/2} \end{pmatrix}$$

$$\begin{pmatrix} a_{k,m} \\ b_{k,m} \end{pmatrix} = \begin{pmatrix} -sign(k)\sqrt{\frac{2k+1-m}{2(2k+1)}} \\ \sqrt{\frac{2k+1+m}{2(2k+1)}} \end{pmatrix}$$

Applying the selection rules as above to k and m we find:

$$\Delta k = -2k, \pm1$$

$$\Delta m = 0, \pm2$$

The k selection rule gives the correct answer, that at maximum only three final states can be reached from a given initial state. The exceptions still present are initial $s_{1/2}$ and $p_{1/2}$ states, where only two final states can be reached. The transitions $\Delta k=+1$ or $\Delta k=-1$ lead to not existing final states with $k=0$, in these cases.

A table with the possible transitions and quantum numbers is given below .

initial state		final state		
ℓ, j	k	ℓ', j'	k'	Δk
$s_{1/2}$	-1	$p_{1/2}$	1	2
		$p_{3/2}$	-2	-1
$p_{1/2}$	1	$s_{1/2}$	-1	-2
		$d_{3/2}$	2	1
$p_{3/2}$	-2	$s_{1/2}$	-1	1
		$d_{3/2}$	2	4
		$d_{5/2}$	-3	-1
$d_{3/2}$	2	$p_{1/2}$	1	-1
		$p_{3/2}$	-2	-4

		$f_{5/2}$	3	1
$d_{5/2}$	-3	$p_{3/2}$	-2	1
		$f_{5/2}$	3	6
		$f_{7/2}$	-4	-1
$f_{5/2}$	3	$d_{3/2}$	2	-1
		$d_{5/2}$	-3	-6
		$g_{7/2}$	4	1
$f_{7/2}$	-4	$d_{5/2}$	-3	1
		$g_{7/2}$	4	8
		$g_{9/2}$	-5	-1

I.5.1 The Spinor Spherical Harmonics for s- to g- states

The Spinor Spherical Harmonics for s- to d- states are given explicitly by:

a) $\ell=0$:

$$\Omega_{-1,+1} = s_{1/2,+1/2} = \begin{pmatrix} Y_{00} \\ 0 \end{pmatrix} = Y_{00}|\uparrow\rangle$$

$$\Omega_{-1,-1} = s_{1/2,-1/2} = \begin{pmatrix} 0 \\ Y_{00} \end{pmatrix} = Y_{00}|\downarrow\rangle$$

$$W_{1/2,1/2} = |Y_{00}|^2 = \frac{1}{4\pi}$$

b) $\ell=1$

b1) j=1/2; $p_{1/2}$

$$\Omega_{1,+1} = p_{1/2,+1/2} = \begin{pmatrix} -\sqrt{\frac{1}{3}} \cdot Y_{10} \\ \sqrt{\frac{2}{3}} \cdot Y_{11} \end{pmatrix}$$

$$\Omega_{1,-1} = p_{1/2,-1/2} = \begin{pmatrix} -\sqrt{\frac{2}{3}} \cdot Y_{1-1} \\ \sqrt{\frac{1}{3}} \cdot Y_{10} \end{pmatrix}$$

$$W_{1/2,1/2} = |Y_{00}|^2 = \frac{1}{4\pi}$$

b2) j=3/2; $p_{3/2}$

$$\Omega_{-2,+3} = p_{3/2,+3/2} = \begin{pmatrix} Y_{11} \\ 0 \end{pmatrix} \qquad \Omega_{-2,+1} = p_{3/2,+1/2} = \begin{pmatrix} \sqrt{\frac{2}{3}} \cdot Y_{10} \\ \sqrt{\frac{1}{3}} \cdot Y_{11} \end{pmatrix}$$

$$\Omega_{-2,-3} = p_{3/2,-3/2} = \begin{pmatrix} 0 \\ Y_{1-1} \end{pmatrix} \text{ and } \qquad \Omega_{-2,-1} = p_{3/2,-1/2} = \begin{pmatrix} \sqrt{\frac{1}{3}} \cdot Y_{1-1} \\ \sqrt{\frac{2}{3}} \cdot Y_{10} \end{pmatrix}$$

$$W_{3/2,3/2} = |Y_{11}|^2 = \frac{3}{8\pi}\sin^2\vartheta \qquad W_{3/2,1/2} = \frac{1}{3}\{2|Y_{10}|^2 + |Y_{11}|^2\} = \frac{1}{8\pi}(3\cos^2\vartheta + 1)$$

c) $\ell=2$; d

c1) j=3/2; $d_{3/2}$

$$\Omega_{2,+3} = d_{3/2,+3/2} = \begin{pmatrix} -\sqrt{\frac{1}{5}} \cdot Y_{21} \\ \sqrt{\frac{4}{5}} \cdot Y_{22} \end{pmatrix} \qquad \Omega_{2,+1} = d_{3/2,+1/2} = \begin{pmatrix} -\sqrt{\frac{2}{5}} \cdot Y_{20} \\ \sqrt{\frac{3}{5}} \cdot Y_{21} \end{pmatrix}$$

$$\Omega_{2,-3} = d_{3/2,-3/2} = \begin{pmatrix} -\sqrt{\frac{4}{5}} \cdot Y_{2-2} \\ \sqrt{\frac{1}{5}} \cdot Y_{2-1} \end{pmatrix} \text{ and } \qquad \Omega_{2,-1} = d_{3/2,-1/2} = \begin{pmatrix} -\sqrt{\frac{3}{5}} \cdot Y_{2-1} \\ \sqrt{\frac{2}{5}} \cdot Y_{20} \end{pmatrix}$$

$$W_{3/2,3/2} = \frac{3}{8\pi}\sin^2\vartheta \qquad W_{3/2,1/2} = \frac{1}{8\pi}(3\cos^2\vartheta + 1)$$

c2) j=5/2; $d_{5/2}$

$$\Omega_{-3,+5} = d_{5/2,+5/2} = \begin{pmatrix} Y_{22} \\ 0 \end{pmatrix}$$

$$\Omega_{-3,-5} = d_{5/2,-5/2} = \begin{pmatrix} 0 \\ Y_{2-2} \end{pmatrix}$$

$$W_{5/2,5/2} = \frac{15}{32\pi}\sin^4\vartheta$$

$$\Omega_{-3,+2} = d_{5/2,+3/2} = \begin{pmatrix} \sqrt{\frac{4}{5}} \cdot Y_{21} \\ \sqrt{\frac{1}{5}} \cdot Y_{22} \end{pmatrix}$$

$$\Omega_{-3,-3} = d_{5/2,-3/2} = \begin{pmatrix} \sqrt{\frac{1}{5}} \cdot Y_{2-2} \\ \sqrt{\frac{4}{5}} \cdot Y_{2-1} \end{pmatrix}$$

$$W_{5/2,3/2} = \frac{3}{32\pi} \sin^2\vartheta[15\cos^2\vartheta + 1]$$

$$\Omega_{-3,+1} = d_{5/2,+1/2} = \begin{pmatrix} \sqrt{\frac{3}{5}} \cdot Y_{20} \\ \sqrt{\frac{2}{5}} \cdot Y_{21} \end{pmatrix}$$

$$\Omega_{-3,-1} = d_{5/2,-1/2} = \begin{pmatrix} \sqrt{\frac{2}{5}} \cdot Y_{2-1} \\ \sqrt{\frac{3}{5}} \cdot Y_{20} \end{pmatrix}$$

$$W_{5/2,1/2} = \frac{3}{16\pi}[5\cos^4\vartheta - 2\cos^2\vartheta + 1]$$

where $W_{j,m}$ are the probability distribution functions that describe the angular distribution of the electrons (independent of ϑ and φ).

From $W_{1/2,1/2}=|Y_{00}|^2$ we see that the distribution of electrons in the $p_{1/2}$- or $s_{1/2}$- states is spherical symmetric and moreover for all filled shells a spherical symmetric charge distribution is obtained in averaging over all m_j substates for given total angular momentum j.

I.6 The Spinor Gaunt-coefficients

The Spinor Gaunt-coefficients are defined by:

$$\gamma^l_\beta(j,m_j,j',m_j') = \int_0^\pi \left\{ \int_0^{2\pi} \Omega^{l+}_{j',m_j'} \sqrt{\tfrac{2\pi}{3}}\, Y_{k=1,\beta=0,\pm1} \Omega^l_{j,m_j} d\varphi \right\} \sin(\vartheta) d\vartheta$$

$$= \sqrt{\tfrac{2\pi}{3}} \iint \begin{pmatrix} a' Y^*_{l',m_j'-1/2} & b' Y^*_{l',m_j'+1/2} \end{pmatrix} Y_{k=1,\beta=0,\pm1} \begin{pmatrix} a Y_{l,m_j-1/2} \\ b Y_{l,m_j+1/2} \end{pmatrix} d\varphi \sin(\vartheta) d\vartheta$$

$$= \{a'a \cdot g(l\pm1, m_j+\beta-1/2, l, m_j-1/2) + b'b \cdot g(l\pm1, m_j+\beta+1/2, l, m_j+1/2)\}$$

where the abbreviations $a=a_\beta(j,m_j)$ and $b=b_\beta(j,m_j)$, and similar for the primed coefficients, are used.

The following Spinor Gaunt-coefficients for spinflip emission are observed from the equation above:

a) $s \rightarrow p$

	$p_{3/2,3/2}$	$p_{3/2,1/2}$	$p_{1/2,1/2}$	$p_{1/2,-1/2}$	$p_{3/2,-1/2}$	$p_{3/2,-3/2}$
β=	1	0		−1		−
$s_{1/2,1/2}$	1/√6	1/3	−√2/6	−1/3	√2/6	−
β=	−	1		0		−1
$s_{1/2,-1/2}$	−	√2/6	1/3	√2/6	1/3	1/√6

b1) $p \rightarrow s$

β=	−1		0		1	
	$s_{1/2,-1/2}$	$s_{1/2,+1/2}$	$s_{1/2,-1/2}$	$s_{1/2,+1/2}$	$s_{1/2,-1/2}$	$s_{1/2,+1/2}$
$p_{1/2,-1/2}$	−	−	√2/6	−	−	1/3
$p_{1/2,+1/2}$	−1/3	−	−	−√2/6	−	−
$p_{3/2,-3/2}$	−	−	−	−	−1/√6	−
$p_{3/2,-1/2}$	−	−	1/3	−	−	−√2/6
$p_{3/2,+1/2}$	−√2/6	−	−	1/3	−	−
$p_{3/2,+3/2}$	−	−1/√6	−	−	−	−

b2) $p \rightarrow d$

β=	−1		0		1	
	$d_{3/2,-3/2}$	$d_{3/2,-1/2}$	$d_{3/2,-1/2}$	$d_{3/2,+1/2}$	$d_{3/2,+1/2}$	$d_{3/2,+3/2}$
$p_{1/2,+1/2}$	−	√2/6	−	1/3	−	1/√6
$p_{1/2,-1/2}$	1/√6	−	1/3	−	√2/6	−
	$d_{5/2,+1/2}$	$d_{3/2,+1/2}$	$d_{5/2,+3/2}$	$d_{3/2,+3/2}$	$d_{5/2,+5/2}$	
$p_{3/2,+3/2}$	√2/10	−√3/15	√2/√5	−√2/10	1/√5	
	$d_{5/2,-1/2}$	$d_{3/2,-1/2}$	$d_{5/2,+1/2}$	$d_{3/2,+1/2}$	$d_{5/2,+3/2}$	$d_{3/2,+3/2}$
$p_{3/2,+1/2}$	√6/10	−2/15	√3/5	−√2/30	√3/5	√3/15
	$d_{5/2,-3/2}$	$d_{3/2,-3/2}$	$d_{5/2,-1/2}$	$d_{3/2,-1/2}$	$d_{5/2,+1/2}$	$d_{3/2,+1/2}$
$p_{3/2,-1/2}$	√3/5	−√3/15	√3/5	−√2/30	√6/10	2/15
		$d_{5/2,-5/2}$	$d_{5/2,-3/2}$	$d_{3/2,-3/2}$	$d_{5/2,-1/2}$	$d_{3/2,-1/2}$
$p_{3/2,-3/2}$		1/√5	√2/√5	√2/10	√2/10	√3/15

I.6.1 Some final states

a1) Initial state $s_{1/2,+1/2}$

for $\Delta m=1$	Final states	$p_{3/2,+3/2}$
for $\Delta m=-1$		$p_{3/2,-1/2}$ and $p_{1/2,-1/2}$
for $\Delta m=0$		$p_{3/2,+1/2}$ and $p_{1/2,+1/2}$

a2) Initial state $s_{1/2,-1/2}$

for $\Delta m=1$	Final states	$p_{3/2,+1/2}$ and $p_{1/2,+1/2}$
for $\Delta m=-1$		$p_{3/2,-3/2}$
for $\Delta m=0$		$p_{3/2,-1/2}$ and $p_{1/2,-1/2}$

b11) Initial state $p_{1/2,+1/2}$

for $\Delta m=1$	Final states	$d_{3/2,+3/2}$
for $\Delta m=-1$		$s_{1/2,-1/2}$ and $d_{3/2,-1/2}$
for $\Delta m=0$		$s_{1/2,1/2}$ and $d_{3/2,+1/2}$

b12) Initial state $p_{1/2,-1/2}$

for $\Delta m=1$	Final states	$s_{1/2,+1/2}$ and $d_{3/2,+1/2}$
for $\Delta m=-1$		$d_{3/2,-3/2}$
for $\Delta m=0$		$s_{1/2,-1/2}$ and $d_{3/2,-1/2}$

b21) Initial state $p_{3/2,+1/2}$

for $\Delta m=1$	Final states	$d_{5/2,+3/2}$ and $d_{3/2,+3/2}$
for $\Delta m=-1$		$s_{1/2,-1/2}$ and $d_{5/2,-1/2}$ and $d_{3/2,-1/2}$
for $\Delta m=0$		$s_{1/2,1/2}$ and $d_{5/2,+1/2}$ and $d_{3/2,+1/2}$

b22) Initial state $p_{3/2,-1/2}$

for $\Delta m=1$	Final states	$s_{1/2,1/2}$ and $d_{5/2,+1/2}$ and $d_{3/2,+1/2}$
for $\Delta m=-1$		$d_{5/2,-3/2}$ and $d_{3/2,-3/2}$
for $\Delta m=0$		$s_{1/2,-1/2}$ and $d_{5/2,-1/2}$ and $d_{3/2,-1/2}$

b31) Initial state $p_{3/2,+3/2}$

for $\Delta m=1$	Final states	$d_{5/2,+5/2}$
for $\Delta m=-1$		$s_{1/2,+1/2}$ and $d_{5/2,+1/2}$ and $d_{3/2,+1/2}$

for $\Delta m=0$		$d_{5/2,+3/2}$ and $d_{3/2,+3/2}$

b32) Initial state $p_{3/2,-3/2}$

for $\Delta m=1$	Final states	$s_{1/2,-1/2}$ and $d_{5/2,-1/2}$ and $d_{3/2,-1/2}$
for $\Delta m=-1$		$d_{5/2,-5/2}$
for $\Delta m=0$		$d_{5/2,-3/2}$ and $d_{3/2,-3/2}$

I.7 The Properties of Spherical functions under Co-ordinate Transformations

I.7.1 Transformation of Spherical Harmonics

Here the properties of the spherical harmonics under co-ordinate transformations are given. In the following it is always used that r'=r.

a) Co-ordinate Inversion

$$\hat{P}_r Y_{lm} = Y_{lm}(\pi - \vartheta, \varphi - \pi) = (-1)^l Y_{lm}$$

b) General Rotations

Applying a rotation about the Euler angles $\underline{\omega}=(\alpha,\beta,\gamma)$ to the spherical harmonics has the result:

$$\hat{D}(\underline{\omega}) Y_{lm}(\vartheta,\varphi) = Y_{lm'}(\vartheta',\varphi') = \sum_{m=-l}^{l} Y_{lm}(\vartheta,\varphi) D^l_{mm'}(\alpha,\beta,\gamma)$$

The rotational D-functions using Wigner d-functions are given by:

$$D^l_{m,m'} = \exp(-im\alpha)\cdot d^l_{m,m'}(\beta)\cdot\exp(-im'\gamma)$$

$$d^j_{m,m'} = (-1)^{j+m}\sqrt{(j+m)!\cdot(j-m)!\cdot(j+m')!\cdot(j-m')!}\cdot\sum_k \frac{(-1)^k\cdot\cos^{2k-m-m'}(\beta/2)\cdot\sin^{2j+m-m'-2k}(\beta/2)}{k!\cdot(j+m-k)!\cdot(j+m'-k)!\cdot(k-m-m')!}$$

the sum has N+1 terms with N=min{j+m, j-m, j+m', j-m'} .The Wigner d-functions can be expressed alternatively using Jacobi-Polinomials JP(x):

$$d^j_{m',m}(\beta) = \sqrt{\frac{(j+m')!\cdot(j-m')!}{(j+m)!\cdot(j-m)!}}\cdot\sin(\beta/2)^{m'+m}\cdot\cos(\beta/2)^{m'-m}\cdot JP^{m'-m,m'+m}_{j-m'}(\cos(\beta))$$

$$JP^{\alpha,\beta}_n(x) = \frac{(-1)^n}{2^n\cdot n!}\cdot\frac{\frac{d^n}{dx^n}\{(1-x)^{\alpha+n}\cdot(1+x)^{\beta+n}\}}{(1-x)^\alpha\cdot(1+x)^\beta} = 2^{-n}\sum_{i=1}^{n}\binom{n+\alpha}{i}\binom{n+\beta}{n-i}(x-1)^{n-i}\cdot(x+1)^i$$

here we used the j,m',m convention of Edmonds (Angular Momentum...)

c) Rotational matrices

Here we give the case where the state is aligned in the x-y plane and we have to apply the rotation to this case. The angle μ is measured with respect to the x-axis, so that the set of Euler angles describing this case is given by $\underline{\omega}_\mu=(\mu,\pi/2,\pi/2)$ and we have:

$$D_\mu = e^{-i m\cdot\mu}\cdot d^l_{m'm}\left(\frac{\pi}{2}\right)\cdot e^{-i m'\cdot\frac{\pi}{2}}$$

this operation describes the x'y'-plane in the surface. For μ=0 it transfers: x⇔z', y⇔x', z⇔y' and for μ=90° it transfers: x⇔−x', y⇔z', z⇔y' .

the inverse rotation is described by $\underline{\omega}^{-1}_\mu=(\pi/2,\pi/2,\pi-\mu)$ leading to:

$$D^{-1}_\mu = e^{-i m\cdot\frac{\pi}{2}}\cdot d^l_{m'm}\left(\frac{\pi}{2}\right)\cdot e^{-i m'(\pi-\mu)}$$

Applying these rotations we find for ℓ=1 states:

D_μ		m' = 1	m' = 0	m' = -1	$e^{-im\mu}$	$e^{-im0°}$	$e^{-im90°}$
m	1	½	$-1/\sqrt{2}$	½	$e^{-i\mu}$	1	-i
	0	$1/\sqrt{2}$	0	$-1/\sqrt{2}$	1	1	1
	-1	½	$1/\sqrt{2}$	½	$e^{i\mu}$	1	i
	$e^{-im'\pi/2}$	-i	1	i			

and inverted

$D^{-1}_\mu(\ell=1)$		m' = 1	m' = 0	m' = -1	$e^{-im\pi/2}$
m	1	½	$-1/\sqrt{2}$	½	-i
	0	$1/\sqrt{2}$	0	$-1/\sqrt{2}$	1
	-1	½	$1/\sqrt{2}$	½	i
	$e^{-im'(\pi-\mu)}$	$-e^{i\mu}$	1	$-e^{-i\mu}$	
	$e^{-im'(\pi-0°)}$	-1	1	-1	
	$e^{-im'(\pi-90°)}$	-i	1	i	

For initial ℓ=2 states we find:

D_μ		m' = 2	m' = 1	m' = 0	m' = -1	m' = -2	$e^{-im\mu}$	$e^{-im0°}$	$e^{-im90°}$
m	2	¼	-1/2	$\sqrt{3}/\sqrt{8}$	-1/2	¼	$e^{-i2\mu}$	1	-1
	1	½	½	0	-1/2	-1/2	$e^{-i\mu}$	1	-i
	0	$\sqrt{3}/\sqrt{8}$	0	-1/2	0	$\sqrt{3}/\sqrt{8}$	1	1	1
	-1	½	-1/2	0	½	-1/2	$e^{i\mu}$	1	i
	-2	¼	-1	$\sqrt{3}/\sqrt{8}$	½	¼	$e^{i2\mu}$	1	-1
	$e^{-im'\pi/2}$	-1	-i	1	i	-1			

and inverted:

D_μ	m' = 2	m' = 1	m' = 0	m' = -1	m' = -2	$e^{-im\pi/2}$

m	2	¼	-1/2	√3/√8	-1/2	¼	-1
	1	½	½	0	-1/2	-1/2	-i
	0	√3/√8	0	-1/2	0	√3/√8	1
	-1	½	-1/2	0	½	-1/2	i
	-2	¼	-1	√3/√8	½	¼	-1
	$e^{-im'(\pi-\mu)}$	$e^{i2\mu}$	$-e^{i\mu}$	1	$-e^{-i\mu}$	$e^{-i2\mu}$	
	$e^{-im'(\pi-0°)}$	1	-1	1	-1	1	
	$e^{-im'(\pi-90°)}$	-1	-i	1	i	-1	

The rotational matrix for f_{gg} or states with higher angular momentum are too big to be reproduced here, because the matrices are of the order $(2l+1)^2$. The corresponding Wigner d-functions can be found in Varshallovich.

d) Special Rotations by π

about x-axis

$$\vartheta' = \pi - \vartheta$$
$$\varphi' = 2\pi - \varphi$$
$$\rightarrow Y_{lm}(\pi-\vartheta, 2\pi-\varphi) = (-1)^l Y_{l-m}$$

about y-axis

$$\vartheta' = \pi - \vartheta$$
$$\varphi' = \pi - \varphi$$
$$\rightarrow Y_{lm}(\pi-\vartheta, \pi-\varphi) = (-1)^{l-m} Y_{l-m}$$

about z-axis

$$\vartheta' = \vartheta$$
$$\varphi' = \pi + \varphi$$
$$\rightarrow Y_{lm}(\vartheta, \pi+\varphi) = (-1)^m Y_{lm}$$

e) Mirror operations

reflection on equatorial plane $\vartheta_m=\pi/2$ (x-y-plane)

$$\vartheta' = \pi - \vartheta \qquad \varphi' = \varphi$$
$$\rightarrow \quad Y_{lm}(\pi-\vartheta, \varphi) = (-1)^{l+m} Y_{lm}$$

or

$$\hat{M}_{x-y} Y_{lm}(\vartheta, \varphi) = (-1)^{l+m} Y_{lm}$$

reflection on meridian plane $\varphi_m=\varphi_0$, $\varphi_m=\pi+\varphi_0$ ($\varphi_0=0$ in x-z or $\varphi_0=\pi/2$ in y-z-plane)

$$\vartheta' = \vartheta \qquad \varphi' = 2\varphi_0 - \varphi$$
$$\rightarrow \quad Y_{lm}(\vartheta, 2\varphi_0+\varphi) = (-1)^m \exp\{i2m\varphi_0\} Y_{l-m}$$

or

$$\hat{M}^{\parallel}_{y-z} Y_{lm}(\vartheta, \varphi) = i \cdot (-1)^m Y_{l-m}(\vartheta, \varphi)$$

$$\hat{M}^{\perp}_{x-z} Y_{lm}(\vartheta, \varphi) = (-1)^m Y_{l-m}(\vartheta, \varphi)$$

I.7.2 Transformation of Spinor Spherical Harmonics

a) Co-ordinate Inversion

$$\hat{P}_r \Omega^l_{j,m} = \Omega^l_{j,m}(\pi-\vartheta, \pi+\varphi) = (-1)^l \Omega^l_{j,m}$$

b) General Rotation

Applying a rotation about the Euler angles $\underline{\omega}=(\alpha,\beta,\gamma)$ to the spinor spherical harmonics has the result:

$$\hat{D}(\underline{\omega})\Omega^l_{jm}(\vartheta,\varphi) = \Omega^l_{jm'}(\vartheta',\varphi') = \sum_{m=-j}^{j} \Omega^l_{jm}(\vartheta,\varphi) D^j_{mm'}(\alpha,\beta,\gamma)$$

The rotational D-functions using Wigner d-functions are given by:

$$D^l_{m,m'} = \exp(-ima) \cdot d^l_{m,m'}(\beta) \cdot \exp(-im'\gamma)$$

c) Special rotational matrices

The magnetisation is in the x-y plane, in most magnetic surface science experiments and we have to apply the rotation to this case. The angle μ of the magnetisation is measured with respect to the x-axis, so that $M^{\parallel}=M_x=M\cos(\mu)$ and $M^{\perp}=M_y=M\sin(\mu)$. The set of Euler angles is given by $\underline{\omega}_\mu=(\mu,\pi/2,\pi/2)$ it describes the x'-y'-plane in the surface. For μ=0 it transfers: x→z', y→x', z→y' and for μ=90° it transfers: x→-x', y→z', z→y'.The inverse rotation needed to describe the magnetised states in the x,y,z-coordinates is given by: $\underline{\omega}^{-1}{}_\mu=(\pi/2,\pi/2,\pi-\mu)$.To describe the magnetic field in the x-y-plane we use the rotational matrix and its inverse as follows:

$$D_\mu = e^{-i\cdot m\cdot\mu} \cdot d^l_{m'm}\left(\frac{\pi}{2}\right) \cdot e^{-i\cdot m'\frac{\pi}{2}}$$

$$D^{-1}_\mu = e^{-i\cdot m\cdot\frac{\pi}{2}} \cdot d^l_{m'm}\left(\frac{\pi}{2}\right) \cdot e^{-i\cdot m'(\pi-\mu)}{}_\mu$$

For initial j=1/2 states we find:

D_μ		m'				
		1/2	-1/2	$e^{-im\mu}$	$e^{-im0°}$	$e^{-im\pi/2}$
m	1/2	$1/\sqrt{2}$	$-1/\sqrt{2}$	$e^{-i\mu/2}$	1	$(1-i)/\sqrt{2}$
	-1/2	$1/\sqrt{2}$	$1/\sqrt{2}$	$e^{i\mu/2}$	1	$(1+i)/\sqrt{2}$
	$e^{-im'\pi/2}$	$(1-i)/\sqrt{2}$	$(1+i)/\sqrt{2}$			

and the inverse:

$D^{-1}{}_\mu$		m'		
		1/2	-1/2	$e^{-im\pi/2}$
m	1/2	$1/\sqrt{2}$	$-1/\sqrt{2}$	$(1-i)/\sqrt{2}$
	-1/2	$1/\sqrt{2}$	$1/\sqrt{2}$	$(1+i)/\sqrt{2}$
	$e^{-im'(\pi-\mu)}$	$-i\,e^{i\mu/2}$	$i\,e^{-i\mu/2}$	
	$e^{-im'\pi}$	$-i$	i	
	$e^{im'\pi/2}$	$(1-i)/\sqrt{2}$	$(1+i)/\sqrt{2}$	

The magnetised p'-states are described for the parallel and perpendicular orientations of the magnetic field in the x-y laboratory co-ordinates by:

$M_\perp \rightarrow D^{-1}{}_\perp$	
$p'_{1/2,+1/2}=$	$-[i\,p_{1/2,+1/2}+p_{1/2,-1/2}]/\sqrt{2}$
$p'_{1/2,-1/2}=$	$[p_{1/2,+1/2}+i\,p_{1/2,-1/2}]/\sqrt{2}$

$M_\parallel \rightarrow D^{-1}{}_\parallel$	
$p'_{1/2,+1/2}=$	$-[p_{1/2,+1/2}+p_{1/2,-1/2}](1+i)/2$
$p'_{1/2,-1/2}=$	$[p_{1/2,+1/2}-p_{1/2,-1/2}](1-i)/2$

The $D_\perp$ operation converts the p_y state to $-p'_z$ as we have seen in the case of reel orbitals because the x'z' plane is in the surface. The alternative rotation and its inverse with the y'z' plane in the surface can be reached with: $\underline{\omega}_\perp=(\pi/2,\pi/2,\pi)$ and $\underline{\omega}^{-1}{}_\perp=(0,\pi/2,\pi/2)$. In this case the magnetised states are described by:

$M_\perp(y'z') \rightarrow D^{-1}{}_\perp(y'z')$	
$p'_{1/2,+1/2}=$	$[(1-i)\,p_{1/2,+1/2}-(1+i)p_{1/2,-1/2}]/2$
$p'_{1/2,-1/2}=$	$[(1-i)\,p_{1/2,+1/2}+(1+i)p_{1/2,-1/2}]/2$

for initial j=3/2 states we find:

D_μ		m'						
		3/2	½	-1/2	-3/2	$e^{-im\mu}$	$e^{-im0°}$	$e^{-im\pi/2}$
m	3/2	1	$-\sqrt{3}$	$\sqrt{3}$	-1	$e^{-i3\mu/2}$	1	$-(1-i)/\sqrt{2}$
	½	$\sqrt{3}$	-1	-1	$\sqrt{3}$	$e^{-i\mu/2}$	1	$(1-i)/\sqrt{2}$
	-1/2	$\sqrt{3}$	1	-1	$-\sqrt{3}$	$e^{i\mu/2}$	1	$(1+i)/\sqrt{2}$
	-3/2	1	$\sqrt{3}$	$\sqrt{3}$	1	$e^{i3\mu/2}$	1	$-(1+i)/\sqrt{2}$
	$e^{-im'\pi/2}$	$-(1-i)/\sqrt{2}$	$(1-i)/\sqrt{2}$	$(1+i)/\sqrt{2}$	$-(1+i)/\sqrt{2}$			

and the inverse:

$D^{-1}{}_\mu$		m'				
		3/2	½	-1/2	-3/2	$e^{-im\pi/2}$
m	3/2	1	$-\sqrt{3}$	$\sqrt{3}$	-1	$-(1-i)/\sqrt{2}$
	½	$\sqrt{3}$	-1	-1	$\sqrt{3}$	$(1-i)/\sqrt{2}$
	-1/2	$\sqrt{3}$	1	-1	$-\sqrt{3}$	$(1+i)/\sqrt{2}$
	-3/2	1	$\sqrt{3}$	$\sqrt{3}$	1	$-(1+i)/\sqrt{2}$
	$e^{-im'(\pi-\mu)}$	$i\,e^{i3\mu/2}$	$-i\,e^{i\mu/2}$	$i\,e^{-i\mu/2}$	$-i\,e^{-i3\mu/2}$	
	$e^{-im'\pi}$	i	$-i$	i	$-i$	
	$e^{-im'\pi/2}$	$-(1-i)/\sqrt{2}$	$(1-i)/\sqrt{2}$	$(1+i)/\sqrt{2}$	$-(1+i)/\sqrt{2}$	

The rotational matrix for $d_{5/2}$ or states with higher angular momentum are too big to be reproduced here, because the matrices are of the order $(2j+1)^2$.